Out-of-Plane Shaketable Testing of Unreinforced Masonry Walls in Two-Way Bending: Supplementary Material

J. Vaculik and M. C. Griffith

December 21, 2017

Abstract

The present document[1] contains supplementary material for the journal article *Vaculik and Griffith* (2017), whose full reference is as follows:

Vaculik J. and Griffith M.C. (2017) Out-of-plane shaketable testing of unreinforced masonry walls in two-way bending, *Bulletin of Earthquake Engineering*.
DOI: 10.1007/s10518-017-0282-8

This document is structured as follows:

- Section S.1 describes test methods and results of material tests;
- Section S.2 describes naming convention for main wall tests;
- Section S.3 describes the earthquake motions used for shaketable input;
- Section S.4 describes basic processing of raw data to obtain time-domain response parameters of interest, including wall acceleration and displacement. Peak values of key response parameters from individual test runs are also reported;
- Section S.5 describes the method used to derive values of key cyclic properties (such as wall vibrational frequency, hysteretic damping and effective stiffness) and reports their values for individual test runs;
- Section S.6 describes the frequency-domain filters applied to the data in post-processing;
- Section S.7 provides force-displacement plots for the individual test runs;
- Section S.8 provides photographs of the walls at the conclusion of testing; and
- Section S.9 describes the contents of the attached test data.

[1] Available at DOI: 10.4225/55/5a0138124b6c0

S.1 Material Testing

S.1.1 Introduction

Key material properties of the masonry used in the main test study were quantified through a series of tests on small-sized masonry specimens, as reported herein. The main engineering parameters of interest were:

- Flexural tensile strength of the masonry, f_{mt} (Section S.1.2).
- Unconfined compressive strength of the masonry, f_{mc} (Section S.1.3).
- Young's modulus of elasticity of the brick units (E_u), mortar joints (E_j), and overall masonry (E_m) (Section S.1.3).
- Coefficient of friction along the masonry bond, μ_m (Section S.1.4).

All masonry used throughout this test campaign (including the main wall tests and material tests described herein) was constructed using half-scale solid clay bricks with dimensions $110 \times 50 \times 39$ mm. These bricks were obtained from solid paving units cut lengthwise into multiple half-scale units. The mortar joints in the material test specimens were made to a 5 mm thickness, equal to that used in the construction of the main walls.

S.1.2 Flexural Tensile Strength

S.1.2.1 Test Method

The flexural tensile strength of the masonry, f_{mt}, was determined by the bond wrench method as prescribed by AS 3700 (*Standards Australia*, 2011), with masonry couplets used as test specimens (two bricks joined together with a mortar joint along the bed joint). A total of 12 joints were tested for each of the four mortar batches used in constructing the main test walls.

The test arrangement involved the bottom brick of the couplet being secured within a timber grip vice and the bond wrench being attached to the top brick (Figure S.1). An individual test was performed by manually applying a downward load onto the wrench handle, thus subjecting the joint to a bending moment in addition to a small compressive load. The load was slowly increased until failure of the bond. A calibrated strain gauge on the horizontal arm of the wrench conveyed the applied load to the data acquisition system. For each joint tested, the failure load was recorded and used to calculate the corresponding f_{mt} based on the procedure outlined in Section S.1.2.2.

S.1.2.2 Calculation of f_{mt}

Calculation of f_{mt} assumes that up to the point of failure the bonded interface exhibits a linear stress profile, and that failure occurs at the point when the stress in the extreme tensile fibre exceeds the tensile strength. By accounting for the combination of stress from applied moment and axial load, the tensile bond strength is calculated as

$$f_{mt} = \frac{M}{Z} - \frac{P}{A}, \tag{S.1}$$

where M is the applied moment at failure, P is the applied axial load at failure, Z is the elastic modulus of the bedded section, and A is the area of the bedded section.

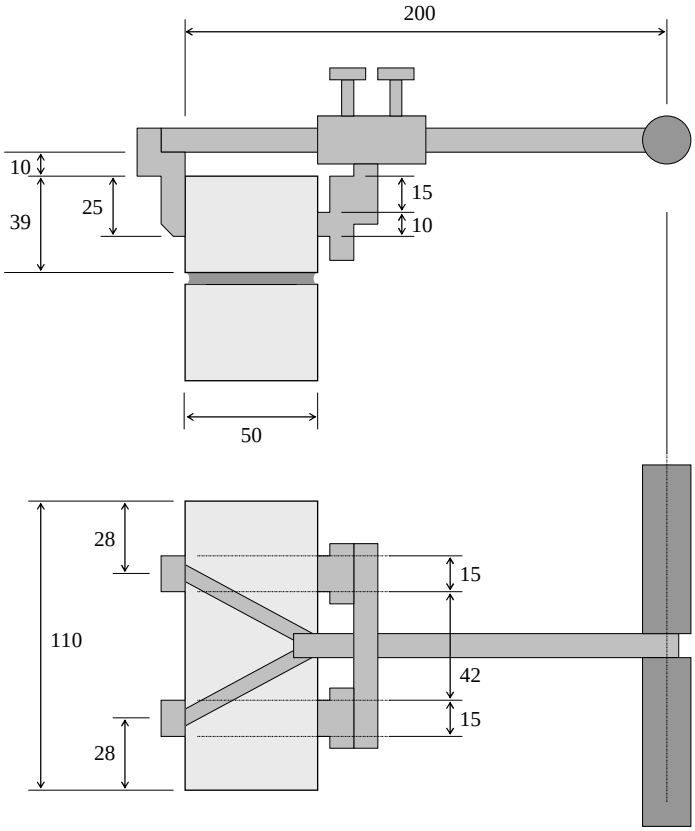

Figure S.1: Bond wrench test arrangement. Bottom brick in the couplet was clamped within a timber-grip vice (not shown). Dimensions are in millimetres.

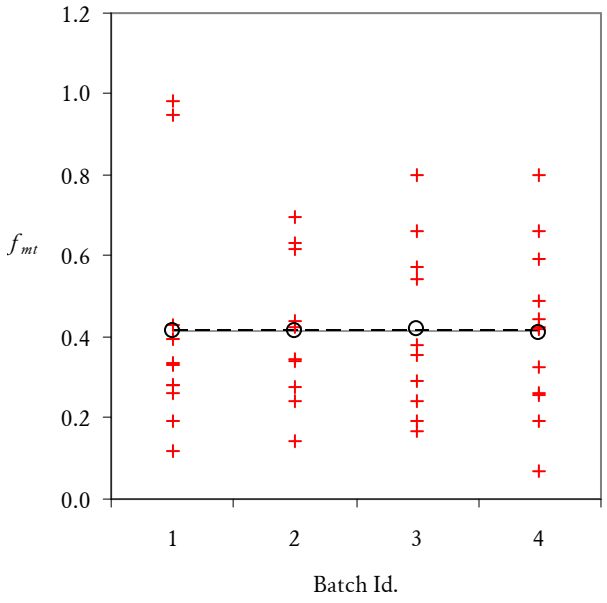

Figure S.2: Measured f_{mt} data in (in MPa) for the four mortar batches. Red crosses (+) show individual joint data; black circles (○) show mean values for each batch; solid gray line (——) shows the average f_{mt} for the wall, calculated as the mean of the batch averages; and dashed black line (----) shows the average f_{mt} for the wall, calculated as the mean of the individual bond data.

Table S.1: Results of bond wrench tests.

Batch	Sample consisting of bond data within batch				Sample consisting of pooled bond data			Sample consisting of batch averages		
	n	mean f_{mt} [MPa]	COV	t-test P-value	n	mean f_{mt} [MPa]	COV	n	mean f_{mt} [MPa]	COV
1	11	0.414	0.69	0.99	43	0.415	0.53	4	0.416	0.01
2	10	0.416	0.44	0.99						
3	10	0.421	0.51	0.94						
4	12	0.411	0.51	0.95						

S.1.2.3 Results

In the majority of joints tested, the failure plane followed the interface between the mortar and one of the bricks in the couplet, leaving the mortar completely adhered to the second brick. This suggests that the tensile strength of the bond was considerably weaker than the tensile strength of the mortar.

Figure S.2 graphs f_{mt} data for the four mortar batches tested. The results are also provided in Table S.1 for three alternate methods of data grouping: individual joints grouped by batch (columns 2–5), pooled data for all joints tested (columns 6–8), and data comprising the averages of the individual batches (columns 9–11). The mean values of f_{mt} for the four batches all range between 0.411 and 0.421 MPa. It is seen that although the coefficient of variation (COV; defined as ratio of the mean to the standard deviation) of all batches is high, their mean values are consistent.

Student's t-test was used to assess whether the four batches can be considered to all originate from the same batch. The resulting P-values of the t-test are provided in the 5th column of Table S.1.

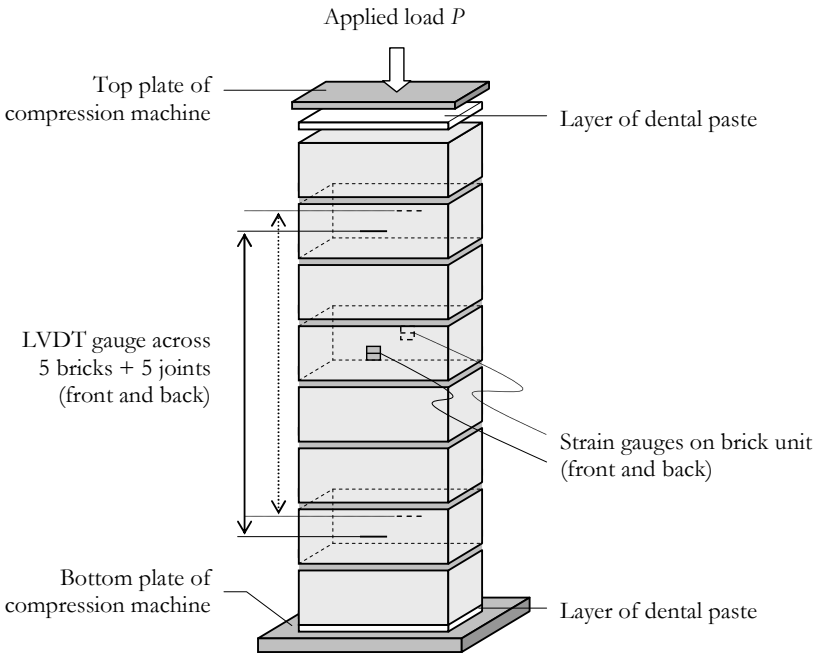

Figure S.3: Compression test arrangement.

That the P-values for all four batches are greater than 0.9 suggests that they can be treated as originating from the same batch. Pooling the data from the individual batches together gives a single data set consisting of 43 data points, with a mean f_{mt} of 0.415 MPa and a coefficient of variation of 0.53.

S.1.3 Compression Tests

Compression tests were performed to determine the compressive strength of the masonry (f_{mc}); and the Young's modulus of elasticity of the brick units (E_u), mortar joints (E_j), and overall masonry (E_m).

S.1.3.1 Test Method

Test specimens used for compression tests were seven-brick prisms as shown in Figure S.3. A single specimen was tested for each mortar batch.

For the purpose of quantifying the modulus of elasticity of the bricks, deformations in the central brick unit were measured using a pair of strain gauges positioned on opposite sides of the specimen. Deformation across the overall masonry (bricks + mortar joints) were measured using a pair of linear variable differential transformer (LVDT) displacement transducers across a five brick gauge length. In the subsequent data processing, measurements made on the opposite sides of the specimen were averaged to remove any effect of unintended bending of the specimen due to incidental eccentricity of the applied load.

The prisms were tested using a mechanical compression rig capable of imposing loads up to 1000 kN. Prior to applying any load, a moderate quantity of dental paste was applied to both the top and bottom loading faces of the prism and left to harden against the machine platens to promote a uniform distribution of the compressive load.

Each test was conducted by slowly applying a compressive load to the specimen up to 35 kN (approximately 25% of the failure load), during which data were recorded by a data acquisition system. The load was gradually released and reapplied for a total of four repetitions. Of these, the first load application was used to 'settle' the specimen and only the last three were subsequently used in calculating the modulus of elasticity. Finally the specimen was subjected to an increasing load until failure.

S.1.3.2 Calculation of f_{mc}

The unconfined compressive strength of the masonry, f_{mc}, was determined in accordance with AS 3700 as

$$f_{mc} = k_a \left(\frac{F_{sp}}{A_d} \right), \tag{S.2}$$

where F_{sp} is the applied compressive force at failure; A_d is the bedded area; and k_a is a factor used to account for the effects of horizontal confinement of the specimen due to platen restraint, taken as 1.0 in this case.

S.1.3.3 Calculation of E_u, E_j and E_m

The recorded data were converted to a stress-strain (σ-ϵ) format and from that, the modulus of elasticity was determined for the brick units (E_u), mortar joints (E_j) and the overall masonry comprising bricks plus mortar (E_m).

Stiffness of the brick (E_u) was directly measured in each prism, even though its value is independent of any properties of the mortar batch. The procedure used to quantify the stiffness of the mortar joint (E_j) in each batch used a back-calculation process which assumed that the stiffness of the central brick in the prism was equal to the directly measured value E_u and that the stiffness of the remaining bricks was equal to the mean E_u measured across all specimens. This was then followed by a forward-calculation process to determine E_m for each batch based on the back-calculated value of E_j and mean value of E_u. Additional detail regarding this procedure is provided in *Vaculik* (2012).

S.1.3.4 Results

Each of the four specimens tested underwent splitting failure as shown by Figure S.4. The onset of failure could be described as 'gentle' and was preceded by a reduction in the resisted load.

Stress-strain curves measured in each specimen are shown by Figure S.5 for both the overall masonry (5-brick gauge) and central brick. It is seen that the curves are consistent between the four specimens, except for the prism made with batch no. 3, which had one of its mortar joints broken during transportation and exhibited a much softer response than the other three. Note that this specimen was ignored in calculating E_j and E_m.

Results for each specimen are given in Table S.2. The calculated mean material properties are: $E_u = 32{,}100$ MPa, $E_j = 1{,}410$ MPa, $E_m = 9{,}180$ MPa, and $f_{mc} = 25.9$ MPa.

S.1.4 Coefficient of Friction

These tests were undertaken to quantify the coefficient of friction along the broken brick-to-mortar joint interface, μ_m.

Figure S.4: Typical compressive failure.

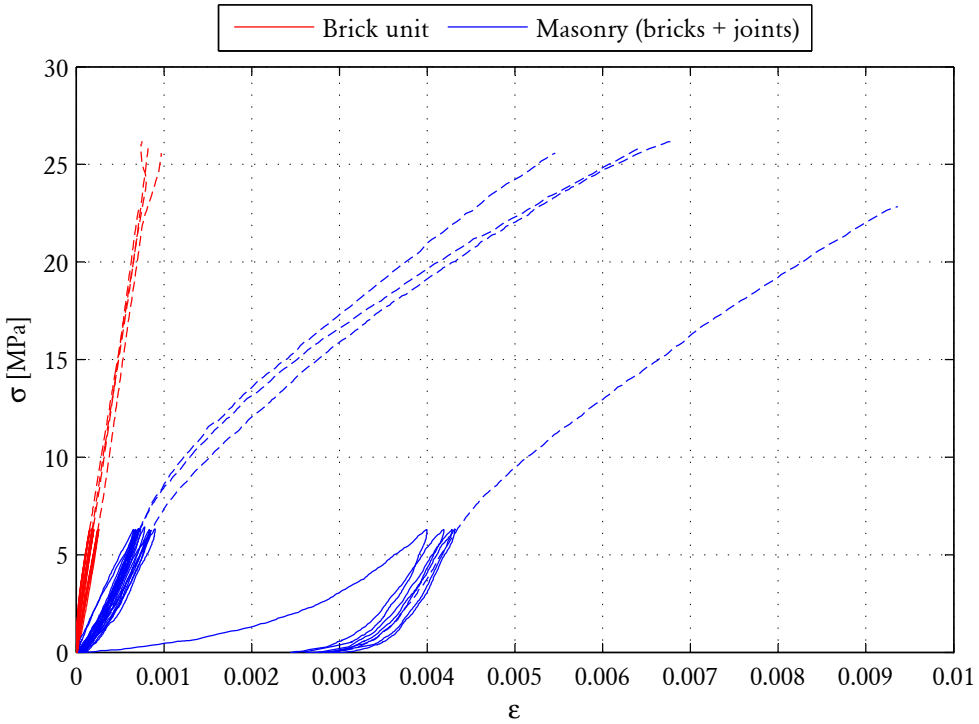

Figure S.5: Stress versus strain plots from compression tests. All four tests conducted are superimposed. The solid lines show tests used to calculate the Young's moduli and dashed line shows the push to failure. The rightmost curve (resisting load for approx. $\epsilon > 0.003$) is the response of specimen 3 which was broken prior to testing and was ignored in calculating modulus of elasticity of the masonry. Curves are only shown up to ultimate load, as the deformation measurements became inaccurate beyond this point.

Table S.2: Results of compression tests.

Batch	E_m [MPa]	E_u [MPa]	E_j [MPa]	f_{mc} [MPa]
1	7,720	37,900	1,110	26.2
2	9,360	33,600	1,430	26.1
3	–	31,100	–	22.9
4	10,500	25,700	1,670	28.6
Mean	9,180	32,100	1,410	25.9
COV	0.15	0.16	0.20	0.09

Table S.3: Coefficient of friction (μ_m) at different levels of axial stress (σ_v).

σ_v [MPa]	n	mean μ_m	COV	t-test P-value
0.037	8	0.582	0.13	0.80
0.073	8	0.583	0.08	0.77
0.108	8	0.569	0.12	0.78
0.144	8	0.570	0.08	0.79
Pooled	32	0.576	0.10	

S.1.4.1 Test Method

The test apparatus is shown by Figure S.6. The specimens used were reconstructed from broken couplets left over from the bond wrench tests (described in Section S.1.2.1). Each specimen consisted of three bricks with their originally adhered mortar, stacked together. A vertical load was applied to the top brick using either a 20, 40, 60 or 80 kg mass. These weights were chosen to generate similar levels of vertical stress to those in the main test walls.

A single test was conducted by applying a horizontal load to the central brick using a hand-operated hydraulic ram, while the top and bottom units were horizontally restrained. The load exerted by the ram and displacement of the central brick were conveyed to a data acquisition system. The test was stopped when the central brick displaced by approximately 16 mm. A total of eight specimens were tested at each level of axial compression.

S.1.4.2 Calculation of μ_m

The forces applied to the specimen are shown by Figure S.6. Since the specimen is subjected to the fixed vertical force F_v, at the point of slip, the horizontal forces across the two joints must be $\mu_1 F_v$ and $\mu_2 F_v$, where μ_1 and μ_2 are their respective friction coefficients. Therefore, from horizontal force equilibrium, the average friction coefficient for the two joints is

$$\mu_m = \frac{\mu_1 + \mu_2}{2} = \frac{F_h}{2F_v}, \tag{S.3}$$

where F_h is the applied horizontal load.

S.1.4.3 Results

Figure S.7 shows the typical measured response in terms of the friction coefficient μ_m [calculated from the resisted horizontal force F_h using Eq. (S.3)] versus the horizontal displacement of the central brick, Δ. Response is highly ductile and approximately elastoplastic. The friction coefficient for each specimen was calculated as the average value over the displacement range of 2 to 15 mm.

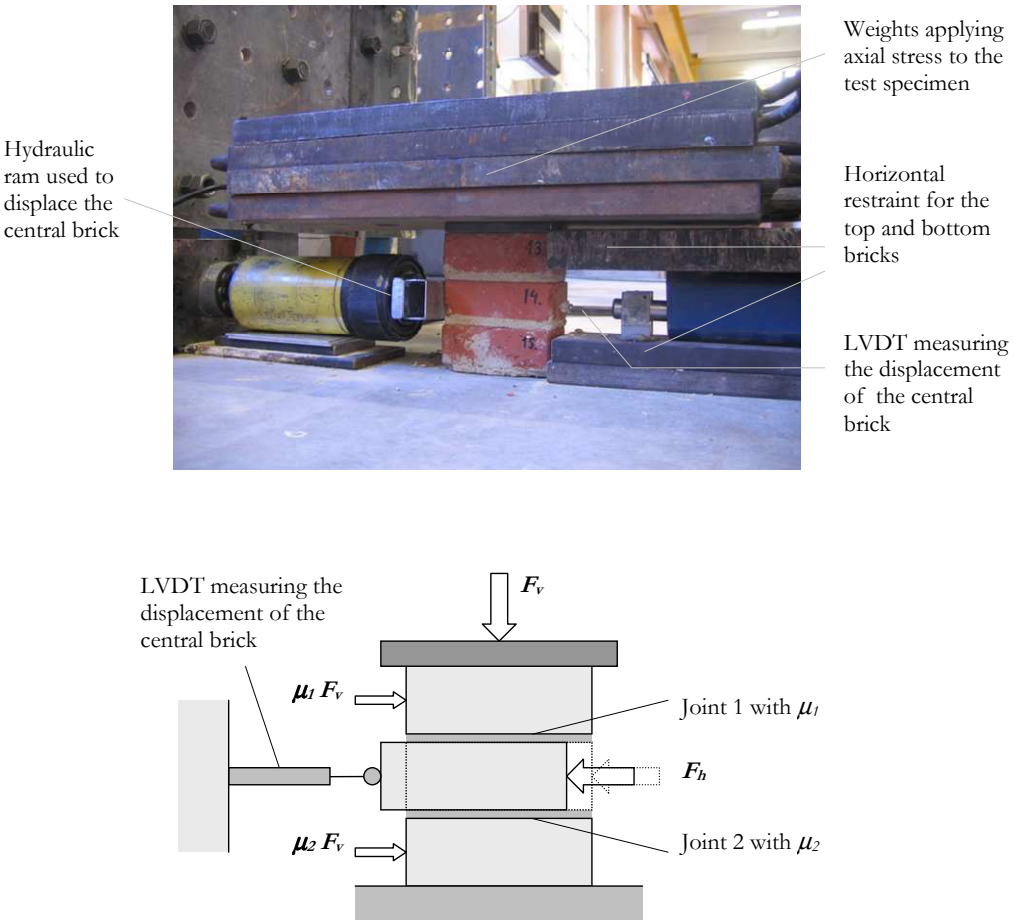

Figure S.6: Friction test arrangement (top) and forces applied to the test specimen at the instance of slip (bottom).

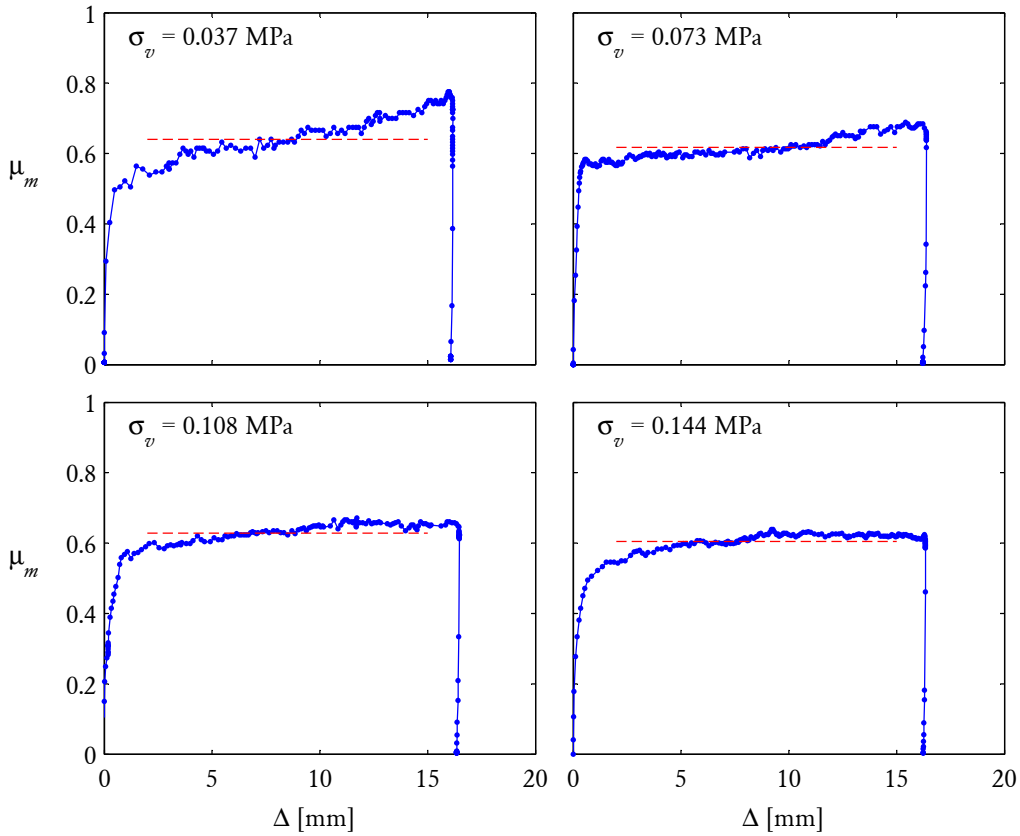

Figure S.7: Typical response of frictional resistance (as μ_m) at varied displacement (Δ). These results correspond to a single specimen under different levels axial stress σ_v. Dashed red line (----) shows the mean value calculated over the displacement range 2–15 mm.

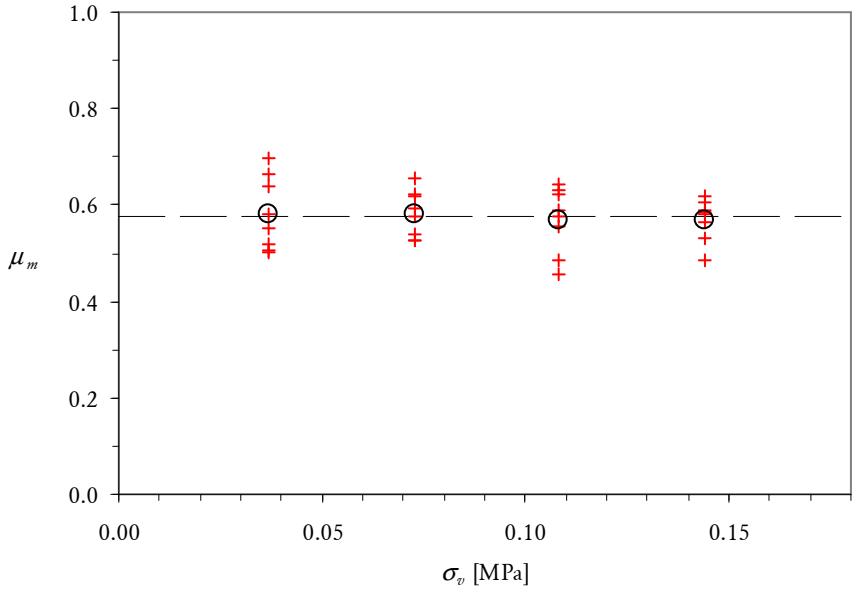

Figure S.8: Measured friction coefficient data at different levels of axial stress. Red crosses (+) indicate individual data points; black circles (○) show the mean values at each level of axial stress; and dashed black line (----) shows the overall mean value.

The μ_m data for individual specimens are plotted in Figure S.8 for different levels of axial stress. The associated mean values and COV are summarised in Table S.3. Whilst the coefficient of friction is typically assumed to be independent of the acting normal stress, a Student's t-test was conducted to assess whether there was a statistically significant difference in the measured μ_m values at different levels of σ_v. The large t-test P-values indicate that σ_v had negligible influence on μ_m and that all data may be assumed to come from the same distribution. Pooling the entire data set gives a mean μ_m value of 0.576.

S.2 Test Run Nomenclature

A standardised convention is used for naming individual test runs which uses several descriptors separated by underscores. The first three arguments are standard[2] and provide the following information:

1. Name of the wall; for example D1, D2, D3,...
2. Index of the test run for the particular wall.
3. Type of test: `R` = pulse test, `H` = harmonic test, and `EQ` = earthquake motion test.

For example, test `d2_06_R_8mm_100ms` was the sixth test run performed on wall D2 and used a pulse input motion.

The remaining arguments contain specific information relating to the different types of tests, as follows:

Pulse Tests (`R`) These tests used a simple displacement step function as the table input motion (Figure S.9). The first argument after `R` denotes the displacement step and the second argument the time step (defined respectively by x_o and $\mathrm{d}t$ in Figure S.9). For example, in test `d2_06_R_8mm_100ms` the table was subjected to a displacement step of 8 millimetres over 100 milliseconds.

Harmonic Tests (`H`) These tests used a sinusoidal harmonic input motion as shown by Figure S.10. The first argument after `R` denotes the excitation frequency, and the second argument denotes the table displacement amplitude (defined respectively by f_o and x_o in Figure S.10). For example, in test `d2_29_H_12Hz_0.3mm` the table was subjected to a harmonic motion at a frequency of 12 Hz with a targeted amplitude of 0.3 mm.

Earthquake Motion Tests (`EQ`) These tests used earthquake motions defined using a digitised displacement record. The first argument after `EQ` refers to the name of the earthquake motion: either `Taft` or one of the synthetic motions `Synth0x`. Details of these motions are presented in Section S.3. The second argument refers to the motion's peak ground displacement (PGD) with '+' or '−' denoting the directionality (as defined in Figure S.15). For example, test `d2_39_EQ_Taft_+80mm` ran the Taft motion at a PGD of 80 mm in the positive direction.

It should be noted that the table displacements specified within the test name were for the *input* motion. Actual PGD of the motions generated, as recorded using instrumentation, are reported in Table S.9.

[2] Exceptions include test runs 1–6, 8–10 and 89–91 for wall D1, which also provide a value of the non-standard axial stress applied at the top of the wall as one of the first four arguments.

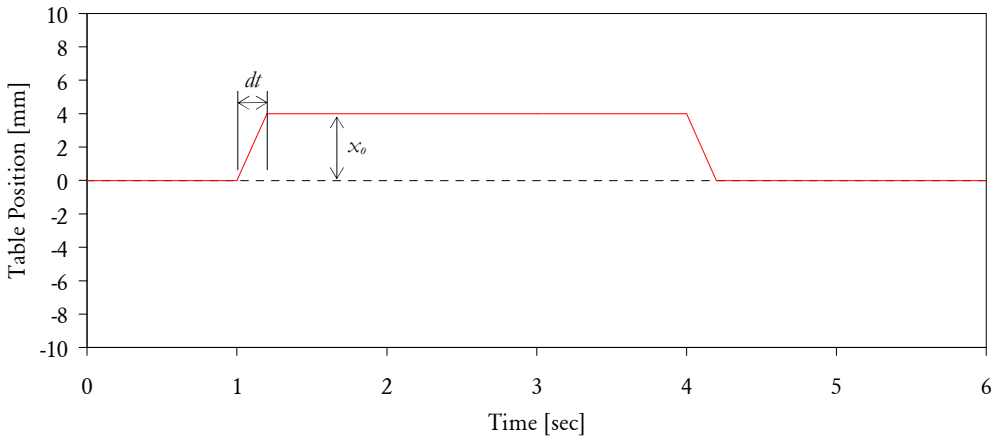

Figure S.9: Table displacement step function used for pulse tests. Each run consisted of a pair of pulses: one forward and one backward. The function is defined by the table displacement x_o and time interval dt over which it moves from $x = 0$ to $x = x_o$ at constant velocity.

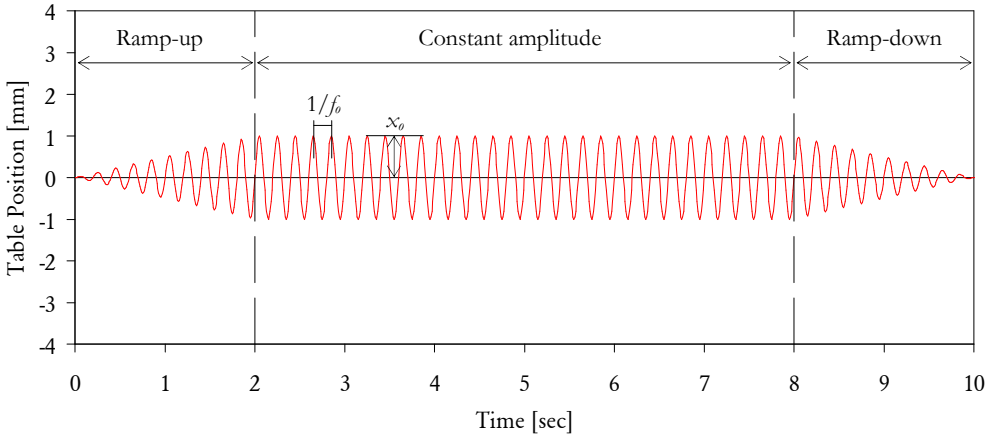

Figure S.10: Sinusoidal table displacement function used for harmonic tests, as defined by excitation frequency f_o and displacement amplitude x_o.

Table S.4: Synthetic earthquake motion cutoff frequencies.

Quake	Cutoff Frequency [Hz]
Synth01	6
Synth03	8
Synth05	12

S.3 Earthquake Input Motions

Time and frequency domain representations of the Taft earthquake motion, which served as the main input motion during these tests, are shown by Figure S.11.

In addition, three synthetic motions were used: Synth01, Synth03 and Synth05. The procedure used to generate each motion consisted of the following steps:

1. Digitised Gaussian noise was randomly generated in the time domain.
2. A lowpass filter was applied to the noise in the frequency domain, using the cutoff frequencies given in Table S.4.
3. A shape function was applied to the waveform in the time domain, consisting of three regions: linear ramp-up, constant amplitude, and linear ramp-down.
4. The resulting waveform was used as the synthetic motion's velocity vector.
5. The velocity was integrated to determine the displacement vector, and differentiated to determine the acceleration vector.
6. During the tests, the motion was scaled to achieve a required PGD.

The motions are shown by Figures S.12, S.13 and S.14.

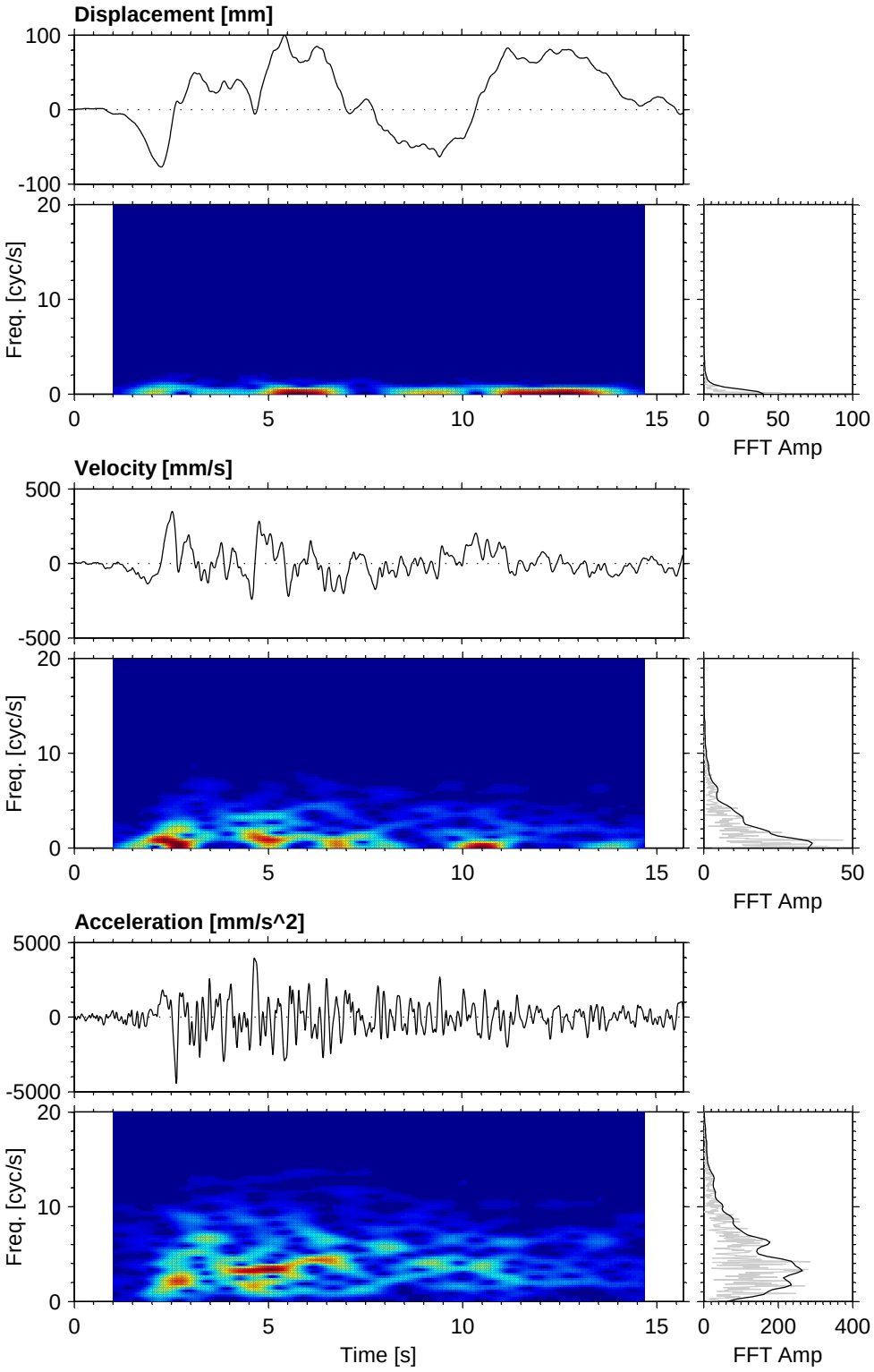

Figure S.11: Taft input motion in the time and frequency domains. (Scaled such that PGD = +100 mm)

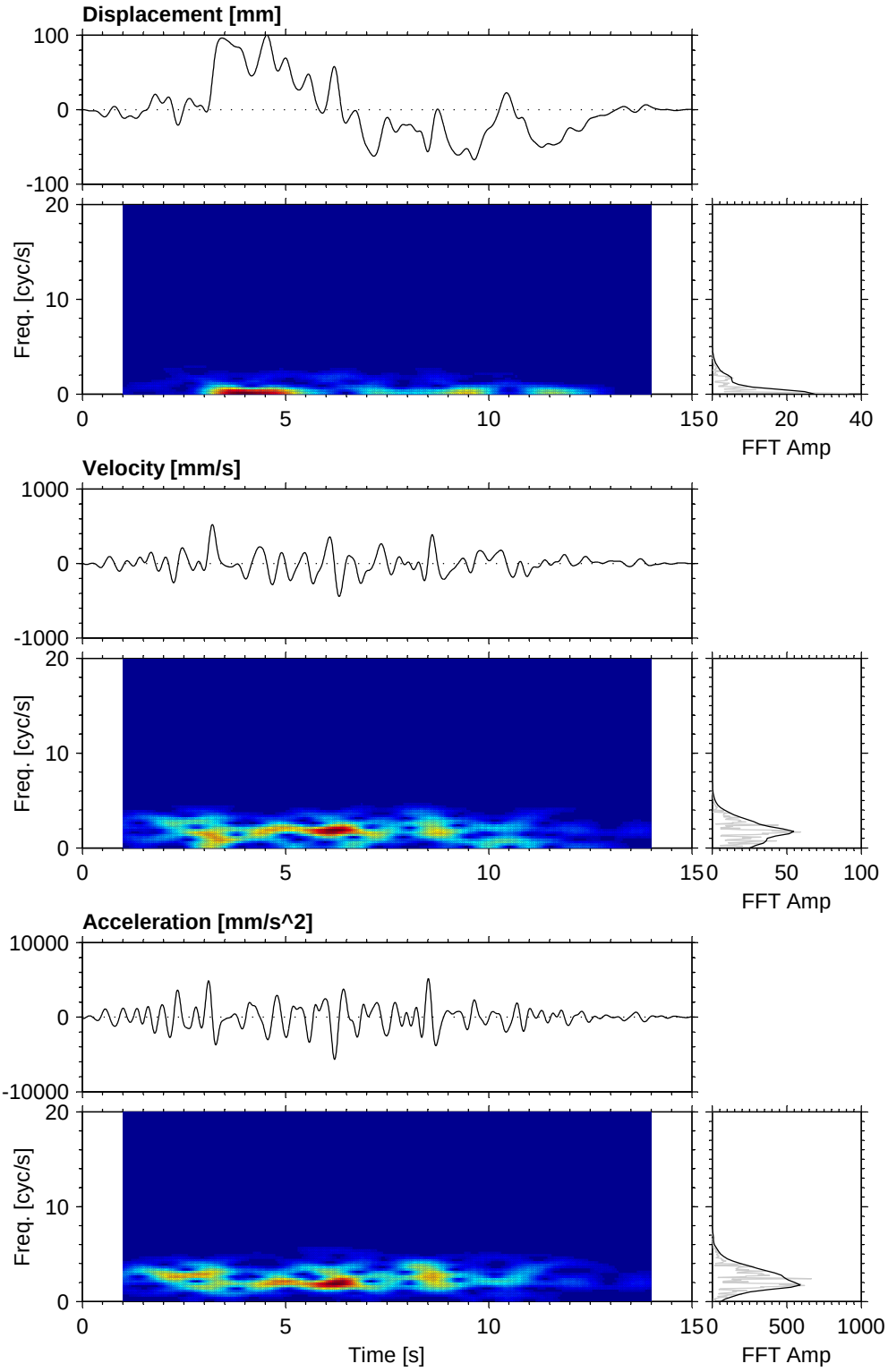

Figure S.12: Synth01 input motion in the time and frequency domains. (Scaled such that PGD = +100 mm)

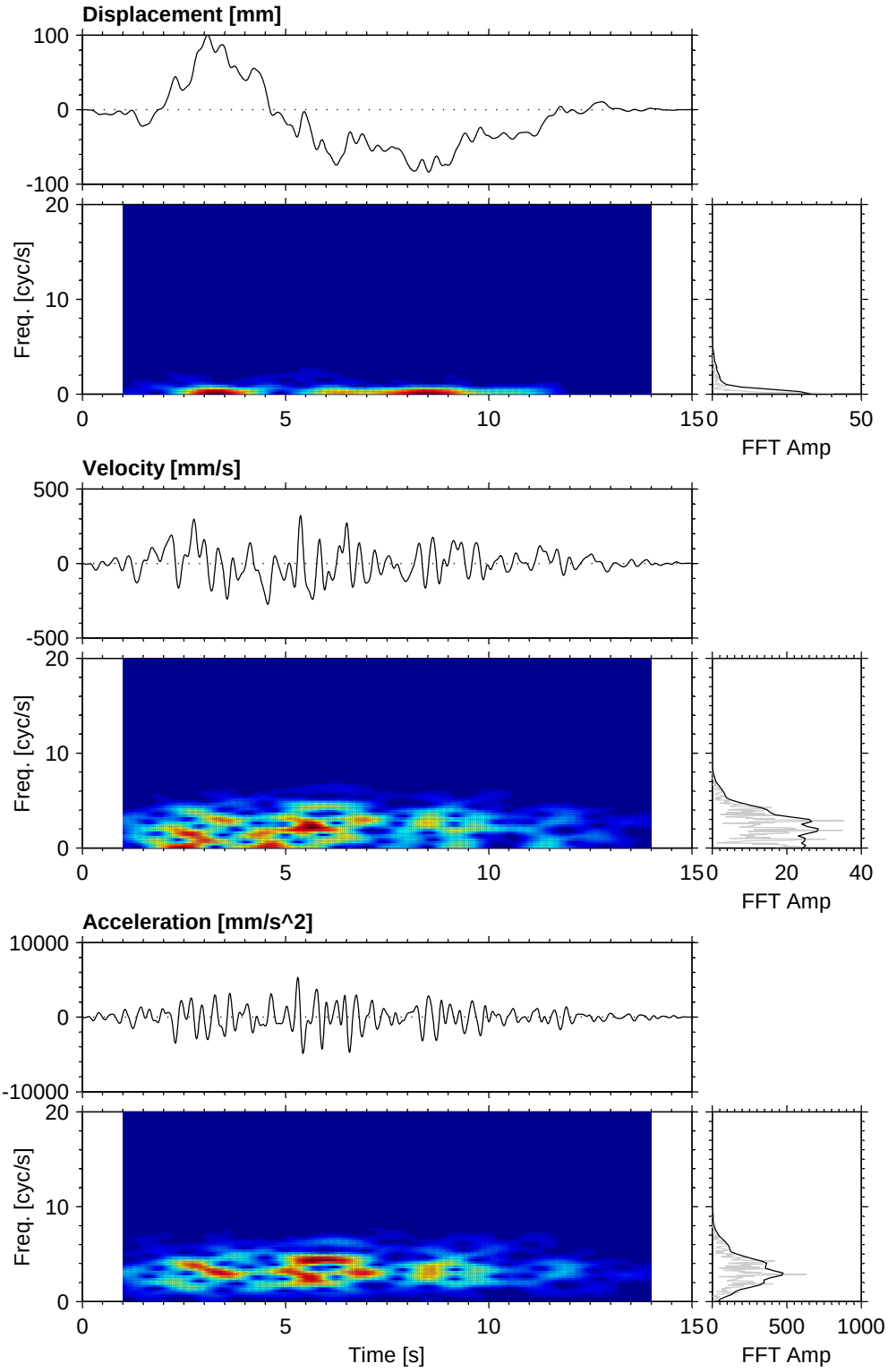

Figure S.13: Synth03 input motion in the time and frequency domains. (Scaled such that PGD = +100 mm)

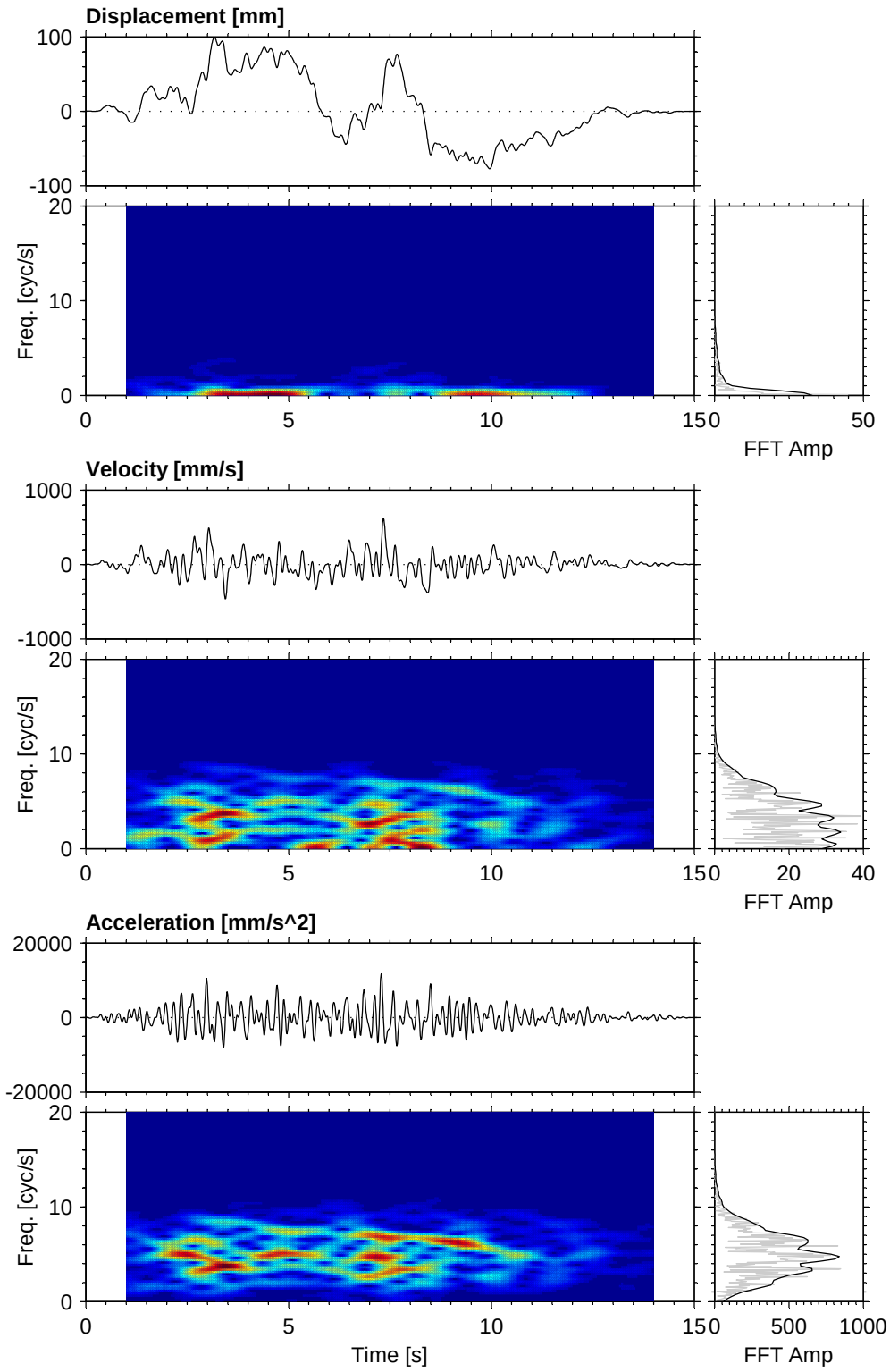

Figure S.14: Synth05 input motion in the time and frequency domains. (Scaled such that PGD = +100 mm)

S.4 Standard Data Processing

Section S.4.1 describes the data processing routine used to calculated key response variables such as wall displacement and force resistance. Section S.4.2 reports peak values of selected response variables for each test run.

S.4.1 Calculation of Time-Domain Response Vectors

The raw data acquired during testing consisted of output from ten accelerometers and six displacement transducers collected at 200 Hz sampling rate (Figure S.15). A computer routine was implemented to process the data and derive other time-domain vectors for variables of interest.[3] (N.B. The term 'vector' refers to data sampled over time; i.e. varying in the time domain.)

S.4.1.1 Positions and Displacements

Variables corresponding to positions and displacements are listed below.[4] Locations of the displacement transducers are shown in Figure S.15.

VECTOR	DESCRIPTION
$\boldsymbol{x}_{\text{tab}}$ and $\boldsymbol{x}_{\text{sup.bot}}$	Position of the table ($\boldsymbol{x}_{\text{tab}}$) and position of the wall's bottom support ($\boldsymbol{x}_{\text{sup.bot}}$) measured by displacement transducer DT4. These were treated as equal, since slip between the table and slab was shown to be negligible.
$\boldsymbol{x}_{\text{sup.top}}$	Position of the wall's top support as measured by displacement transducer DT3.
$\boldsymbol{x}_{\text{sup.avg}}$	Average position of the wall's top and bottom supports: $$\boldsymbol{x}_{\text{sup.avg}} = \frac{\boldsymbol{x}_{\text{sup.bot}} + \boldsymbol{x}_{\text{sup.top}}}{2}. \quad \text{(S.4)}$$
$\boldsymbol{\Delta}_{\text{slab-tab}}$	Slip between the concrete slab and the table, measured using displacement transducer DT5. Shown to be negligible throughout the course of testing.
$\boldsymbol{\Delta}_{\text{w.bot-slab}}$	Displacement between the wall's bottom edge and the concrete slab, as measured by displacement transducer DT5. The displacement transducer was located on the second course of bricks from the bottom of the wall.
$\boldsymbol{\Delta}_{\text{sup.top-tab}}$	Relative displacement between the top and bottom supports (i.e. interstorey drift): $$\boldsymbol{\Delta}_{\text{sup.top-tab}} = \boldsymbol{x}_{\text{sup.top}} - \boldsymbol{x}_{\text{sup.bot}}. \quad \text{(S.5)}$$
$\boldsymbol{\Delta}_{\text{w.cent}}$	The wall's central displacement, defined as the position of the wall's centre relative to the average position of its top and bottom supports. Calculated by firstly determining the wall's central position $\boldsymbol{x}_{\text{w.cent}}$ by averaging data from displacement transducers DT1 and DT2 to minimise noise. The central displacement was then taken as $$\boldsymbol{\Delta}_{\text{w.cent}} = \boldsymbol{x}_{\text{w.cent}} - \boldsymbol{x}_{\text{sup.avg}}. \quad \text{(S.6)}$$
$\boldsymbol{\Delta}_{\text{w.cent0}}$	The wall's central displacement ($\boldsymbol{\Delta}_{\text{w.cent}}$) zeroed at the start of each test run.

[3] Vector variables are denoted by bold symbols (e.g. $\boldsymbol{x}$ or $\boldsymbol{a}$) and scalar variables by italicised symbols (e.g. x or a).

[4] Note the subtle difference between these two parameters: Positions (x) are measured with respect to the *absolute* reference frame, whilst displacements (Δ) measure the relative difference between two positions.

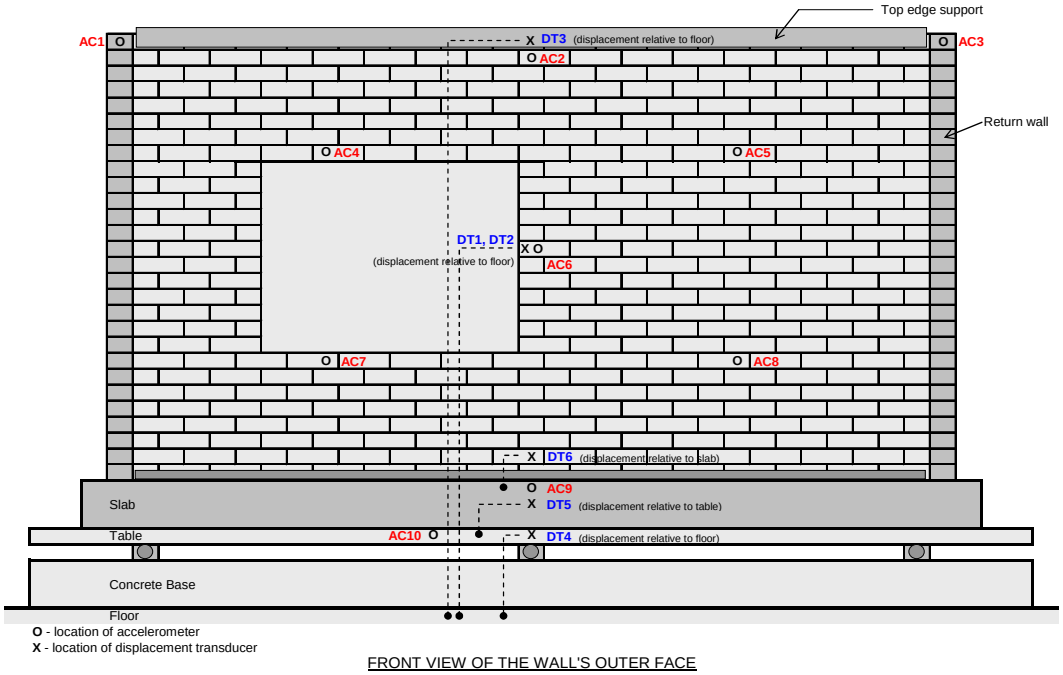

Figure S.15: Map of the instrumentation, comprising of 10 accelerometers (labelled AC1–AC10) and 6 displacement transducers (labelled DT1–DT6). Diagram is applicable to walls both with and without openings.

S.4.1.2 Accelerations

The following accelerations were determined. Locations of accelerometers are shown in Figure S.15.

VECTOR	DESCRIPTION
$\boldsymbol{a}_{\text{w.tl.corner}}$	Acceleration at the top left corner of the wall, as measured by accelerometer AC1 which was located at the top course of the return wall.
$\boldsymbol{a}_{\text{w.t.edge}}$	Acceleration at the top edge of the wall, as measured by accelerometer AC2. The accelerometer was located on the second topmost course of bricks, just below the top edge restraint member.
$\boldsymbol{a}_{\text{w.tr.corner}}$	Acceleration at the top right corner of the wall, as measured by accelerometer AC3 which was located at the top course of the return wall.
$\boldsymbol{a}_{\text{w.tl.quad}}$	Acceleration at the centre of the top left quadrant of the wall, as measured by accelerometer AC4.
$\boldsymbol{a}_{\text{w.tr.quad}}$	Acceleration at the centre of the top right quadrant of the wall, as measured by accelerometer AC5.
$\boldsymbol{a}_{\text{w.cent}}$	Acceleration at the centre of the wall, as measured by accelerometer AC6.
$\boldsymbol{a}_{\text{w.bl.quad}}$	Acceleration at the centre of the bottom left quadrant of the wall, as measured by accelerometer AC7.
$\boldsymbol{a}_{\text{w.br.quad}}$	Acceleration at the centre of the bottom right quadrant of the wall, as measured by accelerometer AC8.
$\boldsymbol{a}_{\text{slab}}$	Acceleration at the centre of the slab supporting the wall, as measured by accelerometer AC9.
$\boldsymbol{a}_{\text{tab}}$	Acceleration at the centre of the table, as measured by accelerometer AC10.
$\boldsymbol{a}_{\text{sup.avg}}$	Average acceleration of the wall's supports. Calculated as a weighted average of the slab (50% contribution) and the top left and right corners of the wall (25% contribution each): $$\boldsymbol{a}_{\text{sup.avg}} = 0.5\,\boldsymbol{a}_{\text{slab}} + 0.25\,\boldsymbol{a}_{\text{w.tl.corner}} + 0.25\,\boldsymbol{a}_{\text{w.tr.corner}}. \quad \text{(S.7)}$$
$\boldsymbol{a}_{\text{w.avg}}$	Average acceleration of the wall, calculated as a weighted average of the contributions of the 10 accelerometers according to the summation $$\boldsymbol{a}_{\text{w.avg}} = \sum_{k=1}^{10} r_k\,\boldsymbol{a}_k, \quad \text{(S.8)}$$ where k refers to the index of each accelerometer, with $\boldsymbol{a}_k$ being its acceleration and r_k its weighting factor. The weighting factor for each accelerometer was taken as its percentage of the tributary area along the wall (Figure S.16). The resulting vector $\boldsymbol{a}_{\text{w.avg}}$ was used for computing the wall's resisting force and pressure.
$\boldsymbol{a}_{\text{w.cent-sup.avg}}$	Relative acceleration between the wall's centre and its top and bottom supports, calculated as $$\boldsymbol{a}_{\text{w.cent-sup.avg}} = \boldsymbol{a}_{\text{w.cent}} - \boldsymbol{a}_{\text{sup.avg}}. \quad \text{(S.9)}$$ The primary purpose of this response variable was for use in a subsequent spectral analysis for determining the wall's vibrational frequency, since it best captures the wall's fundamental mode of vibration. For comparison, this relative acceleration was also calculated by double differentiating the wall's central displacement $\Delta_{\text{w.cent}}$. The response vector resulting from this latter approach exhibited greater levels of data noise than that calculated using the above equation. However, at larger levels of shaking the resulting vectors were very similar in their peak response, waveform and spectral content.

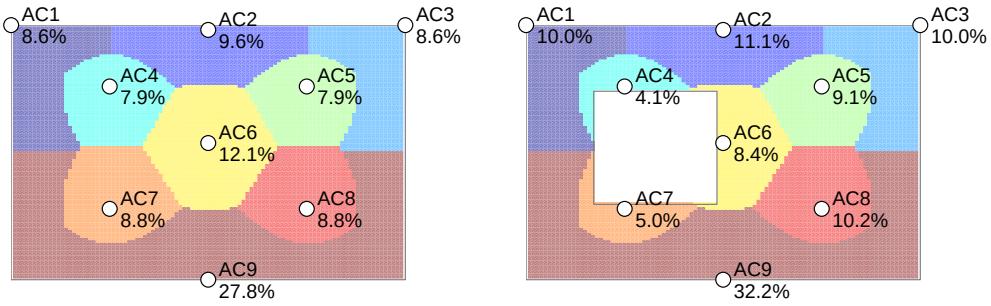

(a) Solid walls.

(b) Walls with window.

Figure S.16: Accelerometer tributary area percentages, used as weighting factors in calculation of the wall's average acceleration.

S.4.1.3 Pressure and Force

The pressure and force resisted by the wall were calculated using the wall's average acceleration $\boldsymbol{a}_{\text{w.avg}}$. These calculations are based on the equation of motion and the assumption of negligible viscous (velocity-proportional) forces.

VECTOR	DESCRIPTION
$\boldsymbol{q_w}$	Uniformly distributed face pressure resisted by the wall, calculated as $$\boldsymbol{q_w} = -\frac{\gamma\, t_u}{g}\, \boldsymbol{a}_{\text{w.avg}}, \quad \text{(S.10)}$$ where γ is the unit weight of the masonry, t_u is the thickness of the wall and g is acceleration due to gravity.
$\boldsymbol{F_w}$	Force resisted by the wall, calculated as $$\boldsymbol{F_w} = -m_w\, \boldsymbol{a}_{\text{w.avg}}. \quad \text{(S.11)}$$ In this expression, m_w is the mass of the wall, which is equal to $$m_w = \frac{\gamma\, t_u\, A_w}{g}, \quad \text{(S.12)}$$ where A_w is the wall's net area.

S.4.2 Results

Table S.9 summarises the peak values for key variables in each test run performed, and also provides miscellaneous notes relating to individual test runs. Note that the reported values were determined from unfiltered data (i.e. not incorporating the frequency domain filters described in Section S.6; Filtered data were only used in the cyclic response analysis reported in Section S.5).

Table S.8: Legend for the notes column in Table S.9.

⊠	New cracking occurred during the test.
□	No new cracking occurred during the test. This is only shown for tests between initial and full cracking of the wall.
ϟ	Shaketable underwent unexpected 'impacts' which generated spikes in its acceleration response [refer to Appendix D in *Vaculik* (2012)]. These were ultimately found to be due to a velocity limitation of the hydraulic ram used to drive the shaketable.
🎥	Test was recorded using video camera.
📷	Cracking pattern was photographed after the test.

Table S.9: Peak response of key variables during individual test runs. The tests are listed in the order in which they were performed. Table S.8 provides an explanation of the symbols used in the notes column.

Test Name	Notes	Table and Supports					Wall Response					
		x_{tab} [mm]	$x_{\text{sup.avg}}$ [mm]	$\Delta_{\text{sup.top-tab}}$ [mm]	a_{tab} [g]	$a_{\text{sup.avg}}$ [g]	$\Delta_{\text{w.cent}}$ [mm]	$\Delta_{\text{w.cent0}}$ [mm]	$a_{\text{w.cent}}$ [g]	$a_{\text{w.avg}}$ [g]	q_w [kPa]	F_w [N]
d5_01_H_14Hz_0.05mm		0.1	0.2	0.4	0.08	0.08	0.3	0.3	0.19	0.10	0.10	203
d5_02_H_14Hz_0.1mm		0.2	0.4	0.5	0.21	0.23	0.5	0.5	0.57	0.29	0.30	593
d5_03_H_14Hz_0.15mm		0.6	0.8	0.6	0.50	0.54	1.3	1.3	1.51	0.72	0.76	1501
d5_04_H_14Hz_0.2mm	⊠ 📷 🎥	0.9	1.2	0.9	0.80	0.88	2.6	2.6	2.61	1.20	1.27	2498
d5_05_R_2mm_200ms	□[5]	2.2	2.2	0.2	0.08	0.09	0.5	0.3	0.36	0.10	0.11	214
d5_06_R_4mm_200ms	□	4.4	4.4	0.3	0.13	0.15	0.6	0.5	0.59	0.20	0.21	408
d5_07_R_4mm_100ms	□	4.7	4.7	0.5	0.35	0.36	1.3	1.2	1.23	0.42	0.45	875
d5_08_H_14Hz_0.2mm	□ 🎥	0.3	0.5	0.6	0.31	0.31	2.4	2.3	2.11	0.68	0.72	1416
d5_09_H_14Hz_0.25mm	⊠ 📷 🎥	1.0	1.2	0.8	0.94	1.01	5.9	5.7	3.32	0.96	1.02	2003
d5_10_R_2mm_200ms	□	2.2	2.2	0.3	0.08	0.08	0.7	0.5	0.30	0.08	0.08	158
d5_11_R_4mm_200ms	□	4.5	4.5	0.5	0.14	0.16	1.1	0.9	0.55	0.16	0.17	339
d5_12_R_4mm_100ms	□	4.7	4.8	0.4	0.35	0.39	2.4	2.2	1.03	0.30	0.32	624
d5_13_H_14Hz_0.3mm	⊠[6] 🎥	1.4	1.8	1.0	1.54	1.58	8.3	8.0	3.92	0.85	0.90	1762
d5_14_R_2mm_200ms		2.2	2.2	0.2	0.09	0.10	1.6	0.5	0.31	0.08	0.08	166
d5_15_R_4mm_200ms		4.4	4.4	0.4	0.14	0.16	2.1	1.1	0.49	0.13	0.14	270
d5_16_R_4mm_100ms		4.8	4.8	0.4	0.36	0.40	3.5	2.4	0.91	0.28	0.29	573
d5_17_EQ_Taft_-6mm	🎥	5.5	5.5	0.4	0.04	0.05	1.2	0.2	0.12	0.04	0.04	85
d5_18_EQ_Taft_+6mm	🎥	5.7	5.7	0.4	0.04	0.05	1.3	0.3	0.12	0.04	0.04	78
d5_19_EQ_Taft_+11mm	🎥	11.3	11.3	0.5	0.09	0.11	1.5	0.5	0.29	0.07	0.08	148
d5_20_EQ_Taft_-11mm	🎥	11.2	11.2	0.3	0.08	0.08	1.5	0.5	0.22	0.06	0.07	135
d5_21_EQ_Taft_-17mm	🎥	17.0	16.9	0.5	0.11	0.11	1.7	0.6	0.34	0.09	0.10	195
d5_22_EQ_Taft_+17mm	🎥	16.9	16.9	0.4	0.13	0.15	1.7	0.7	0.48	0.10	0.11	211
d5_23_EQ_Taft_+22mm	🎥	22.5	22.6	0.5	0.16	0.17	1.9	0.9	0.55	0.13	0.13	260
d5_24_EQ_Taft_-22mm	🎥	22.3	22.3	0.4	0.18	0.19	2.0	1.0	0.44	0.14	0.14	284
d5_25_EQ_Taft_-28mm	🎥	28.1	28.1	0.4	0.20	0.20	2.2	1.1	0.49	0.16	0.17	326
d5_26_EQ_Taft_+28mm	🎥	28.0	28.0	0.4	0.23	0.24	2.1	1.2	0.62	0.17	0.18	359
d5_27_EQ_Taft_+33mm	🎥	33.5	33.5	0.5	0.28	0.29	2.5	1.5	0.77	0.20	0.21	418
d5_28_EQ_Taft_-33mm	🎥	33.3	33.4	0.5	0.23	0.28	2.3	1.4	0.58	0.19	0.20	390
d5_29_EQ_Taft_-39mm	🎥	39.0	39.0	0.5	0.30	0.37	2.5	1.6	0.63	0.23	0.25	482
d5_30_EQ_Taft_+39mm	🎥	39.4	39.5	0.4	0.32	0.36	2.7	1.8	0.87	0.26	0.27	537
d5_31_EQ_Taft_+45mm	🎥	44.9	44.9	0.4	0.37	0.41	2.9	2.2	0.96	0.29	0.31	605
d5_32_EQ_Taft_-45mm	🎥	45.0	45.0	0.4	0.35	0.42	2.9	2.0	0.76	0.29	0.30	593
d5_33_EQ_Taft_-50mm	🎥	50.1	50.1	0.5	0.46	0.46	4.2	3.3	1.07	0.38	0.41	798
d5_34_EQ_Taft_+50mm	📷 🎥	50.3	50.5	0.5	0.39	0.45	3.4	2.4	1.10	0.33	0.34	676
d5_35_EQ_Taft_+56mm	🎥	56.1	56.0	0.7	0.49	0.52	2.9	2.8	1.19	0.39	0.41	810
d5_36_EQ_Taft_-56mm	ϟ 🎥	56.2	56.1	0.9	1.06	1.04	6.5	6.8	2.00	0.74	0.79	1544
d5_37_EQ_Taft_-67mm	ϟ 🎥	66.7	66.6	1.4	1.96	1.76	12.0	12.1	3.52	1.29	1.37	2680

continued on next page

[5]These three free vibration tests (5–7) showed the wall's frequency to be approximately 15-20 Hz. However, a preliminary free vibration test performed prior to test no. 1 by impacting the wall with a rubber mallet showed a strong signal at approximately 35 Hz. It is likely that the reduction in frequency from 35 Hz to 15-20 Hz was a result of the initial cracking of the wall.

[6]Wall became fully cracked.

Bull Earthquake Eng, DOI: 10.1007/s10518-017-0282-8
SUPPLEMENTARY MATERIAL

Table S.9: (cont'd).

Test Name	Notes	Table and Supports					Wall Response					
		x_{tab} [mm]	$x_{\text{sup.avg}}$ [mm]	$\Delta_{\text{sup.top-tab}}$ [mm]	a_{tab} [g]	$a_{\text{sup.avg}}$ [g]	$\Delta_{\text{w.cent}}$ [mm]	$\Delta_{\text{w.cent0}}$ [mm]	$a_{\text{w.cent}}$ [g]	$a_{\text{w.avg}}$ [g]	q_w [kPa]	F_w [N]
d5_38_EQ_Taft_+67mm	ϟ 📹	67.3	67.2	0.8	1.35	1.42	8.9	9.0	3.61	1.17	1.24	2426
d5_39_R_2mm_200ms		2.4	2.2	0.6	0.08	0.10	0.8	0.5	0.29	0.07	0.08	154
d5_40_R_4mm_200ms		4.6	4.4	0.7	0.14	0.15	1.2	0.9	0.42	0.12	0.13	257
d5_41_R_4mm_100ms		5.1	4.9	0.7	0.36	0.40	2.8	2.3	0.81	0.29	0.31	610
d5_42_EQ_Taft_+73mm	ϟ 📹	72.6	72.5	1.2	1.97	1.90	13.0	12.6	3.89	1.52	1.61	3159
d5_43_EQ_Taft_-73mm	ϟ 📹	73.0	72.9	1.4	1.98	1.81	14.8	14.5	2.67	1.21	1.29	2523
d5_44_EQ_Taft_-78mm	ϟ 📹	78.2	77.9	1.1	1.83	1.81	13.1	13.0	2.75	1.12	1.18	2321
d5_45_EQ_Taft_+78mm	ϟ 📹	78.2	78.1	1.4	2.41	2.32	17.1	16.6	3.94	1.43	1.52	2976
d5_46_R_2mm_200ms		2.5	2.3	0.8	0.11	0.09	3.1	0.6	0.23	0.07	0.07	140
d5_47_R_4mm_200ms		4.6	4.5	0.6	0.13	0.17	3.9	1.3	0.36	0.13	0.13	261
d5_48_R_4mm_100ms		5.1	4.9	0.6	0.38	0.37	6.0	3.8	0.80	0.31	0.32	635
d5_49_EQ_Taft_+22mm	📹	21.8	22.3	1.4	0.13	0.19	3.8	1.9	0.35	0.13	0.14	276
d5_50_EQ_Taft_-22mm	📹	22.8	22.3	1.4	0.15	0.18	3.8	1.9	0.41	0.15	0.16	305
d5_51_EQ_Taft_-45mm	📹	45.8	45.2	1.6	0.30	0.33	6.4	4.7	0.91	0.28	0.30	591
d5_52_EQ_Taft_+45mm	📹	44.3	44.8	1.3	0.36	0.38	6.1	4.4	0.69	0.30	0.32	629
d5_53_EQ_Taft_+67mm	ϟ 📹	66.5	67.1	1.6	1.18	1.09	8.9	10.6	2.38	0.81	0.86	1685
d5_54_EQ_Taft_-67mm	ϟ 📹	67.4	66.6	1.8	1.95	1.64	15.6	13.9	2.48	1.13	1.20	2353
d5_55_EQ_Taft_-84mm	ϟ 📹	84.3	83.4	2.1	1.52	1.22	10.9	10.7	1.71	0.88	0.93	1829
d5_56_EQ_Taft_+84mm	ϟ 📹	83.7	84.2	2.1	2.55	2.64	19.0	18.5	4.91	1.50	1.59	3112
d5_57_EQ_Taft_+89mm	ϟ 📹	88.7	89.2	2.0	2.47	2.35	17.1	17.4	4.95	1.42	1.50	2940
d5_58_EQ_Taft_-89mm	ϟ 📹	89.9	89.0	2.1	1.27	1.16	15.9	15.4	1.59	0.67	0.71	1389
d5_59_EQ_Taft_-95mm	ϟ 📹	95.0	94.2	2.2	1.34	1.13	18.0	18.8	1.90	0.80	0.84	1653
d5_60_EQ_Taft_+95mm	ϟ 📷 📹	94.2	94.7	1.8	2.30	2.07	19.9	19.2	2.90	1.25	1.32	2594
d5_61_EQ_Taft_+100mm	ϟ 📹	100.2	100.8	1.9	2.31	1.88	22.2	22.2	2.30	1.33	1.41	2771
d5_62_EQ_Taft_-100mm	ϟ[7] 📷 📹	100.9	100.1	2.3	1.45	1.25	22.6	24.5	2.79	0.94	1.00	1963
d3_01_R_2mm_200ms		2.2	2.1	0.5	0.09	0.10	0.5	0.4	0.15	0.11	0.11	226
d3_02_R_4mm_200ms		4.1	4.2	0.3	0.17	0.17	0.3	0.3	0.25	0.19	0.20	399
d3_03_R_4mm_100ms		4.5	4.5	0.5	0.34	0.35	0.3	0.3	0.46	0.38	0.40	793
d3_04_R_8mm_100ms		8.9	9.1	0.7	0.74	0.79	0.7	0.6	1.37	0.92	0.97	1909
d3_05_H_13Hz_0.05mm	📹	0.4	0.2	0.5	0.08	0.08	0.3	0.2	0.11	0.08	0.09	169
d3_06_H_13Hz_0.1mm	📹	0.6	0.4	0.5	0.22	0.20	0.3	0.3	0.32	0.23	0.24	476
d3_07_H_13Hz_0.15mm	📹	0.6	0.6	0.8	0.41	0.54	0.5	0.4	0.68	0.45	0.48	940
d3_08_H_13Hz_0.2mm	📹	0.6	0.8	0.9	0.55	0.71	0.5	0.5	1.07	0.65	0.69	1358
d3_09_H_13Hz_0.25mm	📹	0.8	1.1	1.0	0.70	1.00	0.8	0.9	1.65	0.96	1.02	1999
d3_10_H_13Hz_0.3mm	[8] 📷 📹	1.1	1.5	1.3	0.94	1.30	1.1	1.1	2.08	1.41	1.50	2940
d3_11_H_13Hz_0.3mm	⊠[9] 📹	1.9	2.7	2.2	1.68	2.05	4.7	4.2	4.97	2.40	2.54	4983
d3_12_R_4mm_200ms	□	4.0	4.1	0.4	0.15	0.14	1.3	0.3	0.24	0.16	0.17	342
d3_13_R_4mm_100ms	□	4.3	4.5	0.4	0.32	0.31	1.5	0.5	0.65	0.35	0.37	723
d3_14_R_8mm_100ms	□	8.7	8.9	0.6	0.72	0.68	2.2	1.1	1.59	0.80	0.85	1670

continued on next page

[7] Lintel fell out due to a loss of connection with the wall at one of its ends.
[8] Precompression springs underwent severe horizontal vibration during test 10.
[9] Precompression springs were restrained prior to conducting this test. The revised test setup was retained for all subsequent tests with precompression.

Table S.9: (cont'd).

Test Name	Notes	Table and Supports					Wall Response					
		x_{tab} [mm]	$x_{\text{sup.avg}}$ [mm]	$\Delta_{\text{sup.top-tab}}$ [mm]	a_{tab} [g]	$a_{\text{sup.avg}}$ [g]	$\Delta_{\text{w.cent}}$ [mm]	$\Delta_{\text{w.cent0}}$ [mm]	$a_{\text{w.cent}}$ [g]	$a_{\text{w.avg}}$ [g]	q_w [kPa]	F_w [N]
d3_15_H_13Hz_0.35mm	⊠ 🎥	1.8	2.8	2.6	1.54	2.22	5.7	4.6	5.49	2.52	2.67	5247
d3_16_H_13Hz_0.4mm	⊠ 📷 🎥	1.6	2.5	2.5	1.41	2.07	6.7	5.6	5.29	2.45	2.59	5082
d3_17_R_4mm_200ms	□	4.1	4.2	0.6	0.15	0.18	1.0	0.4	0.49	0.20	0.21	414
d3_18_R_4mm_100ms	□	4.3	4.4	0.4	0.32	0.32	1.3	0.7	0.80	0.35	0.37	733
d3_19_R_8mm_100ms	□	8.6	8.8	0.7	0.75	0.63	2.1	1.5	1.67	0.78	0.82	1616
d3_20_H_12Hz_0.4mm	⊠[10] 📷 🎥	1.8	2.5	2.0	1.31	1.80	8.2	8.8	4.77	2.10	2.23	4374
d3_21_R_4mm_200ms		4.2	4.2	0.5	0.14	0.16	1.4	0.6	0.44	0.15	0.16	318
d3_22_R_4mm_100ms		4.6	4.6	0.4	0.33	0.34	2.4	1.6	1.06	0.32	0.34	660
d3_23_R_8mm_100ms		8.8	9.0	0.5	0.75	0.67	4.3	3.5	2.18	0.59	0.62	1222
d3_24_EQ_Taft_-5mm	🎥	5.0	5.0	0.3	0.04	0.05	1.1	0.3	0.13	0.06	0.07	128
d3_25_EQ_Taft_+5mm		5.1	5.1	0.6	0.04	0.05	1.1	0.3	0.15	0.07	0.07	136
d3_26_EQ_Taft_+10mm	🎥	10.1	10.1	0.5	0.08	0.08	1.1	0.5	0.34	0.13	0.13	262
d3_27_EQ_Taft_-10mm		9.9	9.9	0.5	0.07	0.08	1.1	0.3	0.25	0.10	0.11	214
d3_28_EQ_Taft_-20mm		20.0	20.0	0.6	0.12	0.15	1.3	0.5	0.35	0.18	0.19	370
d3_29_EQ_Taft_+20mm		19.9	19.9	0.5	0.13	0.15	1.2	0.5	0.49	0.23	0.24	476
d3_30_EQ_Taft_+30mm		30.2	29.9	0.6	0.20	0.23	1.4	0.6	0.58	0.27	0.28	555
d3_31_EQ_Taft_-30mm		30.1	30.1	0.6	0.18	0.21	1.3	0.6	0.56	0.20	0.22	425
d3_32_EQ_Taft_-40mm		39.8	39.8	0.5	0.28	0.25	1.6	0.9	0.65	0.27	0.28	558
d3_33_EQ_Taft_+40mm		40.1	40.1	0.5	0.29	0.28	1.5	0.9	0.82	0.40	0.42	822
d3_34_EQ_Taft_+50mm		49.8	49.9	0.4	0.34	0.41	1.9	1.2	0.98	0.54	0.57	1122
d3_35_EQ_Taft_-50mm		49.7	49.7	0.5	0.40	0.41	1.9	1.2	0.84	0.35	0.37	729
d3_36_EQ_Taft_-60mm	ϟ	60.0	60.1	1.1	1.50	1.34	5.9	5.2	3.17	1.11	1.18	2315
d3_37_EQ_Taft_+60mm	🎥	59.8	60.0	0.5	0.45	0.45	2.6	2.1	1.42	0.57	0.61	1193
d3_38_EQ_Taft_+70mm	ϟ 🎥	70.3	70.6	1.0	1.71	1.57	9.5	8.9	3.69	1.59	1.68	3299
d3_39_EQ_Taft_-70mm	ϟ 🎥	69.9	70.0	1.5	2.16	2.04	8.5	9.3	4.89	1.39	1.47	2879
d3_40_EQ_Taft_-80mm	ϟ 🎥	79.4	79.4	1.2	1.79	1.74	7.5	8.1	4.49	1.18	1.25	2451
d3_41_EQ_Taft_+80mm	ϟ 🎥	80.0	80.1	1.8	2.73	2.77	15.7	15.2	4.78	1.86	1.97	3870
d3_42_R_4mm_200ms		4.2	4.3	0.4	0.16	0.16	1.8	0.8	0.52	0.22	0.24	462
d3_43_R_4mm_100ms		4.5	4.5	0.3	0.33	0.34	2.6	1.6	0.88	0.36	0.38	749
d3_44_R_8mm_100ms		8.9	9.0	0.6	0.76	0.75	5.0	3.8	2.04	0.65	0.69	1349
d3_45_EQ_Taft_+90mm	ϟ 🎥	89.7	89.8	2.1	2.62	2.97	17.2	16.3	5.03	1.76	1.87	3665
d3_46_EQ_Taft_-90mm	ϟ 🎥	89.6	89.7	1.0	1.37	1.33	7.8	6.6	3.52	0.98	1.04	2036
d3_47_R_4mm_200ms		4.2	4.3	0.5	0.15	0.16	1.6	0.8	0.53	0.19	0.20	385
d3_48_R_4mm_100ms		4.5	4.5	0.3	0.33	0.31	2.5	1.5	0.96	0.38	0.40	789
d3_49_R_8mm_100ms		8.9	9.0	0.6	0.75	0.77	5.2	4.2	1.99	0.63	0.66	1302
d3_50_EQ_Taft_-100mm	ϟ	99.5	99.6	0.8	1.46	1.45	6.8	6.7	3.46	1.47	1.56	3059
d3_51_EQ_Taft_+100mm	ϟ	100.2	100.4	1.7	2.47	2.33	15.5	14.7	4.31	1.50	1.59	3118
d3_52_EQ_Taft_+110mm	ϟ 📷 🎥	108.8	109.1	2.2	3.15	2.42	14.8	13.8	4.28	1.76	1.87	3665
d3_53_EQ_Taft_-110mm	ϟ 🎥	108.3	108.3	1.4	2.32	1.91	11.1	9.9	4.28	1.86	1.97	3871
d3_54_EQ_Taft_-120mm	ϟ 🎥	119.4	119.6	1.6	3.22	2.68	15.3	14.3	4.54	2.21	2.34	4595
d3_55_EQ_Taft_+120mm	ϟ 🎥	118.4	118.7	2.4	3.55	2.80	16.3	15.2	5.18	1.81	1.91	3754
d3_56_EQ_Taft_+60mm	🎥	59.7	60.0	0.6	0.50	0.57	3.7	2.5	1.06	0.48	0.51	1006
d3_57_EQ_Taft_-60mm	ϟ 🎥	60.2	60.3	0.9	1.64	1.34	8.6	7.3	2.94	1.02	1.08	2125

continued on next page

[10] Wall became fully cracked.

Bull Earthquake Eng, DOI: 10.1007/s10518-017-0282-8
SUPPLEMENTARY MATERIAL

Table S.9: (cont'd).

Test Name	Notes	Table and Supports					Wall Response					
		x_{tab} [mm]	$x_{\text{sup.avg}}$ [mm]	$\Delta_{\text{sup.top-tab}}$ [mm]	a_{tab} [g]	$a_{\text{sup.avg}}$ [g]	$\Delta_{\text{w.cent}}$ [mm]	$\Delta_{\text{w.cent0}}$ [mm]	$a_{\text{w.cent}}$ [g]	$a_{\text{w.avg}}$ [g]	q_w [kPa]	F_w [N]
d3_58_H_12Hz_0.1mm	📹	0.4	0.2	0.5	0.10	0.19	2.6	1.5	0.84	0.26	0.27	535
d3_59_H_12Hz_0.2mm	📹	0.5	0.4	0.4	0.16	0.32	3.4	2.4	1.32	0.35	0.37	722
d3_60_H_12Hz_0.4mm	📷 📹	1.4	1.5	0.5	0.92	0.92	7.5	6.5	2.78	0.45	0.48	945
d4_01_R_4mm_200ms		4.2	4.3	0.4	0.18	0.18	0.3	0.2	0.27	0.21	0.22	434
d4_02_R_4mm_100ms		4.5	4.6	0.4	0.33	0.36	0.3	0.2	0.51	0.40	0.42	824
d4_03_R_8mm_100ms		9.2	9.4	1.0	0.95	0.93	0.5	0.4	1.55	1.12	1.18	2319
d4_04_H_13Hz_0.05mm		0.3	0.2	0.4	0.08	0.08	0.2	0.2	0.10	0.08	0.08	160
d4_05_H_13Hz_0.10mm	📹	0.4	0.3	0.5	0.23	0.25	0.2	0.3	0.33	0.25	0.26	515
d4_06_EQ_Taft_-40mm	[11]	40.0	39.9	0.6	0.30	0.32	0.4	0.4	0.45	0.36	0.38	740
d4_07_EQ_Taft_+40mm		40.1	40.3	0.6	0.31	0.32	0.4	0.5	0.51	0.37	0.40	778
d4_08_EQ_Taft_+80mm	⊠, ϟ	79.0	78.2	4.1	2.54	2.22	2.0	2.0	4.46	2.51	2.65	5210
d4_09_EQ_Taft_-80mm	⊠, ϟ	78.4	79.5	4.1	1.96	2.14	3.3	3.0	3.18	2.15	2.28	4466
d4_10_R_4mm_200ms	□	5.4	4.2	2.6	0.17	0.19	0.8	0.3	0.38	0.22	0.23	447
d4_11_R_4mm_100ms	□	5.5	4.5	2.6	0.33	0.30	1.0	0.5	0.59	0.34	0.36	711
d4_12_R_8mm_100ms	□	10.1	9.1	2.8	0.76	0.56	1.4	0.9	1.15	0.66	0.70	1365
d4_13_H_13Hz_0.15mm	□	1.7	0.6	2.6	0.35	0.34	0.9	0.6	0.69	0.43	0.45	885
d4_14_H_13Hz_0.20mm	□ 📹	1.7	0.7	2.6	0.45	0.34	1.2	0.7	0.93	0.48	0.51	1005
d4_15_H_13Hz_0.25mm	□ 📹	1.9	0.8	2.8	0.62	0.50	1.5	0.9	1.35	0.58	0.62	1213
d4_16_H_13Hz_0.30mm	□ 📹	1.9	0.9	2.9	0.67	0.68	1.6	1.1	1.48	0.66	0.70	1376
d4_17_H_13Hz_0.35mm	□ 📹	1.9	1.1	3.4	0.75	1.07	2.2	1.7	1.81	0.99	1.05	2068
d4_18_H_13Hz_0.40mm	⊠ 📹	2.2	1.3	4.1	0.87	1.30	3.0	2.3	2.53	1.33	1.41	2768
d4_19_R_4mm_200ms	□	5.6	4.1	3.2	0.14	0.15	1.4	0.4	0.36	0.17	0.18	350
d4_20_R_4mm_100ms	□	5.9	4.4	3.3	0.35	0.28	1.5	0.6	0.75	0.33	0.35	689
d4_21_R_8mm_100ms	□	10.5	9.2	3.7	0.71	0.60	2.2	1.4	1.60	0.63	0.67	1307
d4_22_H_13Hz_0.45mm	⊠ 📹	2.7	1.8	4.7	0.97	1.32	4.4	3.3	3.00	1.25	1.32	2595
d4_23_H_13Hz_0.50mm	⊠ 📹	3.5	1.9	5.4	1.32	0.83	5.0	3.4	3.34	0.90	0.96	1880
d4_24_R_4mm_200ms	□	2.6	4.2	5.1	0.14	0.15	2.2	0.3	0.32	0.16	0.17	340
d4_25_R_4mm_100ms	□	6.9	4.5	5.1	0.34	0.28	2.7	0.7	0.65	0.29	0.30	598
d4_26_R_8mm_100ms	□	11.5	9.2	5.2	0.87	0.54	3.7	1.8	1.33	0.55	0.58	1145
d4_27_H_6Hz_0.10mm	□	2.8	0.2	5.2	0.04	0.05	2.4	0.3	0.08	0.04	0.04	80
d4_28_H_6Hz_0.20mm	□	2.7	0.3	5.1	0.06	0.08	2.5	0.4	0.18	0.09	0.09	183
d4_29_H_6Hz_0.30mm	□	2.9	0.5	5.1	0.07	0.10	2.5	0.4	0.23	0.11	0.12	232
d4_30_H_6Hz_0.40mm	□	3.1	0.6	5.2	0.09	0.12	2.4	0.4	0.30	0.13	0.13	260
d4_31_H_6Hz_0.50mm	□	3.0	0.6	5.2	0.11	0.14	2.5	0.4	0.29	0.15	0.16	305
d4_32_H_6Hz_0.75mm	□	3.3	1.0	5.2	0.15	0.17	2.4	0.4	0.30	0.17	0.18	349
d4_33_H_6Hz_1.0mm	□	3.7	1.4	5.3	0.26	0.24	2.6	0.4	0.37	0.24	0.25	489
d4_34_H_6Hz_1.5mm	□	4.8	2.3	5.3	0.43	0.45	3.4	1.8	0.82	0.48	0.51	996
d4_35_R_4mm_200ms	□	5.1	4.2	2.0	0.17	0.18	0.9	0.4	0.52	0.20	0.21	408
d4_36_R_4mm_100ms	□	5.3	4.5	2.1	0.35	0.34	1.3	0.6	0.69	0.34	0.37	717
d4_37_R_8mm_100ms	□	9.7	9.0	2.2	0.78	0.68	3.1	2.5	2.29	0.66	0.69	1362
d4_38_H_13Hz_0.10mm	□	1.2	0.3	2.0	0.15	0.14	1.1	0.3	0.26	0.15	0.16	305

continued on next page

[11] These Taft earthquake runs (6–9) were conducted early in the test sequence in order to observe the response of an uncracked wall subjected to an earthquake motion. Previously, earthquake runs were only performed once the wall was fully cracked.

Table S.9: (cont'd).

Test Name	Notes	Table and Supports					Wall Response					
		x_{tab} [mm]	$x_{\text{sup.avg}}$ [mm]	$\Delta_{\text{sup.top-tab}}$ [mm]	a_{tab} [g]	$a_{\text{sup.avg}}$ [g]	$\Delta_{\text{w.cent}}$ [mm]	$\Delta_{\text{w.cent0}}$ [mm]	$a_{\text{w.cent}}$ [g]	$a_{\text{w.avg}}$ [g]	q_w [kPa]	F_w [N]
d4_39_H_13Hz_0.20mm	□	1.3	0.6	2.1	0.36	0.36	1.8	1.2	1.20	0.42	0.45	883
d4_40_H_13Hz_0.30mm	□	1.4	0.7	2.1	0.53	0.48	4.2	3.5	2.33	0.78	0.82	1614
d4_41_H_13Hz_0.40mm	⊠[12]	2.1	1.5	2.3	1.00	1.22	6.4	5.4	3.96	0.92	0.97	1904
d4_42_R_4mm_200ms		5.0	4.2	1.8	0.16	0.17	1.5	0.5	0.28	0.18	0.19	368
d4_43_R_4mm_100ms		5.3	4.5	2.0	0.34	0.35	2.2	1.0	0.72	0.33	0.35	688
d4_44_R_8mm_100ms		9.9	9.2	2.1	0.93	0.82	4.0	3.1	1.75	0.63	0.67	1310
d4_45_EQ_Taft_-10mm		9.2	10.1	2.0	0.06	0.06	1.5	0.3	0.16	0.08	0.09	171
d4_46_EQ_Taft_+10mm		10.6	9.7	1.9	0.07	0.08	1.5	0.3	0.19	0.10	0.10	204
d4_47_EQ_Taft_+20mm		21.2	20.5	2.0	0.16	0.14	1.6	0.5	0.29	0.16	0.17	328
d4_48_EQ_Taft_-20mm		18.6	19.4	1.9	0.12	0.12	1.6	0.4	0.28	0.14	0.15	295
d4_49_EQ_Taft_-30mm		30.7	31.3	1.9	0.19	0.18	1.8	0.6	0.35	0.19	0.20	393
d4_50_EQ_Taft_+30mm		29.3	28.6	2.0	0.22	0.22	1.8	0.6	0.42	0.24	0.25	492
d4_51_EQ_Taft_+40mm		41.1	40.5	2.2	0.30	0.28	2.0	0.9	0.54	0.29	0.31	603
d4_52_EQ_Taft_-40mm		39.5	40.2	2.0	0.27	0.29	1.9	0.8	0.47	0.28	0.30	582
d4_53_EQ_Taft_-50mm		49.5	50.1	2.1	0.39	0.40	2.2	1.2	0.66	0.38	0.40	792
d4_54_EQ_Taft_+50mm		51.2	50.5	2.0	0.38	0.37	2.6	1.4	0.78	0.40	0.43	838
d4_55_EQ_Taft_+60mm		60.5	59.9	2.1	0.49	0.54	2.8	1.7	1.04	0.53	0.56	1104
d4_56_EQ_Taft_-60mm	↯	59.7	60.5	2.6	1.66	1.43	6.5	5.5	2.98	1.24	1.31	2578
d4_57_R_4mm_200ms		5.3	4.3	2.0	0.12	0.13	1.4	0.3	0.22	0.13	0.14	278
d4_58_R_4mm_100ms		5.3	4.5	1.9	0.34	0.34	2.1	1.0	0.71	0.32	0.34	669
d4_59_R_8mm_100ms		9.9	9.1	2.1	0.90	0.78	4.0	3.1	1.74	0.61	0.65	1274
d4_60_EQ_Taft_+60mm	[13]	61.2	60.6	1.9	0.39	0.41	2.3	1.5	0.77	0.40	0.42	823
d4_61_EQ_Taft_-60mm	↯	59.8	60.6	2.2	1.07	1.00	4.3	3.7	1.95	0.92	0.97	1912
d4_62_EQ_Taft_-70mm	↯	69.1	69.8	2.5	1.33	1.18	6.1	4.8	2.73	1.06	1.12	2198
d4_63_EQ_Taft_+70mm	↯	71.6	70.8	2.1	0.93	0.99	4.6	3.4	2.14	0.91	0.96	1890
d4_64_EQ_Taft_+70mm	↯[14]	71.4	70.7	2.0	0.66	0.69	3.6	2.4	1.48	0.67	0.71	1388
d4_65_EQ_Taft_-70mm	↯	69.4	70.1	2.2	0.78	0.77	3.7	2.7	1.47	0.71	0.75	1471
d4_66_R_4mm_200ms	[15]	5.0	4.3	2.0	0.18	0.17	1.8	0.5	0.38	0.17	0.18	355
d4_67_R_4mm_100ms		5.3	4.5	1.9	0.37	0.35	2.3	1.1	0.76	0.32	0.34	667
d4_68_R_8mm_100ms		9.7	9.0	2.1	0.89	0.78	4.1	3.1	1.78	0.61	0.65	1267

continued on next page

[12]Wall became fully cracked.

[13]Tests 60–61 were repeats of tests 55–56 in that both used the same PGD; however, the PID setting of the controller was reduced from 36 dB to 30 dB in the latter tests. This was to investigate whether shaketable impacts [refer Appendix D in *Vaculik* (2012)] could be stopped from occurring by lowering the PID setting. However, whilst this caused the PGA generated to reduce, the impacts still occurred for the +60 mm PGD run as before. The reduced PID setting of 30 dB was also retained in tests 62–63. The influence of the PID is discussed in Appendix D of *Vaculik* (2012).

[14]In tests 64–65, the PID was further reduced to 25 dB, but the impacts still continued to occur, even though there was a reduction in the generated PGA relative to tests 62–63 which were carried out at the same PGD.

[15]In test 66 and onwards, the PID was restored to 36 dB after it was concluded that reducing the PID setting of the controller was an unviable method of limiting the influence of the shaketable impacts.

Bull Earthquake Eng, DOI: 10.1007/s10518-017-0282-8
SUPPLEMENTARY MATERIAL

Table S.9: (cont'd).

Test Name	Notes	Table and Supports					Wall Response					
		x_{tab} [mm]	$x_{\text{sup.avg}}$ [mm]	$\Delta_{\text{sup.top-tab}}$ [mm]	a_{tab} [g]	$a_{\text{sup.avg}}$ [g]	$\Delta_{\text{w.cent}}$ [mm]	$\Delta_{\text{w.cent0}}$ [mm]	$a_{\text{w.cent}}$ [g]	$a_{\text{w.avg}}$ [g]	q_w [kPa]	F_w [N]
d4_69_EQ_Taft_+70mm	ϟ[16]	70.9	70.2	2.0	1.46	1.47	5.8	5.3	2.75	1.25	1.33	2603
d4_70_EQ_Taft_-70mm	ϟ	69.0	69.8	2.9	2.19	1.86	9.5	8.2	4.89	1.54	1.64	3209
d4_71_EQ_Taftbf05_-70mm	ϟ	69.0	69.8	2.9	2.05	1.77	9.4	7.8	4.53	1.44	1.53	2999
d4_72_EQ_Taftbf05_+70mm	ϟ	70.5	69.9	2.0	1.43	1.37	6.3	5.3	2.86	1.23	1.30	2546
d4_73_EQ_Taftbf10_+70mm	ϟ	70.6	69.9	2.2	1.28	1.27	5.9	4.6	2.53	1.10	1.17	2293
d4_74_EQ_Taftbf10_-70mm	ϟ	69.1	69.9	2.8	1.96	1.73	9.6	8.2	4.66	1.39	1.47	2892
d4_75_EQ_Taftbf20_-70mm	ϟ	69.0	69.7	2.8	1.81	1.54	8.5	6.9	3.92	1.29	1.36	2671
d4_76_EQ_Taftbf20_+70mm	ϟ	70.5	69.9	2.0	1.25	1.22	5.6	4.4	2.39	1.08	1.14	2234
d4_77_EQ_Taftbf30_+70mm	ϟ	70.5	69.9	2.2	0.97	1.01	5.0	3.5	2.02	0.88	0.93	1826
d4_78_EQ_Taftbf30_-70mm	ϟ	69.0	69.7	2.7	1.72	1.45	8.3	6.7	3.89	1.23	1.31	2564
d4_79_EQ_Taftbf50_-70mm	ϟ	69.0	69.7	2.5	1.44	1.26	7.1	5.5	3.06	1.07	1.13	2215
d4_80_EQ_Taftbf50_+70mm	ϟ	70.5	69.8	1.9	0.82	0.78	4.3	2.8	1.63	0.73	0.77	1517
d4_81_EQ_Taftbf75_+70mm	ϟ	70.6	69.9	2.0	0.68	0.69	4.0	2.4	1.52	0.63	0.67	1309
d4_82_EQ_Taftbf75_-70mm	ϟ	68.9	69.6	2.5	1.26	1.16	6.5	4.9	2.73	0.96	1.02	2004
d4_83_EQ_Taftbf100_-70mm	ϟ	69.0	69.7	2.3	1.10	1.00	5.8	4.3	2.30	0.85	0.90	1771
d4_84_EQ_Taftbf100_+70mm	ϟ	70.4	69.7	2.0	0.62	0.63	4.4	2.9	1.77	0.60	0.63	1237
d4_85_R_4mm_200ms		5.0	4.1	1.9	0.16	0.16	2.2	0.6	0.35	0.15	0.16	314
d4_86_R_4mm_100ms		5.4	4.6	1.9	0.33	0.31	2.8	1.3	0.69	0.29	0.31	612
d4_87_R_8mm_100ms		9.7	9.0	2.1	0.85	0.73	4.5	3.2	1.80	0.59	0.62	1221
d4_88_H_13Hz_0.2mm		1.3	0.8	2.0	0.52	0.49	4.1	2.6	1.61	0.21	0.23	444
d4_89_H_13Hz_0.4mm		2.1	1.5	2.4	1.00	1.18	6.5	5.3	3.19	0.52	0.55	1079
d4_90_H_13Hz_0.6mm		2.9	2.3	2.8	1.70	1.74	8.9	7.4	4.66	0.65	0.69	1348
d4_91_R_4mm_200ms		5.0	4.2	1.9	0.13	0.15	2.5	0.6	0.36	0.13	0.14	278
d4_92_R_4mm_100ms		5.2	4.5	1.9	0.34	0.34	3.4	1.6	0.74	0.28	0.29	572
d4_93_R_8mm_100ms		9.9	9.1	2.1	0.85	0.68	5.4	3.8	1.98	0.56	0.59	1162
d4_94_EQ_Taft_+70mm	ϟ	70.9	70.3	2.3	1.69	1.64	8.7	7.7	3.49	1.37	1.45	2840
d4_95_EQ_Taft_-70mm	ϟ	69.2	70.0	2.7	2.13	1.70	12.3	10.5	5.01	1.43	1.52	2974
d4_96_EQ_Taft_-80mm	ϟ	78.8	79.6	2.7	1.74	1.59	11.8	9.8	4.66	1.26	1.34	2622
d4_97_EQ_Taft_+80mm	ϟ	80.3	79.7	2.9	2.62	2.25	12.3	11.7	4.82	1.74	1.84	3615
d4_98_EQ_Taft_+90mm	ϟ	90.2	89.5	2.9	2.48	2.49	12.2	12.5	4.56	1.72	1.82	3566
d4_99_EQ_Taft_-90mm	ϟ	88.9	89.7	2.4	1.32	1.13	10.1	8.4	3.67	0.95	1.01	1975
d4_100_EQ_Taft_-100mm	ϟ	98.9	99.7	2.4	1.39	1.27	10.4	8.4	3.51	1.00	1.06	2083
d4_101_EQ_Taft_+100mm	ϟ	100.6	100.1	3.0	2.27	2.03	10.7	11.6	4.07	1.66	1.76	3445
d4_102_EQ_Taft_+110mm	ϟ	109.5	109.0	3.5	3.00	2.50	11.6	13.5	4.74	2.05	2.17	4258
d4_103_EQ_Taft_-110mm	ϟ	107.8	108.5	2.5	2.15	1.97	12.9	11.1	4.98	1.48	1.56	3069
d4_104_EQ_Taft_-120mm	ϟ	118.7	119.7	3.0	3.06	2.64	16.7	14.8	5.56	1.94	2.05	4032
d4_105_EQ_Taft_+120mm	ϟ	119.1	118.6	3.8	3.27	2.77	12.1	14.1	4.36	2.22	2.35	4611
d4_106_R_4mm_200ms		5.1	4.3	1.8	0.13	0.14	2.7	0.8	0.38	0.13	0.14	275
d4_107_R_4mm_100ms		5.3	4.6	1.8	0.34	0.33	3.5	1.8	0.77	0.28	0.29	575

continued on next page

[16] In a further attempt to prevent the shaketable impacts, tests 69–84 trialled alternate versions of the Taft motion. Runs 69–70 used the standard Taft motion as a control reference, whilst runs 71–84 used Taft motions which had been filtered using a binomial filter in the time domain. The period of the filter (number of data points used for weighted averaging) are indicated in the test name. For example, `Taftbf05` means that the binomial filter averaged five adjacent data points in the original motion. Even though the PGA reduced as the severity of filtration was increased, the impacts still continued to occur. Hence, the original Taft motion was restored in subsequent tests.

Table S.9: (cont'd).

Test Name	Notes	Table and Supports					Wall Response					
		x_{tab} [mm]	$x_{\text{sup.avg}}$ [mm]	$\Delta_{\text{sup.top-tab}}$ [mm]	a_{tab} [g]	$a_{\text{sup.avg}}$ [g]	$\Delta_{\text{w.cent}}$ [mm]	$\Delta_{\text{w.cent0}}$ [mm]	$a_{\text{w.cent}}$ [g]	$a_{\text{w.avg}}$ [g]	q_w [kPa]	F_w [N]
d4_108_R_8mm_100ms		10.0	9.3	2.0	0.85	0.72	5.4	3.8	1.87	0.53	0.56	1093
d4_109_H_13Hz_0.1mm		1.1	0.2	1.9	0.10	0.12	2.5	0.6	0.30	0.05	0.05	95
d4_110_H_13Hz_0.2mm		1.4	0.6	1.9	0.39	0.40	3.6	2.0	1.17	0.16	0.17	337
d4_111_H_13Hz_0.3mm		2.0	1.5	2.3	0.97	0.92	6.0	4.1	2.45	0.30	0.32	623
d4_112_H_13Hz_0.4mm		2.2	1.7	2.5	1.22	1.27	7.3	5.9	3.52	0.49	0.52	1018
d4_113_H_13Hz_0.5mm		2.6	2.1	2.7	1.47	1.58	8.6	7.1	3.94	0.65	0.69	1348
d4_114_R_4mm_200ms		5.0	4.2	1.8	0.14	0.15	3.6	0.6	0.44	0.15	0.16	309
d4_115_R_4mm_100ms		5.2	4.6	1.9	0.34	0.34	4.3	1.4	0.77	0.30	0.32	622
d4_116_R_8mm_100ms	📷	9.9	9.2	2.1	0.86	0.72	6.2	3.8	1.68	0.57	0.61	1192
d2_01_R_4mm_200ms		4.4	4.4	0.3	0.12	0.15	0.2	0.2	0.18	0.16	0.17	386
d2_02_R_4mm_100ms		4.6	4.7	0.4	0.23	0.26	0.3	0.2	0.35	0.30	0.31	713
d2_03_R_8mm_100ms		9.6	9.6	0.6	0.55	0.54	0.3	0.3	0.76	0.61	0.65	1474
d2_04_R_4mm_200ms		4.1	4.1	0.3	0.16	0.19	0.2	0.2	0.24	0.21	0.22	494
d2_05_R_4mm_100ms		4.4	4.6	0.4	0.35	0.38	0.3	0.3	0.57	0.45	0.48	1080
d2_06_R_8mm_100ms	☒[17]	9.3	9.7	1.5	1.17	1.48	0.9	0.9	1.96	1.63	1.72	3905
d2_07_H_12Hz_0.05mm	☐	0.3	0.3	0.6	0.06	0.08	0.5	0.3	0.08	0.07	0.07	164
d2_08_H_12Hz_0.1mm	☐	0.5	0.5	0.7	0.27	0.34	0.5	0.4	0.52	0.40	0.42	948
d2_09_H_12Hz_0.2mm	☒	1.3	1.5	1.0	0.96	1.28	0.9	0.7	1.34	1.25	1.33	3007
d2_10_R_4mm_200ms	☐	4.2	4.2	0.3	0.16	0.20	0.4	0.3	0.27	0.22	0.23	527
d2_11_R_4mm_100ms	☐	4.4	4.5	0.5	0.34	0.39	0.5	0.3	0.55	0.44	0.47	1061
d2_12_R_8mm_100ms	☒	9.1	9.5	1.0	0.93	1.21	1.1	0.9	1.27	1.12	1.19	2697
d2_13_H_12Hz_0.25mm	☒	1.3	1.6	1.0	1.02	1.46	1.9	2.1	1.58	1.39	1.47	3339
d2_14_H_12Hz_0.25mm	☒	0.7	0.7	0.7	0.36	0.47	1.6	1.7	0.90	0.55	0.58	1311
d2_15_Z		0.3	0.1	0.4	0.02	0.02	1.3	0.2	0.03	0.01	0.01	28
d2_16_R_4mm_200ms	☐	4.1	4.2	0.7	0.17	0.18	1.3	0.3	0.31	0.22	0.23	521
d2_17_R_4mm_100ms	☐	4.1	4.3	0.5	0.36	0.36	1.4	0.5	0.70	0.46	0.49	1108
d2_18_R_8mm_100ms	☒[18]	8.9	9.3	0.8	0.84	0.68	2.5	1.5	1.92	0.95	1.01	2285
d2_19_Z		0.3	0.2	0.4	0.01	0.02	1.2	0.2	0.03	0.01	0.01	30
d2_20_H_12Hz_0.1mm	☐	0.3	0.3	0.4	0.12	0.15	1.3	0.4	0.22	0.16	0.17	376
d2_21_H_12Hz_0.2mm	☒[19]	0.7	0.8	0.6	0.52	0.51	2.2	1.9	1.30	0.84	0.88	2005
d2_22_Z		0.3	0.2	0.4	0.01	0.02	1.7	0.2	0.03	0.01	0.01	26
d2_23_H_12Hz_0.1mm	☐	0.5	0.3	0.4	0.09	0.13	1.8	0.3	0.25	0.15	0.16	370
d2_24_H_12Hz_0.2mm	☒	0.6	0.7	0.7	0.43	0.57	4.1	2.6	1.96	1.02	1.08	2439
d2_25_R_4mm_200ms	☐	4.4	4.3	0.3	0.16	0.18	2.1	0.5	0.38	0.20	0.21	472
d2_26_R_4mm_100ms	☐	4.4	4.4	0.4	0.33	0.36	2.7	1.2	0.82	0.40	0.42	956
d2_27_R_8mm_100ms	☒	8.7	8.8	0.6	0.87	0.83	4.6	3.3	2.59	0.83	0.88	2003
d2_28_H_12Hz_0.25mm	☒	0.9	1.0	0.6	0.63	0.45	5.1	3.4	1.72	0.60	0.63	1439

continued on next page

[17] Unusually, first cracking occurred during a pulse test. All other walls tested were able to withstand the initial pulse tests without cracking.

[18] After test 18, the vertical edges were restrained using timber members to prevent rocking of the wall away from the returns. The revised arrangement is shown in the main body of the paper (*Vaculik and Griffith*, 2017).

[19] After test 21, the new vertical edge restraint was further stiffened using timber wedges. This setup was retained for the remainder of tests, including the current wall, D2, and the final wall tested, D1.

Bull Earthquake Eng, DOI: 10.1007/s10518-017-0282-8
SUPPLEMENTARY MATERIAL

Table S.9: (cont'd).

Test Name	Notes	Table and Supports					Wall Response					
		x_{tab} [mm]	$x_{sup.avg}$ [mm]	$\Delta_{sup.top-tab}$ [mm]	a_{tab} [g]	$a_{sup.avg}$ [g]	$\Delta_{w.cent}$ [mm]	$\Delta_{w.cent0}$ [mm]	$a_{w.cent}$ [g]	$a_{w.avg}$ [g]	q_w [kPa]	F_w [N]
d2_29_H_12Hz_0.3mm	⊠[20]	1.0	1.1	0.6	0.73	0.54	4.8	3.4	1.45	0.26	0.28	632
d2_30_R_4mm_200ms		4.3	4.4	0.3	0.16	0.19	2.2	0.8	0.37	0.15	0.16	371
d2_31_R_4mm_100ms		4.3	4.5	0.4	0.35	0.39	3.1	1.9	0.74	0.30	0.31	712
d2_32_R_8mm_100ms		9.2	9.4	0.7	1.24	1.19	4.9	3.7	1.54	0.60	0.64	1445
d2_33_EQ_Taft_-20mm		20.3	20.3	0.7	0.16	0.22	2.4	0.9	0.45	0.26	0.28	632
d2_34_EQ_Taft_+20mm		19.9	20.0	0.6	0.17	0.21	2.3	0.9	0.37	0.22	0.23	517
d2_35_EQ_Taft_+40mm		40.2	40.2	0.6	0.39	0.40	3.4	2.1	0.82	0.43	0.45	1021
d2_36_EQ_Taft_-40mm		40.3	40.2	0.7	0.41	0.40	3.4	2.0	0.91	0.46	0.49	1108
d2_37_EQ_Taft_-60mm	ϟ	60.5	60.3	1.0	1.58	1.69	6.0	5.5	2.15	1.19	1.26	2856
d2_38_EQ_Taft_+60mm		59.5	59.4	0.7	0.60	0.65	3.9	3.1	1.04	0.58	0.62	1398
d2_39_EQ_Taft_+80mm	ϟ	79.5	79.6	1.8	3.08	3.06	10.2	8.8	3.83	1.85	1.96	4445
d2_40_EQ_Taft_-80mm	ϟ	79.7	79.3	1.6	2.34	2.85	7.2	8.0	2.96	1.58	1.67	3795
d2_41_EQ_Taft_-100mm	ϟ	99.3	99.1	1.6	1.85	1.85	8.9	7.5	2.08	1.14	1.21	2745
d2_42_EQ_Taft_+100mm	ϟ	99.4	99.6	1.9	2.71	3.72	10.5	11.4	2.98	1.73	1.83	4144
d2_43_R_4mm_200ms		4.3	4.4	0.3	0.16	0.17	2.0	1.2	0.33	0.16	0.17	381
d2_44_R_4mm_100ms		4.5	4.5	0.4	0.36	0.38	2.9	2.0	0.56	0.26	0.28	625
d2_45_R_8mm_100ms		9.3	9.6	0.8	1.31	1.21	5.1	4.5	1.46	0.84	0.89	2010
d2_46_EQ_Taft_+60mm	🎥	59.5	59.6	0.6	0.68	0.72	5.6	4.5	1.04	0.57	0.60	1357
d2_47_EQ_Taft_-60mm	ϟ 🎥	60.4	60.2	0.8	1.55	1.57	6.3	7.4	1.72	0.98	1.03	2340
d2_48_EQ_Taft_-120mm	ϟ 🎥	118.5	118.4	1.8	2.82	2.71	13.4	12.5	2.75	1.70	1.80	4076
d2_49_EQ_Taft_+120mm	ϟ 🎥	117.4	117.5	1.8	3.36	3.28	13.8	15.2	3.34	2.15	2.28	5165
d2_50_R_4mm_200ms		4.3	4.3	0.3	0.16	0.17	2.0	1.3	0.30	0.14	0.14	325
d2_51_R_4mm_100ms		4.5	4.6	0.5	0.39	0.38	2.7	2.2	0.58	0.26	0.28	632
d2_52_R_8mm_100ms		9.4	9.7	0.9	1.46	1.40	5.8	5.3	1.28	0.93	0.99	2242
d2_53_EQ_Synth01_+20mm		19.7	19.8	0.6	0.20	0.23	2.1	1.3	0.32	0.17	0.18	406
d2_54_EQ_Synth01_-20mm		20.2	20.2	0.8	0.20	0.22	1.9	1.5	0.29	0.17	0.18	419
d2_55_EQ_Synth01_-40mm	ϟ	40.1	40.0	0.7	1.23	1.21	5.9	6.6	1.48	0.77	0.81	1839
d2_56_EQ_Synth01_+40mm		39.9	40.0	0.6	0.56	0.54	2.9	2.8	0.56	0.35	0.37	839
d2_57_EQ_Synth01_+60mm	ϟ	59.4	59.5	1.2	2.24	2.30	8.6	9.2	2.14	1.43	1.51	3430
d2_58_EQ_Synth01_-60mm	ϟ	60.1	59.9	1.4	2.21	2.17	9.7	10.9	2.13	1.40	1.48	3364
d2_59_EQ_Synth01_-80mm	ϟ, [21] 📷	79.3	79.0	2.2	3.49	3.86	14.4	15.1	3.77	2.33	2.47	5598
d2_60_R_4mm_200ms		4.3	4.3	0.3	0.16	0.18	3.1	1.4	0.33	0.12	0.13	295
d2_61_R_4mm_100ms		4.5	4.6	0.3	0.37	0.37	3.7	2.4	0.54	0.26	0.27	617
d2_62_R_8mm_100ms	📷	9.3	9.5	0.9	1.41	1.27	5.7	5.9	1.11	0.81	0.86	1955
d1_01_0MPa_R_4mm_200ms	[22]	4.2	4.3	0.5	0.18	0.17	0.2	0.2	0.29	0.21	0.22	495
d1_02_0MPa_R_4mm_100ms		4.2	4.4	0.6	0.38	0.37	0.3	0.2	0.61	0.47	0.50	1127
d1_03_0MPa_R_8mm_100ms		9.2	9.7	1.3	1.23	1.35	0.7	0.7	1.86	1.45	1.54	3482

continued on next page

[20] Wall became fully cracked.

[21] During test 59, the sub-plates forming the mechanism underwent severe sliding along diagonal cracks. They were pushed back together prior to conducting the final free vibration tests 60–62, due to a risk of collapse.

[22] To observe the free vibration response for the same wall at different levels of axial stress, pulse tests were firstly conducted without any precompression in tests 1–3. The precompression was then increased to an intermediate value of 0.05 MPa in tests 4–6 and finally to the full value of 0.10 MPa prior to test 8.

Table S.9: (cont'd).

Test Name	Notes	Table and Supports					Wall Response					
		x_{tab} [mm]	$x_{\text{sup.avg}}$ [mm]	$\Delta_{\text{sup.top-tab}}$ [mm]	a_{tab} [g]	$a_{\text{sup.avg}}$ [g]	$\Delta_{\text{w.cent}}$ [mm]	$\Delta_{\text{w.cent0}}$ [mm]	$a_{\text{w.cent}}$ [g]	$a_{\text{w.avg}}$ [g]	q_w [kPa]	F_w [N]
d1_04_0.05MPa_R_4mm_200ms	[23]	4.4	4.5	0.4	0.20	0.21	0.2	0.2	0.27	0.23	0.24	540
d1_05_0.05MPa_R_4mm_100ms		4.4	4.4	0.5	0.38	0.36	0.2	0.2	0.58	0.43	0.46	1040
d1_06_0.05MPa_R_8mm_100ms		9.0	9.3	0.8	0.88	0.79	0.5	0.5	1.33	0.92	0.97	2204
d1_07_0.10MPa_Z		0.3	0.2	0.4	0.01	0.02	0.2	0.2	0.03	0.01	0.01	27
d1_08_0.10MPa_R_4mm_200ms	[24]	4.5	4.5	0.3	0.18	0.19	0.2	0.2	0.27	0.23	0.24	543
d1_09_0.10MPa_R_4mm_100ms		4.3	4.4	0.4	0.38	0.37	0.2	0.2	0.51	0.41	0.44	989
d1_10_0.10MPa_R_8mm_100ms		9.1	9.3	0.9	0.92	0.87	0.4	0.4	1.38	1.07	1.13	2561
d1_11_H_13Hz_0.25mm		1.5	1.9	1.2	1.69	1.52	0.4	0.4	1.94	1.50	1.59	3595
d1_12_H_13Hz_0.5mm		2.0	2.4	1.4	1.87	1.75	0.7	0.7	2.40	1.91	2.02	4572
d1_13_H_13Hz_0.75mm		2.4	3.0	1.6	2.18	2.12	0.9	0.9	2.97	2.27	2.40	5448
d1_14_H_13Hz_1mm		2.9	3.5	2.1	2.65	2.47	1.4	1.4	3.35	2.53	2.68	6078
d1_15_EQ_Taft_-40mm		40.6	40.7	0.6	0.40	0.41	0.5	0.4	0.70	0.51	0.54	1224
d1_16_EQ_Taft_+40mm		40.3	40.4	0.6	0.42	0.39	0.4	0.4	0.68	0.47	0.50	1137
d1_17_EQ_Taft_+60mm		60.3	60.6	0.8	0.57	0.57	0.5	0.4	0.85	0.67	0.71	1599
d1_18_EQ_Taft_-60mm	ϟ	60.1	60.1	1.4	1.62	1.50	0.6	0.7	2.40	1.69	1.78	4043
d1_19_EQ_Taft_-80mm	⊠, ϟ	80.1	80.2	2.3	2.45	2.24	2.1	1.9	4.60	3.07	3.25	7368
d1_20_EQ_Taft_+80mm	⊠, ϟ	79.7	80.1	2.9	3.13	2.48	2.5	2.3	5.81	3.73	3.95	8957
d1_21_EQ_Taft_+100mm	⊠, ϟ	98.6	98.8	2.7	2.90	2.53	3.4	3.5	5.78	3.64	3.85	8736
d1_22_EQ_Taft_-100mm	⊠, ϟ	99.7	99.5	1.6	1.77	1.59	1.7	1.7	3.38	1.73	1.83	4159
d1_23_EQ_Taft_-120mm	⊠, ϟ	118.5	118.6	2.8	3.55	2.96	5.9	5.9	6.40	2.85	3.02	6839
d1_24_EQ_Taft_+120mm	⊠, ϟ 📷	119.3	119.8	2.7	3.65	3.15	7.9	7.7	6.15	2.82	2.98	6760
d1_25_R_4mm_200ms	□	4.3	4.4	0.5	0.20	0.20	0.6	0.3	0.37	0.23	0.24	540
d1_26_R_4mm_100ms	□	4.3	4.4	0.5	0.38	0.38	0.7	0.4	0.70	0.44	0.46	1044
d1_27_R_8mm_100ms	□	8.8	9.2	0.8	0.88	0.80	1.3	1.0	1.78	0.88	0.94	2123
d1_28_H_13Hz_0.1mm	□	0.5	0.2	0.5	0.04	0.05	0.5	0.3	0.06	0.04	0.05	105
d1_29_H_13Hz_0.2mm	□	0.6	0.4	0.5	0.27	0.25	0.5	0.2	0.35	0.26	0.27	619
d1_30_H_13Hz_0.4mm	⊠[25]	1.5	2.0	1.5	1.64	1.29	8.5	8.2	5.39	2.16	2.29	5188
d1_31_R_4mm_200ms		4.3	4.5	0.7	0.18	0.18	1.1	0.3	0.47	0.26	0.28	634
d1_32_R_4mm_100ms		4.3	4.4	0.5	0.38	0.39	1.3	0.5	0.82	0.43	0.46	1040
d1_33_R_8mm_100ms		8.8	9.1	0.9	0.86	0.80	2.5	1.7	1.90	0.88	0.93	2103
d1_34_EQ_Taft_+40mm		40.3	40.5	0.7	0.47	0.45	1.4	0.6	0.89	0.49	0.52	1173
d1_35_EQ_Taft_-40mm		40.3	40.3	0.7	0.44	0.45	1.3	0.6	0.91	0.44	0.47	1058
d1_36_EQ_Taft_-60mm	ϟ	60.5	60.5	1.2	1.64	1.57	4.3	3.5	3.33	1.42	1.51	3415
d1_37_EQ_Taft_+60mm		59.7	59.8	1.0	0.76	0.78	2.0	1.2	1.58	0.83	0.88	2002
d1_38_EQ_Taft_+80mm	ϟ	79.3	79.7	2.6	3.13	2.54	12.8	12.0	6.19	2.14	2.27	5146
d1_39_EQ_Taft_-80mm	ϟ	79.5	79.3	1.7	2.56	2.76	9.9	8.8	5.82	1.84	1.95	4421
d1_40_EQ_Taft_-100mm	ϟ	99.4	99.1	1.8	1.88	1.73	6.0	5.5	4.14	1.64	1.74	3935
d1_41_EQ_Taft_+100mm	ϟ	99.5	100.1	2.2	2.86	2.67	14.0	13.1	6.35	2.08	2.20	4988
d1_42_R_4mm_200ms		4.3	4.6	0.5	0.20	0.20	1.5	0.3	0.57	0.28	0.30	672
d1_43_R_4mm_100ms		4.1	4.3	0.6	0.38	0.38	1.6	0.6	0.84	0.42	0.45	1013

continued on next page

[23] Wall was subjected to 0.05 MPa precompression.
[24] The wall was subjected to the full precompression of 0.10 MPa in test 8 and onwards.
[25] Wall became fully cracked.

Bull Earthquake Eng. DOI: 10.1007/s10518-017-0282-8
SUPPLEMENTARY MATERIAL

Table S.9: (cont'd).

Test Name	Notes	Table and Supports					Wall Response					
		x_{tab} [mm]	$x_{\text{sup.avg}}$ [mm]	$\Delta_{\text{sup.top-tab}}$ [mm]	a_{tab} [g]	$a_{\text{sup.avg}}$ [g]	$\Delta_{\text{w.cent}}$ [mm]	$\Delta_{\text{w.cent0}}$ [mm]	$a_{\text{w.cent}}$ [g]	$a_{\text{w.avg}}$ [g]	q_w [kPa]	F_w [N]
d1_44_R_8mm_100ms		9.0	9.0	0.9	0.92	0.83	3.0	2.0	1.86	0.84	0.89	2015
d1_45_EQ_Taft_+120mm	ϟ	117.5	117.6	2.4	3.57	2.96	11.2	10.1	5.34	2.36	2.50	5674
d1_46_EQ_Taft_-120mm	ϟ[26]	119.2	119.1	2.9	3.61	3.00	12.6	11.5	5.53	2.50	2.65	5997
d1_47_R_4mm_200ms		4.3	4.5	0.5	0.20	0.20	1.7	0.3	0.56	0.26	0.28	631
d1_48_R_4mm_100ms		4.1	4.3	0.5	0.38	0.38	1.9	0.6	0.87	0.42	0.44	1006
d1_49_R_8mm_100ms	📷	8.7	9.0	0.9	0.89	0.83	3.3	1.9	1.91	0.92	0.97	2200
d1_50_H_12Hz_0.1mm		0.5	0.3	0.7	0.05	0.06	1.4	0.3	0.11	0.06	0.06	144
d1_51_H_12Hz_0.2mm		1.5	1.6	1.6	1.17	1.02	7.3	6.1	3.36	1.63	1.73	3912
d1_52_R_4mm_200ms	[27]	4.3	4.4	0.8	0.21	0.23	1.4	0.2	0.48	0.25	0.26	592
d1_53_R_4mm_100ms		4.2	4.3	0.7	0.39	0.38	1.6	0.4	0.74	0.43	0.46	1034
d1_54_R_8mm_100ms		8.7	9.1	1.1	0.92	0.84	2.7	1.6	1.86	0.88	0.93	2111
d1_55_Z		0.3	0.2	0.7	0.02	0.02	1.2	0.2	0.02	0.01	0.01	26
d1_56_EQ_Synth01_+20mm		19.8	20.0	0.8	0.25	0.24	1.5	0.4	0.64	0.34	0.36	820
d1_57_EQ_Synth01_-20mm		20.4	20.3	0.8	0.21	0.23	1.4	0.4	0.41	0.29	0.30	688
d1_58_EQ_Synth01_-40mm	ϟ	40.2	40.1	1.0	1.17	1.11	3.0	2.3	2.28	1.12	1.18	2675
d1_59_EQ_Synth01_+40mm		40.0	40.0	0.9	0.50	0.51	1.6	0.6	0.95	0.55	0.58	1311
d1_60_EQ_Synth01_+60mm	ϟ	59.1	59.2	1.8	2.50	2.07	9.0	8.0	4.48	1.75	1.85	4190
d1_61_EQ_Synth01_-60mm	ϟ	60.3	60.3	1.6	2.12	1.81	7.8	7.0	3.83	1.58	1.68	3800
d1_62_EQ_Synth01_-80mm	ϟ	79.1	78.7	3.2	4.28	3.51	14.1	13.3	6.19	2.48	2.62	5945
d1_63_EQ_Synth01_+80mm	ϟ	79.6	80.1	2.9	3.92	3.55	12.1	11.3	5.60	2.35	2.49	5633
d1_64_R_4mm_200ms		4.2	4.5	0.6	0.21	0.20	1.1	0.4	0.56	0.27	0.28	639
d1_65_R_4mm_100ms		4.2	4.3	0.7	0.37	0.39	1.4	0.6	0.92	0.41	0.44	988
d1_66_R_8mm_100ms		8.6	9.1	0.9	0.91	0.84	2.8	2.0	1.92	0.88	0.94	2121
d1_67_EQ_Synth03_-20mm		20.4	20.3	0.7	0.26	0.29	1.1	0.4	0.55	0.34	0.35	805
d1_68_EQ_Synth03_+20mm		20.1	20.2	0.8	0.28	0.32	1.2	0.4	0.56	0.34	0.36	805
d1_69_EQ_Synth03_+40mm		40.2	40.3	0.9	0.45	0.51	1.4	0.7	0.98	0.60	0.64	1451
d1_70_EQ_Synth03_-40mm		40.5	40.4	1.0	0.40	0.44	1.5	0.8	1.00	0.57	0.60	1371
d1_71_EQ_Synth03_-60mm	ϟ	60.5	60.3	0.9	1.06	1.02	2.5	1.7	1.89	0.89	0.95	2142
d1_72_EQ_Synth03_+60mm		59.7	59.9	0.9	0.84	0.82	1.9	1.5	1.56	0.80	0.85	1923
d1_73_EQ_Synth03_+80mm	ϟ	79.6	79.9	2.5	2.75	2.34	9.3	8.6	4.52	1.99	2.10	4768
d1_74_EQ_Synth03_-80mm	ϟ	80.0	80.0	1.7	2.72	2.49	9.6	8.8	4.69	1.91	2.03	4593
d1_75_EQ_Synth03_-100mm	ϟ	99.9	99.5	2.4	3.47	2.90	11.2	10.5	5.51	2.15	2.28	5168
d1_76_EQ_Synth03_+100mm	ϟ	99.9	100.5	2.7	3.48	2.88	13.3	12.5	5.23	2.26	2.39	5421
d1_77_R_4mm_200ms		4.2	4.5	0.7	0.19	0.18	1.2	0.3	0.52	0.24	0.25	576
d1_78_R_4mm_100ms		4.1	4.3	0.6	0.38	0.39	1.5	0.6	0.88	0.41	0.43	977
d1_79_R_8mm_100ms		8.6	8.9	1.0	0.89	0.82	3.2	2.2	1.88	0.86	0.91	2063
d1_80_EQ_Synth05_-20mm		20.6	20.6	0.9	0.49	0.52	1.8	1.3	1.27	0.67	0.71	1601
d1_81_EQ_Synth05_+20mm		20.2	20.4	0.9	0.43	0.49	2.1	1.3	1.22	0.64	0.68	1536
d1_82_EQ_Synth05_+40mm	ϟ	41.0	41.4	1.3	1.18	1.17	4.0	3.2	2.46	1.18	1.25	2836
d1_83_EQ_Synth05_-40mm	ϟ	40.4	40.4	1.3	1.86	1.65	5.8	4.9	3.07	1.52	1.61	3640

continued on next page

[26] Severe sliding became evident along diagonal cracks between sub-plates of the mechanism after test 46. This state was left unaltered during tests 47–51, after which the wall was repaired.

[27] The wall was repaired by pushing the sub-plates back together prior to test 52.

Table S.9: (cont'd).

Test Name	Notes	Table and Supports					Wall Response					
		x_{tab} [mm]	$x_{\text{sup.avg}}$ [mm]	$\Delta_{\text{sup.top-tab}}$ [mm]	a_{tab} [g]	$a_{\text{sup.avg}}$ [g]	$\Delta_{\text{w.cent}}$ [mm]	$\Delta_{\text{w.cent0}}$ [mm]	$a_{\text{w.cent}}$ [g]	$a_{\text{w.avg}}$ [g]	q_w [kPa]	F_w [N]
d1_84_EQ_Synth05_-60mm	ϟ	60.5	61.0	2.3	3.65	3.37	12.8	12.0	5.85	2.27	2.40	5435
d1_85_EQ_Synth05_+60mm	ϟ	60.8	61.4	2.4	3.47	3.69	12.1	12.0	5.91	2.20	2.33	5281
d1_86_R_4mm_200ms		4.2	4.5	0.6	0.22	0.22	1.3	0.4	0.51	0.23	0.24	548
d1_87_R_4mm_100ms		4.1	4.3	0.7	0.36	0.36	1.6	0.7	0.86	0.38	0.40	917
d1_88_R_8mm_100ms		8.6	9.0	1.1	0.87	0.81	3.4	2.4	1.94	0.89	0.94	2134
d1_89_0MPa_R_4mm_200ms	[28]	4.1	4.3	0.8	0.17	0.17	3.8	1.9	0.42	0.19	0.21	467
d1_90_0MPa_R_4mm_100ms		4.1	4.5	0.7	0.39	0.37	5.3	3.3	0.70	0.26	0.27	615
d1_91_0MPa_R_8mm_100ms	📷	9.1	9.7	1.3	1.58	1.57	10.3	7.9	1.76	0.79	0.84	1900

[28] Vertical precompression was removed from the wall and a final pulse test was conducted in runs 89–91.

Bull Earthquake Eng, DOI: 10.1007/s10518-017-0282-8
SUPPLEMENTARY MATERIAL

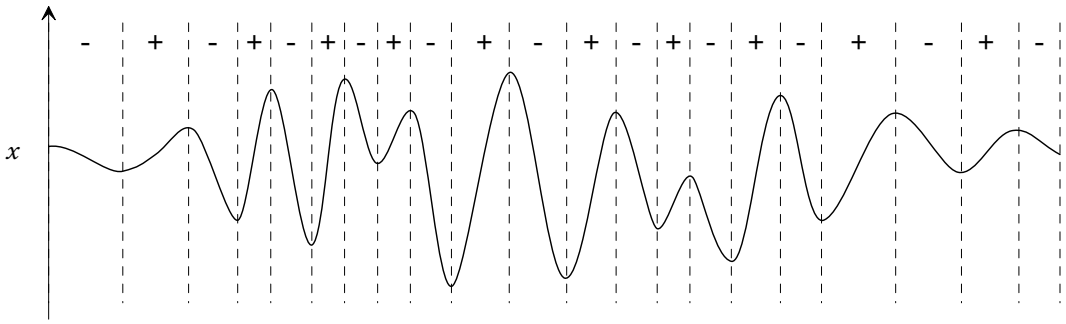

Figure S.17: Division of a generic waveform into segments for the purpose of isolating individual cycles. The segments correspond to regions of alternating positive and negative directions of movement, as indicated by the + and − signs.

S.5 Cyclic Response Analysis

This section describes an analysis procedure that was developed for the purpose of processing the wall's force-displacement data (obtained by methods outlined in Section S.4) to quantify key response parameters such as the effective stiffness, equivalent viscous damping and response period. A significant aspect of the procedure is its applicability to all types of tests performed, regardless of whether the input motion was periodic (i.e. harmonic sinusoidal motion tests) or non-periodic (i.e. pulse and earthquake motion tests).

The basis of the analysis was to firstly employ a time-domain search algorithm to find and isolate individual cycles in the wall's displacement response in a particular test run. This process is described in Section S.5.1. For every valid cycle identified, the properties of interest were then calculated using the process described in Section S.5.2. Average values of each property were then determined by grouping cycles within a specific range of displacement (including cycles close to the maximum response, and cycles at small displacements). Examples of the computer program output are shown in Section S.5.3. Detailed results of the analysis are presented in Section S.5.4.

Note that prior to implementing these processes, the data were filtered (using the techniques described in Section S.6).

S.5.1 Cycle Isolation Algorithm

The objective of the cycle isolation algorithm is to find individual cycles in the waveform of a generic time-domain vector variable, which in the upcoming descriptions is denoted using the arbitrary symbol $\boldsymbol{x}$. In implementing this procedure to the test data, the wall's initially zeroed central displacement ($\Delta_{\text{w.cent0}}$) was used for this purpose.

S.5.1.1 Step 1: Division of the Waveform into Segments

The first step in the procedure is to identify points in the waveform $\boldsymbol{x}$ corresponding to reversals of direction. These points are referred to as 'vertices'. The regions between vertices are referred to as 'segments'. This process is illustrated by Figure S.17, which shows that neighbouring segments always alternate between ascending and descending.

As shown by Figure S.18, a segment (denoted by the index i) is considered ascending if the values at its vertices, x_i and x_{i+1}, are such that $x_i < x_{i+1}$, or descending if $x_i > x_{i+1}$. The cycle amplitude

(a) Ascending segment ($x_i < x_{i+1}$). (b) Descending segment ($x_i > x_{i+1}$).

Figure S.18: Definition of segment direction and amplitude.

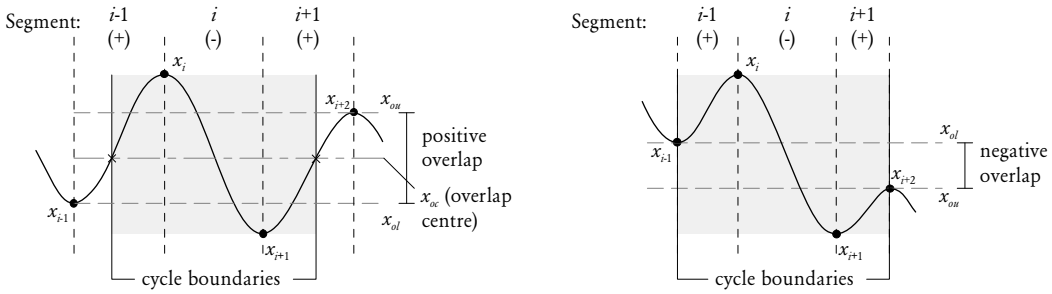

(a) Closed cycle. (b) Open cycle.

Figure S.19: Definition of closed and open cycles, and their boundaries. Shown for the case of a descending middle segment. Any segment i together with its two neighbouring segments $i-1$ and $i+1$ can be classified as one of these cycle types. Closed cycles have overlap across the $i-1$ and $i+1$ segments, whilst open cycles do not. For closed cycles the boundaries are taken at the central value of the overlapping region in the outside segments, whilst for open cycles the boundaries are taken at the exterior limits of the outside segments.

of a segment (x_{amp}) is taken as half of the absolute difference between its two vertices:

$$x_{\text{amp}} = 0.5\,|x_{i+1} - x_i|\,. \tag{S.13}$$

The remaining steps 2–4 were performed on every segment in the waveform, with the exception of the first and last segments.

S.5.1.2 Step 2: Classification of Cycle as Either Open or Closed

Once the waveform $\boldsymbol{x}$ has been divided into segments, it becomes possible for any segment (denoted by the index i) together with its two neighbouring segments (denoted by the indices $i-1$ and $i+1$) to be classified as either a closed or open cycle. As illustrated by Figure S.19, the type of cycle formed depends on whether there is any overlap between the outer segments $i-1$ and $i+1$. A *closed cycle* is defined as having an overlapping region, whilst an *open cycle* is defined as having no overlap (or negative overlap).

To quantify the amount of overlap, the upper and lower bounds of the overlapping region are determined. The overlap upper bound is calculated as

$$x_{ou} = \begin{cases} \min(x_i, x_{i+2})\,, & \text{if segment } i \text{ is descending } (x_i > x_{i+1}); \\ \min(x_{i-1}, x_{i+1})\,, & \text{if segment } i \text{ is ascending } (x_i < x_{i+1}). \end{cases}$$

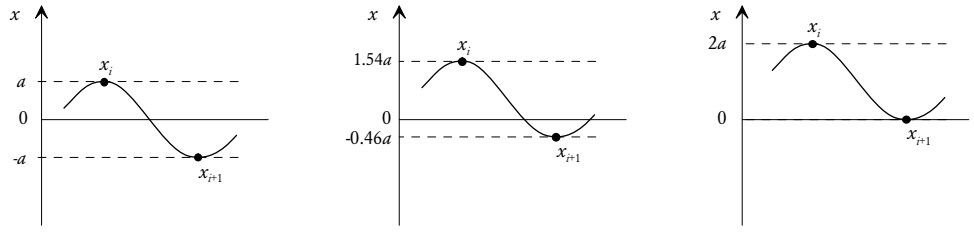

(a) $R_C = 1$. (b) $R_C = 0.3$. (c) $R_C = 0$.

Figure S.20: Demonstration of the cycle centrality parameter R_C. The cycle amplitude is denoted as a.

The overlap lower bound is calculated as

$$x_{ol} = \begin{cases} \max(x_{i-1}, x_{i+1}), & \text{if segment } i \text{ is descending } (x_i > x_{i+1}); \\ \max(x_i, x_{i+2}), & \text{if segment } i \text{ is ascending } (x_i < x_{i+1}). \end{cases}$$

The total overlap x_o is then taken as the difference:

$$x_o = x_{ou} - x_{ol}. \tag{S.14}$$

It is possible for the resulting value of x_o to be either positive or negative. This leads to the definition of closed and open cycles, such that if $x_o \geq 0$, then the cycle is classified as closed, and conversely if $x_o < 0$, then it is classified as open. It is worth noting that closed cycles were found to be far more common that open cycles in the test data analysed.

S.5.1.3 Step 3: Omission of Invalid Cycles

Cycles which failed to meet minimum centrality and minimum overlap criteria were excluded from subsequent calculation of hysteretic properties (refer to Section S.5.2). These selection conditions will now be briefly discussed.

Minimum Centrality Condition The first requirement for a cycle to be considered valid was to be sufficiently centred about $x = 0$ (i.e. zero displacement). This condition was implemented to ensure that the cycle was not biased toward a particular displacement direction. It also served to eliminate cycles which could potentially be in the 'plastic' range of the force-displacement response, as such cycles were likely to have unrealistically low effective stiffness. It was also noticed that non-centred cycles had a tendency to exhibit unrealistically large fluctuation in their equivalent viscous damping ratio.

The degree of centrality for a cycle was quantified using the parameter R_C, calculated as

$$R_C = \begin{cases} -x_i/x_{i+1}, & \text{if } |x_i| \leq |x_{i+1}|; \\ -x_{i+1}/x_i, & \text{if } |x_i| > |x_{i+1}|. \end{cases} \tag{S.15}$$

It is possible for R_C to range between the limits $-1 < R_C \leq 1$, with several cases shown in Figure S.20. A perfectly centred cycle, in which the values at the two vertices are equal and opposite, results in $R_C = 1$. A positive value of R_C corresponds to a cycle that crosses the line $x = 0$, whilst a negative value corresponds to a cycle that does not. A value of $R_C = 0$ results when one of the vertices touches the line $x = 0$. In analysing the wall test data, a minimum centrality condition of $R_C > 0.3$ was enforced for admissible cycles, which is illustrated by Figure S.20b.

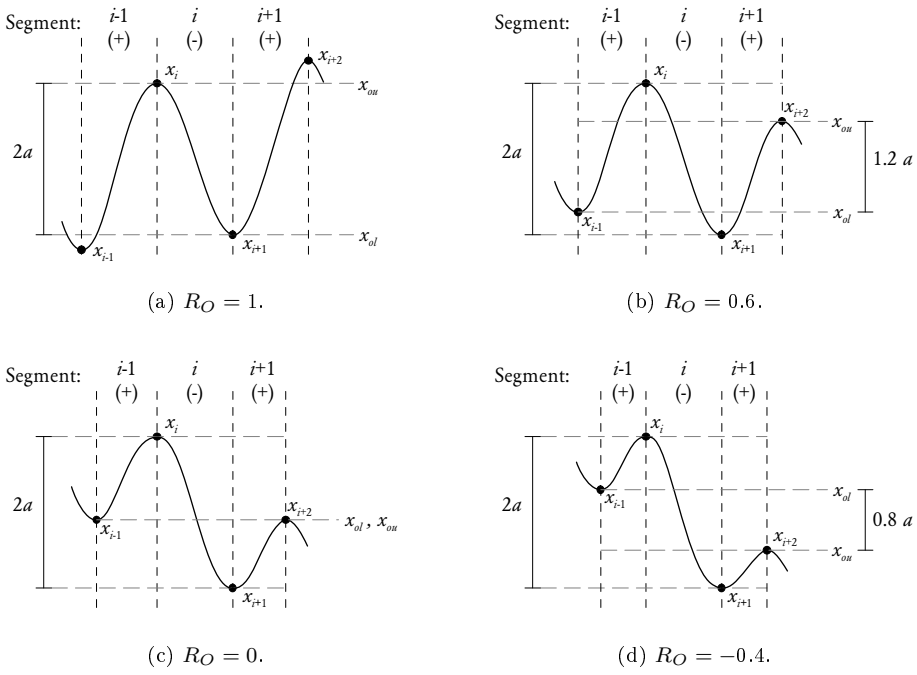

(a) $R_O = 1$. (b) $R_O = 0.6$.

(c) $R_O = 0$. (d) $R_O = -0.4$.

Figure S.21: Demonstration of the cycle overlap parameter R_O. The cycle amplitude is denoted as a.

Minimum Overlap Condition The second requirement for a cycle to be considered valid was to be 'sufficiently closed'. This required the cycle's outer segments (with indices $i-1$ and $i+1$, as shown by Figure S.19) to have sufficient overlap. The reason for implementing this condition was that closed cycles were deemed to be more likely to yield a representative value of the wall's equivalent viscous damping calculated based on the area enclosed within the hysteresis loop.

The degree of overlap was quantified using the parameter R_O, calculated as

$$R_O = \frac{x_o}{2\,x_{\text{amp}}}, \tag{S.16}$$

where x_o is the length of the overlap given by Eq. (S.14) and x_{amp} is the cycle amplitude given by Eq. (S.13). It is possible for R_O to range between the limits $-1 < R_O \leq 1$, with several different cases shown in Figure S.21. In processing the test data, the condition $R_O > -0.4$ was enforced for cycles to be admissible. The limiting case is illustrated by Figure S.21d.

S.5.1.4 Step 4: Definition of Cycle Boundaries and Extraction of Data

Once a cycle was declared valid by satisfying the conditions outlined in step 3, its load and displacement data were extracted from the full data. In order to do this however it was first necessary to define the cycle's boundaries in the time domain (i.e. its first and last data points). The method used to define these boundaries was dependent on whether the cycle was closed or open.

The approach used for closed cycles was to firstly calculate the central overlap value x_{oc} as the average of the upper and lower bounds of the overlap:

$$x_{oc} = 0.5\,(x_{ou} + x_{ol})\,. \tag{S.17}$$

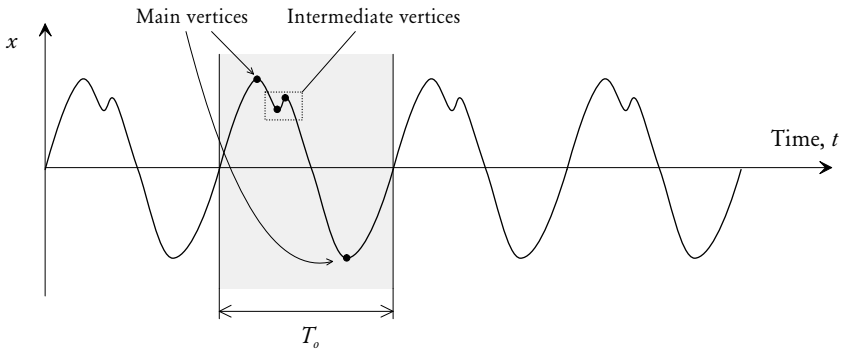

Figure S.22: Example of scenario where the cycle detection algorithm fails to detect the main response cycles in the waveform.

The points defining the cycle's boundaries were then taken at the intersections of the waveform with the value x_{oc} inside the outer segments, as shown by Figure S.19a. As these boundaries did not generally coincide with discrete data points, values at the boundary points were were determined by interpolation.

For open cycles, the cycle boundaries were simply taken at the ends of the outer segments, as shown by Figure S.19b.

Once the cycle's boundaries were defined, its displacement and acceleration data vectors ($\Delta_{\text{w.cent0}}$, $a_{\text{w.cent}}$ and $a_{\text{w.avg}}$) were extracted for subsequent calculation of key cyclic properties as described in Section S.5.2.

S.5.1.5 Remarks

Although the cycle isolation algorithm described is fairly versatile in that it can be applied to data regardless of whether the input motion is periodic or non-periodic, a degree of care has to be exercised in its application. For instance, there are certain scenarios where the algorithm will fail to isolate 'true' cycles in the wall's response. Such an example is illustrated by the hypothetical case in Figure S.22, which shows the displacement response during a harmonic excitation test at the excitation period T_o in the presence of higher frequency interference. While the dominant component of the response occurs at the period T_o, presence of higher frequency interference can cause additional minor peaks and troughs in the resulting waveform as shown. Even though it is obvious that the cycles of interest are those responding at the excitation period, the algorithm fails to detect them due to the presence of the intermediate vertices. Such behaviour was observed in a small number of harmonic tests which contained high frequency interference thought to be either due to higher vibrational modes in the wall's response or vibration of the restraint frame. The problem was overcome by firstly filtering the recorded data in the frequency domain to eliminate the contributions from the higher order harmonics which removed the intermediate vertices. The filters used are described in Section S.6.

S.5.2 Evaluation of Key Cyclic Properties

S.5.2.1 Calculation of Properties from Each Cycle

For each valid cycle isolated using the procedure described in Section S.5.1, several key properties were calculated from its displacement and acceleration data (Figure S.23), including: displacement

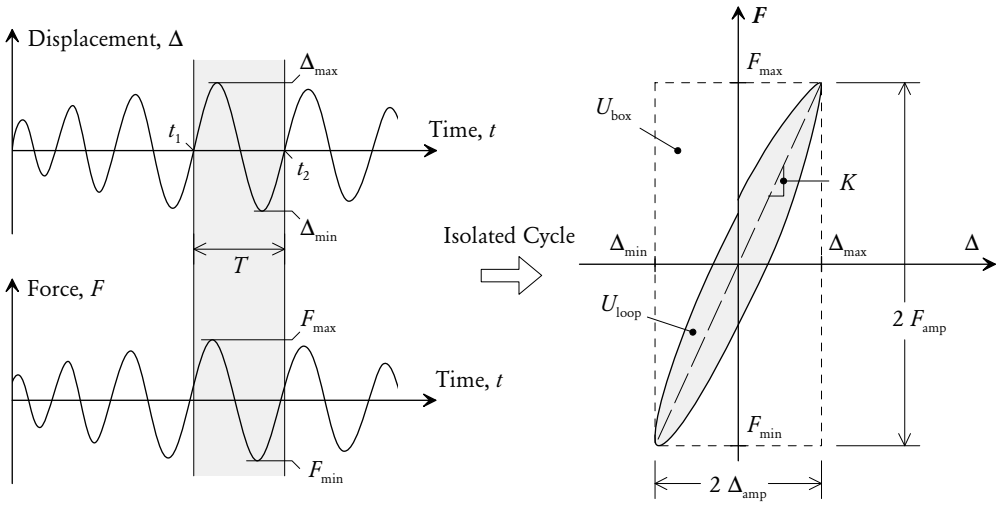

Figure S.23: Isolated hysteresis loop and the properties derived.

and force amplitudes, effective stiffness, equivalent viscous damping, and period. The methods used to calculate these properties will now be described.

Displacement Cycle Amplitude Since the displacement response of a cycle was not necessarily symmetrical about zero displacement ($\Delta = 0$), the displacement amplitude Δ_{amp} was taken as

$$\Delta_{\text{amp}} = \frac{\Delta_{\max} - \Delta_{\min}}{2}, \tag{S.18}$$

where $\Delta_{\max}$ and $\Delta_{\min}$ are the maximum and minimum displacements excursions in the loop.

Force or Acceleration Cycle Amplitude Due to the direct proportionality between the wall's restoring force F_w and its average acceleration $a_{\text{w.avg}}$ [through Eq. (S.11)], these variables are effectively interchangeable (with the relevant proportionality factors). The acceleration amplitude a_{amp} was taken as

$$a_{\text{amp}} = \frac{a_{\max} - a_{\min}}{2}, \tag{S.19}$$

where $a_{\max}$ and $a_{\min}$ are the maximum and minimum accelerations excursions. Similarly, for force:

$$F_{\text{amp}} = \frac{F_{\max} - F_{\min}}{2}. \tag{S.20}$$

Effective Stiffness Two alternative methods were used to calculate the effective secant stiffness, K: In the first method, the stiffness was determined by fitting a linear regression to the individual F-Δ data points. In the second method, the stiffness was calculated as the slope of the line passing through the corner points of the loop's bounding box, as shown by Figure S.23, which is equivalent to

$$K = \frac{F_{\text{amp}}}{\Delta_{\text{amp}}}. \tag{S.21}$$

It was found that both methods produced very similar values; therefore, the second approach [based on Eq. (S.21)] was adopted, since it is less computationally intensive.

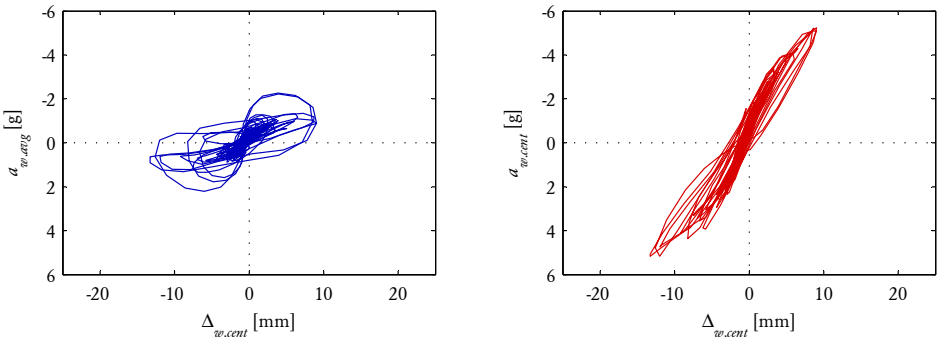

(a) Earthquake test run `d1_76_EQ_Synth03_+100mm`.

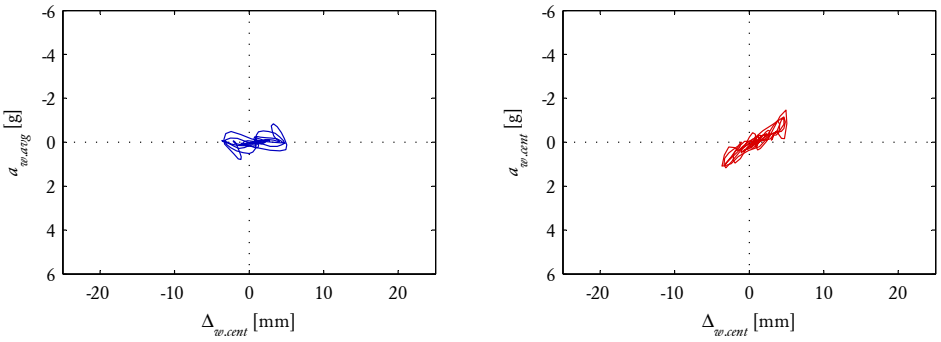

(b) Pulse test run `d2_45_R_8mm_100ms`.

Figure S.24: Typical examples demonstrating the difference between hysteresis loops based on the average wall acceleration, $a_{\mathrm{w.avg}}$ (left) and the central wall acceleration, $a_{\mathrm{w.cent}}$ (right).

Equivalent Viscous Damping The equivalent viscous damping ξ_{hyst} was calculated using the area-based method, according to the equation

$$\xi_{\mathrm{hyst}} = \frac{2}{\pi}\frac{U_{\mathrm{loop}}}{U_{\mathrm{box}}}, \tag{S.22}$$

where U_{loop} is area enclosed within the hysteresis loop, and U_{box} is the area inside the loop's bounding box. From Figure S.23 it can be seen that

$$U_{\mathrm{box}} = 4\,F_{\mathrm{amp}}\,\Delta_{\mathrm{amp}}. \tag{S.23}$$

The energy U_{loop} dissipated during a cycle is evaluated by the integral

$$U_{\mathrm{loop}} = \int_{t=t_1}^{t_2} F\,\mathrm{d}\Delta, \tag{S.24}$$

in which t_1 is the time at the start of the cycle and t_2 the time at the end of the cycle. This integral was evaluated numerically using the Δ and F vectors for the cycle.

The computed values of ξ_{hyst} are reported in Section S.5.4. It should be noted that the reported damping values are based on energies U_{loop} and U_{box} determined from the wall's central acceleration ($a_{\mathrm{w.cent}}$) instead of its average acceleration ($a_{\mathrm{w.avg}}$). Comparison of typical hysteresis loop shapes obtained using these alternate approaches is shown by Figure S.24. The reason for selecting $a_{\mathrm{w.cent}}$ is that it is thought to have more accurately represented the wall's fundamental flexural mode of vibration, which is evidenced by the 'clean' shape of the hysteresis loops. By contrast, $a_{\mathrm{w.avg}}$, which was calculated as a weighted average of the 10 accelerometers mounted on the wall [as per

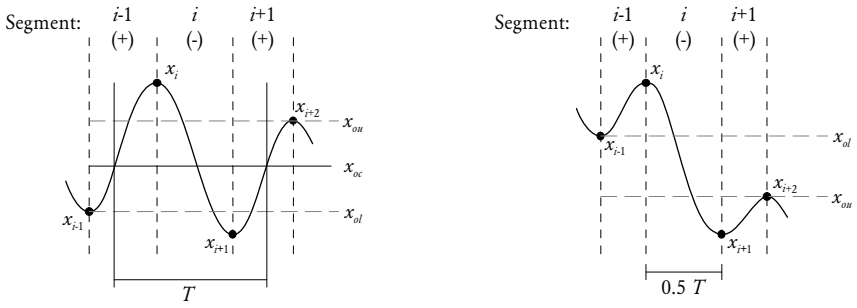

(a) Closed cycle. (b) Open cycle.

Figure S.25: Method used for estimating the cycle period T in closed and open cycles.

Eq. (S.8)], is thought to have received interference from higher vibrational modes (possibly twisting of the specimens), resulting in distortion of the apparent phase relationship between F and Δ and ultimately producing fatter and more ragged loops. Furthermore, damping values (ξ_{hyst}) calculated using $a_{\text{w.avg}}$ generally ranged between 0.15 and 0.4 and were thought to be uncharacteristically high (unconservative).

Period and Frequency As shown by Figure S.25, the method used to evaluate the period T of the cycle depended on whether the cycle was closed or open.[29] For closed cycles, the period was taken as the duration between the start and end boundaries (Figure S.25a). These boundary points were determined using the procedure described in Section S.5.1, as illustrated by Figure S.19a. For open cycles, the period was taken as twice the duration between the cycle's peak and trough vertices (Figure S.25b).

S.5.2.2 Calculation of Average Values in Each Test Run

Once the aforementioned properties were calculated for all valid cycles within a test run, their average values were computed over two ranges of displacement response:

Short Displacement Range This range was intended to capture response along the initial loading branch of the force-displacement curve and included any cycles whose displacement amplitude was inside the range 0.5 mm $\leq \Delta_{\text{amp}} \leq$ 3 mm. To ensure a good spread of response, average values were only calculated for runs in which the maximum displacement amplitude exceeded 95% of the upper limit value of 3 mm (i.e. $\max \Delta_{\text{amp}} > 2.85$ mm). For this range, 'average' values of the effective stiffness K, equivalent viscous damping ξ_{hyst} and period T, were calculated as the interquartile mean to reduce the influence of outlying values due to noise.

Peak Response Range This range was intended to capture the behaviour near the maximum displacement response in the test run, and included all cycles whose displacement amplitude was at least 70% of maximum value. Average values of properties within this range were calculated as the direct mean.

[29] Initial attempts to quantify the walls' vibration frequency were made using Fourier-based (FFT) processing of the displacement and acceleration response. However, this strategy was ultimately abandoned due to the discovery of interference from additional higher frequency signals in the response thought to be due to some aspect of the test arrangement such as the wall restraint frame and the shaketable rig itself.

S.5.3 Examples

The overall data processing routine described was implemented in MATLAB. Examples of typical graphical output are provided by Figures S.26, S.27 and S.28 for a pulse test, harmonic test and earthquake motion test, respectively.

S.5.4 Results

Results of the cyclic analysis are presented in Table S.10 for each individual test run. The corresponding hysteresis curves are provided in Section S.7.

Column 1 of the table provides the test run name. Column 2 describes the frequency filter used to clean the data (refer to Section S.6). In the case of pulse and earthquake motion tests the column gives the cutoff frequency (f_c) of the applied lowpass filter (Butterworth filter with order $n = 10$). A value of 'default' refers to the filter for harmonic tests, which was a Butterworth comb filter passing the first three harmonics of the excitation frequency with a normalised bandwidth of 0.2 (refer to Section S.6.1). Columns 3–5 provide peak amplitudes of the respective properties occurring in the test run. Columns 7–12 and 13–18 provide average values for cycles in the large and small displacement ranges, respectively. Within each range, n is the number of valid cycles used for averaging, K is the average effective stiffness, ξ_{hyst} is the average equivalent viscous damping ratio, f is the average cycle frequency, with other properties as defined previously. Note that f is not provided for harmonic test runs, since throughout these tests the wall simply responded at the excitation frequency.

Whilst the table omits the amplitude of the wall's restoring force (F_{amp}), it can be calculated directly from the average wall acceleration amplitude using the relationship

$$F_{\text{amp}} = W_w \frac{a_{a\,\text{amp}}}{g}, \tag{S.25}$$

where W_w is the weight of the wall (equal to 2400 N for walls D1 and D2, and 2079 N for walls D3, D4 and D5).

Figures S.29–S.33 together with the legend in Table S.11 graphically show a sequential plot of each wall's main response properties in each test run, including the load (or acceleration), displacement, effective stiffness, hysteretic damping, and frequency.

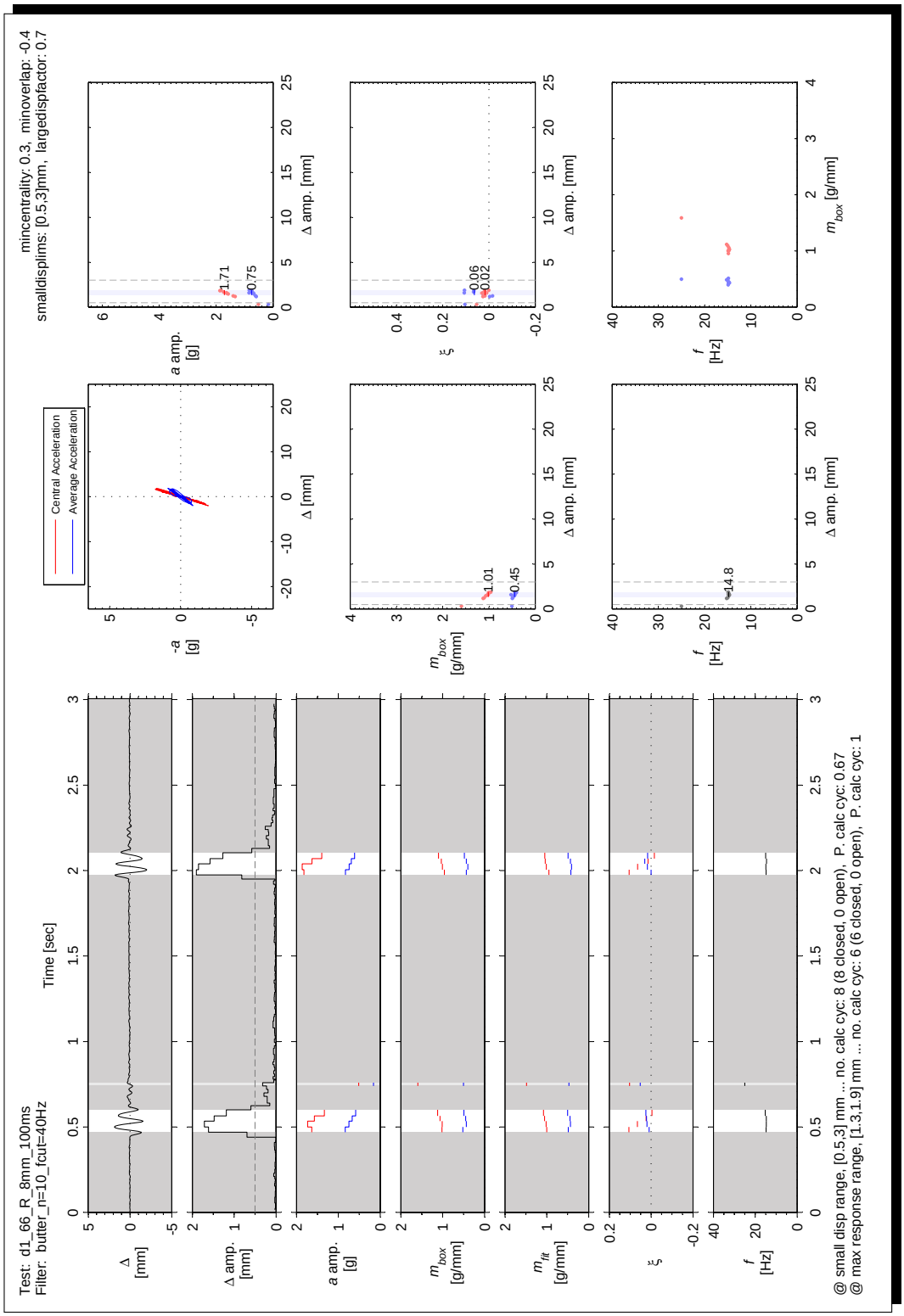

Figure S.26: Example of graphical output from the cyclic analysis of a pulse test (d1_66_R_8mm_100ms).

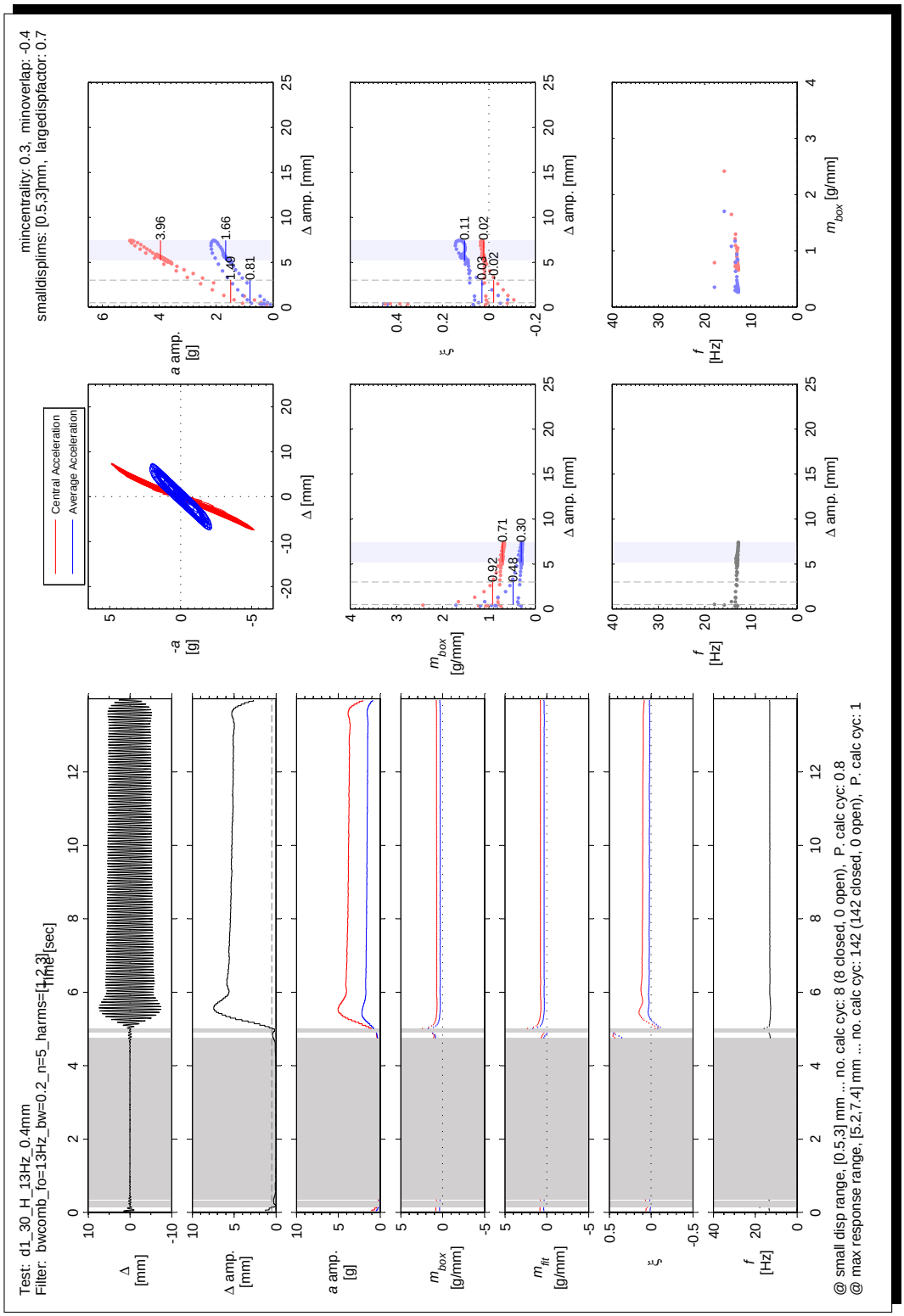

Figure S.27: Example of graphical output from the cyclic analysis of a harmonic test (d1_30_H_13Hz_0.4mm).

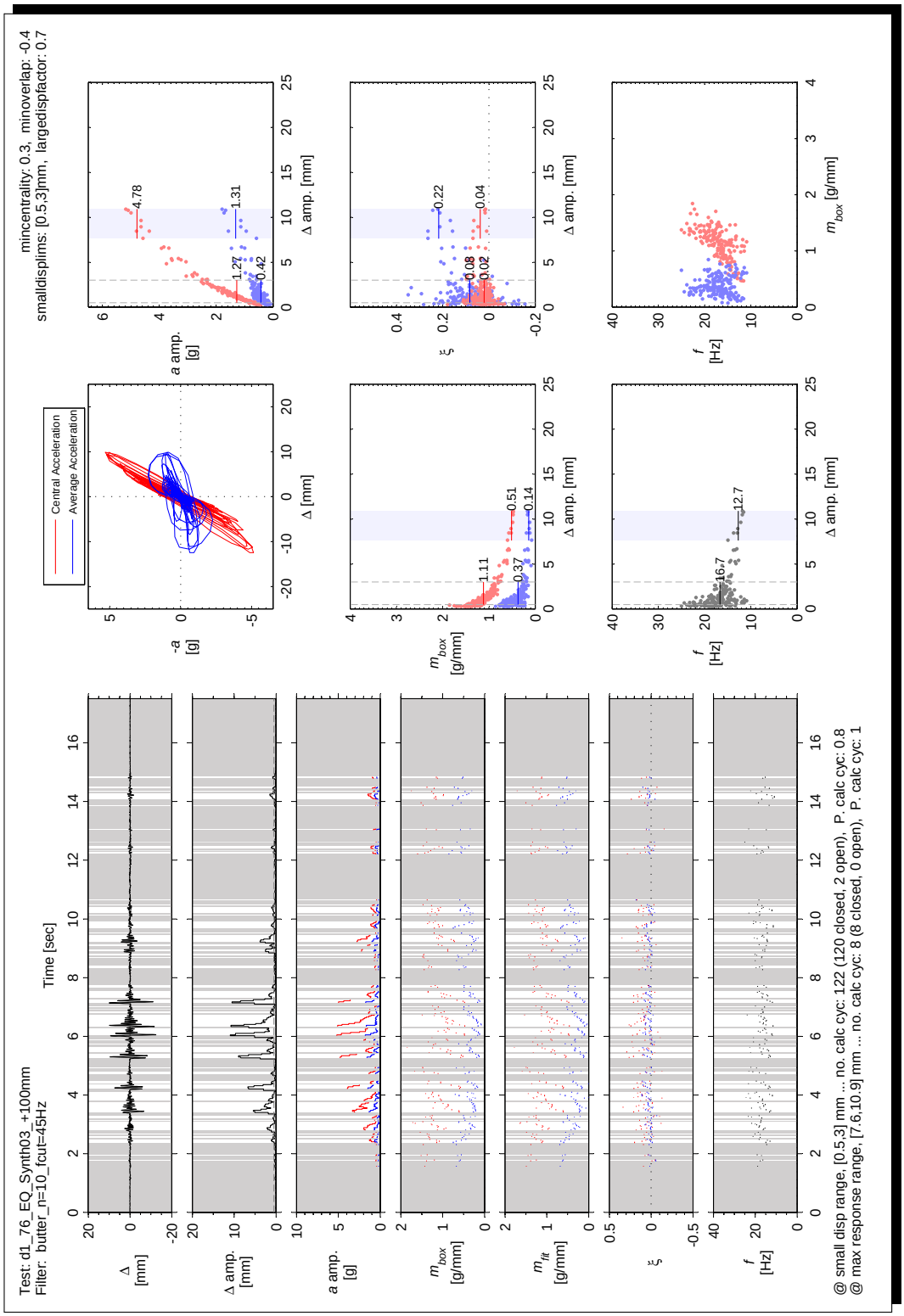

Figure S.28: Example of graphical output from the cyclic analysis of an earthquake motion test (d1_76_EQ_Synth03_+100mm).

Table S.10: Cyclic analysis results for individual test runs.

Test Name	Filter	Peak response cycles			Avg. results for cycles with $\Delta_{amp} \geq 0.7\ \max(\Delta_{amp})$						Avg. results for cycles with $0.5\,mm \leq \Delta_{amp} \leq 3\,mm$					
	f_c [Hz]	Δ_{amp} [mm]	$a_{c\,amp}$ [g]	$a_{a\,amp}$ [g]	n	Δ_{amp} [mm]	$a_{a\,amp}$ [g]	K [N/mm]	ξ_{hyst}	f [Hz]	n	Δ_{amp} [mm]	$a_{a\,amp}$ [g]	K [N/mm]	ξ_{hyst}	f [Hz]
d1_01_0MPa_R_4mm_200ms	40	–	–	–	0	–	–	–	–	–	0	–	–	–	–	–
d1_02_0MPa_R_4mm_100ms	40	–	–	–	0	–	–	–	–	–	0	–	–	–	–	–
d1_03_0MPa_R_8mm_100ms	40	0.6	1.76	1.36	6	0.5	1.18	5980	0.13	16.3	2	–	–	–	–	–
d1_04_0.05MPa_R_4mm_200ms	40	–	–	–	0	–	–	–	–	–	0	–	–	–	–	–
d1_05_0.05MPa_R_4mm_100ms	40	–	–	–	0	–	–	–	–	–	0	–	–	–	–	–
d1_06_0.05MPa_R_8mm_100ms	40	–	–	–	0	–	–	–	–	–	0	–	–	–	–	–
d1_08_0.10MPa_R_4mm_200ms	40	–	–	–	0	–	–	–	–	–	0	–	–	–	–	–
d1_09_0.10MPa_R_4mm_100ms	40	–	–	–	0	–	–	–	–	–	0	–	–	–	–	–
d1_10_0.10MPa_R_8mm_100ms	40	–	–	–	0	–	–	–	–	–	0	–	–	–	–	–
d1_11_H_13Hz_0.25mm	default	–	–	–	0	–	–	–	–	–	0	–	–	–	–	–
d1_12_H_13Hz_0.5mm	default	–	–	–	93	0.4	1.40	8680	0.20	–	0	–	–	–	–	–
d1_13_H_13Hz_0.75mm	default	0.6	2.06	1.81	13	0.5	1.63	7740	0.16	–	8	–	–	–	–	–
d1_14_H_13Hz_1mm	default	1.2	3.07	2.35	39	1.0	2.05	5010	0.11	–	60	–	–	–	–	–
d1_15_EQ_Taft_-40mm	40	–	–	–	0	–	–	–	–	–	0	–	–	–	–	–
d1_16_EQ_Taft_+40mm	40	–	–	–	0	–	–	–	–	–	0	–	–	–	–	–
d1_17_EQ_Taft_+60mm	40	–	–	–	0	–	–	–	–	–	0	–	–	–	–	–
d1_18_EQ_Taft_-60mm	40	0.6	2.33	1.45	1	0.6	1.45	5570	0.08	18.4	1	–	–	–	–	–
d1_19_EQ_Taft_-80mm	45	1.6	4.07	2.70	1	1.6	2.70	4180	0.07	17.6	5	–	–	–	–	–
d1_20_EQ_Taft_+80mm	45	2.3	5.20	3.25	2	2.1	3.11	3530	0.07	17.9	6	–	–	–	–	–
d1_21_EQ_Taft_+100mm	45	3.2	5.42	3.00	4	2.9	2.50	2030	0.05	18.7	14	1.4	1.50	2980	0.06	15.2
d1_22_EQ_Taft_-100mm	45	1.6	3.17	1.56	3	1.5	1.34	2210	0.04	20.8	3	–	–	–	–	–
d1_23_EQ_Taft_-120mm	45	5.5	5.95	2.70	3	4.7	2.46	1280	0.05	15.6	30	1.1	0.91	2110	0.05	21.0
d1_24_EQ_Taft_+120mm	45	6.6	5.85	2.44	5	5.9	1.99	802	0.05	15.3	50	1.0	0.69	1810	0.04	20.1
d1_25_R_4mm_200ms	40	–	–	–	0	–	–	–	–	–	0	–	–	–	–	–
d1_26_R_4mm_100ms	40	–	–	–	1	0.3	0.37	2760	0.03	20.9	0	–	–	–	–	–
d1_27_R_8mm_100ms	40	0.9	1.66	0.86	2	0.9	0.84	2320	0.02	15.3	3	–	–	–	–	–
d1_28_H_13Hz_0.1mm	default	–	–	–	0	–	–	–	–	–	0	–	–	–	–	–
d1_29_H_13Hz_0.2mm	default	–	–	–	0	–	–	–	–	–	0	–	–	–	–	–
d1_30_H_13Hz_0.4mm	default	7.4	5.03	2.18	142	5.6	1.66	713	0.02	–	8	1.5	0.81	1150	−0.02	–
d1_31_R_4mm_200ms	40	–	–	–	0	–	–	–	–	–	0	–	–	–	–	–
d1_32_R_4mm_100ms	40	–	–	–	2	0.4	0.37	2060	−0.01	18.4	0	–	–	–	–	–
d1_33_R_8mm_100ms	40	1.5	1.76	0.84	4	1.3	0.78	1390	0.04	15.6	7	–	–	–	–	–
d1_34_EQ_Taft_+40mm	35	–	–	–	17	0.4	0.27	1750	0.03	20.8	0	–	–	–	–	–
d1_35_EQ_Taft_-40mm	35	–	–	–	16	0.4	0.28	1740	0.04	20.6	0	–	–	–	–	–
d1_36_EQ_Taft_-60mm	40	3.4	3.25	1.37	3	3.2	1.06	797	0.02	16.0	26	0.8	0.40	1480	0.04	19.0
d1_37_EQ_Taft_+60mm	40	1.2	1.58	0.63	3	1.0	0.62	1440	0.03	17.7	15	–	–	–	–	–
d1_38_EQ_Taft_+80mm	45	9.3	5.47	2.13	3	8.2	1.77	516	0.04	13.5	25	0.8	0.43	1390	0.02	19.2
d1_39_EQ_Taft_-80mm	45	8.7	5.18	1.79	3	7.6	1.60	509	0.03	13.9	56	0.8	0.46	1390	0.02	18.1
d1_40_EQ_Taft_-100mm	45	5.3	3.92	1.42	3	4.6	1.22	641	0.02	14.9	84	1.1	0.53	1280	0.02	18.1
d1_41_EQ_Taft_+100mm	45	10.3	5.68	2.03	3	8.9	1.70	458	0.04	13.5	82	1.1	0.50	1170	0.02	17.6
d1_42_R_4mm_200ms	40	–	–	–	1	0.3	0.24	1860	0.04	20.4	0	–	–	–	–	–
d1_43_R_4mm_100ms	40	0.5	0.80	0.39	2	0.5	0.36	1750	−0.01	15.0	1	–	–	–	–	–
d1_44_R_8mm_100ms	40	1.7	1.75	0.84	4	1.6	0.79	1190	0.02	15.4	8	–	–	–	–	–
d1_45_EQ_Taft_+120mm	45	9.0	5.30	2.01	4	7.6	1.60	506	0.03	13.3	109	1.0	0.46	1180	0.02	17.7

continued on next page

Table S.10: (cont'd).

Test Name	Filter	Peak response cycles			Avg. results for cycles with $\Delta_{amp} \geq 0.7\ \max(\Delta_{amp})$						Avg. results for cycles with $0.5\,mm \leq \Delta_{amp} \leq 3\,mm$					
	f_c [Hz]	Δ_{amp} [mm]	$a_{c\,amp}$ [g]	$a_{a\,amp}$ [g]	n	Δ_{amp} [mm]	$a_{a\,amp}$ [g]	K [N/mm]	ξ_{hyst}	f [Hz]	n	Δ_{amp} [mm]	$a_{a\,amp}$ [g]	K [N/mm]	ξ_{hyst}	f [Hz]
d1_46_EQ_Taft_-120mm	45	9.8	5.33	2.05	4	9.0	1.73	463	0.05	12.1	118	1.1	0.49	1160	0.03	17.3
d1_47_R_4mm_200ms	40	–	–	–	0	–	–	–	–	–	0	–	–	–	–	–
d1_48_R_4mm_100ms	40	0.6	0.82	0.38	2	0.5	0.37	1650	−0.01	16.6	2	–	–	–	–	–
d1_49_R_8mm_100ms	40	1.7	1.77	0.84	6	1.5	0.74	1200	0.02	15.0	8	–	–	–	–	–
d1_50_H_12Hz_0.1mm	default	–	–	–	0	–	–	–	–	–	0	–	–	–	–	–
d1_51_H_12Hz_0.2mm	default	4.7	3.19	1.51	215	4.5	1.47	792	0.02	–	28	1.7	0.93	1400	0.02	–
d1_52_R_4mm_200ms	40	–	–	–	0	–	–	–	–	–	0	–	–	–	–	–
d1_53_R_4mm_100ms	40	–	–	–	1	0.4	0.38	2390	0.02	17.0	0	–	–	–	–	–
d1_54_R_8mm_100ms	40	1.4	1.74	0.87	3	1.3	0.81	1560	0.04	15.3	7	–	–	–	–	–
d1_56_EQ_Synth01_+20mm	40	–	–	–	0	–	–	–	–	–	0	–	–	–	–	–
d1_57_EQ_Synth01_-20mm	40	–	–	–	0	–	–	–	–	–	0	–	–	–	–	–
d1_58_EQ_Synth01_-40mm	40	2.1	2.28	1.11	2	2.1	1.04	1220	0.01	15.3	8	–	–	–	–	–
d1_59_EQ_Synth01_+40mm	40	–	–	–	11	0.4	0.28	1630	0.01	20.9	0	–	–	–	–	–
d1_60_EQ_Synth01_+60mm	45	7.2	4.23	1.64	6	6.3	1.39	538	0.04	13.7	36	1.1	0.45	1090	0.03	18.8
d1_61_EQ_Synth01_-60mm	45	6.0	3.73	1.43	9	5.0	1.23	598	0.02	14.0	35	1.1	0.41	1010	0.03	18.8
d1_62_EQ_Synth01_-80mm	45	11.3	5.80	1.91	6	9.7	1.38	336	0.04	13.3	82	1.1	0.44	1050	0.02	18.3
d1_63_EQ_Synth01_+80mm	45	10.5	5.55	1.90	6	9.4	1.42	362	0.04	12.8	83	1.3	0.47	941	0.02	17.1
d1_64_R_4mm_200ms	40	–	–	–	1	0.4	0.22	1550	0.06	18.4	0	–	–	–	–	–
d1_65_R_4mm_100ms	40	0.6	0.86	0.40	2	0.6	0.37	1630	0.01	17.4	1	–	–	–	–	–
d1_66_R_8mm_100ms	40	1.9	1.86	0.84	6	1.7	0.75	1070	0.02	14.8	8	–	–	–	–	–
d1_67_EQ_Synth03_-20mm	40	–	–	–	0	–	–	–	–	–	0	–	–	–	–	–
d1_68_EQ_Synth03_+20mm	40	–	–	–	0	–	–	–	–	–	0	–	–	–	–	–
d1_69_EQ_Synth03_+40mm	40	0.7	0.98	0.44	8	0.6	0.33	1440	0.06	17.7	5	–	–	–	–	–
d1_70_EQ_Synth03_-40mm	40	0.6	0.90	0.40	6	0.5	0.30	1360	0.06	18.9	2	–	–	–	–	–
d1_71_EQ_Synth03_-60mm	40	1.6	1.90	0.71	2	1.5	0.61	943	0.00	17.5	27	–	–	–	–	–
d1_72_EQ_Synth03_+60mm	40	1.3	1.48	0.62	12	1.1	0.50	1110	0.03	17.3	37	–	–	–	–	–
d1_73_EQ_Synth03_+80mm	45	8.2	4.37	1.65	2	7.8	1.41	430	0.04	12.5	74	1.0	0.45	1090	0.02	17.5
d1_74_EQ_Synth03_-80mm	45	8.5	4.43	1.64	4	7.3	1.36	454	0.02	13.0	70	0.9	0.39	1090	0.02	17.4
d1_75_EQ_Synth03_-100mm	45	10.2	5.32	1.69	6	8.9	1.36	365	0.03	12.9	101	1.2	0.46	1000	0.02	16.5
d1_76_EQ_Synth03_+100mm	45	10.9	5.17	1.78	8	9.4	1.31	329	0.04	12.7	122	1.2	0.42	886	0.02	16.7
d1_77_R_4mm_200ms	40	–	–	–	1	0.3	0.20	1550	0.04	19.7	0	–	–	–	–	–
d1_78_R_4mm_100ms	40	0.7	0.82	0.39	2	0.6	0.38	1530	−0.02	14.6	2	–	–	–	–	–
d1_79_R_8mm_100ms	40	2.1	1.90	0.81	7	1.8	0.73	948	0.01	14.6	11	–	–	–	–	–
d1_80_EQ_Synth05_-20mm	40	1.0	1.16	0.48	3	0.9	0.41	1150	0.01	17.3	25	–	–	–	–	–
d1_81_EQ_Synth05_+20mm	40	0.8	1.03	0.44	7	0.7	0.35	1260	0.01	17.4	21	–	–	–	–	–
d1_82_EQ_Synth05_+40mm	45	3.1	2.47	0.99	2	3.0	0.91	730	0.03	13.5	125	0.8	0.36	1040	0.01	17.4
d1_83_EQ_Synth05_-40mm	45	4.8	3.05	1.23	4	4.5	1.17	636	0.04	12.5	118	0.9	0.37	1020	0.02	17.3
d1_84_EQ_Synth05_-60mm	50	11.5	5.53	1.71	6	9.2	1.30	334	0.05	12.4	173	1.1	0.42	924	0.02	16.3
d1_85_EQ_Synth05_+60mm	50	11.7	5.64	1.67	3	9.8	1.35	329	0.04	12.6	168	1.2	0.42	881	0.02	16.1
d1_86_R_4mm_200ms	40	–	–	–	1	0.4	0.21	1410	0.10	16.4	0	–	–	–	–	–
d1_87_R_4mm_100ms	40	0.7	0.81	0.38	2	0.6	0.36	1390	0.01	13.6	2	–	–	–	–	–
d1_88_R_8mm_100ms	40	2.3	1.97	0.82	8	2.1	0.73	845	0.01	14.4	12	–	–	–	–	–
d1_89_OMPa_R_4mm_200ms	40	1.7	0.40	0.17	9	1.4	0.14	230	0.05	7.7	13	–	–	–	–	–
d1_90_OMPa_R_4mm_100ms	40	2.7	0.67	0.23	4	2.4	0.22	218	0.06	6.4	9	–	–	–	–	–
d1_91_OMPa_R_8mm_100ms	40	5.8	1.60	0.66	4	5.0	0.57	274	0.02	10.6	6	1.6	0.12	190	0.09	8.1

continued on next page

Bull Earthquake Eng, DOI: 10.1007/s10518-017-0282-8
SUPPLEMENTARY MATERIAL

Table S.10: (cont'd).

Test Name	Filter	Peak response cycles			Avg. results for cycles with $\Delta_{amp} \geq 0.7\ \max(\Delta_{amp})$						Avg. results for cycles with $0.5\,mm \leq \Delta_{amp} \leq 3\,mm$					
	f_c [Hz]	Δ_{amp} [mm]	$a_{c\,amp}$ [g]	$a_{a\,amp}$ [g]	n	Δ_{amp} [mm]	$a_{a\,amp}$ [g]	K [N/mm]	ξ_{hyst}	f [Hz]	n	Δ_{amp} [mm]	$a_{a\,amp}$ [g]	K [N/mm]	ξ_{hyst}	f [Hz]
d2_01_R_4mm_200ms	40	–	–	–	0	–	–	–	–	–	0	–	–	–	–	–
d2_02_R_4mm_100ms	40	–	–	–	0	–	–	–	–	–	0	–	–	–	–	–
d2_03_R_8mm_100ms	40	–	–	–	0	–	–	–	–	–	0	–	–	–	–	–
d2_04_R_4mm_200ms	40	–	–	–	0	–	–	–	–	–	0	–	–	–	–	–
d2_05_R_4mm_100ms	40	–	–	–	0	–	–	–	–	–	0	–	–	–	–	–
d2_06_R_8mm_100ms	40	0.8	1.72	1.47	4	0.7	1.23	4540	0.13	14.6	4	–	–	–	–	–
d2_07_H_12Hz_0.05mm	default	–	–	–	0	–	–	–	–	–	0	–	–	–	–	–
d2_08_H_12Hz_0.1mm	default	–	–	–	0	–	–	–	–	–	0	–	–	–	–	–
d2_09_H_12Hz_0.2mm	default	–	–	–	286	0.5	0.92	4790	0.16	–	0	–	–	–	–	–
d2_10_R_4mm_200ms	40	–	–	–	0	–	–	–	–	–	0	–	–	–	–	–
d2_11_R_4mm_100ms	40	–	–	–	0	–	–	–	–	–	0	–	–	–	–	–
d2_12_R_8mm_100ms	40	0.6	1.26	1.08	4	0.6	0.95	4170	0.16	13.5	3	–	–	–	–	–
d2_13_H_12Hz_0.25mm	default	1.6	1.36	1.17	444	1.3	0.41	734	0.19	–	490	–	–	–	–	–
d2_14_H_12Hz_0.25mm	default	1.4	0.76	0.34	213	1.3	0.31	571	0.20	–	230	–	–	–	–	–
d2_16_R_4mm_200ms	40	–	–	–	0	–	–	–	–	–	0	–	–	–	–	–
d2_17_R_4mm_100ms	40	–	–	–	3	0.4	0.37	2280	0.04	13.8	0	–	–	–	–	–
d2_18_R_8mm_100ms	40	1.3	1.57	0.92	7	1.1	0.79	1760	0.09	13.6	12	–	–	–	–	–
d2_20_H_12Hz_0.1mm	default	–	–	–	0	–	–	–	–	–	0	–	–	–	–	–
d2_21_H_12Hz_0.2mm	default	1.3	1.14	0.72	13	1.1	0.60	1270	0.12	–	210	–	–	–	–	–
d2_23_H_12Hz_0.1mm	default	–	–	–	0	–	–	–	–	–	0	–	–	–	–	–
d2_24_H_12Hz_0.2mm	default	2.5	1.91	1.01	20	2.2	0.88	967	0.03	–	224	–	–	–	–	–
d2_25_R_4mm_200ms	40	–	–	–	3	0.4	0.17	1080	0.08	12.3	0	–	–	–	–	–
d2_26_R_4mm_100ms	40	1.0	0.73	0.36	8	1.0	0.27	691	0.05	13.6	10	–	–	–	–	–
d2_27_R_8mm_100ms	40	3.1	2.11	0.77	9	2.7	0.69	614	0.03	13.4	9	2.4	0.63	624	0.04	13.3
d2_28_H_12Hz_0.25mm	default	3.1	1.55	0.50	193	2.8	0.30	257	0.04	–	192	2.6	0.29	223	0.04	–
d2_29_H_12Hz_0.3mm	default	3.2	1.39	0.24	224	2.9	0.19	156	0.04	–	206	2.7	0.18	151	0.04	–
d2_30_R_4mm_200ms	40	0.7	0.35	0.15	5	0.6	0.14	542	0.11	10.1	6	–	–	–	–	–
d2_31_R_4mm_100ms	40	1.5	0.66	0.27	4	1.4	0.20	346	0.08	10.8	8	–	–	–	–	–
d2_32_R_8mm_100ms	40	3.2	1.34	0.49	8	2.6	0.27	233	0.04	12.2	17	1.7	0.18	209	0.06	12.9
d2_33_EQ_Taft_-20mm	40	0.8	0.38	0.21	8	0.7	0.16	600	0.08	9.8	11	–	–	–	–	–
d2_34_EQ_Taft_+20mm	40	0.8	0.35	0.19	5	0.6	0.16	595	0.09	9.1	12	–	–	–	–	–
d2_35_EQ_Taft_+40mm	40	1.8	0.73	0.36	13	1.5	0.31	490	0.07	8.6	75	–	–	–	–	–
d2_36_EQ_Taft_-40mm	40	2.0	0.81	0.38	7	1.6	0.30	468	0.06	9.0	75	–	–	–	–	–
d2_37_EQ_Taft_-60mm	40	5.1	1.97	0.83	1	5.1	0.83	394	0.05	9.8	120	1.2	0.21	449	0.07	9.2
d2_38_EQ_Taft_+60mm	40	2.8	0.97	0.51	16	2.2	0.38	410	0.06	8.6	130	–	–	–	–	–
d2_39_EQ_Taft_+80mm	50	8.7	3.31	1.52	1	8.7	1.52	420	0.05	12.5	148	1.4	0.21	374	0.06	9.0
d2_40_EQ_Taft_-80mm	50	7.0	2.62	1.42	3	5.8	0.87	346	0.06	8.6	121	1.4	0.18	322	0.07	8.5
d2_41_EQ_Taft_-100mm	50	6.6	1.80	1.00	12	5.3	0.66	302	0.07	6.8	134	1.6	0.19	288	0.07	8.4
d2_42_EQ_Taft_+100mm	50	7.4	2.47	1.59	13	5.9	0.69	276	0.07	6.6	108	1.7	0.19	247	0.07	7.7
d2_43_R_4mm_200ms	40	1.1	0.30	0.14	10	1.0	0.11	259	0.08	7.7	11	–	–	–	–	–
d2_44_R_4mm_100ms	40	2.0	0.53	0.22	4	1.8	0.20	257	0.08	7.3	9	–	–	–	–	–
d2_45_R_8mm_100ms	40	4.4	1.20	0.62	4	3.9	0.61	382	0.04	10.6	6	1.2	0.11	209	0.15	8.3
d2_46_EQ_Taft_+60mm	40	4.3	0.92	0.49	16	3.7	0.38	242	0.08	6.3	145	1.4	0.15	269	0.08	7.5
d2_47_EQ_Taft_-60mm	40	5.6	1.31	0.81	8	4.6	0.50	257	0.08	6.2	123	1.5	0.15	240	0.07	7.1

continued on next page

Table S.10: (cont'd).

Test Name	Filter	Peak response cycles			Avg. results for cycles with $\Delta_{amp} \geq 0.7 \max(\Delta_{amp})$						Avg. results for cycles with $0.5\,mm \leq \Delta_{amp} \leq 3\,mm$					
	f_c [Hz]	Δ_{amp} [mm]	$a_{c\,amp}$ [g]	$a_{a\,amp}$ [g]	n	Δ_{amp} [mm]	$a_{a\,amp}$ [g]	K [N/mm]	ξ_{hyst}	f [Hz]	n	Δ_{amp} [mm]	$a_{a\,amp}$ [g]	K [N/mm]	ξ_{hyst}	f [Hz]
d2_48_EQ_Taft_-120mm	50	9.1	2.15	1.29	6	7.8	0.87	264	0.08	5.9	91	1.7	0.18	230	0.06	8.2
d2_49_EQ_Taft_+120mm	50	8.4	1.59	1.18	6	7.1	0.72	242	0.10	6.1	85	1.8	0.19	230	0.06	7.6
d2_50_R_4mm_200ms	40	1.3	0.28	0.11	10	1.1	0.09	197	0.08	7.3	12	–	–	–	–	–
d2_51_R_4mm_100ms	40	2.1	0.50	0.24	6	1.9	0.18	221	0.07	7.2	10	–	–	–	–	–
d2_52_R_8mm_100ms	40	4.3	1.05	0.71	3	3.7	0.59	389	0.06	11.2	6	1.4	0.16	269	0.12	9.4
d2_53_EQ_Synth01_+20mm	40	1.1	0.21	0.14	1	1.1	0.14	312	0.06	2.9	5	–	–	–	–	–
d2_54_EQ_Synth01_-20mm	40	1.0	0.21	0.14	1	1.0	0.14	329	0.05	3.8	4	–	–	–	–	–
d2_55_EQ_Synth01_-40mm	40	2.4	0.51	0.31	4	2.2	0.24	266	0.07	5.7	32	–	–	–	–	–
d2_56_EQ_Synth01_+40mm	40	1.6	0.49	0.14	4	1.4	0.14	233	0.03	7.8	30	–	–	–	–	–
d2_57_EQ_Synth01_+60mm	50	5.4	1.66	1.08	1	5.4	1.08	482	0.09	12.5	50	1.1	0.13	245	0.05	9.3
d2_58_EQ_Synth01_-60mm	50	3.8	1.00	0.78	2	3.2	0.58	415	0.06	7.6	58	1.3	0.18	298	0.04	9.4
d2_59_EQ_Synth01_-80mm	50	7.9	2.97	1.87	1	7.9	1.87	569	0.12	12.5	40	1.4	0.18	276	0.06	8.8
d2_60_R_4mm_200ms	40	1.4	0.28	0.11	9	1.2	0.09	180	0.05	7.2	13	–	–	–	–	–
d2_61_R_4mm_100ms	40	2.1	0.48	0.24	6	2.0	0.19	221	0.06	6.3	12	–	–	–	–	–
d2_62_R_8mm_100ms	40	3.9	0.96	0.64	3	3.4	0.54	382	0.11	10.0	3	1.5	0.22	372	0.12	8.3
d3_01_R_2mm_200ms	40	–	–	–	0	–	–	–	–	–	0	–	–	–	–	–
d3_02_R_4mm_200ms	40	–	–	–	0	–	–	–	–	–	0	–	–	–	–	–
d3_03_R_4mm_100ms	40	–	–	–	0	–	–	–	–	–	0	–	–	–	–	–
d3_04_R_8mm_100ms	40	–	–	–	4	0.5	0.68	3100	0.14	17.5	0	–	–	–	–	–
d3_05_H_13Hz_0.05mm	default	–	–	–	0	–	–	–	–	–	0	–	–	–	–	–
d3_06_H_13Hz_0.1mm	default	–	–	–	0	–	–	–	–	–	0	–	–	–	–	–
d3_07_H_13Hz_0.15mm	default	–	–	–	0	–	–	–	–	–	0	–	–	–	–	–
d3_08_H_13Hz_0.2mm	default	–	–	–	204	0.3	0.49	2990	0.14	–	0	–	–	–	–	–
d3_09_H_13Hz_0.25mm	default	0.7	1.35	0.87	308	0.6	0.78	2660	0.11	–	257	–	–	–	–	–
d3_10_H_13Hz_0.3mm	default	1.0	1.87	1.25	446	0.9	1.08	2440	0.10	–	467	–	–	–	–	–
d3_11_H_13Hz_0.3mm	default	3.0	3.93	2.15	434	2.8	2.02	1540	0.03	–	474	2.6	1.94	1520	0.03	–
d3_12_R_4mm_200ms	40	–	–	–	0	–	–	–	–	–	0	–	–	–	–	–
d3_13_R_4mm_100ms	40	–	–	–	8	0.4	0.28	1460	0.12	14.4	0	–	–	–	–	–
d3_14_R_8mm_100ms	40	1.0	1.36	0.73	8	0.9	0.63	1440	0.10	14.3	9	–	–	–	–	–
d3_15_H_13Hz_0.35mm	default	3.7	4.22	2.34	455	3.4	1.91	1170	0.02	–	66	1.5	0.95	1330	0.06	–
d3_16_H_13Hz_0.4mm	default	5.0	4.41	2.34	451	4.5	1.85	863	0.03	–	59	1.4	0.76	1130	0.09	–
d3_17_R_4mm_200ms	40	–	–	–	1	0.3	0.18	1250	0.16	16.2	0	–	–	–	–	–
d3_18_R_4mm_100ms	40	0.7	0.70	0.33	7	0.6	0.29	1060	0.07	14.7	6	–	–	–	–	–
d3_19_R_8mm_100ms	40	1.5	1.59	0.68	8	1.3	0.62	998	0.09	14.4	10	–	–	–	–	–
d3_20_H_12Hz_0.4mm	default	7.4	4.35	1.99	398	5.9	1.07	370	0.04	–	48	1.7	0.51	594	0.07	–
d3_21_R_4mm_200ms	30	0.5	0.44	0.15	6	0.5	0.13	624	0.06	14.3	1	–	–	–	–	–
d3_22_R_4mm_100ms	30	1.4	0.95	0.29	8	1.2	0.22	389	0.06	13.7	12	–	–	–	–	–
d3_23_R_8mm_100ms	30	3.2	1.89	0.56	9	2.7	0.37	285	0.02	13.4	12	2.2	0.32	285	0.04	13.2
d3_24_EQ_Taft_-5mm	30	–	–	–	0	–	–	–	–	–	0	–	–	–	–	–
d3_25_EQ_Taft_+5mm	30	–	–	–	0	–	–	–	–	–	0	–	–	–	–	–
d3_26_EQ_Taft_+10mm	30	–	–	–	0	–	–	–	–	–	0	–	–	–	–	–
d3_27_EQ_Taft_-10mm	30	–	–	–	0	–	–	–	–	–	0	–	–	–	–	–
d3_28_EQ_Taft_-20mm	30	–	–	–	1	0.3	0.14	913	0.01	14.8	0	–	–	–	–	–
d3_29_EQ_Taft_+20mm	30	–	–	–	5	0.4	0.15	842	0.07	14.8	0	–	–	–	–	–

continued on next page

Bull Earthquake Eng. DOI: 10.1007/s10518-017-0282-8
SUPPLEMENTARY MATERIAL

Table S.10: (cont'd).

Test Name	Filter	Peak response cycles			Avg. results for cycles with $\Delta_{amp} \geq 0.7\ \max(\Delta_{amp})$						Avg. results for cycles with $0.5\,mm \leq \Delta_{amp} \leq 3\,mm$					
	f_c [Hz]	Δ_{amp} [mm]	$a_{c\,amp}$ [g]	$a_{a\,amp}$ [g]	n	Δ_{amp} [mm]	$a_{a\,amp}$ [g]	K [N/mm]	ξ_{hyst}	f [Hz]	n	Δ_{amp} [mm]	$a_{a\,amp}$ [g]	K [N/mm]	ξ_{hyst}	f [Hz]
d3_30_EQ_Taft_+30mm	30	–	–	–	10	0.4	0.16	790	0.04	14.5	0	–	–	–	–	–
d3_31_EQ_Taft_-30mm	30	0.6	0.52	0.18	7	0.5	0.14	661	0.06	14.7	1	–	–	–	–	–
d3_32_EQ_Taft_-40mm	30	0.7	0.58	0.22	12	0.6	0.18	663	0.06	13.9	10	–	–	–	–	–
d3_33_EQ_Taft_+40mm	30	0.8	0.68	0.25	7	0.7	0.22	719	0.07	13.5	8	–	–	–	–	–
d3_34_EQ_Taft_+50mm	30	1.1	0.87	0.37	10	0.9	0.29	661	0.05	12.4	20	–	–	–	–	–
d3_35_EQ_Taft_-50mm	30	0.9	0.75	0.28	11	0.8	0.22	615	0.04	13.5	29	–	–	–	–	–
d3_36_EQ_Taft_-60mm	30	5.0	2.87	0.95	2	4.7	0.78	339	0.04	12.1	67	0.8	0.22	611	0.07	12.9
d3_37_EQ_Taft_+60mm	30	1.8	1.20	0.39	5	1.6	0.36	491	0.06	12.4	46	–	–	–	–	–
d3_38_EQ_Taft_+70mm	40	7.1	3.43	1.32	2	6.8	1.05	318	0.05	11.4	79	1.0	0.25	582	0.05	12.3
d3_39_EQ_Taft_-70mm	40	8.4	4.12	1.37	3	7.7	0.92	241	0.05	12.0	80	0.9	0.22	547	0.06	12.3
d3_40_EQ_Taft_-80mm	40	7.3	3.56	1.18	3	6.6	0.79	241	0.05	12.1	115	1.0	0.24	526	0.06	12.2
d3_41_EQ_Taft_+80mm	40	11.5	4.44	1.79	1	11.5	1.79	324	0.04	10.2	60	1.3	0.30	505	0.06	11.7
d3_42_R_4mm_200ms	30	0.7	0.44	0.19	13	0.6	0.15	570	0.10	12.8	11	–	–	–	–	–
d3_43_R_4mm_100ms	30	1.3	0.84	0.31	9	1.1	0.22	403	0.05	13.5	12	–	–	–	–	–
d3_44_R_8mm_100ms	30	3.2	1.72	0.62	9	2.9	0.38	268	0.04	13.0	12	1.9	0.25	281	0.08	12.8
d3_45_EQ_Taft_+90mm	40	12.1	4.45	1.75	1	12.1	1.75	301	0.04	9.8	113	1.2	0.26	459	0.05	11.8
d3_46_EQ_Taft_-90mm	40	6.4	2.87	0.87	5	5.4	0.69	264	0.05	11.3	115	1.2	0.27	455	0.06	11.5
d3_47_R_4mm_200ms	30	0.7	0.46	0.17	8	0.6	0.15	553	0.08	12.9	8	–	–	–	–	–
d3_48_R_4mm_100ms	30	1.3	0.82	0.32	7	1.2	0.22	385	0.04	13.5	11	–	–	–	–	–
d3_49_R_8mm_100ms	30	3.3	1.64	0.61	9	2.8	0.35	247	0.03	12.9	13	1.9	0.23	249	0.07	12.7
d3_50_EQ_Taft_-100mm	40	5.8	2.73	0.96	7	5.1	0.74	306	0.05	10.5	142	1.2	0.26	455	0.06	11.9
d3_51_EQ_Taft_+100mm	40	10.3	3.78	1.48	2	8.9	1.27	295	0.04	10.0	120	1.2	0.26	476	0.06	11.2
d3_52_EQ_Taft_+110mm	40	10.0	3.94	1.34	4	8.5	1.10	268	0.04	10.3	115	1.2	0.25	455	0.06	11.3
d3_53_EQ_Taft_-110mm	40	9.7	3.57	1.27	4	8.2	0.95	239	0.07	9.7	144	1.3	0.26	407	0.06	11.4
d3_54_EQ_Taft_-120mm	40	12.6	4.18	1.55	1	12.6	1.55	256	0.03	8.5	121	1.3	0.26	422	0.05	11.4
d3_55_EQ_Taft_+120mm	40	10.8	4.20	1.40	5	8.6	1.00	241	0.05	9.3	138	1.3	0.25	412	0.06	11.2
d3_56_EQ_Taft_+60mm	40	2.0	1.03	0.32	4	1.7	0.24	303	0.06	11.9	84	–	–	–	–	–
d3_57_EQ_Taft_-60mm	40	6.4	2.78	0.82	2	5.5	0.60	218	0.07	10.8	86	0.9	0.19	424	0.05	11.5
d3_58_H_12Hz_0.1mm	default	1.3	0.78	0.23	311	1.2	0.21	364	0.05	–	332	–	–	–	–	–
d3_59_H_12Hz_0.2mm	default	2.1	1.16	0.30	319	2.0	0.28	285	0.04	–	353	–	–	–	–	–
d3_60_H_12Hz_0.4mm	default	5.6	2.63	0.43	310	5.3	0.41	160	0.03	–	50	1.7	0.23	299	0.05	–
d4_01_R_4mm_200ms	40	–	–	–	0	–	–	–	–	–	0	–	–	–	–	–
d4_02_R_4mm_100ms	40	–	–	–	0	–	–	–	–	–	0	–	–	–	–	–
d4_03_R_8mm_100ms	40	–	–	–	2	0.3	0.88	5700	0.16	16.4	0	–	–	–	–	–
d4_04_H_13Hz_0.05mm	default	–	–	–	0	–	–	–	–	–	0	–	–	–	–	–
d4_05_H_13Hz_0.10mm	default	–	–	–	0	–	–	–	–	–	0	–	–	–	–	–
d4_06_EQ_Taft_-40mm	40	–	–	–	0	–	–	–	–	–	0	–	–	–	–	–
d4_07_EQ_Taft_+40mm	40	–	–	–	0	–	–	–	–	–	0	–	–	–	–	–
d4_08_EQ_Taft_+80mm	45	1.5	4.07	2.44	3	1.4	1.57	2360	0.17	16.9	3	–	–	–	–	–
d4_09_EQ_Taft_-80mm	40	2.1	2.85	1.89	1	2.1	1.89	1860	0.14	14.0	2	–	–	–	–	–
d4_10_R_4mm_200ms	40	–	–	–	0	–	–	–	–	–	0	–	–	–	–	–
d4_11_R_4mm_100ms	40	–	–	–	1	0.3	0.33	2070	0.10	20.0	0	–	–	–	–	–
d4_12_R_8mm_100ms	40	0.8	0.99	0.55	5	0.7	0.53	1740	0.25	14.3	5	–	–	–	–	–
d4_13_H_13Hz_0.15mm	default	–	–	–	450	0.4	0.40	2370	0.16	–	0	–	–	–	–	–

continued on next page

Table S.10: (cont'd).

Test Name	Filter	Peak response cycles			Avg. results for cycles with $\Delta_{amp} \geq 0.7\ \max(\Delta_{amp})$						Avg. results for cycles with $0.5\,mm \leq \Delta_{amp} \leq 3\,mm$					
	f_c [Hz]	Δ_{amp} [mm]	$a_{c\,amp}$ [g]	$a_{a\,amp}$ [g]	n	Δ_{amp} [mm]	$a_{a\,amp}$ [g]	K [N/mm]	ξ_{hyst}	f [Hz]	n	Δ_{amp} [mm]	$a_{a\,amp}$ [g]	K [N/mm]	ξ_{hyst}	f [Hz]
d4_14_H_13Hz_0.20mm	default	0.6	0.77	0.43	449	0.5	0.40	1750	0.26	–	83	–	–	–	–	–
d4_15_H_13Hz_0.25mm	default	0.8	1.09	0.51	456	0.7	0.45	1320	0.26	–	460	–	–	–	–	–
d4_16_H_13Hz_0.30mm	default	1.0	1.31	0.58	455	0.9	0.51	1210	0.25	–	467	–	–	–	–	–
d4_17_H_13Hz_0.35mm	default	1.3	1.67	0.82	457	1.3	0.72	1200	0.20	–	479	–	–	–	–	–
d4_18_H_13Hz_0.40mm	default	2.1	2.29	1.11	454	2.0	0.83	883	0.15	–	491	–	–	–	–	–
d4_19_R_4mm_200ms	40	–	–	–	0	–	–	–	–	–	0	–	–	–	–	–
d4_20_R_4mm_100ms	40	–	–	–	4	0.4	0.24	1320	0.20	13.3	0	–	–	–	–	–
d4_21_R_8mm_100ms	40	1.3	1.25	0.51	2	1.1	0.47	892	0.21	15.5	4	–	–	–	–	–
d4_22_H_13Hz_0.45mm	default	2.7	2.84	1.07	460	2.7	0.71	557	0.15	–	502	–	–	–	–	–
d4_23_H_13Hz_0.50mm	default	3.2	2.31	0.80	460	3.0	0.61	428	0.19	–	420	2.8	0.57	412	0.19	–
d4_24_R_4mm_200ms	40	–	–	–	0	–	–	–	–	–	0	–	–	–	–	–
d4_25_R_4mm_100ms	40	–	–	–	2	0.4	0.22	1070	0.27	11.1	0	–	–	–	–	–
d4_26_R_8mm_100ms	40	1.6	0.99	0.43	3	1.5	0.42	601	0.18	10.8	4	–	–	–	–	–
d4_27_H_6Hz_0.10mm	default	–	–	–	0	–	–	–	–	–	0	–	–	–	–	–
d4_28_H_6Hz_0.20mm	default	–	–	–	0	–	–	–	–	–	0	–	–	–	–	–
d4_29_H_6Hz_0.30mm	default	–	–	–	0	–	–	–	–	–	0	–	–	–	–	–
d4_30_H_6Hz_0.40mm	default	–	–	–	0	–	–	–	–	–	0	–	–	–	–	–
d4_31_H_6Hz_0.50mm	default	–	–	–	0	–	–	–	–	–	0	–	–	–	–	–
d4_32_H_6Hz_0.75mm	default	–	–	–	0	–	–	–	–	–	0	–	–	–	–	–
d4_33_H_6Hz_1.0mm	default	–	–	–	0	–	–	–	–	–	0	–	–	–	–	–
d4_34_H_6Hz_1.5mm	default	1.3	0.61	0.42	208	1.3	0.40	651	0.21	–	217	–	–	–	–	–
d4_35_R_4mm_200ms	40	–	–	–	0	–	–	–	–	–	0	–	–	–	–	–
d4_36_R_4mm_100ms	40	0.6	0.68	0.31	5	0.5	0.26	1100	0.14	14.7	2	–	–	–	–	–
d4_37_R_8mm_100ms	40	2.5	1.87	0.59	8	2.0	0.50	526	0.10	14.0	12	–	–	–	–	–
d4_38_H_13Hz_0.10mm	default	–	–	–	0	–	–	–	–	–	0	–	–	–	–	–
d4_39_H_13Hz_0.20mm	default	1.1	1.00	0.40	448	0.9	0.37	854	0.11	–	455	–	–	–	–	–
d4_40_H_13Hz_0.30mm	default	3.2	2.23	0.71	454	2.8	0.55	409	0.07	–	481	2.7	0.53	407	0.07	–
d4_41_H_13Hz_0.40mm	default	5.3	3.61	0.86	461	5.1	0.55	227	0.06	–	41	1.5	0.26	372	0.12	–
d4_42_R_4mm_200ms	30	–	–	–	3	0.4	0.12	678	0.18	13.6	0	–	–	–	–	–
d4_43_R_4mm_100ms	30	1.0	0.60	0.28	3	0.9	0.22	518	0.13	12.2	6	–	–	–	–	–
d4_44_R_8mm_100ms	30	2.6	1.43	0.56	9	2.3	0.32	281	0.08	13.1	14	–	–	–	–	–
d4_45_EQ_Taft_-10mm	30	–	–	–	0	–	–	–	–	–	0	–	–	–	–	–
d4_46_EQ_Taft_+10mm	30	–	–	–	0	–	–	–	–	–	0	–	–	–	–	–
d4_47_EQ_Taft_+20mm	30	–	–	–	1	0.3	0.11	742	0.19	10.3	0	–	–	–	–	–
d4_48_EQ_Taft_-20mm	30	–	–	–	0	–	–	–	–	–	0	–	–	–	–	–
d4_49_EQ_Taft_-30mm	30	–	–	–	2	0.4	0.13	651	0.12	12.1	0	–	–	–	–	–
d4_50_EQ_Taft_+30mm	30	0.5	0.32	0.15	6	0.4	0.12	578	0.17	12.4	1	–	–	–	–	–
d4_51_EQ_Taft_+40mm	30	0.6	0.41	0.21	6	0.5	0.17	661	0.15	11.0	3	–	–	–	–	–
d4_52_EQ_Taft_-40mm	30	0.6	0.41	0.19	4	0.5	0.14	557	0.12	11.9	2	–	–	–	–	–
d4_53_EQ_Taft_-50mm	30	0.8	0.51	0.29	10	0.7	0.21	636	0.14	11.2	14	–	–	–	–	–
d4_54_EQ_Taft_+50mm	30	1.1	0.60	0.28	8	0.9	0.20	453	0.12	11.7	16	–	–	–	–	–
d4_55_EQ_Taft_+60mm	30	1.5	0.82	0.33	5	1.3	0.23	380	0.11	11.9	32	–	–	–	–	–
d4_56_EQ_Taft_-60mm	40	5.4	2.75	1.05	2	4.8	0.82	345	0.08	11.7	34	0.8	0.23	599	0.13	11.0
d4_57_R_4mm_200ms	40	–	–	–	0	–	–	–	–	–	0	–	–	–	–	–
d4_58_R_4mm_100ms	40	1.0	0.61	0.27	4	0.8	0.19	466	0.13	13.0	6	–	–	–	–	–

continued on next page

Bull Earthquake Eng. DOI: 10.1007/s10518-017-0282-8
SUPPLEMENTARY MATERIAL

Table S.10: (cont'd).

Test Name	Filter	Peak response cycles			Avg. results for cycles with $\Delta_{amp} \geq 0.7$ max(Δ_{amp})						Avg. results for cycles with 0.5 mm $\leq \Delta_{amp} \leq$ 3 mm					
	f_c [Hz]	Δ_{amp} [mm]	$a_{c\,amp}$ [g]	$a_{a\,amp}$ [g]	n	Δ_{amp} [mm]	$a_{a\,amp}$ [g]	K [N/mm]	ξ_{hyst}	f [Hz]	n	Δ_{amp} [mm]	$a_{a\,amp}$ [g]	K [N/mm]	ξ_{hyst}	f [Hz]
d4_59_R_8mm_100ms	40	2.7	1.54	0.54	9	2.3	0.32	287	0.08	13.1	14	–	–	–	–	–
d4_60_EQ_Taft_+60mm	40	1.3	0.73	0.35	3	1.2	0.33	578	0.07	10.1	11	–	–	–	–	–
d4_61_EQ_Taft_-60mm	40	3.4	1.88	0.74	1	3.4	0.74	455	0.06	10.3	11	0.9	0.22	555	0.13	11.0
d4_62_EQ_Taft_-70mm	40	4.6	2.48	0.98	2	4.0	0.78	397	0.08	11.2	27	0.9	0.22	532	0.11	10.6
d4_63_EQ_Taft_+70mm	40	3.3	1.74	0.66	2	2.9	0.50	353	0.07	10.4	37	0.8	0.22	576	0.12	10.5
d4_64_EQ_Taft_+70mm	40	2.2	1.24	0.46	1	2.2	0.46	441	0.07	10.0	5	–	–	–	–	–
d4_65_EQ_Taft_-70mm	40	2.6	1.42	0.58	1	2.6	0.58	464	0.06	10.1	10	–	–	–	–	–
d4_66_R_4mm_200ms	40	–	–	–	7	0.4	0.12	682	0.13	12.7	0	–	–	–	–	–
d4_67_R_4mm_100ms	40	1.0	0.63	0.29	8	0.9	0.16	391	0.11	13.3	10	–	–	–	–	–
d4_68_R_8mm_100ms	40	2.7	1.68	0.54	10	2.4	0.32	270	0.06	13.2	16	–	–	–	–	–
d4_69_EQ_Taft_+70mm	40	4.9	2.48	0.97	2	4.5	0.73	328	0.08	11.4	77	1.0	0.22	486	0.09	10.9
d4_70_EQ_Taft_-70mm	40	7.6	4.01	1.30	2	7.3	1.05	297	0.08	12.4	16	0.7	0.20	607	0.13	11.3
d4_71_EQ_Taftbf05_-70mm	40	7.5	3.83	1.17	2	7.1	0.91	264	0.07	12.3	29	0.8	0.23	609	0.13	11.2
d4_72_EQ_Taftbf05_+70mm	40	5.0	2.47	0.90	2	4.5	0.67	299	0.09	10.8	51	1.0	0.22	478	0.10	10.5
d4_73_EQ_Taftbf10_+70mm	40	4.5	2.19	0.80	2	4.0	0.59	293	0.08	10.9	39	0.8	0.18	472	0.10	10.8
d4_74_EQ_Taftbf10_-70mm	40	7.5	3.95	1.15	2	7.3	0.92	260	0.06	12.5	10	0.8	0.21	563	0.10	10.7
d4_75_EQ_Taftbf20_-70mm	40	6.6	3.38	1.04	2	6.2	0.79	262	0.06	11.9	31	0.7	0.16	432	0.09	11.7
d4_76_EQ_Taftbf20_+70mm	40	4.1	2.10	0.77	2	3.8	0.57	303	0.08	10.9	41	0.8	0.16	412	0.08	11.5
d4_77_EQ_Taftbf30_+70mm	40	3.5	1.63	0.61	2	3.2	0.45	287	0.08	11.0	32	0.8	0.15	391	0.08	11.2
d4_78_EQ_Taftbf30_-70mm	40	6.4	3.26	1.02	2	5.9	0.79	270	0.07	11.7	38	0.8	0.15	385	0.08	11.3
d4_79_EQ_Taftbf50_-70mm	40	5.4	2.76	0.89	2	4.9	0.69	287	0.06	11.5	26	0.9	0.15	387	0.07	11.2
d4_80_EQ_Taftbf50_+70mm	40	2.6	1.25	0.47	3	2.2	0.31	285	0.08	10.6	24	–	–	–	–	–
d4_81_EQ_Taftbf75_+70mm	40	2.4	1.16	0.41	3	2.1	0.28	270	0.07	11.1	22	–	–	–	–	–
d4_82_EQ_Taftbf75_-70mm	40	4.8	2.43	0.80	2	4.3	0.61	289	0.06	11.3	31	0.8	0.15	378	0.08	11.0
d4_83_EQ_Taftbf100_-70mm	40	4.1	2.10	0.69	2	3.7	0.53	289	0.06	11.4	22	0.9	0.14	349	0.08	11.2
d4_84_EQ_Taftbf100_+70mm	40	2.7	1.32	0.43	3	2.6	0.32	260	0.06	11.3	22	–	–	–	–	–
d4_85_R_4mm_200ms	40	–	–	–	10	0.4	0.09	484	0.13	12.3	0	–	–	–	–	–
d4_86_R_4mm_100ms	40	1.1	0.59	0.25	3	1.0	0.20	393	0.09	11.7	4	–	–	–	–	–
d4_87_R_8mm_100ms	40	2.8	1.46	0.51	4	2.5	0.35	281	0.05	12.3	14	–	–	–	–	–
d4_88_H_13Hz_0.2mm	default	2.5	1.48	0.20	316	2.1	0.16	160	0.06	–	371	–	–	–	–	–
d4_89_H_13Hz_0.4mm	default	5.0	2.74	0.44	339	4.8	0.41	175	0.05	–	43	1.5	0.13	193	0.08	–
d4_90_H_13Hz_0.6mm	default	7.2	3.88	0.60	345	6.8	0.52	158	0.04	–	28	1.5	0.12	162	0.08	–
d4_91_R_4mm_200ms	40	0.6	0.32	0.10	7	0.5	0.08	320	0.10	11.8	4	–	–	–	–	–
d4_92_R_4mm_100ms	40	1.5	0.71	0.24	2	1.3	0.23	362	0.03	10.5	4	–	–	–	–	–
d4_93_R_8mm_100ms	40	3.4	1.62	0.47	3	3.1	0.36	233	0.05	11.5	13	1.5	0.17	260	0.08	12.2
d4_94_EQ_Taft_+70mm	40	7.4	3.03	0.99	2	6.5	0.69	214	0.09	10.0	109	1.2	0.19	339	0.06	9.8
d4_95_EQ_Taft_-70mm	40	9.5	4.10	1.10	2	8.4	0.73	173	0.06	11.1	91	1.0	0.17	355	0.05	9.8
d4_96_EQ_Taft_-80mm	40	8.4	3.65	1.01	2	7.5	0.69	181	0.05	11.5	111	1.2	0.18	328	0.06	9.7
d4_97_EQ_Taft_+80mm	40	11.0	4.37	1.47	1	11.0	1.47	279	0.05	10.2	124	1.3	0.19	326	0.06	9.9
d4_98_EQ_Taft_+90mm	40	11.4	4.40	1.55	1	11.4	1.55	283	0.05	10.3	142	1.3	0.21	353	0.06	10.0
d4_99_EQ_Taft_-90mm	40	6.8	2.90	0.75	3	6.3	0.64	212	0.05	10.2	120	1.2	0.19	333	0.06	9.7
d4_100_EQ_Taft_-100mm	40	6.8	2.98	0.77	3	6.0	0.63	218	0.05	9.6	141	1.3	0.19	310	0.05	9.6
d4_101_EQ_Taft_+100mm	40	10.0	3.75	1.22	2	9.3	1.11	247	0.04	9.4	139	1.3	0.20	314	0.06	9.5
d4_102_EQ_Taft_+110mm	40	10.8	3.93	1.29	2	9.5	1.10	241	0.05	8.9	136	1.4	0.20	299	0.06	9.3
d4_103_EQ_Taft_-110mm	40	8.8	3.61	0.94	5	7.6	0.80	222	0.06	8.6	141	1.4	0.19	285	0.06	9.3

continued on next page

Table S.10: (cont'd).

Test Name	Filter	Peak response cycles			Avg. results for cycles with $\Delta_{amp} \geq 0.7\ \max(\Delta_{amp})$						Avg. results for cycles with $0.5\,mm \leq \Delta_{amp} \leq 3\,mm$					
	f_c [Hz]	Δ_{amp} [mm]	$a_{c\,amp}$ [g]	$a_{a\,amp}$ [g]	n	Δ_{amp} [mm]	$a_{a\,amp}$ [g]	K [N/mm]	ξ_{hyst}	f [Hz]	n	Δ_{amp} [mm]	$a_{a\,amp}$ [g]	K [N/mm]	ξ_{hyst}	f [Hz]
d4_104_EQ_Taft_-120mm	40	11.6	4.27	1.27	1	11.6	1.27	229	0.05	9.1	151	1.5	0.22	295	0.06	9.2
d4_105_EQ_Taft_+120mm	40	11.1	3.79	1.45	2	9.5	1.17	252	0.05	8.3	138	1.3	0.19	297	0.06	9.3
d4_106_R_4mm_200ms	40	0.7	0.32	0.10	6	0.6	0.08	293	0.08	10.7	5	–	–	–	–	–
d4_107_R_4mm_100ms	40	1.7	0.74	0.24	2	1.5	0.22	318	0.03	9.3	3	–	–	–	–	–
d4_108_R_8mm_100ms	40	3.6	1.58	0.47	2	3.4	0.45	272	0.04	9.4	11	1.3	0.18	274	0.10	10.1
d4_109_H_13Hz_0.1mm	default	–	–	–	324	0.4	0.03	158	0.15	–	0	–	–	–	–	–
d4_110_H_13Hz_0.2mm	default	1.8	0.96	0.13	320	1.5	0.09	129	0.06	–	357	–	–	–	–	–
d4_111_H_13Hz_0.3mm	default	4.0	2.09	0.28	328	3.8	0.26	141	0.02	–	51	1.5	0.10	141	0.06	–
d4_112_H_13Hz_0.4mm	default	5.5	3.16	0.40	337	5.2	0.37	148	0.03	–	48	1.4	0.10	150	0.06	–
d4_113_H_13Hz_0.5mm	default	6.4	3.54	0.54	340	5.8	0.49	177	0.03	–	41	1.6	0.15	212	0.06	–
d4_114_R_4mm_200ms	40	–	–	–	6	0.4	0.11	501	0.12	12.9	0	–	–	–	–	–
d4_115_R_4mm_100ms	40	1.3	0.71	0.24	3	1.1	0.20	376	0.09	11.8	7	–	–	–	–	–
d4_116_R_8mm_100ms	40	3.3	1.39	0.49	3	3.0	0.41	281	0.06	10.8	6	1.8	0.24	256	0.10	12.2
d5_01_H_14Hz_0.05mm	default	–	–	–	0	–	–	–	–	–	0	–	–	–	–	–
d5_02_H_14Hz_0.1mm	default	–	–	–	423	0.3	0.26	1600	0.02	–	0	–	–	–	–	–
d5_03_H_14Hz_0.15mm	default	1.1	1.42	0.72	486	1.0	0.69	1380	−0.01	–	500	–	–	–	–	–
d5_04_H_14Hz_0.2mm	default	2.2	2.45	1.19	487	2.1	0.77	771	0.01	–	539	–	–	–	–	–
d5_05_R_2mm_200ms	40	–	–	–	0	–	–	–	–	–	0	–	–	–	–	–
d5_06_R_4mm_200ms	40	–	–	–	8	0.4	0.13	682	0.06	16.6	0	–	–	–	–	–
d5_07_R_4mm_100ms	40	1.2	1.11	0.38	7	1.0	0.32	655	0.02	15.1	12	–	–	–	–	–
d5_08_H_14Hz_0.2mm	default	2.0	1.75	0.61	493	2.0	0.58	615	0.01	–	550	–	–	–	–	–
d5_09_H_14Hz_0.25mm	default	4.8	2.81	0.89	348	4.0	0.46	245	0.02	–	78	1.7	0.38	488	0.02	–
d5_10_R_2mm_200ms	40	–	–	–	3	0.3	0.06	407	0.06	14.2	0	–	–	–	–	–
d5_11_R_4mm_200ms	40	0.8	0.49	0.13	9	0.7	0.11	322	0.02	12.9	12	–	–	–	–	–
d5_12_R_4mm_100ms	40	1.8	0.93	0.26	4	1.6	0.17	216	0.01	12.9	11	–	–	–	–	–
d5_13_H_14Hz_0.3mm	default	6.2	3.65	0.69	198	4.9	0.55	239	−0.04	–	51	1.6	0.19	245	−0.01	–
d5_14_R_2mm_200ms	40	–	–	–	4	0.4	0.05	264	0.06	11.8	0	–	–	–	–	–
d5_15_R_4mm_200ms	22	0.9	0.41	0.10	4	0.8	0.08	204	0.05	11.3	5	–	–	–	–	–
d5_16_R_4mm_100ms	22	2.2	0.84	0.24	2	2.0	0.23	237	0.02	11.1	7	–	–	–	–	–
d5_17_EQ_Taft_-6mm	25	–	–	–	0	–	–	–	–	–	0	–	–	–	–	–
d5_18_EQ_Taft_+6mm	25	–	–	–	0	–	–	–	–	–	0	–	–	–	–	–
d5_19_EQ_Taft_+11mm	25	–	–	–	6	0.3	0.04	274	0.02	12.5	0	–	–	–	–	–
d5_20_EQ_Taft_-11mm	25	–	–	–	0	–	–	–	–	–	0	–	–	–	–	–
d5_21_EQ_Taft_-17mm	25	–	–	–	14	0.4	0.05	291	0.02	11.4	0	–	–	–	–	–
d5_22_EQ_Taft_+17mm	25	0.6	0.36	0.09	7	0.5	0.06	262	−0.01	12.1	2	–	–	–	–	–
d5_23_EQ_Taft_+22mm	25	0.7	0.42	0.11	15	0.6	0.07	260	0.03	11.1	16	–	–	–	–	–
d5_24_EQ_Taft_-22mm	25	0.6	0.32	0.11	12	0.5	0.08	289	0.01	10.6	9	–	–	–	–	–
d5_25_EQ_Taft_-28mm	25	0.8	0.38	0.14	17	0.7	0.09	283	0.02	10.2	26	–	–	–	–	–
d5_26_EQ_Taft_+28mm	25	0.9	0.48	0.15	9	0.8	0.09	235	0.02	10.6	26	–	–	–	–	–
d5_27_EQ_Taft_+33mm	25	1.2	0.56	0.18	8	1.0	0.12	239	0.02	10.0	54	–	–	–	–	–
d5_28_EQ_Taft_-33mm	25	1.0	0.47	0.17	16	0.8	0.11	272	0.03	9.5	54	–	–	–	–	–
d5_29_EQ_Taft_-39mm	25	1.5	0.57	0.20	6	1.2	0.16	283	0.01	8.8	64	–	–	–	–	–
d5_30_EQ_Taft_+39mm	25	1.5	0.63	0.21	10	1.2	0.13	227	0.02	9.5	68	–	–	–	–	–
d5_31_EQ_Taft_+45mm	25	1.8	0.69	0.24	10	1.5	0.15	218	0.02	9.1	76	–	–	–	–	–

continued on next page

Bull Earthquake Eng. DOI: 10.1007/s10518-017-0282-8
SUPPLEMENTARY MATERIAL

Table S.10: (cont'd).

Test Name	Filter	Peak response cycles			Avg. results for cycles with $\Delta_{amp} \geq 0.7\ \max(\Delta_{amp})$						Avg. results for cycles with $0.5\,mm \leq \Delta_{amp} \leq 3\,mm$					
	f_c [Hz]	Δ_{amp} [mm]	$a_{c\,amp}$ [g]	$a_{a\,amp}$ [g]	n	Δ_{amp} [mm]	$a_{a\,amp}$ [g]	K [N/mm]	ξ_{hyst}	f [Hz]	n	Δ_{amp} [mm]	$a_{a\,amp}$ [g]	K [N/mm]	ξ_{hyst}	f [Hz]
d5_32_EQ_Taft_-45mm	25	1.7	0.62	0.24	15	1.4	0.16	243	0.02	8.5	71	–	–	–	–	–
d5_33_EQ_Taft_-50mm	25	2.2	0.70	0.29	6	1.9	0.23	245	0.03	7.4	85	–	–	–	–	–
d5_34_EQ_Taft_+50mm	25	2.2	0.79	0.25	12	1.8	0.18	210	0.03	8.9	94	–	–	–	–	–
d5_35_EQ_Taft_+56mm	25	2.4	0.88	0.27	18	1.9	0.21	231	0.06	8.5	86	–	–	–	–	–
d5_36_EQ_Taft_-56mm	40	2.6	1.00	0.30	7	2.2	0.26	249	0.04	7.1	91	–	–	–	–	–
d5_37_EQ_Taft_-67mm	40	9.3	3.21	0.96	1	9.3	0.96	214	0.04	9.0	115	1.2	0.13	235	0.06	9.0
d5_38_EQ_Taft_+67mm	40	8.6	3.03	0.77	1	8.6	0.77	187	0.03	10.0	81	1.5	0.15	224	0.06	8.3
d5_39_R_2mm_200ms	30	–	–	–	4	0.4	0.05	283	0.14	11.3	0	–	–	–	–	–
d5_40_R_4mm_200ms	30	0.8	0.40	0.09	4	0.7	0.07	197	0.08	10.6	4	–	–	–	–	–
d5_41_R_4mm_100ms	30	2.2	0.79	0.27	2	2.0	0.26	274	0.05	11.1	7	–	–	–	–	–
d5_42_EQ_Taft_+73mm	40	11.9	3.51	1.09	1	11.9	1.09	191	0.04	10.0	82	1.3	0.12	191	0.07	8.0
d5_43_EQ_Taft_-73mm	40	6.0	1.44	0.45	9	4.9	0.32	137	0.07	5.6	90	1.3	0.11	179	0.07	7.8
d5_44_EQ_Taft_-78mm	40	8.6	2.23	0.89	4	7.1	0.53	150	0.04	7.4	58	1.3	0.12	187	0.07	7.9
d5_45_EQ_Taft_+78mm	40	16.3	2.76	1.24	1	16.3	1.24	158	0.01	4.8	19	1.0	0.08	191	0.08	8.8
d5_46_R_2mm_200ms	30	0.6	0.18	0.05	6	0.5	0.04	193	0.10	7.6	2	–	–	–	–	–
d5_47_R_4mm_200ms	30	1.0	0.28	0.09	6	0.9	0.07	158	0.08	7.2	10	–	–	–	–	–
d5_48_R_4mm_100ms	30	3.3	0.63	0.24	4	3.0	0.21	141	0.06	5.7	7	1.5	0.09	116	0.16	6.3
d5_49_EQ_Taft_+22mm	30	1.6	0.31	0.11	12	1.4	0.09	135	0.08	6.3	51	–	–	–	–	–
d5_50_EQ_Taft_-22mm	30	1.8	0.37	0.11	11	1.5	0.09	125	0.08	6.3	58	–	–	–	–	–
d5_51_EQ_Taft_-45mm	30	4.6	0.72	0.27	8	3.8	0.19	102	0.07	5.5	104	1.2	0.08	135	0.07	6.7
d5_52_EQ_Taft_+45mm	30	4.1	0.61	0.23	11	3.4	0.16	98	0.08	5.8	108	1.3	0.08	139	0.07	6.6
d5_53_EQ_Taft_+67mm	30	8.6	1.56	0.54	4	7.0	0.34	98	0.08	5.1	94	1.4	0.08	121	0.06	6.7
d5_54_EQ_Taft_-67mm	40	11.5	1.72	0.84	1	11.5	0.84	152	0.02	4.3	31	1.6	0.10	127	0.05	6.9
d5_55_EQ_Taft_-84mm	45	9.5	1.40	0.69	10	7.8	0.38	100	0.07	4.8	64	1.6	0.09	118	0.05	7.0
d5_56_EQ_Taft_+84mm	45	17.5	3.29	1.32	1	17.5	1.32	156	−0.01	4.5	23	1.6	0.11	133	0.04	7.3
d5_57_EQ_Taft_+89mm	45	15.6	2.71	1.24	4	12.9	0.67	104	0.03	4.2	17	1.7	0.08	81	0.04	6.6
d5_58_EQ_Taft_-89mm	45	12.4	1.16	0.57	14	10.0	0.33	69	0.09	3.9	26	1.8	0.08	89	0.07	5.3
d5_59_EQ_Taft_-95mm	45	13.4	1.24	0.55	12	11.5	0.35	62	0.09	3.8	34	1.9	0.09	85	0.06	5.4
d5_60_EQ_Taft_+95mm	45	14.7	1.98	1.10	9	11.7	0.45	77	0.07	3.5	36	2.0	0.08	77	0.05	5.7
d5_61_EQ_Taft_+100mm	45	17.1	1.84	1.03	6	13.8	0.47	71	0.09	3.5	11	2.0	0.10	83	0.04	6.0
d5_62_EQ_Taft_-100mm	45	21.6	1.42	0.56	2	19.1	0.45	50	0.09	2.9	16	2.0	0.07	71	0.05	5.6

Table S.11: Legend for Figure S.31.

Colour	Input motion type
■	Pulse test
■	Harmonic test
■	Earthquake test

Data series style	Meaning
—●—	Maximum measured value of the respective properties.
○	Mean result from cyclic response analysis, calculated in the large response range (70–100% of max response).
+	Mean result from cyclic response analysis, calculated in the small response range (0.5–3.0 mm).
– – – – –	Represents the secant stiffness calculated as max force excursion divided by max displacement excursion.

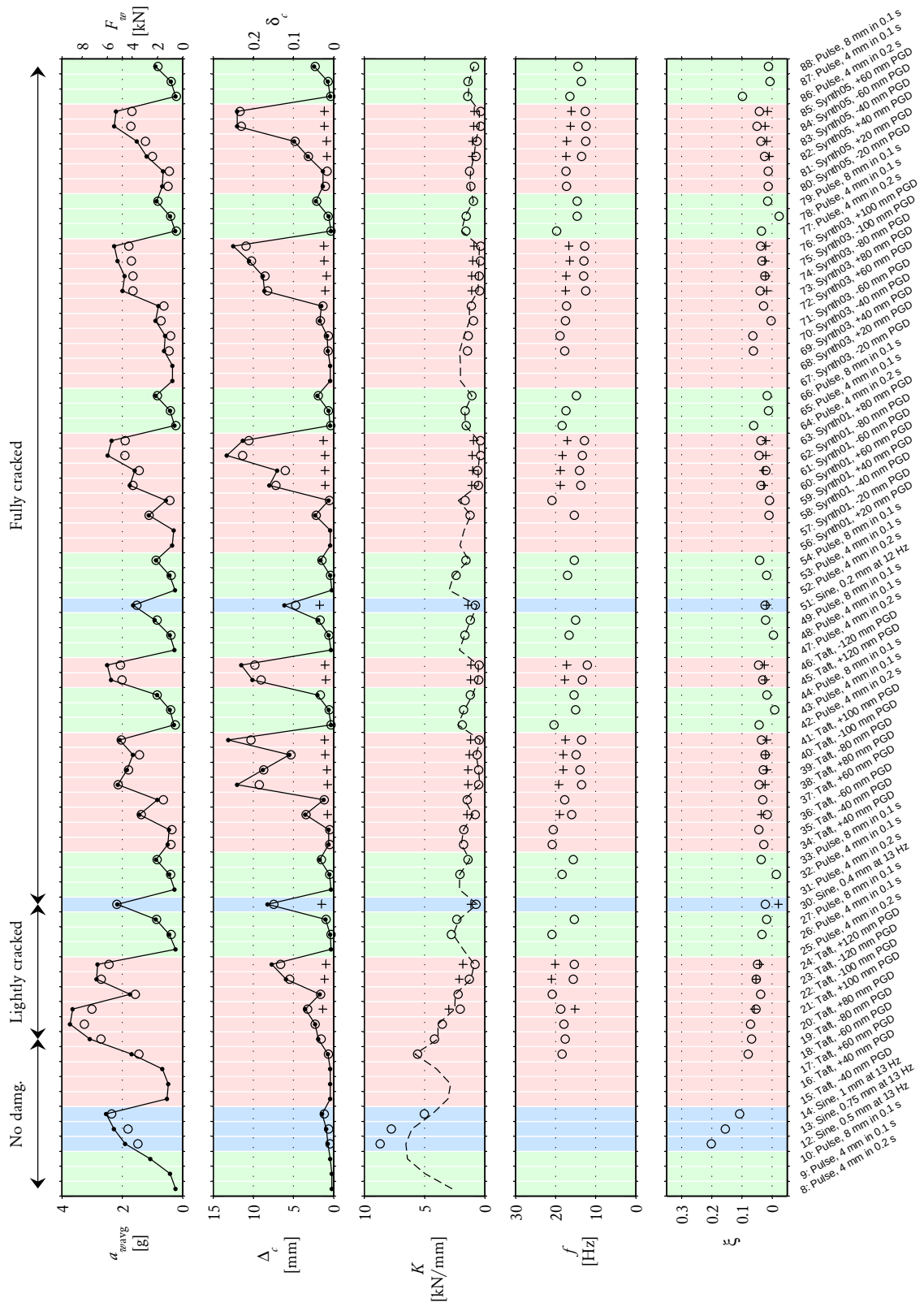

Figure S.29: Test sequence and key results for wall D1. Legend in Table S.11.

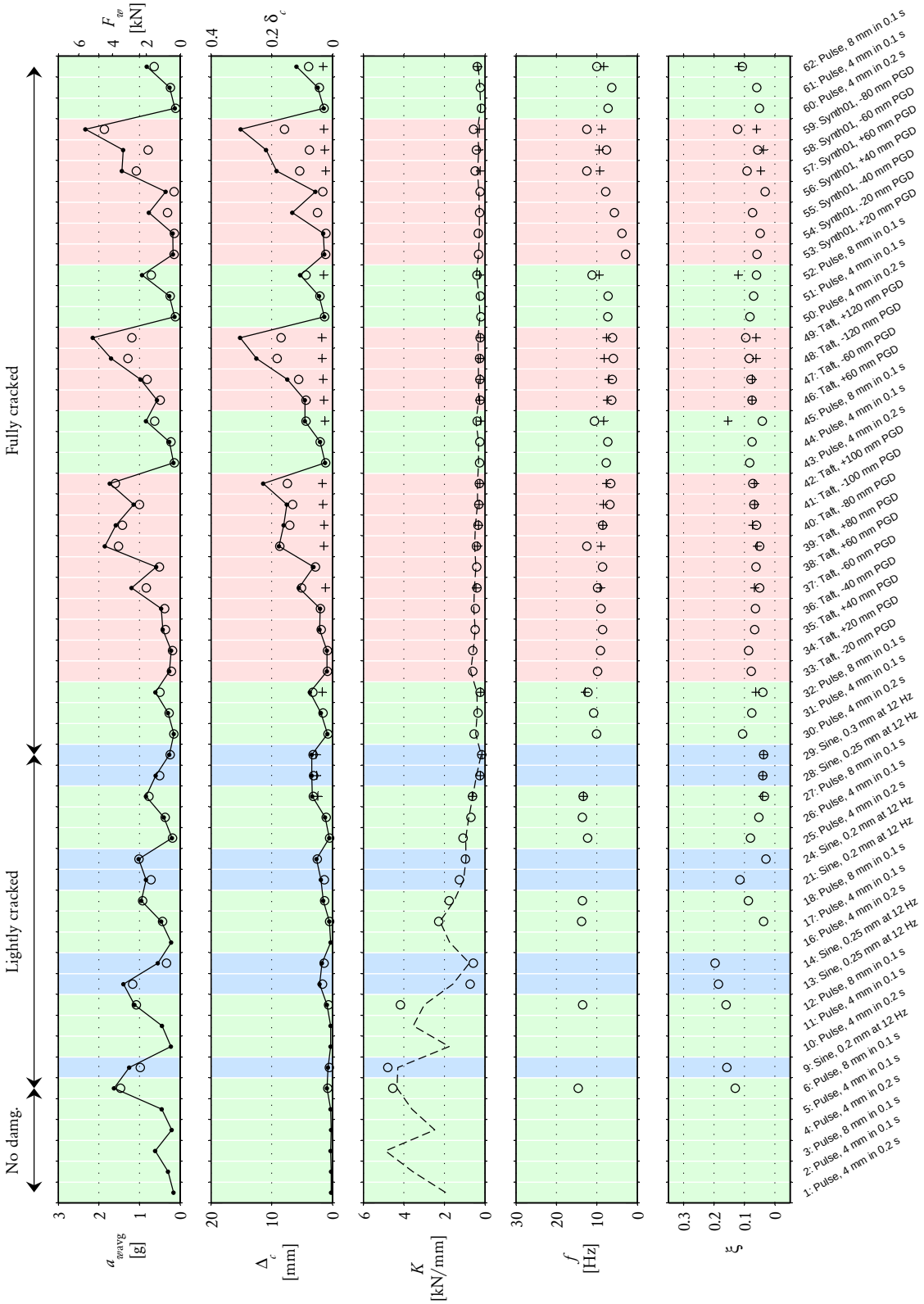

Figure S.30: Test sequence and key results for wall D2. Legend in Table S.11.

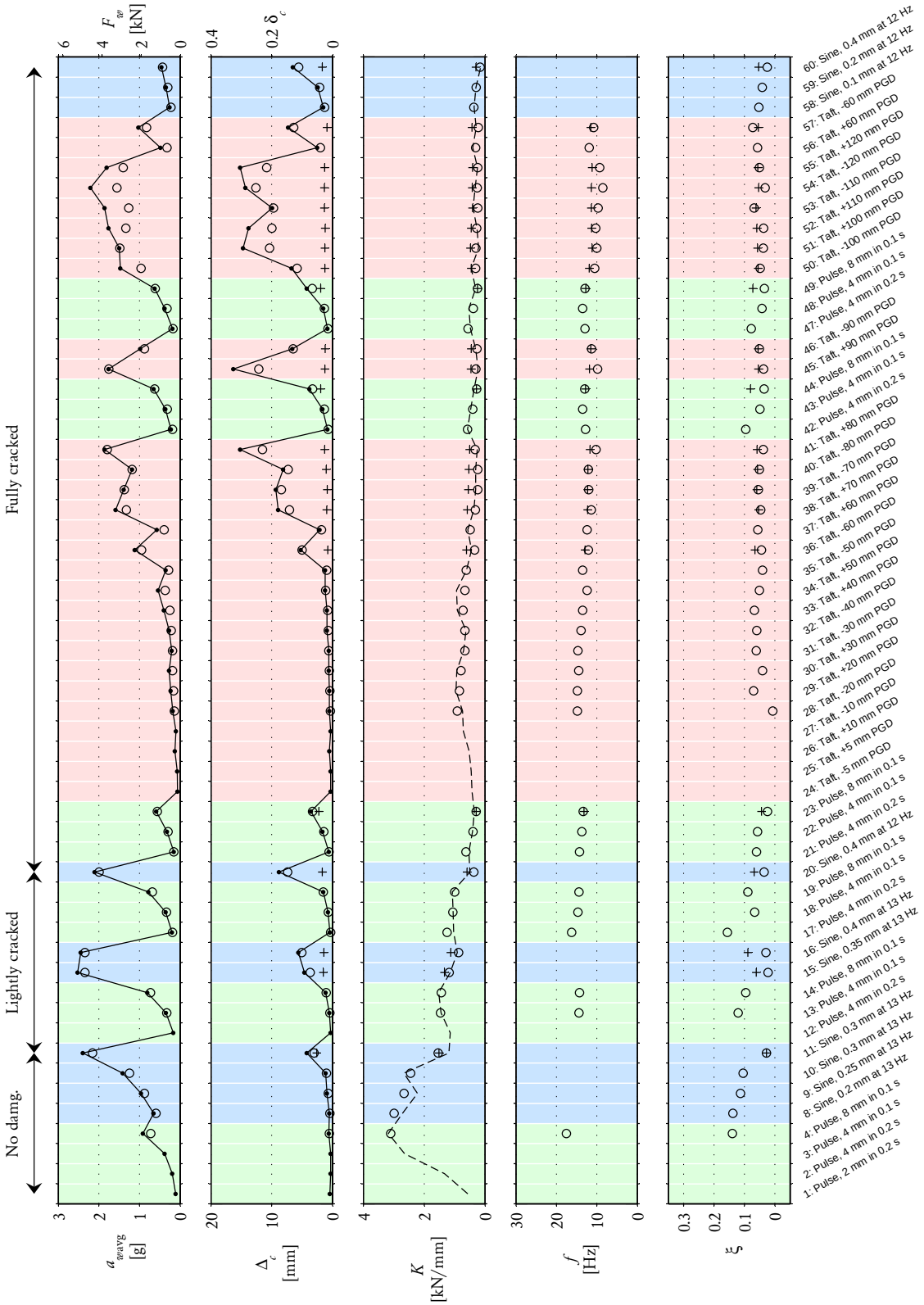

Figure S.31: Test sequence and key results for wall D3. Legend in Table S.11.

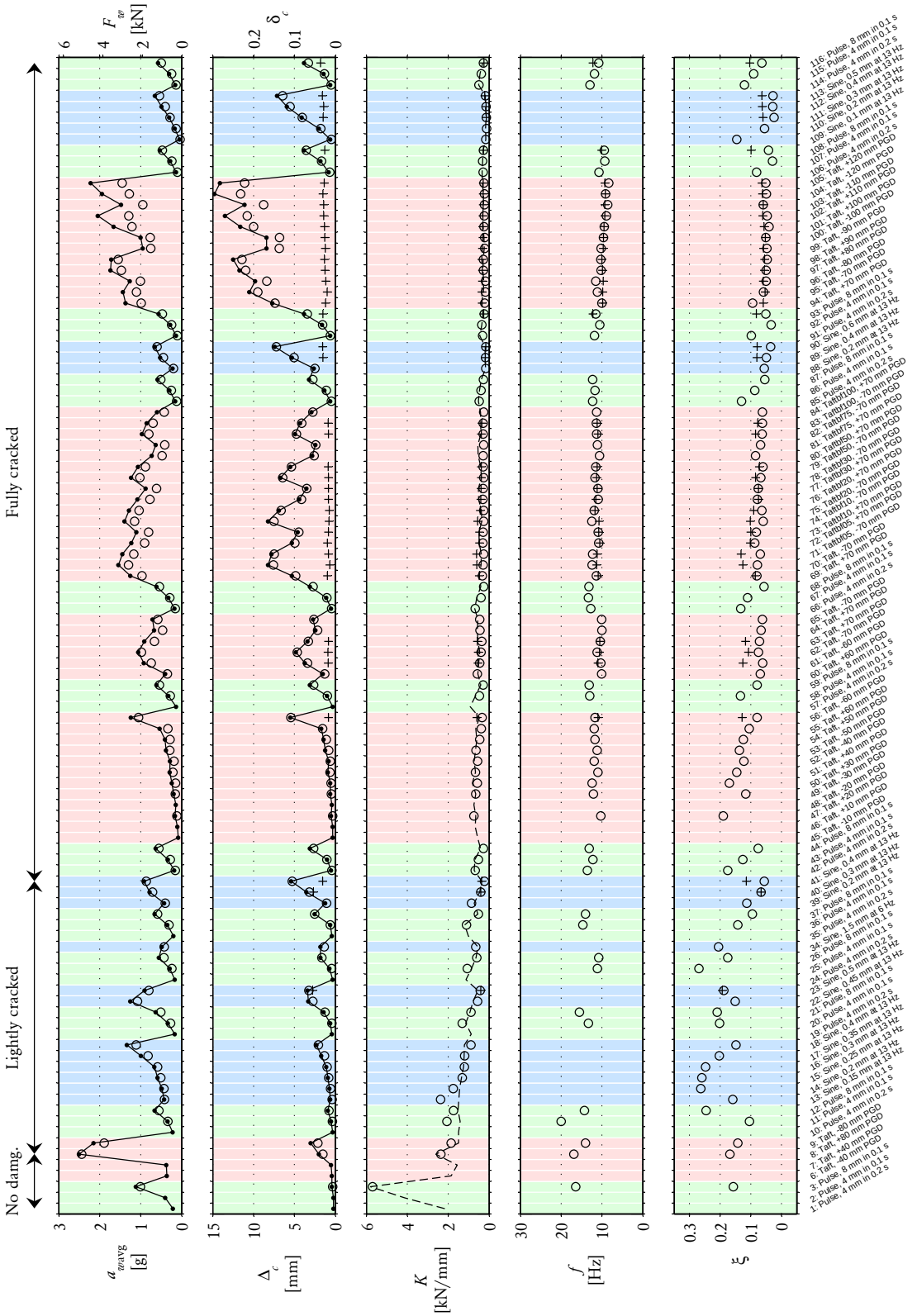

Figure S.32: Test sequence and key results for wall D4. Legend in Table S.11.

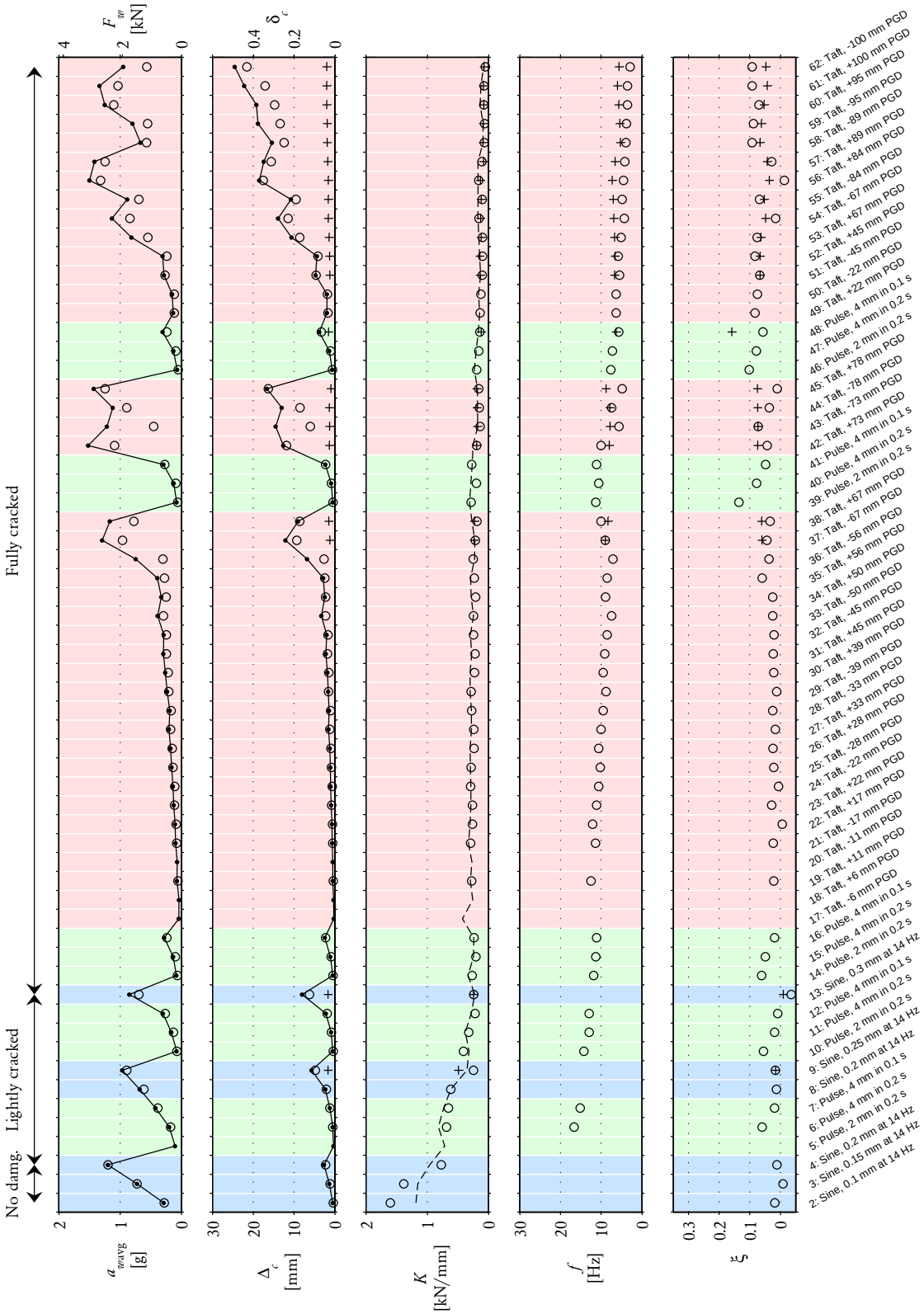

Figure S.33: Test sequence and key results for wall D5. Legend in Table S.11.

S.6 Data Filtering

Although the data acquisition system incorporated an analogue frequency domain filter[30], the recorded data still exhibited some degree of high frequency noise. Therefore, additional frequency domain filtering was performed to remove this noise and thereby 'smoothen' the data for subsequent use in the cyclic response analysis (presented in Section S.5). Different types of filters were applied depending on whether the test was periodic (i.e. harmonic tests) or non-periodic (i.e. pulse and earthquake tests). These will now be described in more detail.

S.6.1 Periodic Tests

Because of the periodicity of the harmonic tests, the associated Fourier spectra for displacement and acceleration data inherently contained peaks at integer multiples of the fundamental excitation frequency f_o. This is demonstrated by Figure S.34 which shows a typical example of unfiltered wall response during a harmonic test. Whilst it can be seen that most spectral content is within the first harmonic, it is the subsequent peaks which are responsible for the more intricate character of the hysteresis loops such as pinching. Several different frequency filters as shown in Figure S.35 were trialled to assess their suitability:

1. $\boldsymbol{f_o}$ **bandpass filter**: Filter retaining only the spectral content at the excitation frequency. The filter tested was a Butterworth filter of order $n = 5$ with a cutoff frequency bandwidth of ± 1 Hz centred around f_o. For example, for $f_o = 12$ Hz a cutoff band of $[11, 13]$ Hz was used.

2. $\boldsymbol{f_o}$**+2**$\boldsymbol{f_o}$ **bandpass filter**: Bandpass filter retaining spectral content across the first and second harmonics (i.e. f_o and $2f_o$). The trialled filter was a Butterworth filter of order $n = 7$ with a cutoff frequency bandwidth between $0.5f_o$ and $2.5f_o$. For example, for $f_o = 12$ Hz a cutoff band of $[6, 30]$ Hz was used.

3. $\boldsymbol{f_o}$**+2**$\boldsymbol{f_o}$ **comb filter**: Comb filter passing only spectral content at the first and second harmonics. This filter was constructed using a Butterworth filter curve, by applying to each peak a pass zone with total frequency bandwidth equal to 20% of f_o at order $n = 5$. For example, for $f_o = 12$ Hz the first harmonic (12 Hz) had a cutoff band of $[10.8, 13.2]$ Hz, and the second harmonic (24 Hz) had a cutoff band of $[22.8, 25.2]$ Hz.

An example of data filtered using each of the above filters is shown in Figure S.36 in terms of the resulting hysteresis loops. It is seen that the f_o bandpass filter has the inherent effect of producing hysteresis loops which are elliptical, since it causes the data approach a sinusoidal shape. Whilst such loops are smoother compared to the unfiltered data, they lose their finer characteristics due to the removal of the spectral content at the higher harmonics ($2f_o$, $3f_o \ldots$). By contrast, the f_o+$2f_o$ bandpass and comb filters preserve some of the additional detail in the shape of the loops.

To provide a quantitative measure of filter performance, a series of analyses were performed in which the indicator parameters Δ_{amp}, a_{amp}, K and ξ_{hyst} were calculated for every cycle occurring during a 2 second time window in the middle of the test run.[31] This process was carried out for every harmonic test run using both unfiltered data as well as data filtered with each of the three candidate filters. The criteria used to evaluate the suitability of the filters were as follows:

- To ensure that the mean values of the indicator parameters computed during the 2 second window did not differ significantly between the filtered and unfiltered data. This criterion was intended to ensure that the data were not over-filtered.

[30] Lowpass Butterworth filter with a cutoff frequency of 50 Hz.

[31] Note that the calculation of these parameters used the wall's average acceleration $a_{\text{w.avg}}$, whereas in the final results reported (in Section S.5) the wall's central acceleration $a_{\text{w.cent}}$ was used to calculate the hysteretic damping ratio ξ_{hyst}.

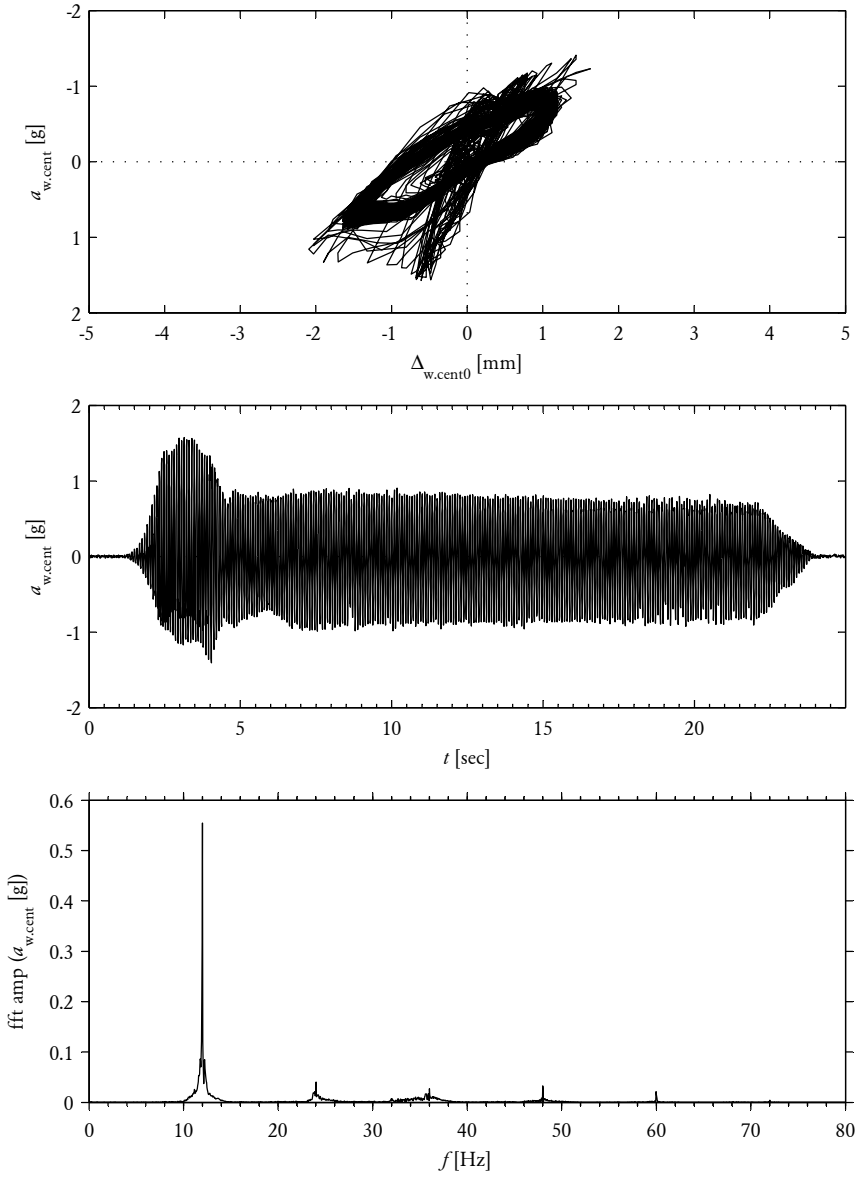

Figure S.34: Example of unfiltered response from harmonic test, including hysteresis plot (top), time domain response (middle) and frequency domain response (bottom). Shown for test run `d2_13_H_12Hz_0.25mm`.

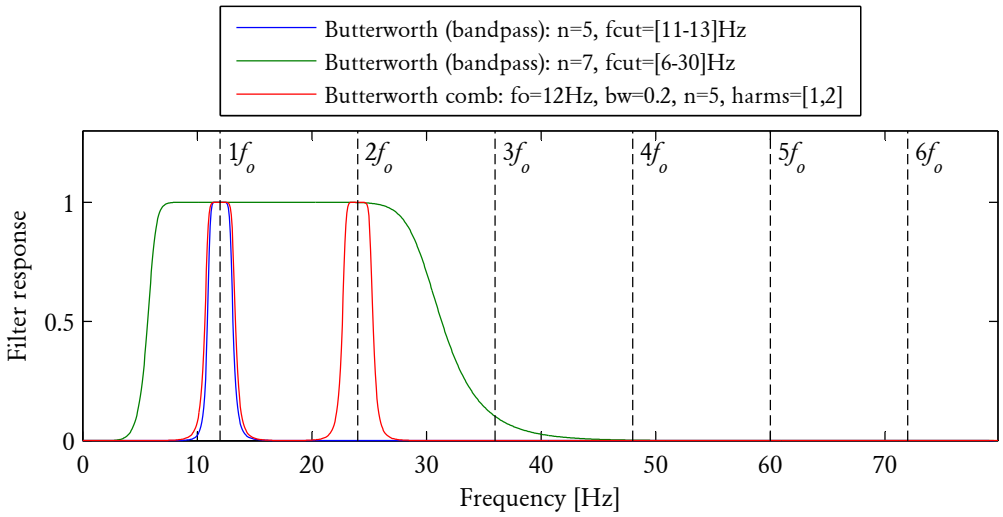

Figure S.35: Types of filters trialled for harmonic test data. For the filters shown, the fundamental frequency is taken as $f_o = 12$ Hz.

- To reduce the amount of data noise. This was assessed by comparing the variability [as the coefficient of variation (COV) or standard deviation (STD)] in the indicator parameter values computed during the 2 second time window. A lower value of COV was deemed to indicate better filter performance.

Of the three filters considered (Figure S.35), the f_o+$2f_o$ comb filter had the best performance with respect to the above criteria. In general, the mean values of parameters obtained using this filter were similar to those from the unfiltered data, whilst considerably improving (i.e. reducing) the variability. This can be seen from Figure S.37 which graphs the filtered versus unfiltered results for each of the four indicator parameters.

By comparison, the f_o bandpass filter produced loops that were inherently elliptical in shape (as shown by the example in Figure S.36b). Whilst this filter was effective in reducing scatter in the results, due to the elliptical shape it had a tendency to produce higher apparent values of equivalent damping ξ_{hyst} and effective stiffness K relative to the unfiltered data. On this basis, this filter was deemed to be unconservative for derivation of these values and therefore unsuitable.

The f_o+$2f_o$ bandpass filter was found to be more effective than the f_o bandpass filter on the basis of mean values, but less effective in terms being able to reduce scatter and therefore sufficiently clean the data. An example of the resulting hysteresis loops is shown by Figure S.36c.

On the basis of this study, the comb filter was deemed to be the most effective and was adopted in subsequent analyses whose results are reported in Section S.5.4. The final choice of filter used for harmonic tests was a comb filter passing the spectral content at the first three harmonics (f_o, $2f_o$ and $3f_o$) with a normalised bandwidth of 0.2 (20% of the fundamental frequency). Figure S.38 shows an example of response obtained using this filter, which can be compared to the original unfiltered response in Figure S.34.

S.6.2 Non-Periodic Tests

Due to the non-periodic nature of the pulse and earthquake tests, the Fourier spectra of the associated data vectors were markedly different to those from the periodic harmonic tests and therefore required a different filtering approach. Typical examples of unfiltered response from

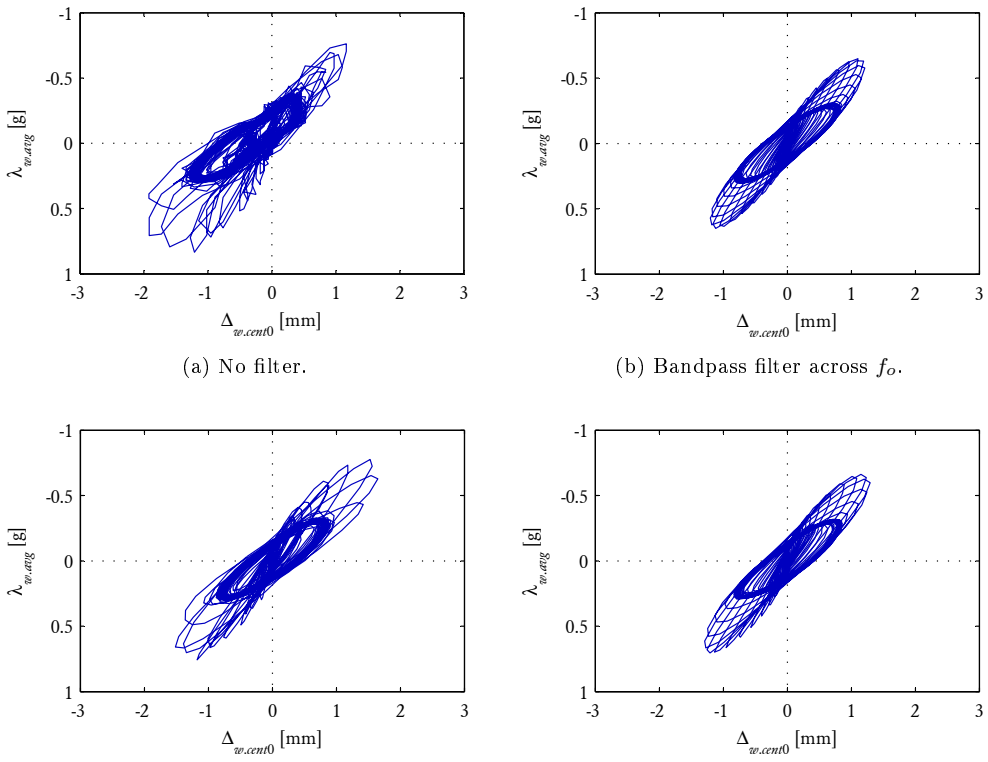

(a) No filter.

(b) Bandpass filter across f_o.

(c) Bandpass filter across f_o and $2f_o$.

(d) Comb filter across f_o and $2f_o$.

Figure S.36: Example comparing the hysteresis loop shape for data filtered using different types of filter. Shown for test run `d2_21_H_12Hz_0.2mm`.

earthquake and pulse tests are shown by Figures S.39 and S.41, respectively, where it is seen that the Fourier spectra contained a broad frequency range, compared to the harmonic tests where the peaks were localised to integer multiples of the fundamental frequency (Figure S.34). This made it possible to utilise a lowpass filter in order to eliminate the high frequency noise. Examples of the filtered response for earthquake and pulse test runs are shown by Figures S.40 and S.42, which can be compared to the original unfiltered the response in Figures S.39 and S.41.

Prior to conducting the cyclic response analysis reported in Section S.5, data from all earthquake and pulse test runs was filtered using a lowpass Butterworth filter with order $n = 10$. The cutoff frequency (f_c) of the filter was manually chosen on a case-by-case basis for each individual test run. The criteria used to select an appropriate value of f_c was to make f_c as low as possible without significantly reducing the maximum response of key variables, including the wall's central displacement ($\Delta_{\text{w.cent}}$), central acceleration ($a_{\text{w.cent}}$), table acceleration (a_{tab}), support acceleration ($a_{\text{sup.avg}}$), and relative acceleration between the centre of the wall and the supports ($a_{\text{w.cent-sup.avg}}$). The cutoff frequency used for each test run is summarised in the main results table for the cyclic response analysis, Table S.10.

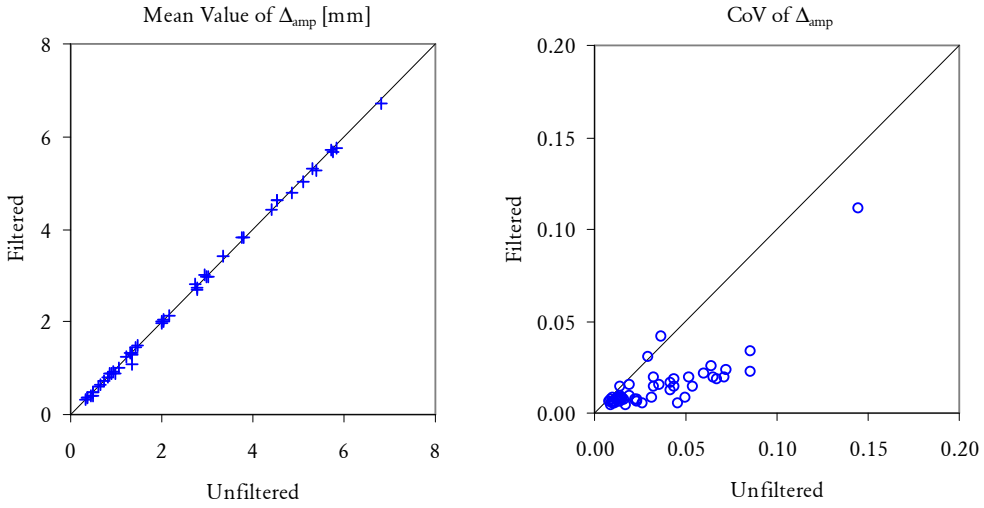

(a) Displacement cycle amplitude Δ_{amp}.

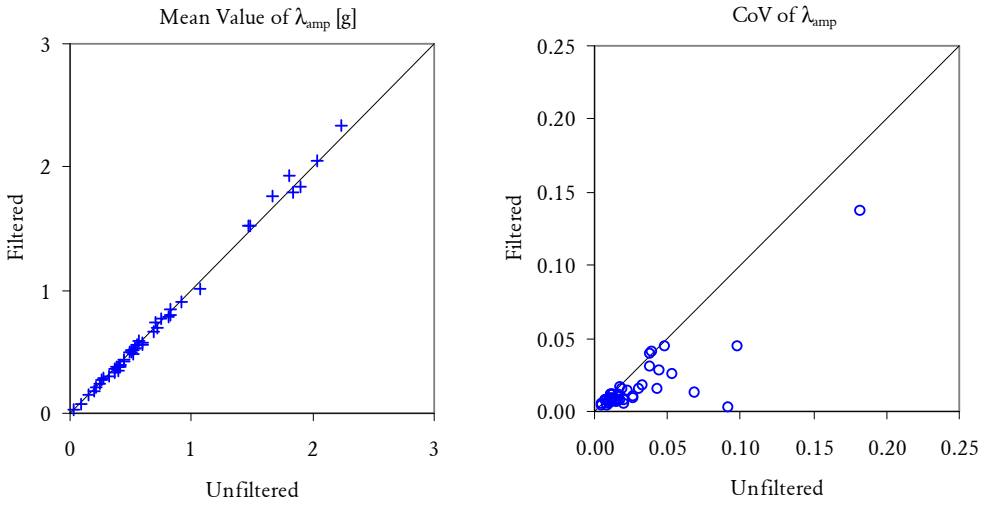

(b) Acceleration cycle amplitude a_{amp}.

Figure S.37: Comparison of key parameters derived from filtered and unfiltered harmonic test data. In the case of filtered data, a comb filter was applied capturing the response at the first and second harmonics of the excitation frequency. Each parameter was calculated over a time window of 2 seconds in the middle of the test run, with the mean value and level of variability (as COV or STD) over this duration being plotted in these graphs. Results are plotted for all harmonic test runs performed, except for runs where the mean displacement amplitude was small (< 0.3 mm), which are omitted.

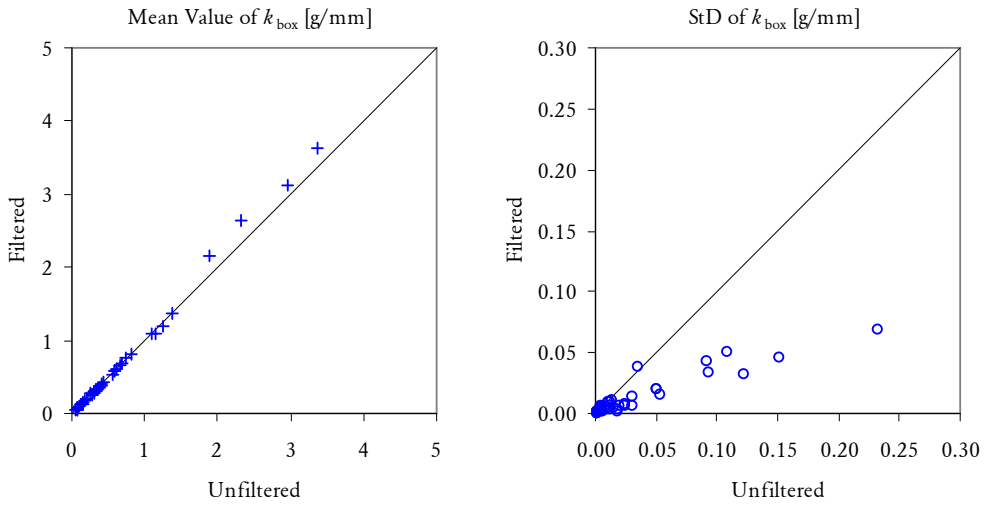

(c) Effective secant stiffness K (as a/Δ).

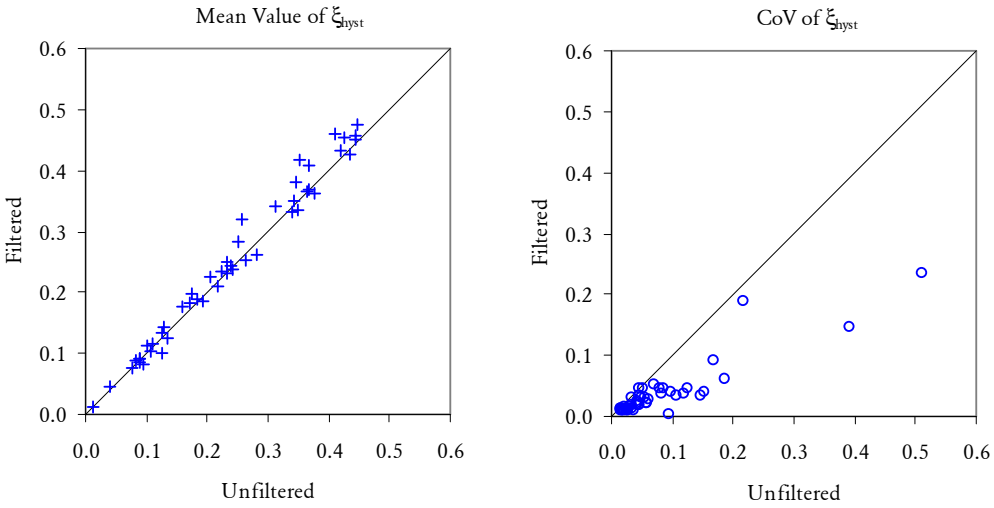

(d) Hysteretic damping ratio ξ_{hyst}.

Figure S.37: (cont'd).

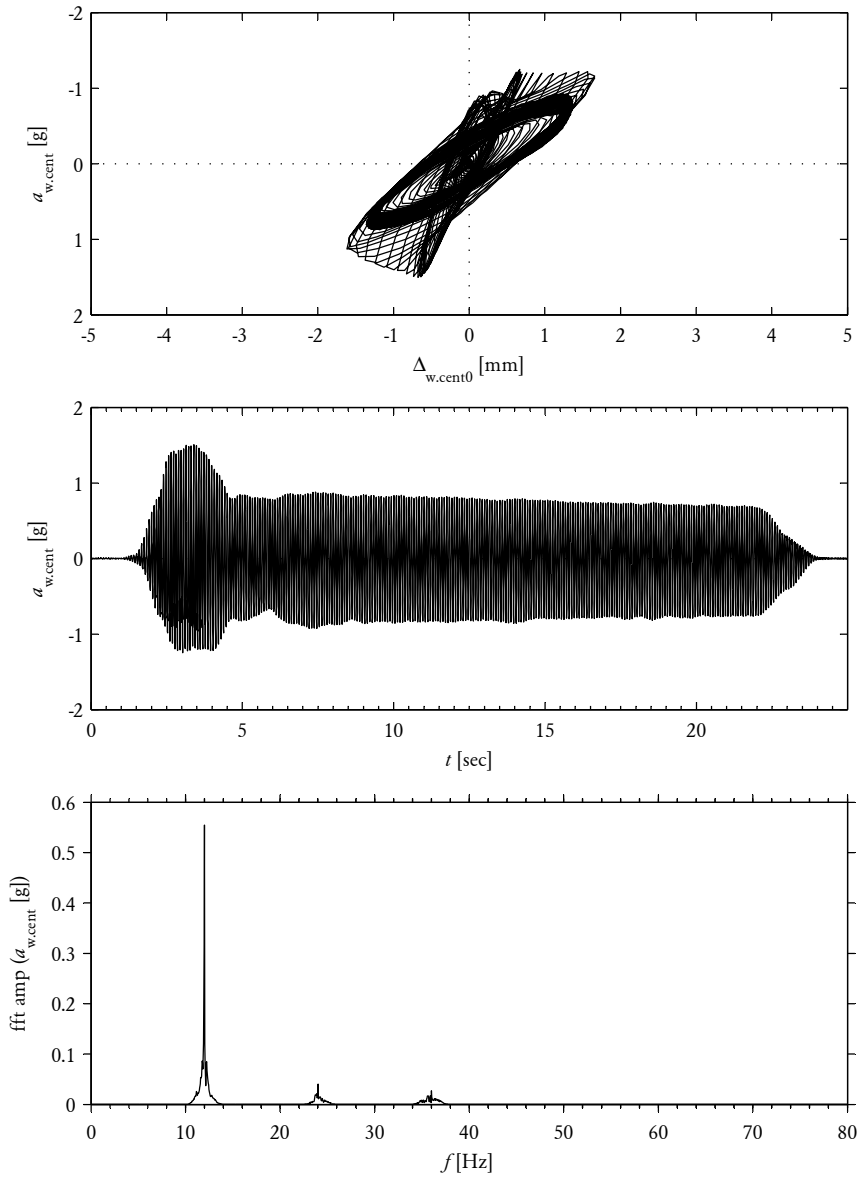

Figure S.38: Example of filtered response from harmonic test, including hysteresis plot (top), time domain response (middle) and frequency domain response (bottom). Shown for test run `d2_13_H_12Hz_0.25mm` combined with comb filter passing the spectral content at the first three harmonics (i.e. f_o, $2f_o$ and $3f_o$).

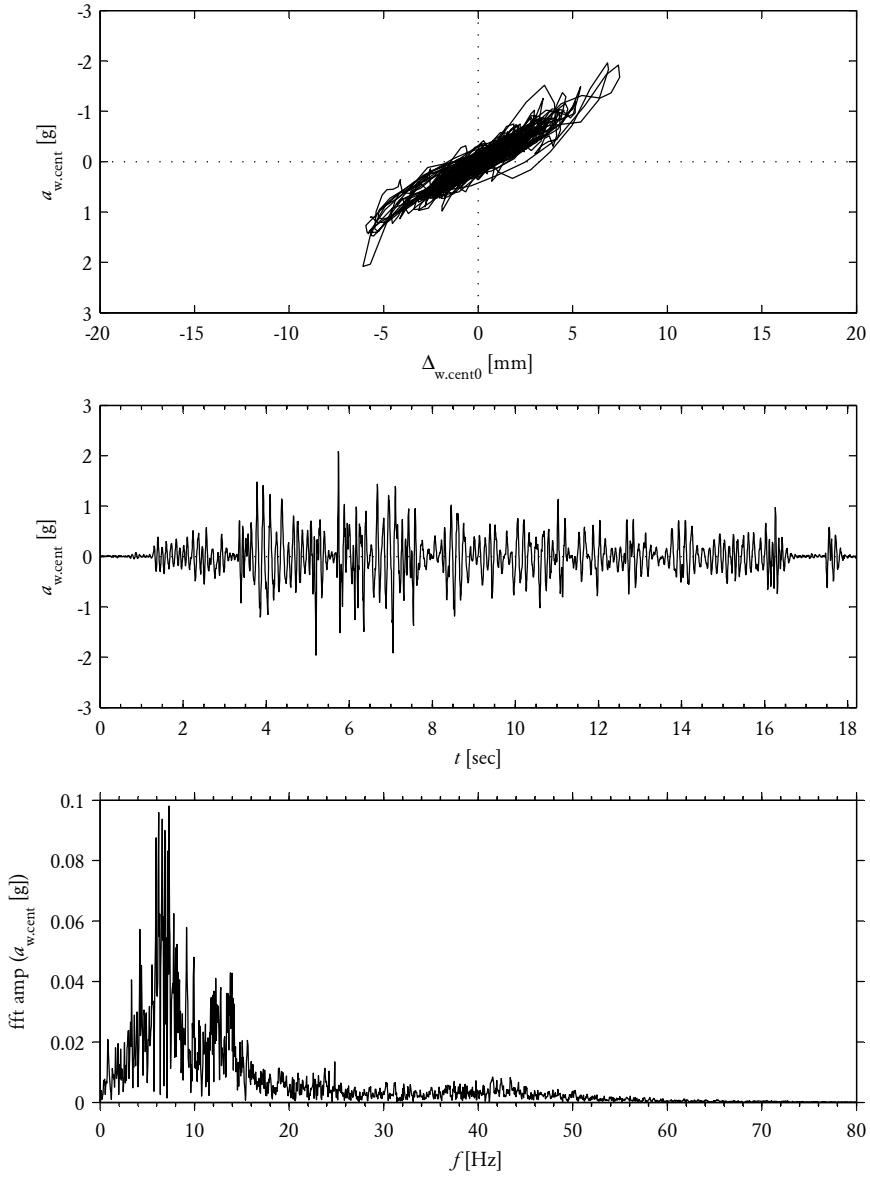

Figure S.39: Example of unfiltered response from earthquake test, including hysteresis plot (top), time domain response (middle) and frequency domain response (bottom). Shown for test run `d2_41_EQ_Taft_-100mm`.

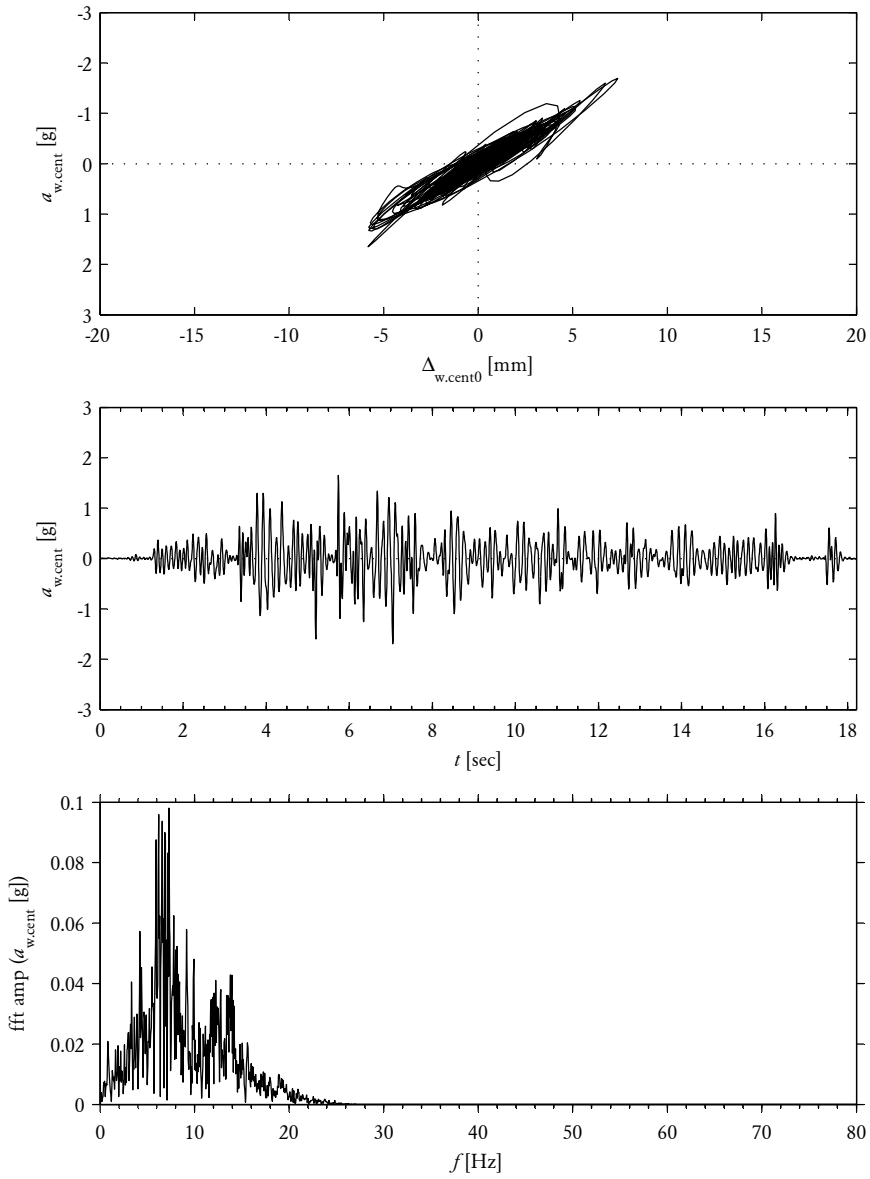

Figure S.40: Example of filtered response from earthquake test, including hysteresis plot (top), time domain response (middle) and frequency domain response (bottom). Shown for test run `d2_41_EQ_Taft_-100mm` combined with lowpass Butterworth filter with order $n = 10$ and cutoff frequency $f_c = 20$ Hz.

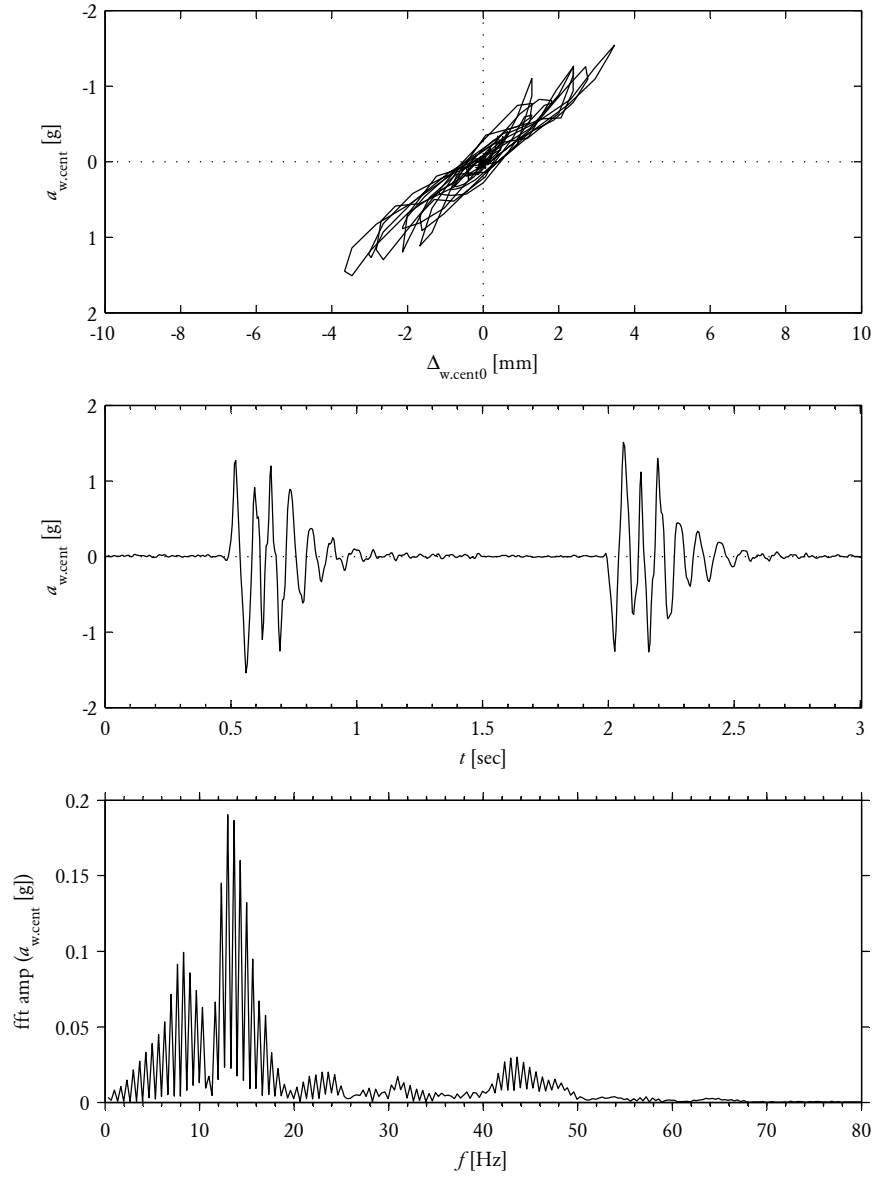

Figure S.41: Example of unfiltered response from pulse test, including hysteresis plot (top), time domain response (middle) and frequency domain response (bottom). Shown for test run `d2_32_R_8mm_100ms`.

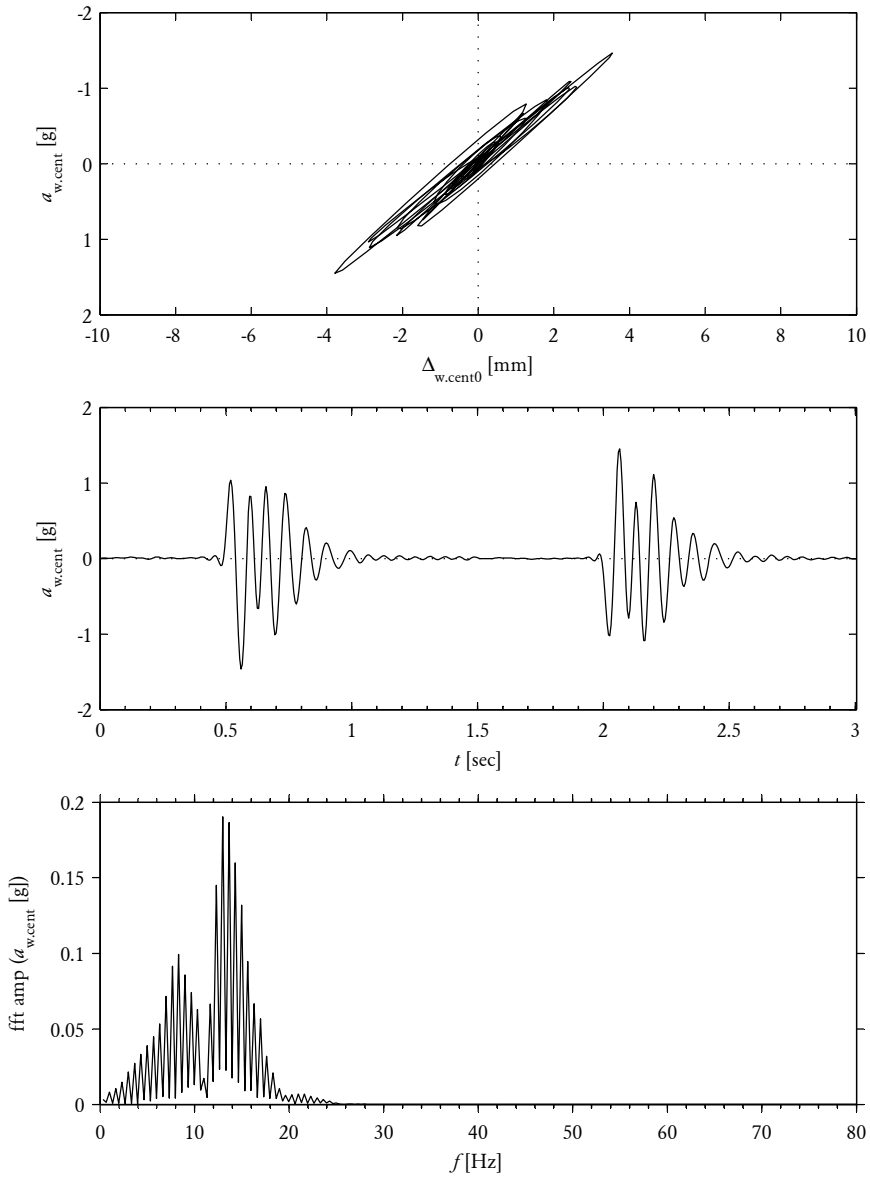

Figure S.42: Example of filtered response from pulse test, including hysteresis plot (top), time domain response (middle) and frequency domain response (bottom). Shown for test run `d2_32_R_8mm_100ms` combined with lowpass Butterworth filter with order $n = 10$ and cutoff frequency $f_c = 20$ Hz.

S.7 Force-Displacement Graphs

This section provides force-displacement response plots from all individual test runs performed. The plotted data were filtered using techniques described in Section S.6 and are the same data used for the cyclic response analysis (Section S.5). Two sets of axes are provided for each test run: The left axes plot the wall's central acceleration $a_{\mathrm{w.cent}}$ versus the normalised central displacement $\delta_{\mathrm{w.cent}}$ (i.e. $\Delta_{\mathrm{w.cent}}$ divided by the wall thickness of 50 mm). The right axes plot the wall's average acceleration $a_{\mathrm{w.avg}}$ versus $\delta_{\mathrm{w.cent}}$. The largest displacement cycle occurring in each test run is also highlighted, but only if the displacement amplitude exceeded 0.3 mm.

S.7.1 Wall D1

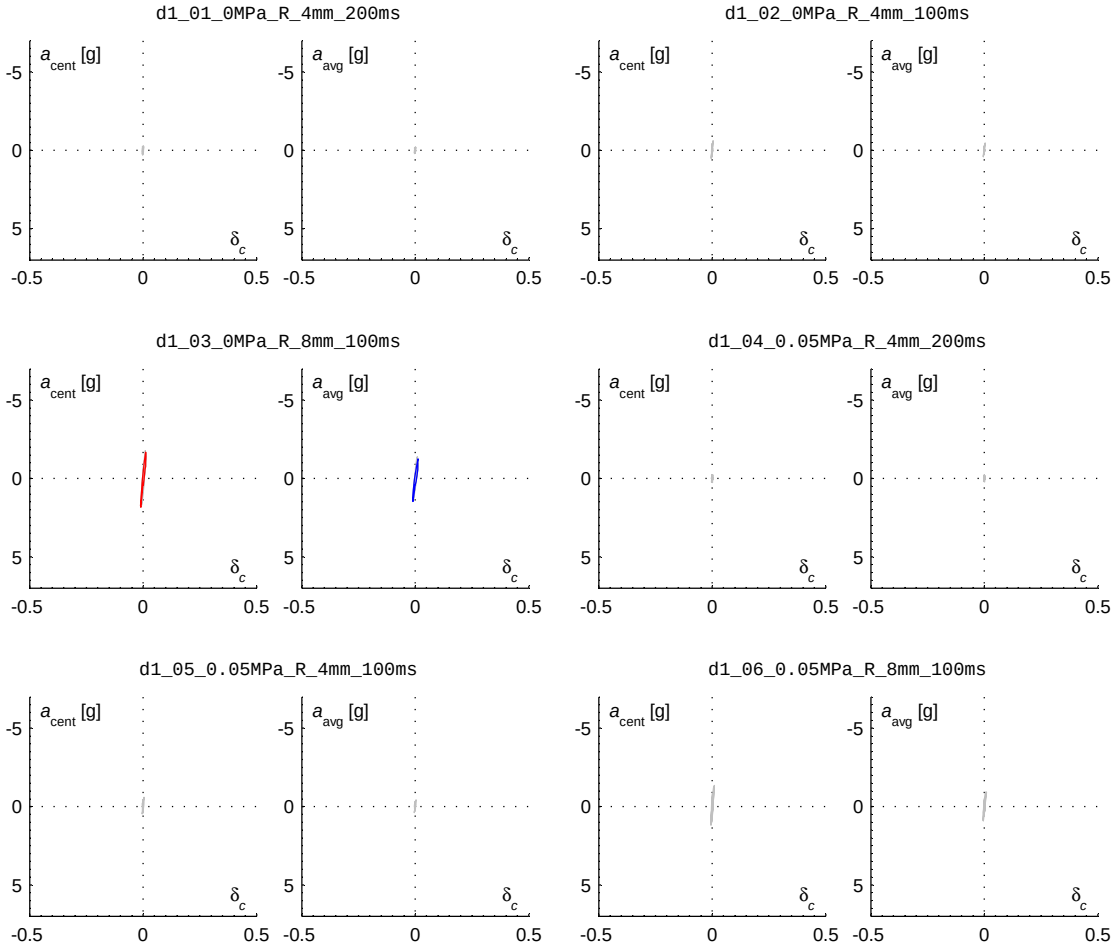

d1_08_0.10MPa_R_4mm_200ms

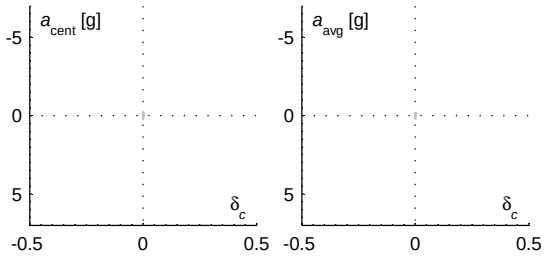

d1_09_0.10MPa_R_4mm_100ms

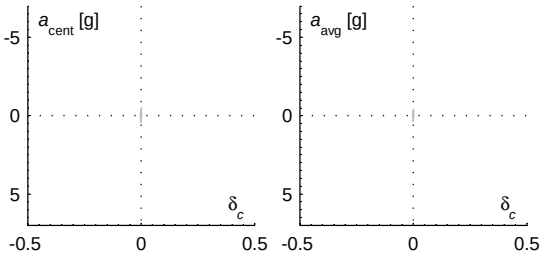

d1_10_0.10MPa_R_8mm_100ms

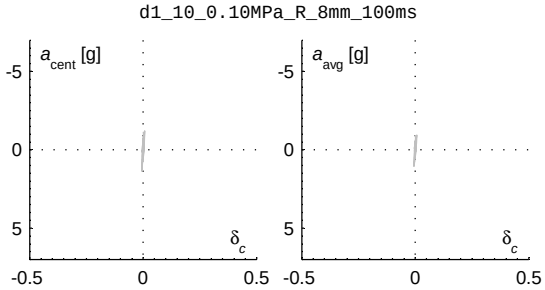

d1_11_H_13Hz_0.25mm

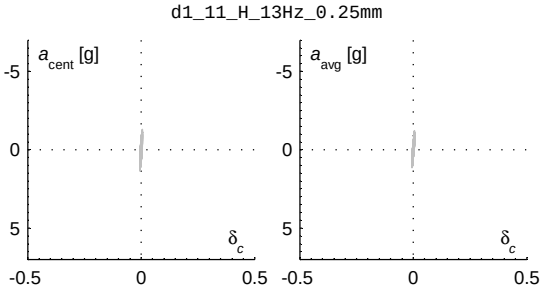

d1_12_H_13Hz_0.5mm

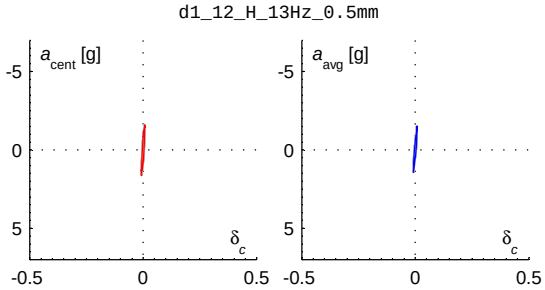

d1_13_H_13Hz_0.75mm

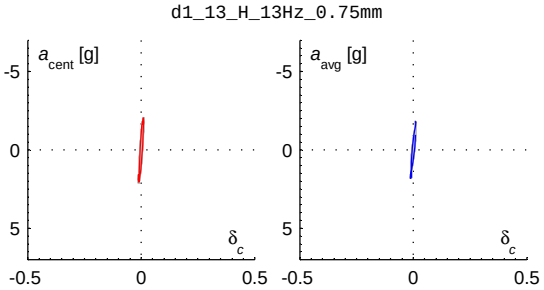

d1_14_H_13Hz_1mm

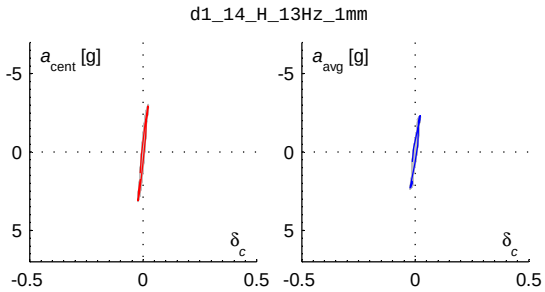

d1_15_EQ_Taft_-40mm

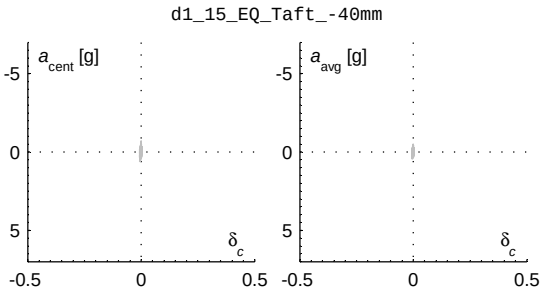

d1_16_EQ_Taft_+40mm

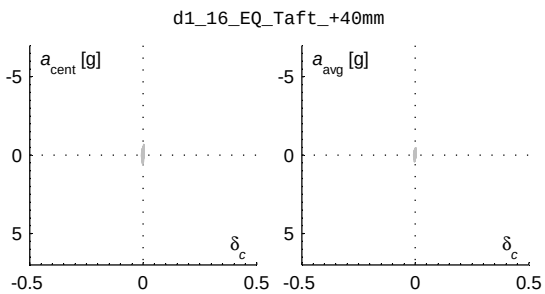

d1_17_EQ_Taft_+60mm

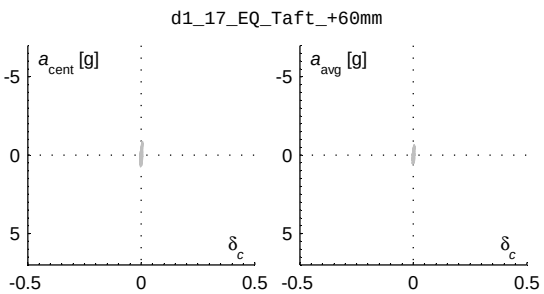

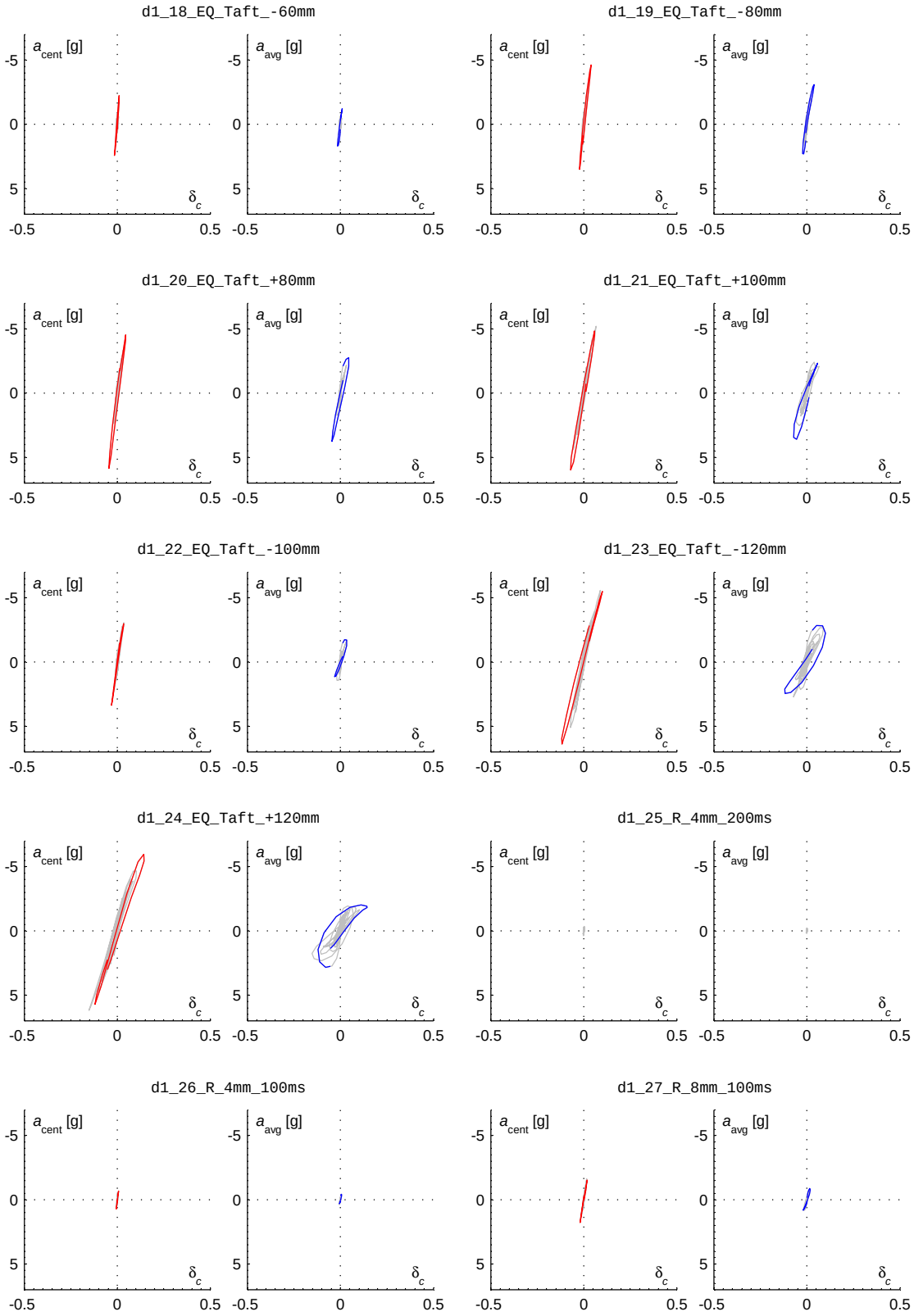
d1_18_EQ_Taft_-60mm
d1_19_EQ_Taft_-80mm
d1_20_EQ_Taft_+80mm
d1_21_EQ_Taft_+100mm
d1_22_EQ_Taft_-100mm
d1_23_EQ_Taft_-120mm
d1_24_EQ_Taft_+120mm
d1_25_R_4mm_200ms
d1_26_R_4mm_100ms
d1_27_R_8mm_100ms
a_cent [g]
a_avg [g]
δ_c
-5
0
5
-0.5
0
0.5

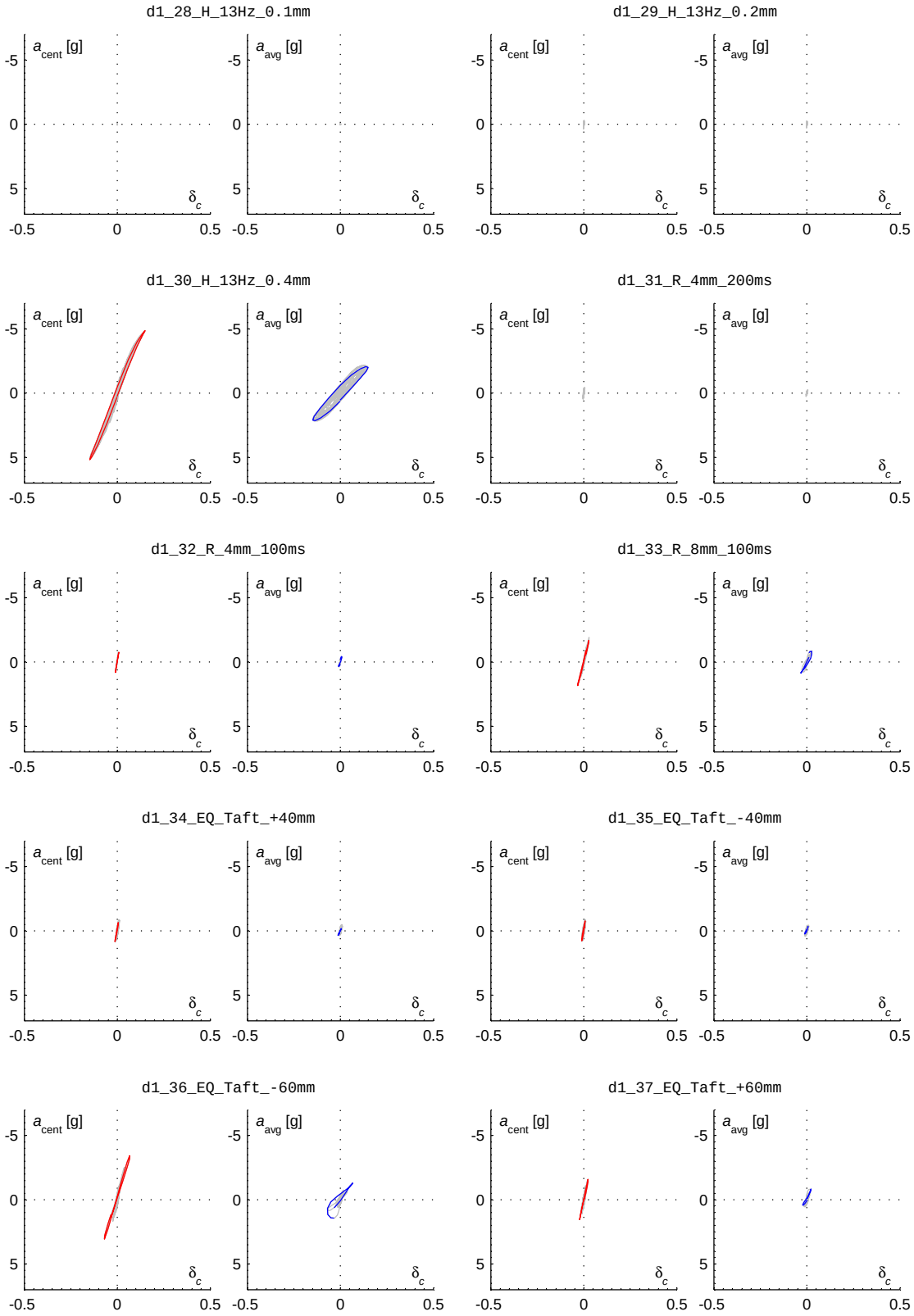
d1_28_H_13Hz_0.1mm
d1_29_H_13Hz_0.2mm
d1_30_H_13Hz_0.4mm
d1_31_R_4mm_200ms
d1_32_R_4mm_100ms
d1_33_R_8mm_100ms
d1_34_EQ_Taft_+40mm
d1_35_EQ_Taft_-40mm
d1_36_EQ_Taft_-60mm
d1_37_EQ_Taft_+60mm
a_cent [g]
a_avg [g]
δ_c
-5
0
5
-0.5
0
0.5

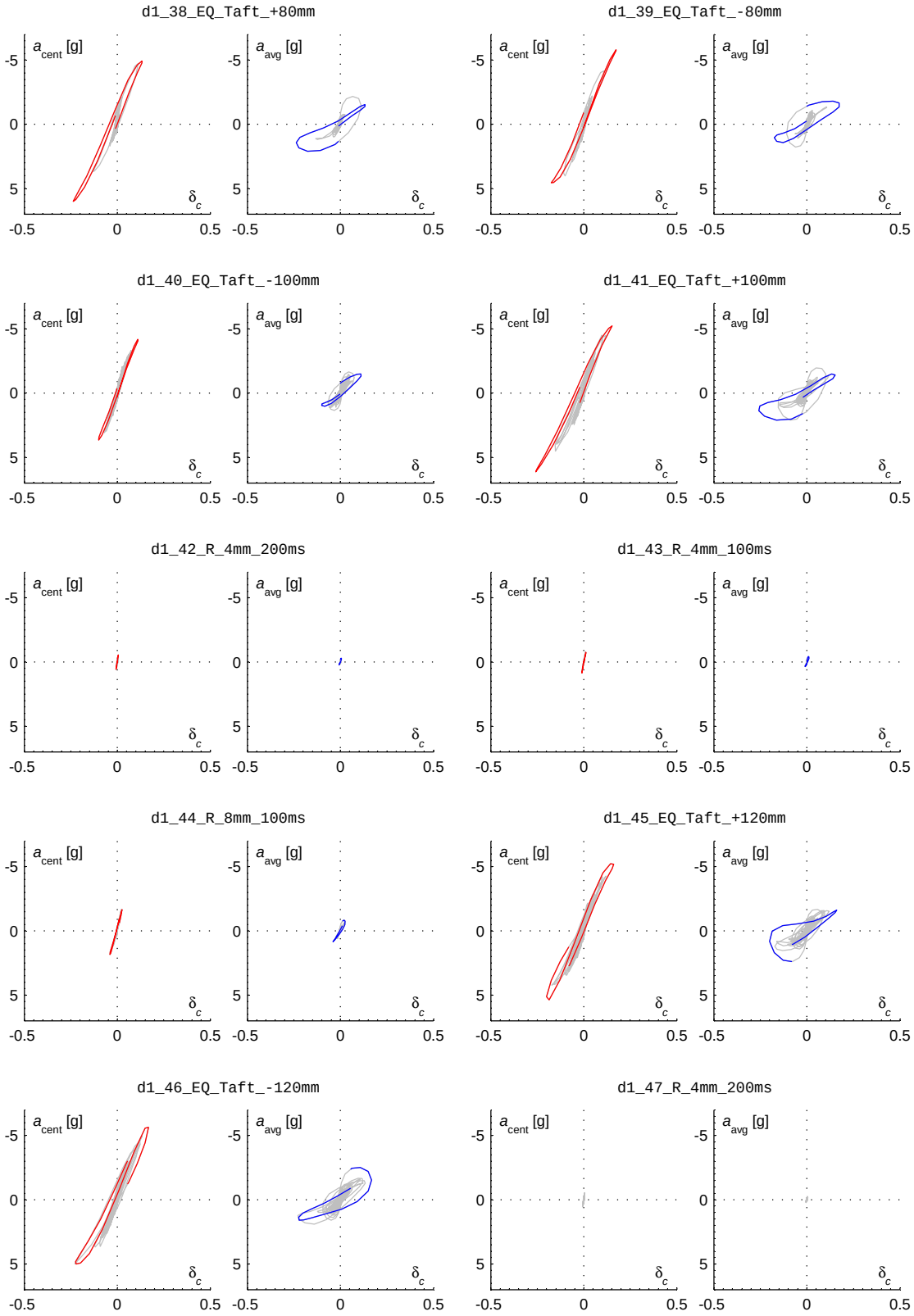
d1_38_EQ_Taft_+80mm
d1_39_EQ_Taft_-80mm
d1_40_EQ_Taft_-100mm
d1_41_EQ_Taft_+100mm
d1_42_R_4mm_200ms
d1_43_R_4mm_100ms
d1_44_R_8mm_100ms
d1_45_EQ_Taft_+120mm
d1_46_EQ_Taft_-120mm
d1_47_R_4mm_200ms
a_cent [g]
a_avg [g]
δ_c
-5
0
5
-0.5
0
0.5

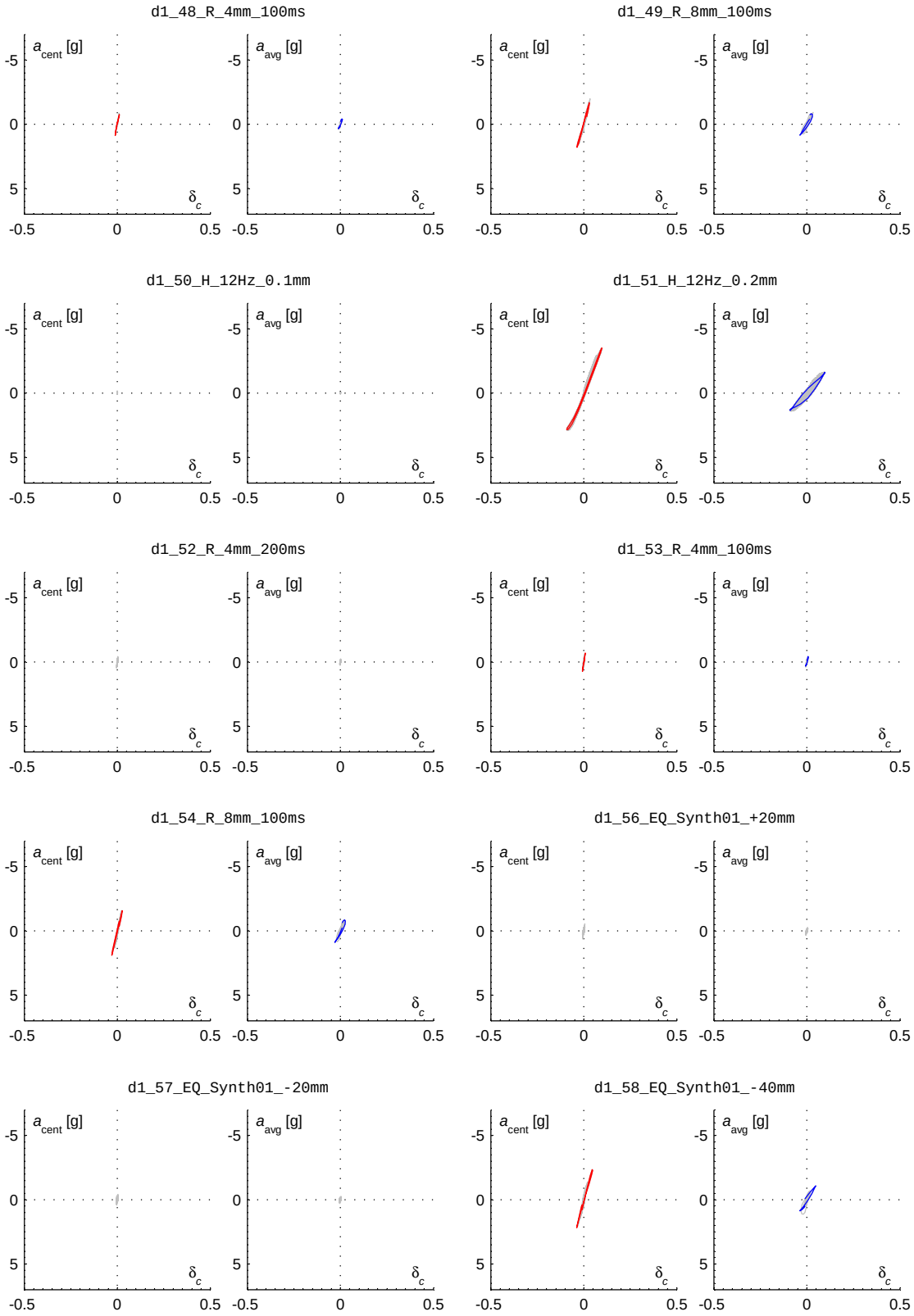
d1_48_R_4mm_100ms
d1_49_R_8mm_100ms
d1_50_H_12Hz_0.1mm
d1_51_H_12Hz_0.2mm
d1_52_R_4mm_200ms
d1_53_R_4mm_100ms
d1_54_R_8mm_100ms
d1_56_EQ_Synth01_+20mm
d1_57_EQ_Synth01_-20mm
d1_58_EQ_Synth01_-40mm
a_cent [g]
a_avg [g]
δ_c
-5
0
5
-0.5
0
0.5

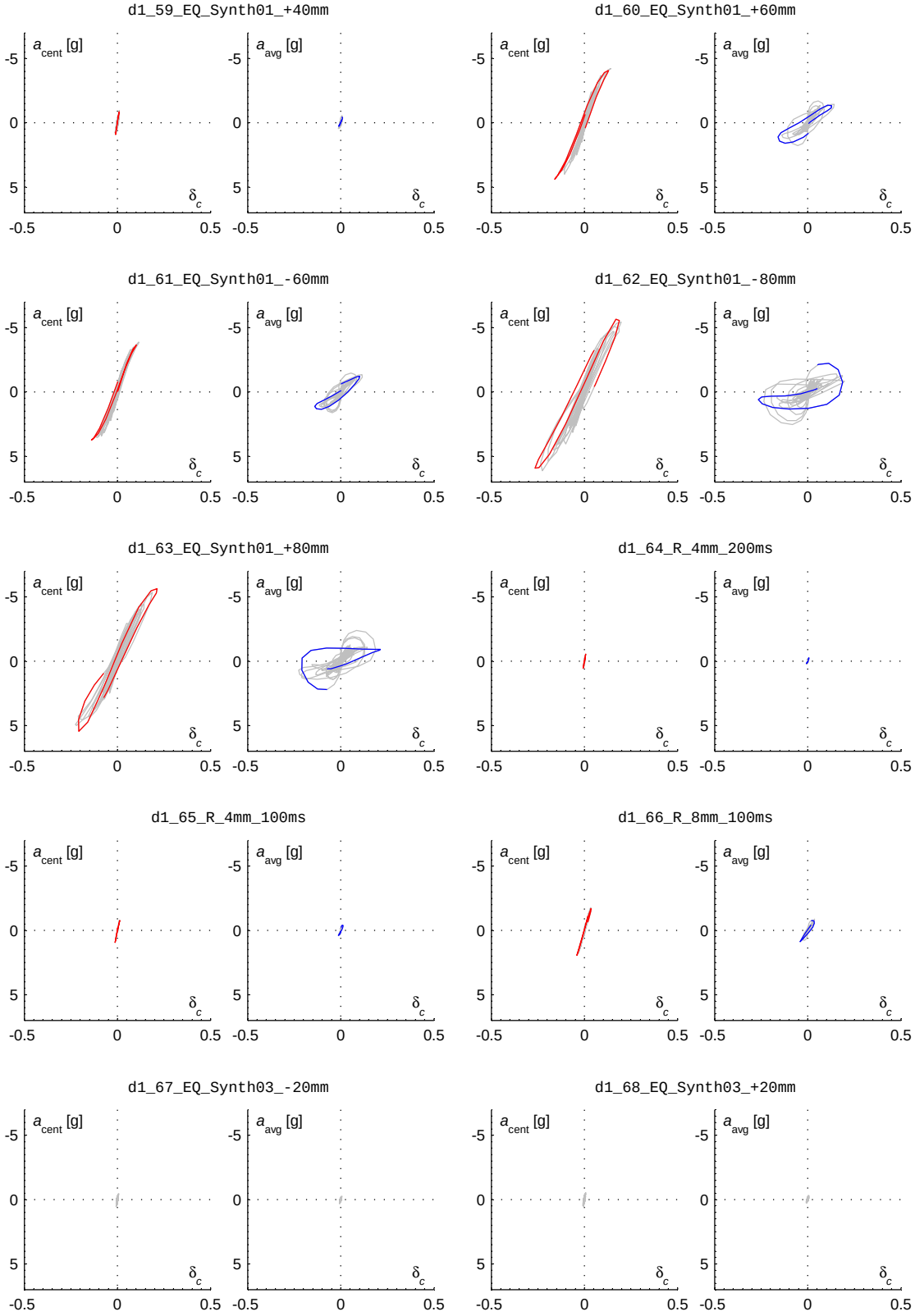
d1_59_EQ_Synth01_+40mm
d1_60_EQ_Synth01_+60mm
d1_61_EQ_Synth01_-60mm
d1_62_EQ_Synth01_-80mm
d1_63_EQ_Synth01_+80mm
d1_64_R_4mm_200ms
d1_65_R_4mm_100ms
d1_66_R_8mm_100ms
d1_67_EQ_Synth03_-20mm
d1_68_EQ_Synth03_+20mm
a_cent [g]
a_avg [g]
δ_c
-5
0
5
-0.5
0
0.5

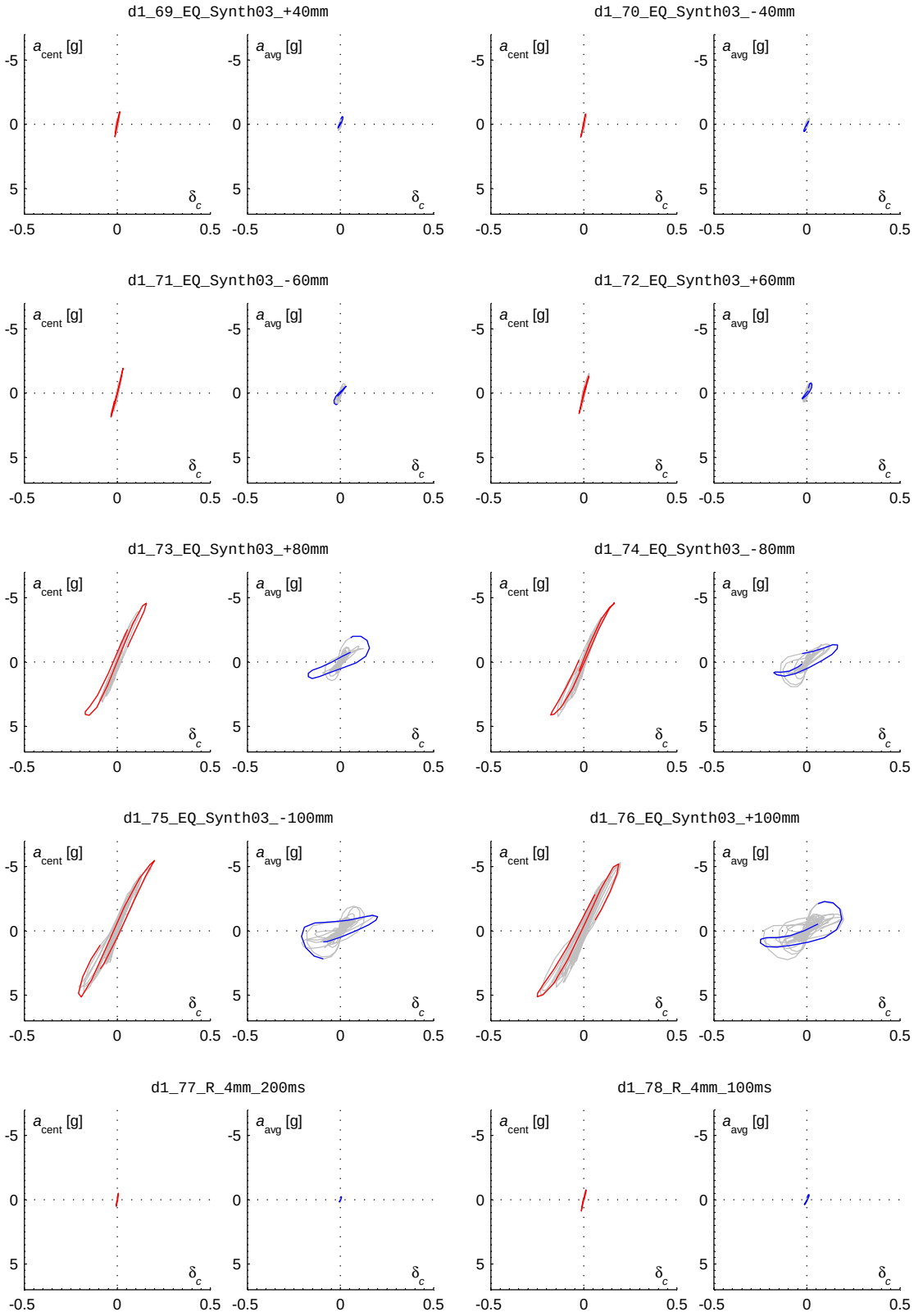
d1_69_EQ_Synth03_+40mm
d1_70_EQ_Synth03_-40mm
d1_71_EQ_Synth03_-60mm
d1_72_EQ_Synth03_+60mm
d1_73_EQ_Synth03_+80mm
d1_74_EQ_Synth03_-80mm
d1_75_EQ_Synth03_-100mm
d1_76_EQ_Synth03_+100mm
d1_77_R_4mm_200ms
d1_78_R_4mm_100ms
a_cent [g]
a_avg [g]
δ_c
-5
0
5
-0.5
0
0.5

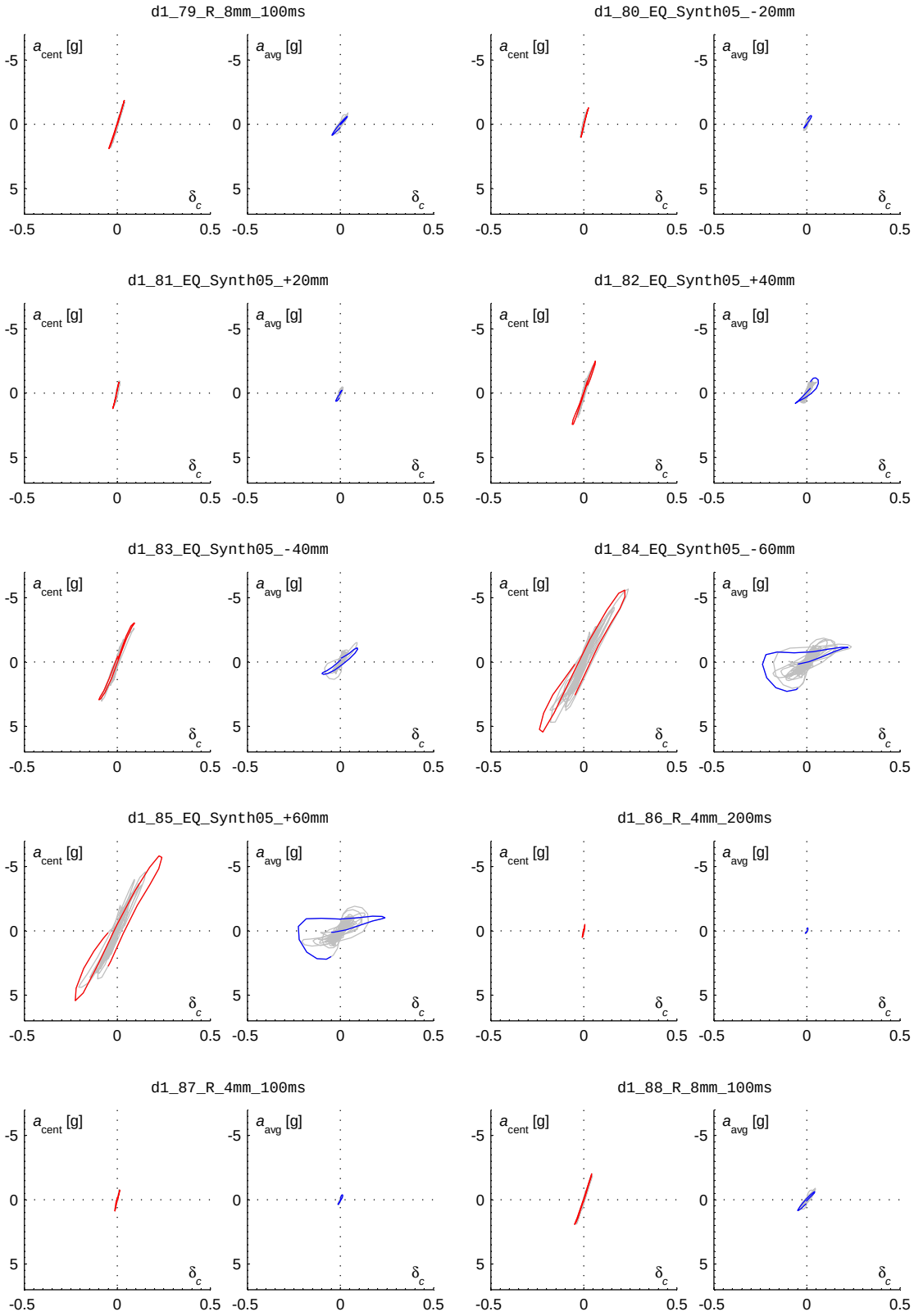
d1_79_R_8mm_100ms
d1_80_EQ_Synth05_-20mm
d1_81_EQ_Synth05_+20mm
d1_82_EQ_Synth05_+40mm
d1_83_EQ_Synth05_-40mm
d1_84_EQ_Synth05_-60mm
d1_85_EQ_Synth05_+60mm
d1_86_R_4mm_200ms
d1_87_R_4mm_100ms
d1_88_R_8mm_100ms
a_cent [g]
a_avg [g]
δ_c
-5
0
5
-0.5
0
0.5

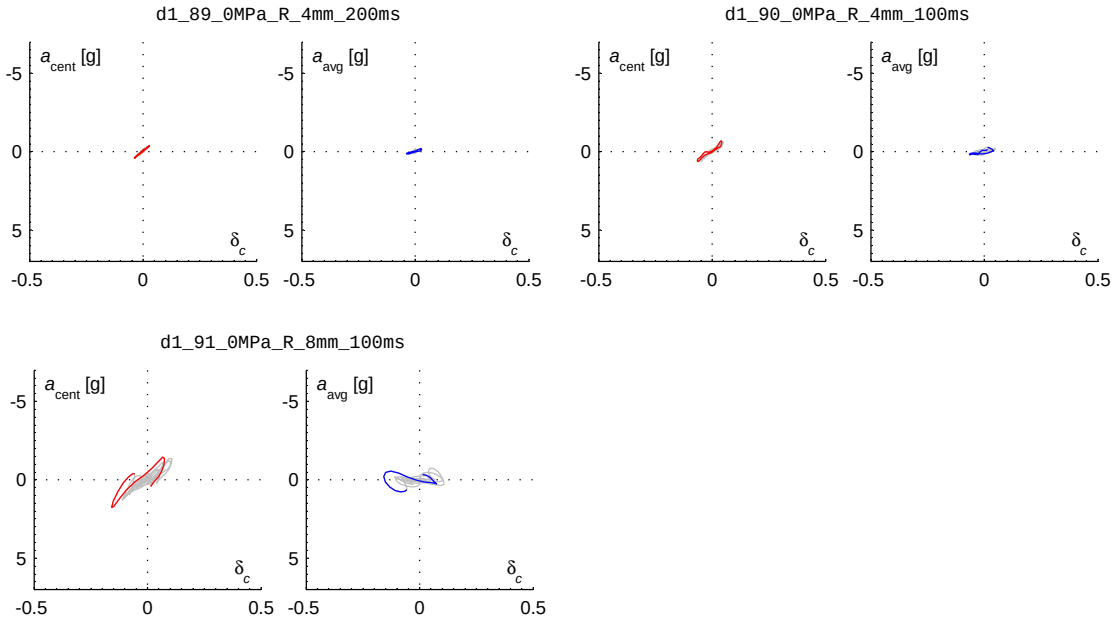
d1_89_0MPa_R_4mm_200ms
d1_90_0MPa_R_4mm_100ms
d1_91_0MPa_R_8mm_100ms
a cent [g]
a avg [g]
δc
-5
0
5
-0.5
0
0.5

S.7.2 Wall D2

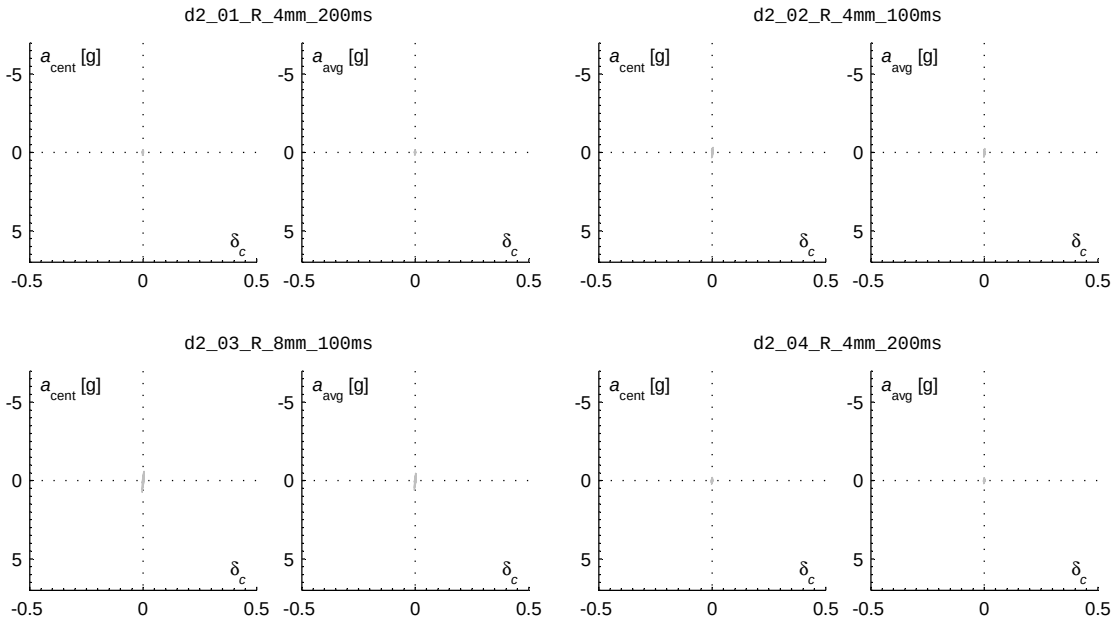
d2_01_R_4mm_200ms
d2_02_R_4mm_100ms
d2_03_R_8mm_100ms
d2_04_R_4mm_200ms
a cent [g]
a avg [g]
δc
-5
0
5
-0.5
0
0.5

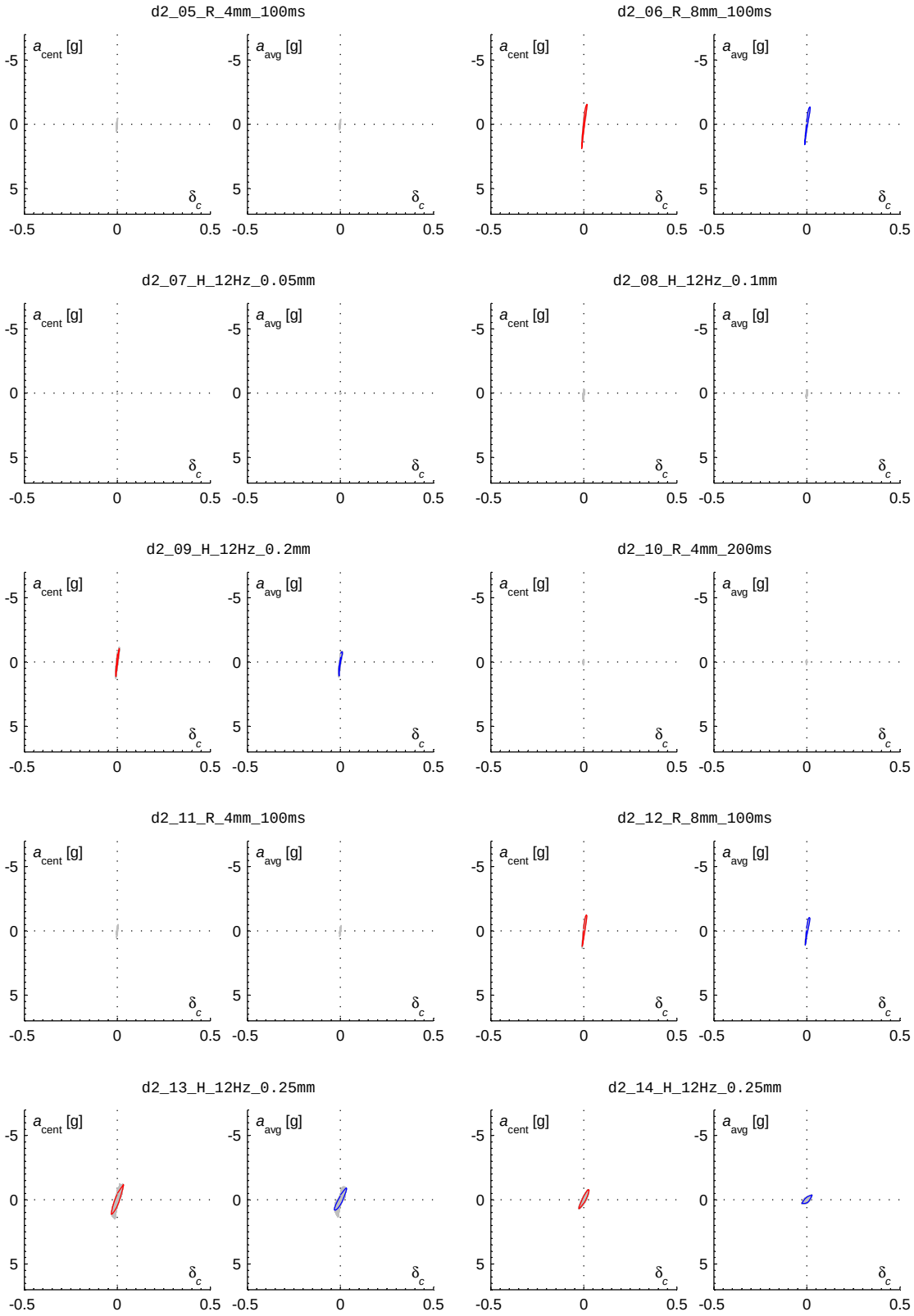
d2_05_R_4mm_100ms
d2_06_R_8mm_100ms
d2_07_H_12Hz_0.05mm
d2_08_H_12Hz_0.1mm
d2_09_H_12Hz_0.2mm
d2_10_R_4mm_200ms
d2_11_R_4mm_100ms
d2_12_R_8mm_100ms
d2_13_H_12Hz_0.25mm
d2_14_H_12Hz_0.25mm
a_cent [g]
a_avg [g]
δ_c
-5
0
5
-0.5
0
0.5

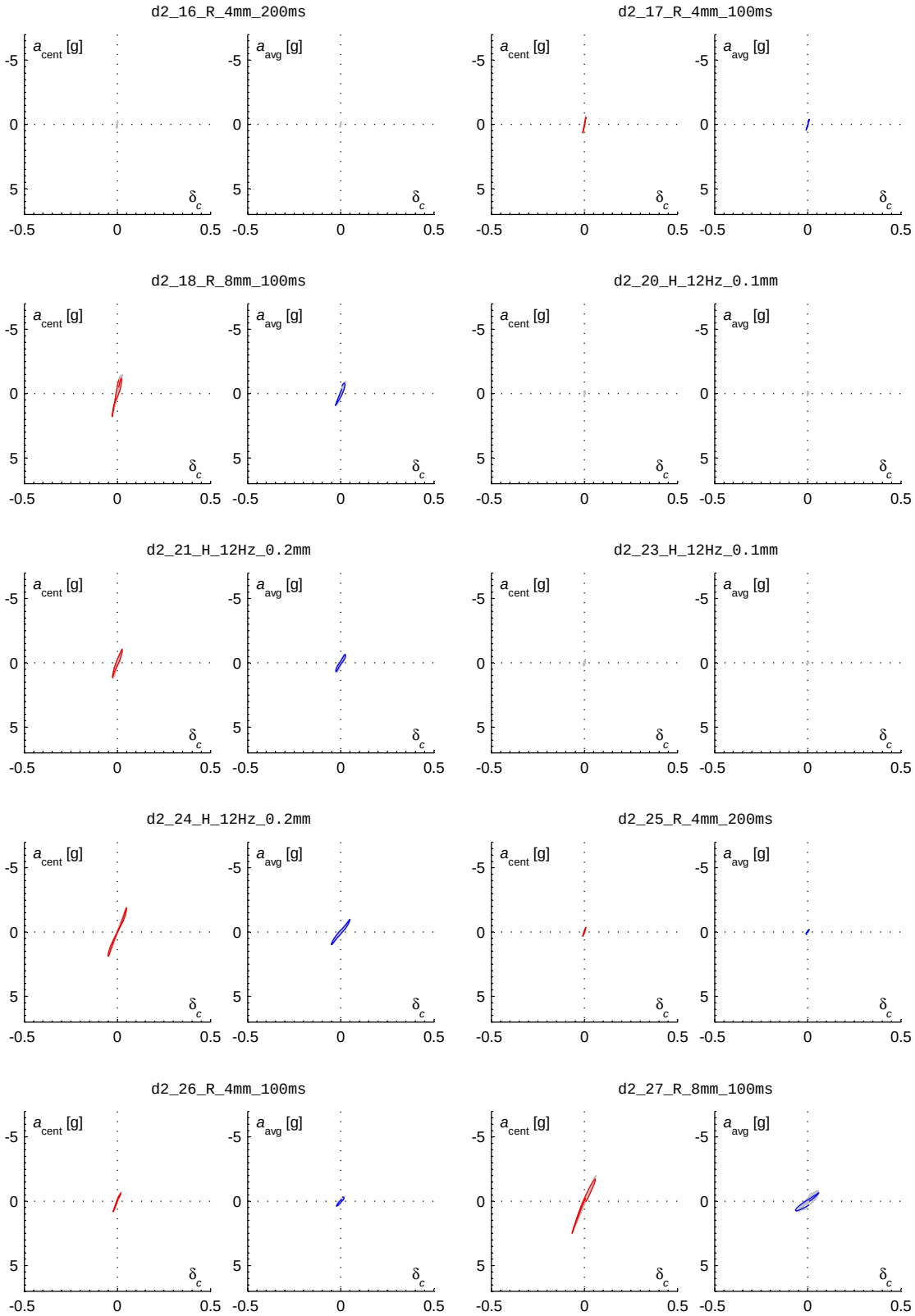
d2_16_R_4mm_200ms
d2_17_R_4mm_100ms
d2_18_R_8mm_100ms
d2_20_H_12Hz_0.1mm
d2_21_H_12Hz_0.2mm
d2_23_H_12Hz_0.1mm
d2_24_H_12Hz_0.2mm
d2_25_R_4mm_200ms
d2_26_R_4mm_100ms
d2_27_R_8mm_100ms
a_cent [g]
a_avg [g]
δ_c
-5
0
5
-0.5
0
0.5

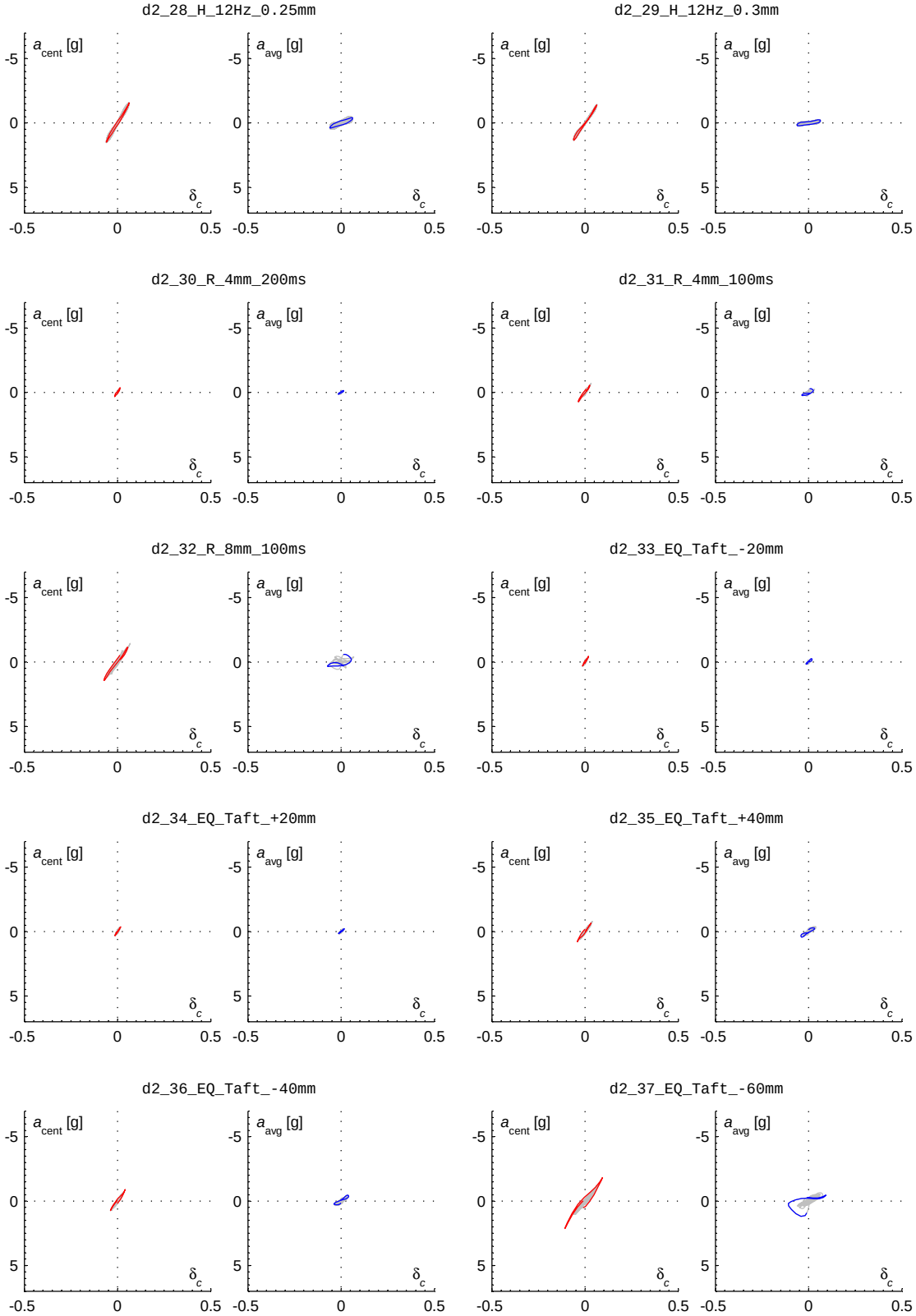
d2_28_H_12Hz_0.25mm
d2_29_H_12Hz_0.3mm
d2_30_R_4mm_200ms
d2_31_R_4mm_100ms
d2_32_R_8mm_100ms
d2_33_EQ_Taft_-20mm
d2_34_EQ_Taft_+20mm
d2_35_EQ_Taft_+40mm
d2_36_EQ_Taft_-40mm
d2_37_EQ_Taft_-60mm
a_cent [g]
a_avg [g]
δ_c
-5
0
5
-0.5
0
0.5

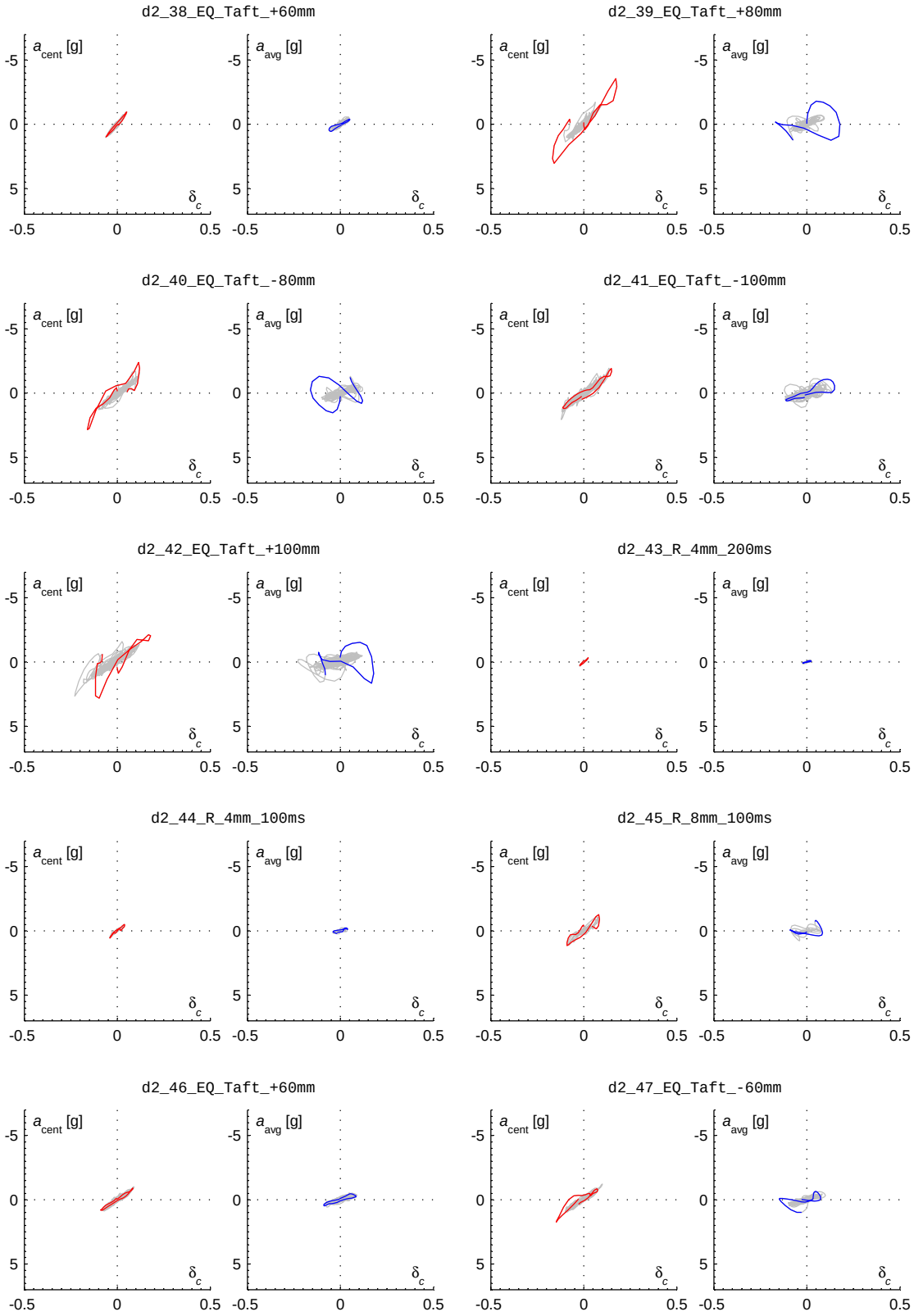
d2_38_EQ_Taft_+60mm
d2_39_EQ_Taft_+80mm
d2_40_EQ_Taft_-80mm
d2_41_EQ_Taft_-100mm
d2_42_EQ_Taft_+100mm
d2_43_R_4mm_200ms
d2_44_R_4mm_100ms
d2_45_R_8mm_100ms
d2_46_EQ_Taft_+60mm
d2_47_EQ_Taft_-60mm
a_cent [g]
a_avg [g]
δ_c
-5
0
5
-0.5
0
0.5

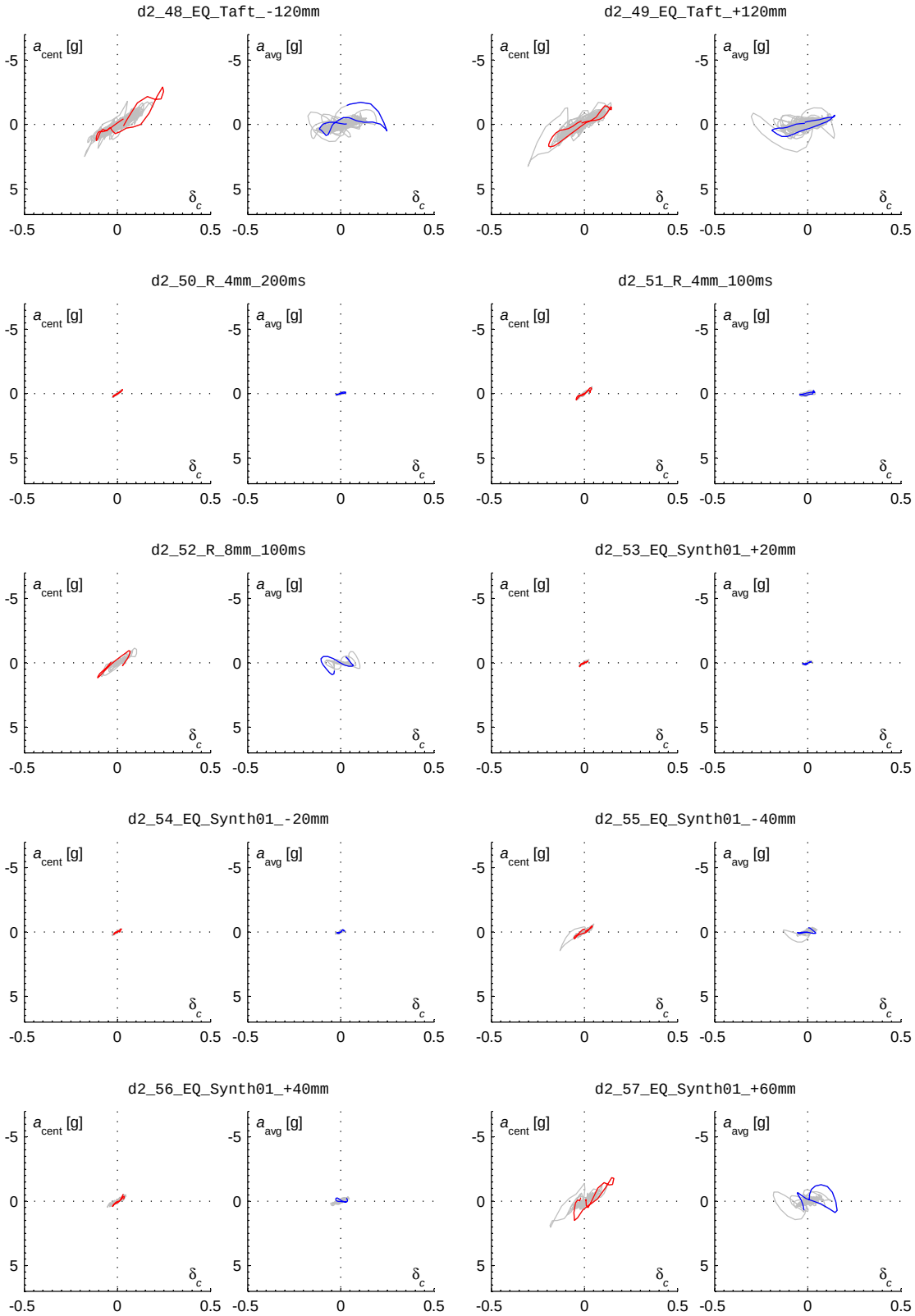
d2_48_EQ_Taft_-120mm
d2_49_EQ_Taft_+120mm
d2_50_R_4mm_200ms
d2_51_R_4mm_100ms
d2_52_R_8mm_100ms
d2_53_EQ_Synth01_+20mm
d2_54_EQ_Synth01_-20mm
d2_55_EQ_Synth01_-40mm
d2_56_EQ_Synth01_+40mm
d2_57_EQ_Synth01_+60mm
a_cent [g]
a_avg [g]
δ_c
-5
0
5
-0.5
0
0.5

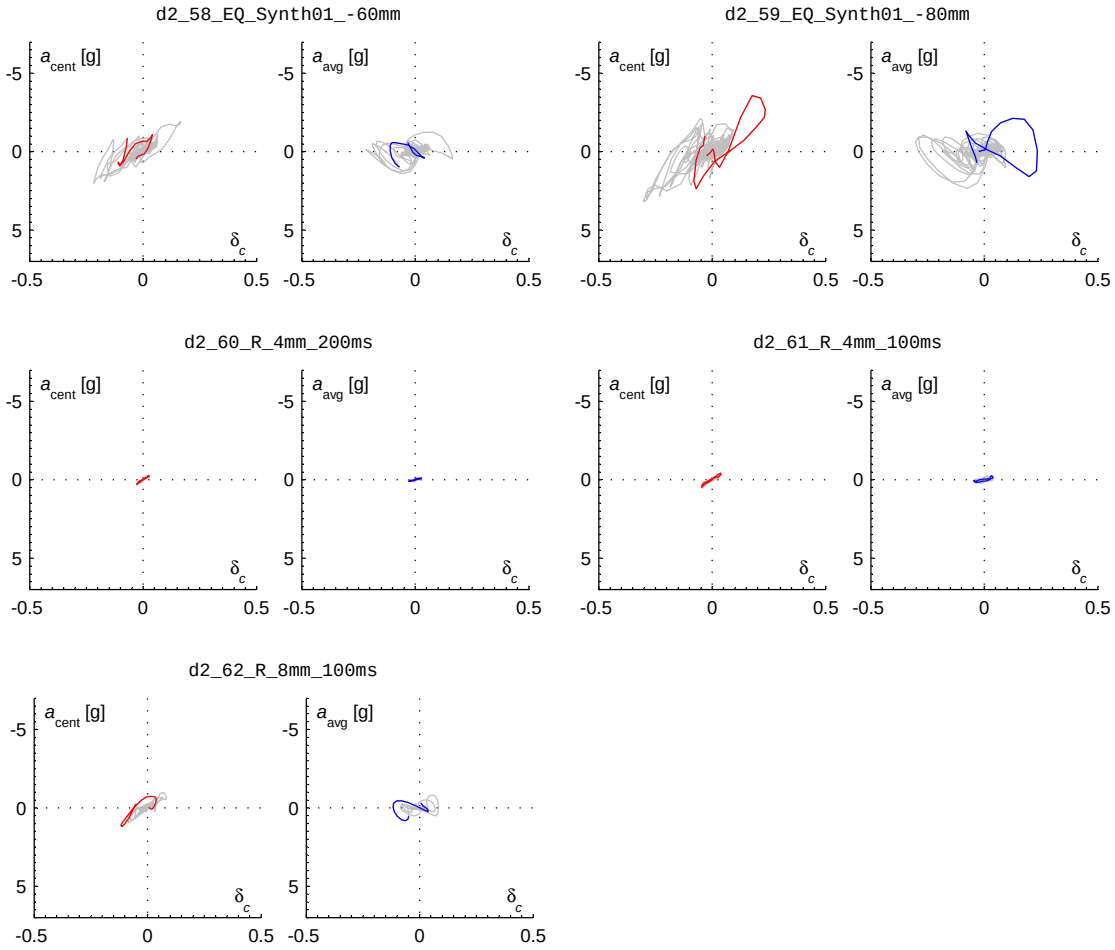
d2_58_EQ_Synth01_-60mm
d2_59_EQ_Synth01_-80mm
d2_60_R_4mm_200ms
d2_61_R_4mm_100ms
d2_62_R_8mm_100ms
a cent [g]
a avg [g]
δc
-5
0
5
-0.5
0
0.5

S.7.3 Wall D3

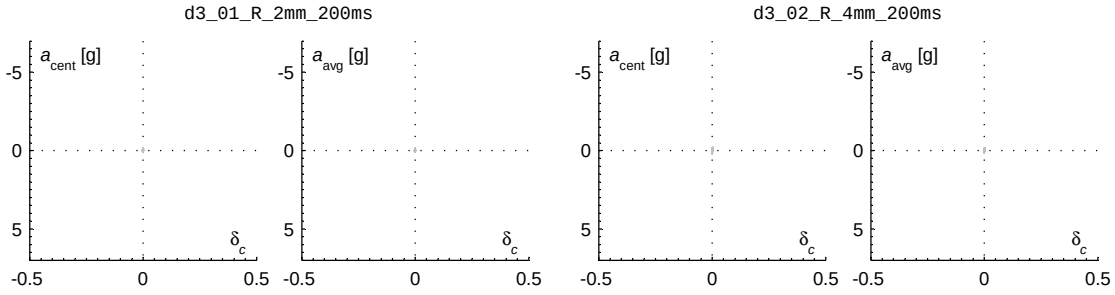
d3_01_R_2mm_200ms
d3_02_R_4mm_200ms
a cent [g]
a avg [g]
δc
-5
0
5
-0.5
0
0.5

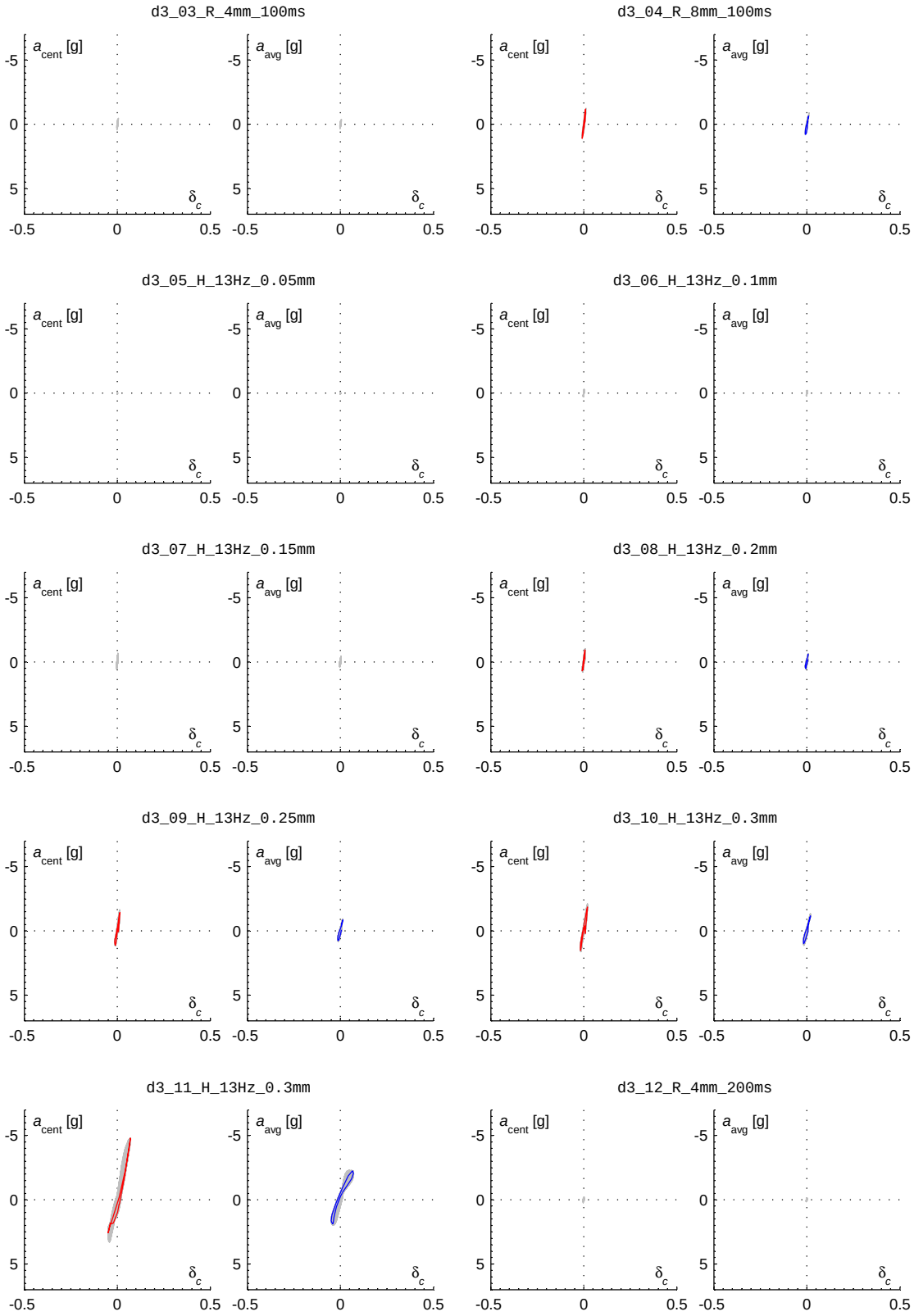
d3_03_R_4mm_100ms
d3_04_R_8mm_100ms
d3_05_H_13Hz_0.05mm
d3_06_H_13Hz_0.1mm
d3_07_H_13Hz_0.15mm
d3_08_H_13Hz_0.2mm
d3_09_H_13Hz_0.25mm
d3_10_H_13Hz_0.3mm
d3_11_H_13Hz_0.3mm
d3_12_R_4mm_200ms
a cent [g]
a avg [g]
δ c
-5
0
5
-0.5
0
0.5

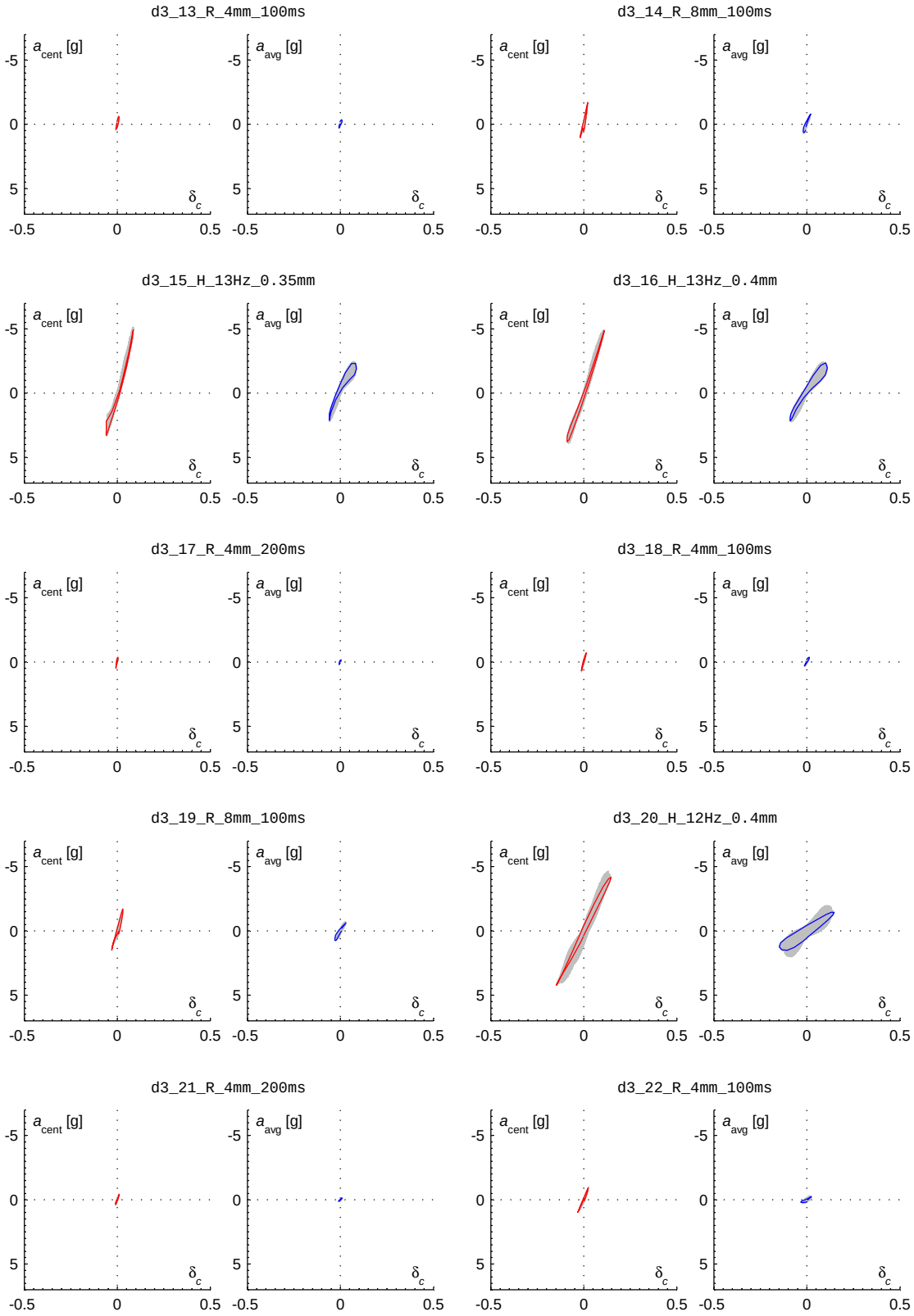
d3_13_R_4mm_100ms
d3_14_R_8mm_100ms
d3_15_H_13Hz_0.35mm
d3_16_H_13Hz_0.4mm
d3_17_R_4mm_200ms
d3_18_R_4mm_100ms
d3_19_R_8mm_100ms
d3_20_H_12Hz_0.4mm
d3_21_R_4mm_200ms
d3_22_R_4mm_100ms
a_cent [g]
a_avg [g]
δ_c
-5
0
5
-0.5
0
0.5

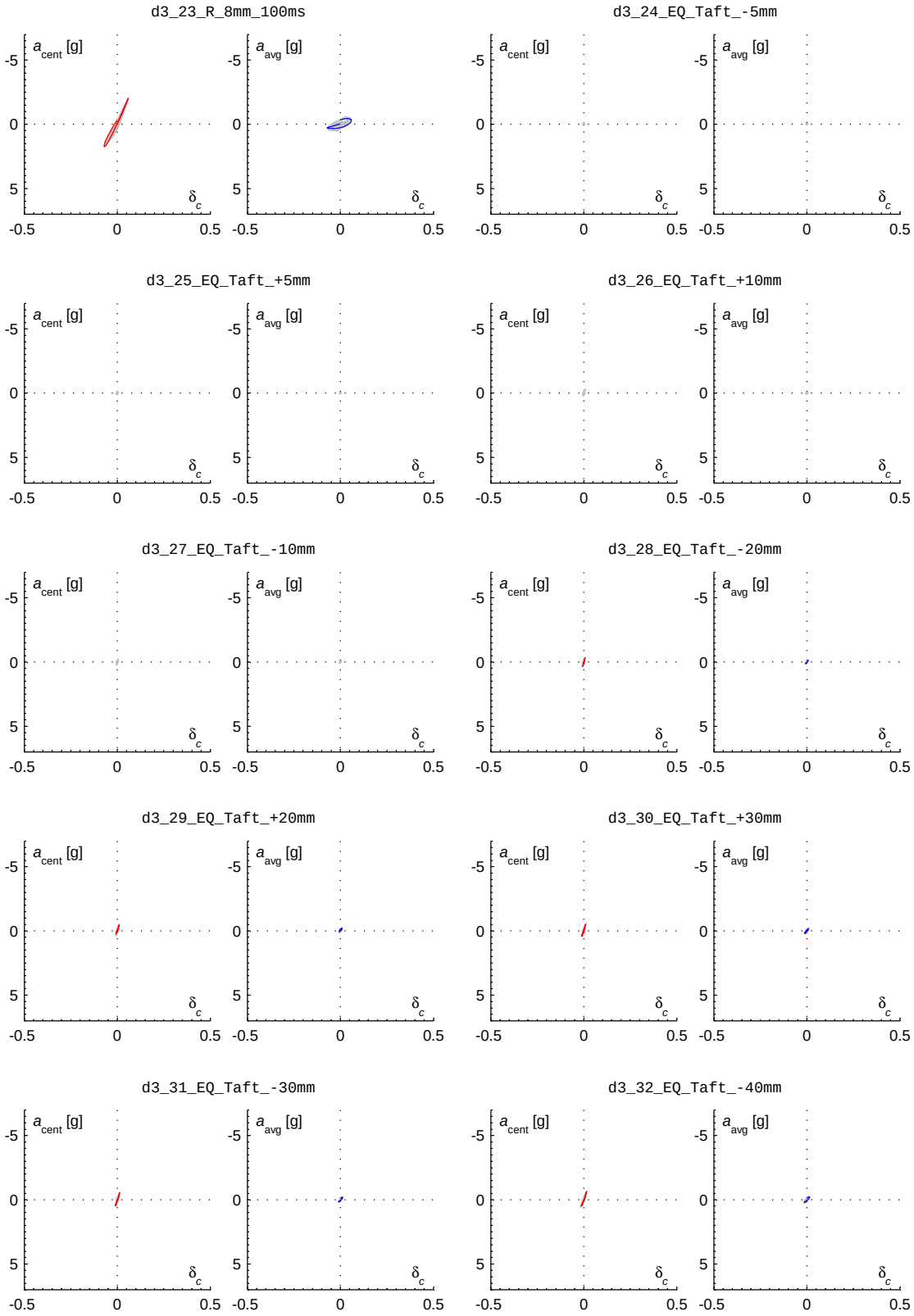
d3_23_R_8mm_100ms
d3_24_EQ_Taft_-5mm
d3_25_EQ_Taft_+5mm
d3_26_EQ_Taft_+10mm
d3_27_EQ_Taft_-10mm
d3_28_EQ_Taft_-20mm
d3_29_EQ_Taft_+20mm
d3_30_EQ_Taft_+30mm
d3_31_EQ_Taft_-30mm
d3_32_EQ_Taft_-40mm
a_cent [g]
a_avg [g]
δ_c
-5
0
5
-0.5
0
0.5

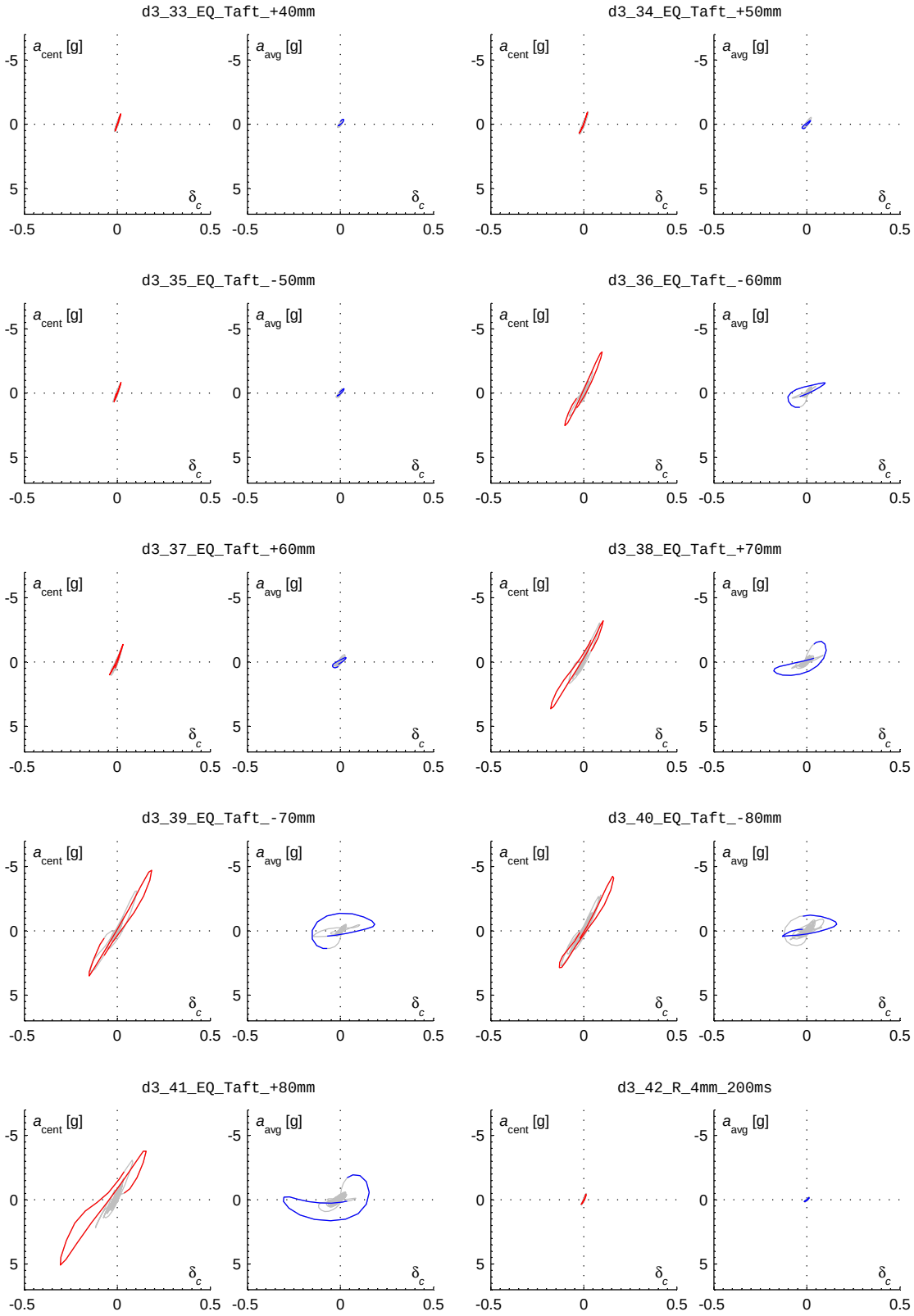
d3_33_EQ_Taft_+40mm
d3_34_EQ_Taft_+50mm
d3_35_EQ_Taft_-50mm
d3_36_EQ_Taft_-60mm
d3_37_EQ_Taft_+60mm
d3_38_EQ_Taft_+70mm
d3_39_EQ_Taft_-70mm
d3_40_EQ_Taft_-80mm
d3_41_EQ_Taft_+80mm
d3_42_R_4mm_200ms
a_cent [g]
a_avg [g]
δ_c
-5
0
5
-0.5
0
0.5

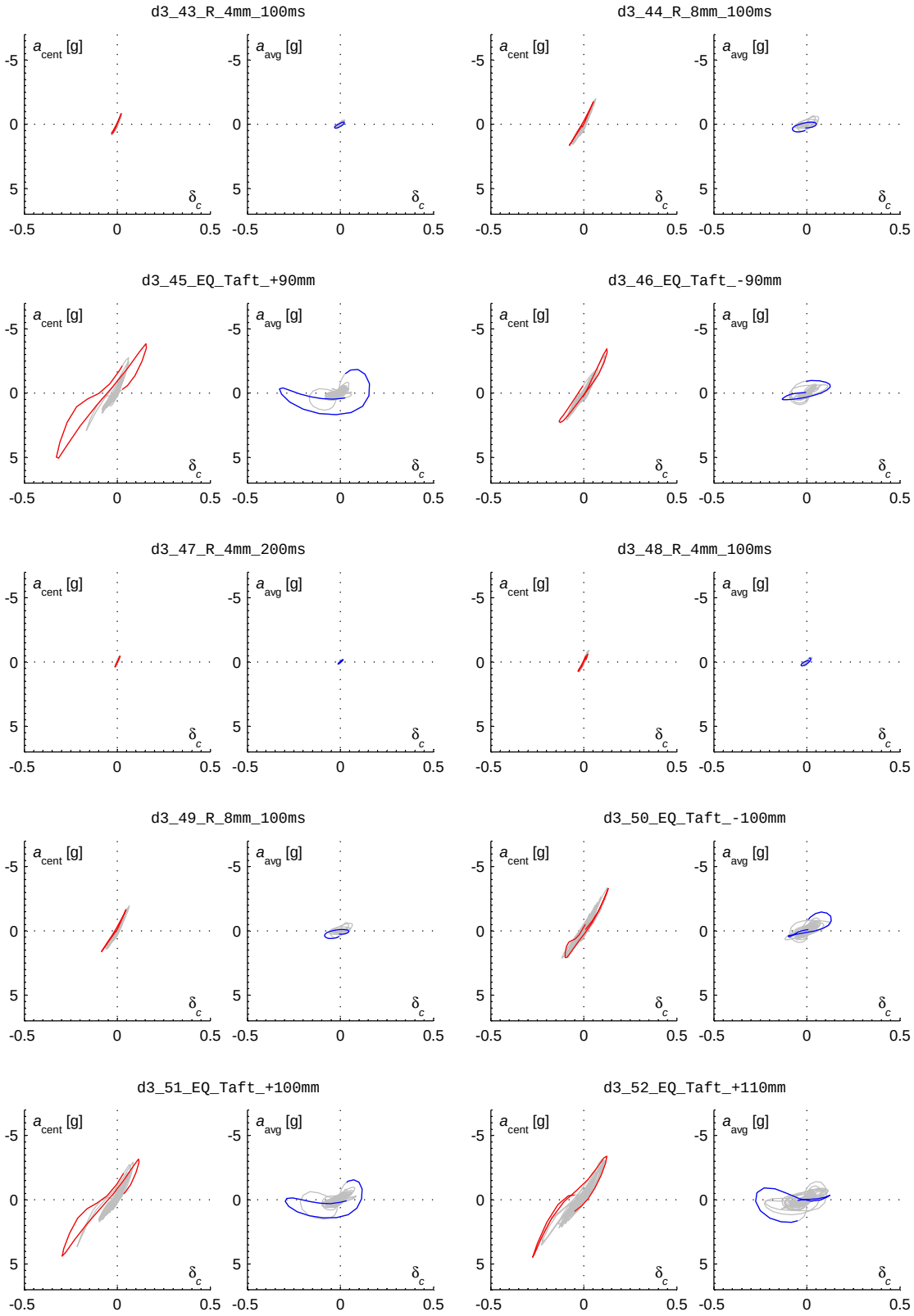
d3_43_R_4mm_100ms
d3_44_R_8mm_100ms
d3_45_EQ_Taft_+90mm
d3_46_EQ_Taft_-90mm
d3_47_R_4mm_200ms
d3_48_R_4mm_100ms
d3_49_R_8mm_100ms
d3_50_EQ_Taft_-100mm
d3_51_EQ_Taft_+100mm
d3_52_EQ_Taft_+110mm
a_cent [g]
a_avg [g]
δ_c
-5
0
5
-0.5
0
0.5

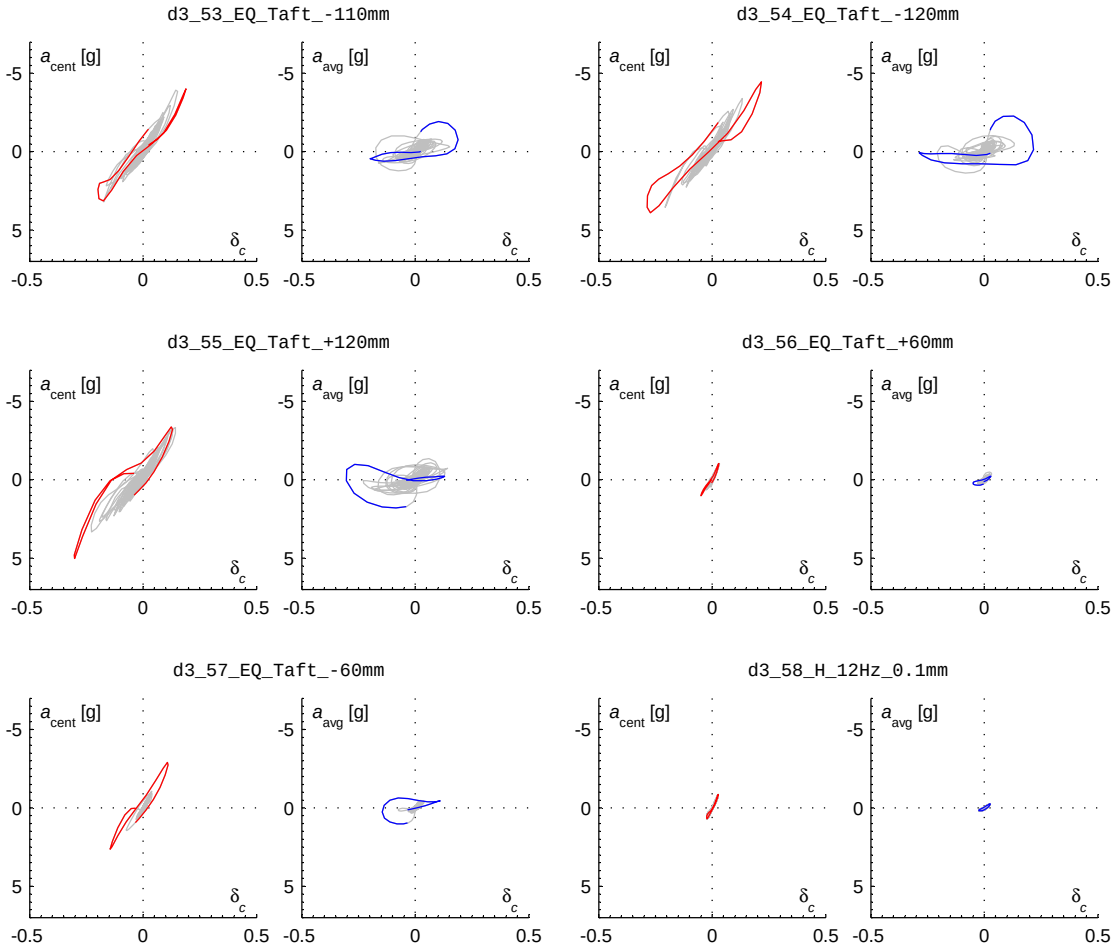
d3_53_EQ_Taft_-110mm
d3_54_EQ_Taft_-120mm
d3_55_EQ_Taft_+120mm
d3_56_EQ_Taft_+60mm
d3_57_EQ_Taft_-60mm
d3_58_H_12Hz_0.1mm
a_cent [g]
a_avg [g]
δ_c
-5
0
5
-0.5
0
0.5

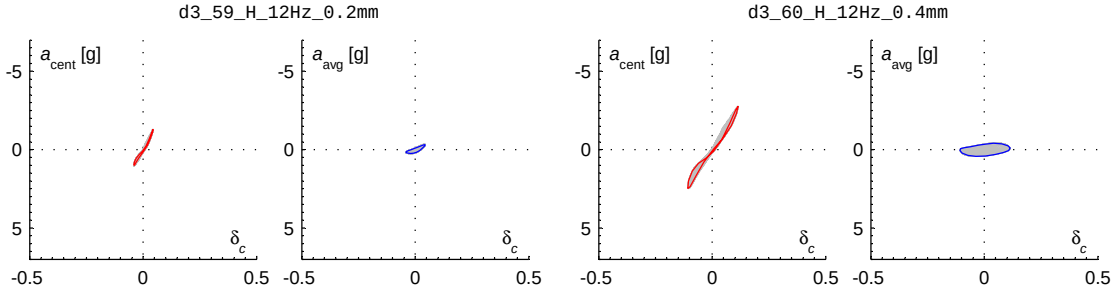
d3_59_H_12Hz_0.2mm
d3_60_H_12Hz_0.4mm
a cent [g]
a avg [g]
δc
-5
0
5
-0.5
0
0.5

S.7.4 Wall D4

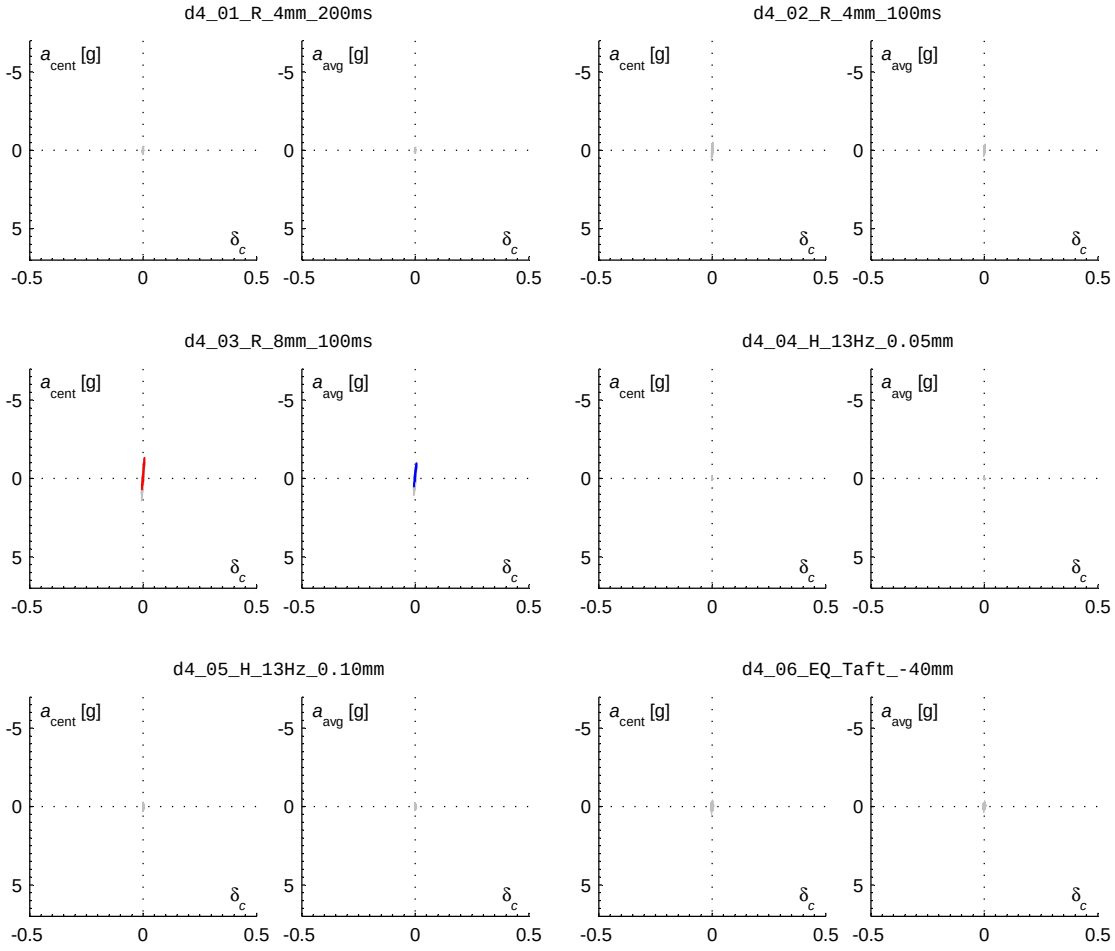
d4_01_R_4mm_200ms
d4_02_R_4mm_100ms
d4_03_R_8mm_100ms
d4_04_H_13Hz_0.05mm
d4_05_H_13Hz_0.10mm
d4_06_EQ_Taft_-40mm
a cent [g]
a avg [g]
δc
-5
0
5
-0.5
0
0.5

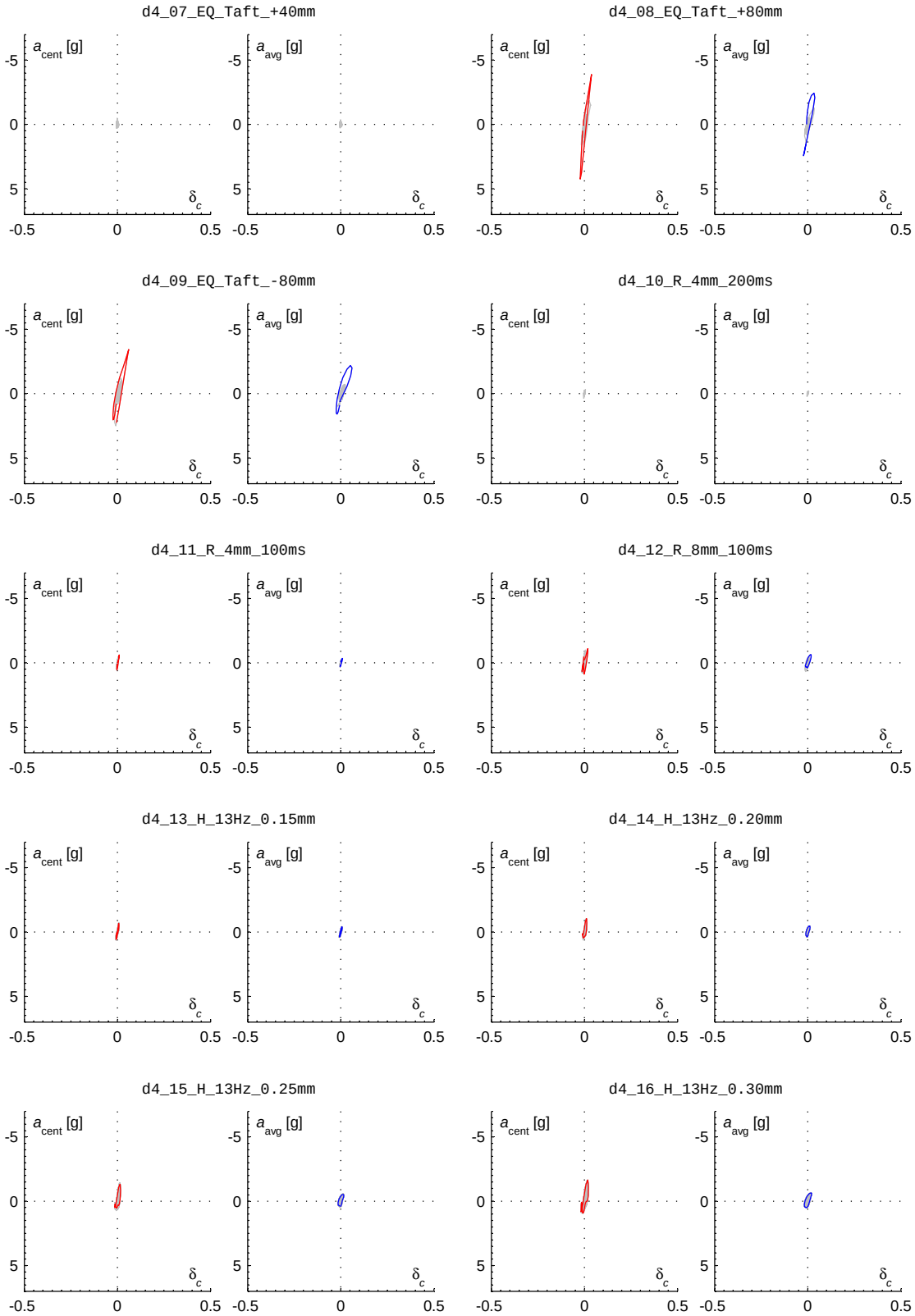
d4_07_EQ_Taft_+40mm
d4_08_EQ_Taft_+80mm
d4_09_EQ_Taft_-80mm
d4_10_R_4mm_200ms
d4_11_R_4mm_100ms
d4_12_R_8mm_100ms
d4_13_H_13Hz_0.15mm
d4_14_H_13Hz_0.20mm
d4_15_H_13Hz_0.25mm
d4_16_H_13Hz_0.30mm
a_cent [g]
a_avg [g]
δ_c
-5
0
5
-0.5
0
0.5

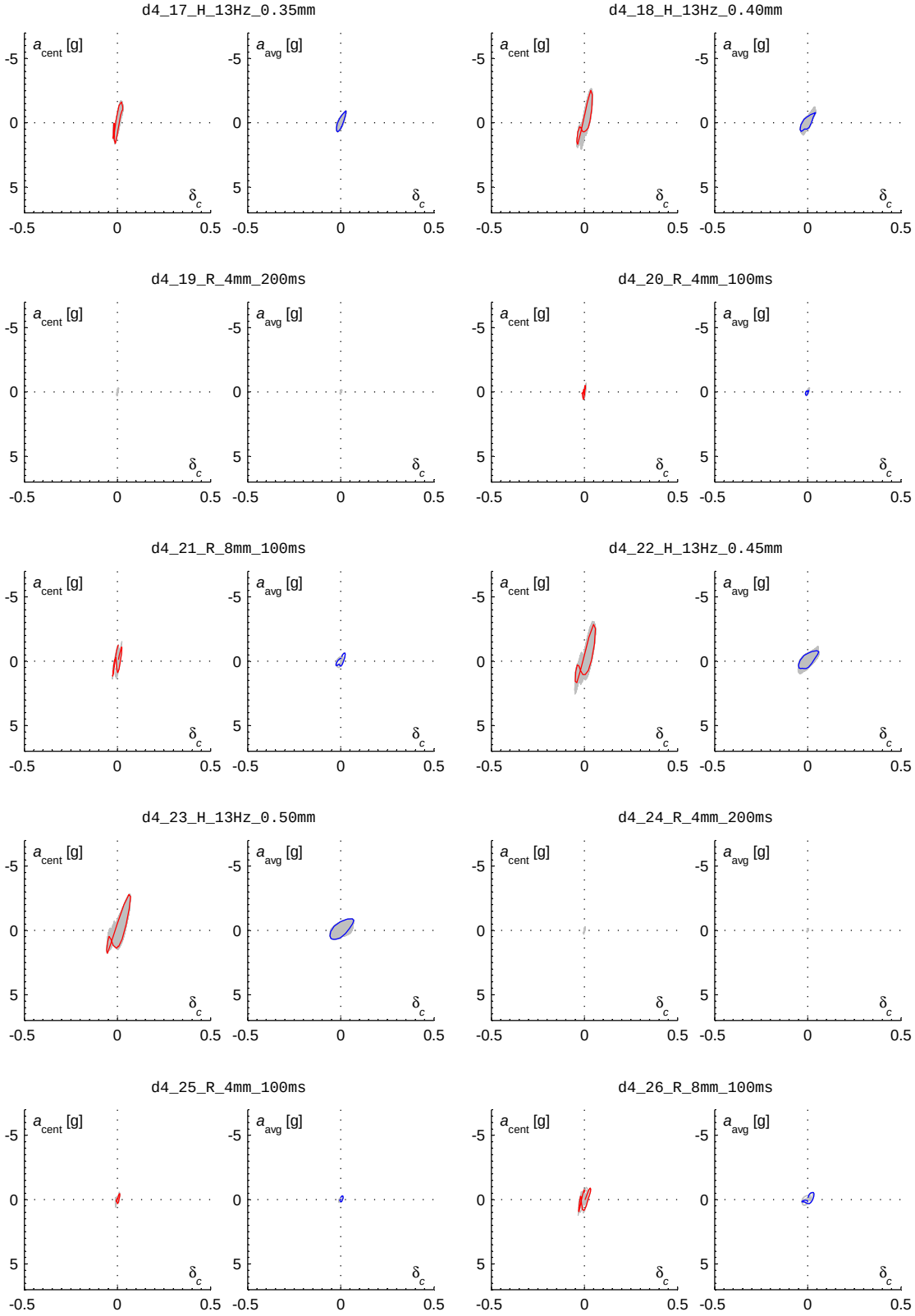
d4_17_H_13Hz_0.35mm
d4_18_H_13Hz_0.40mm
d4_19_R_4mm_200ms
d4_20_R_4mm_100ms
d4_21_R_8mm_100ms
d4_22_H_13Hz_0.45mm
d4_23_H_13Hz_0.50mm
d4_24_R_4mm_200ms
d4_25_R_4mm_100ms
d4_26_R_8mm_100ms
a_cent [g]
a_avg [g]
δ_c
-5
0
5
-0.5
0
0.5

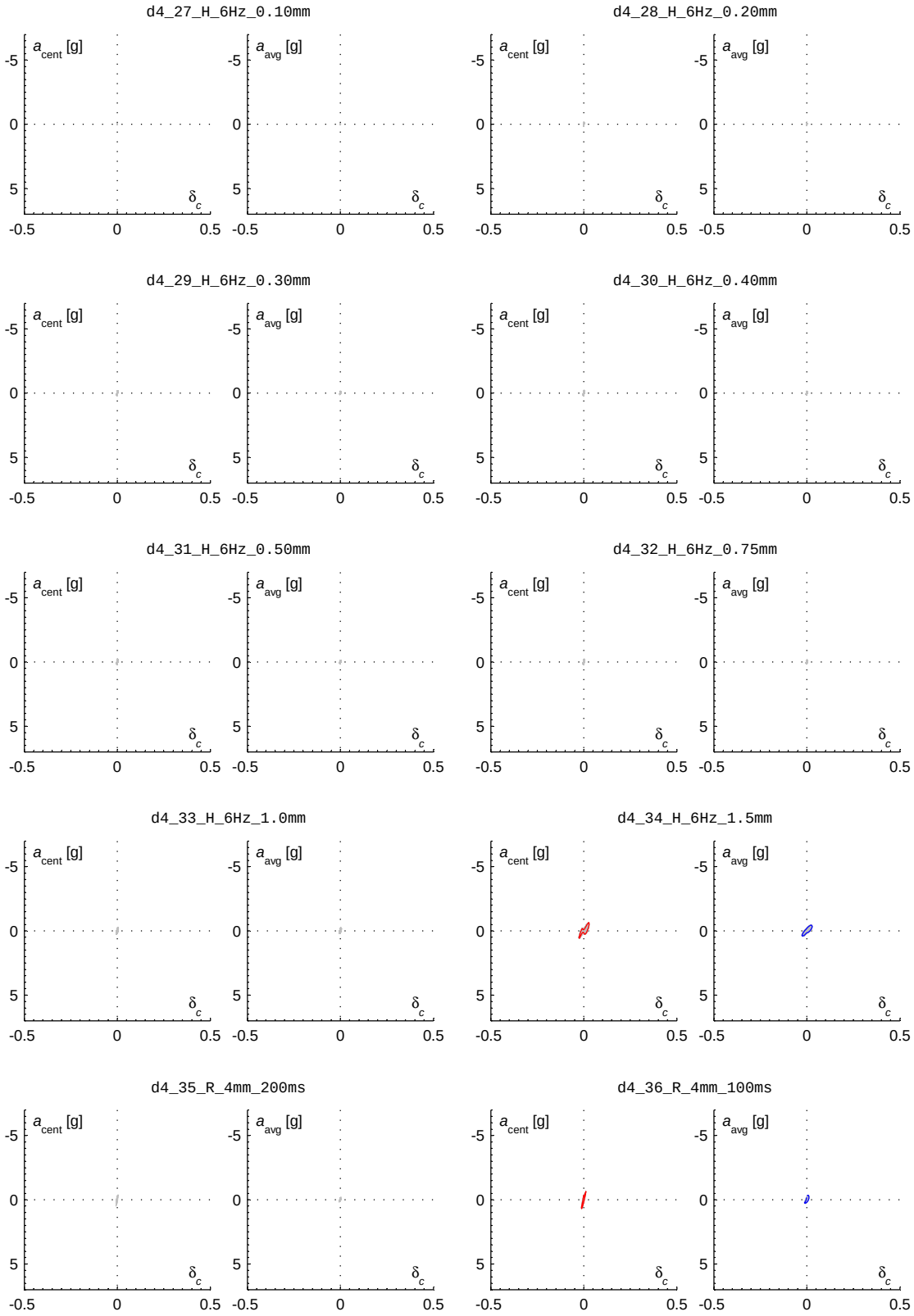
d4_27_H_6Hz_0.10mm
d4_28_H_6Hz_0.20mm
d4_29_H_6Hz_0.30mm
d4_30_H_6Hz_0.40mm
d4_31_H_6Hz_0.50mm
d4_32_H_6Hz_0.75mm
d4_33_H_6Hz_1.0mm
d4_34_H_6Hz_1.5mm
d4_35_R_4mm_200ms
d4_36_R_4mm_100ms
a_cent [g]
a_avg [g]
δ_c
-5
0
5
-0.5
0
0.5

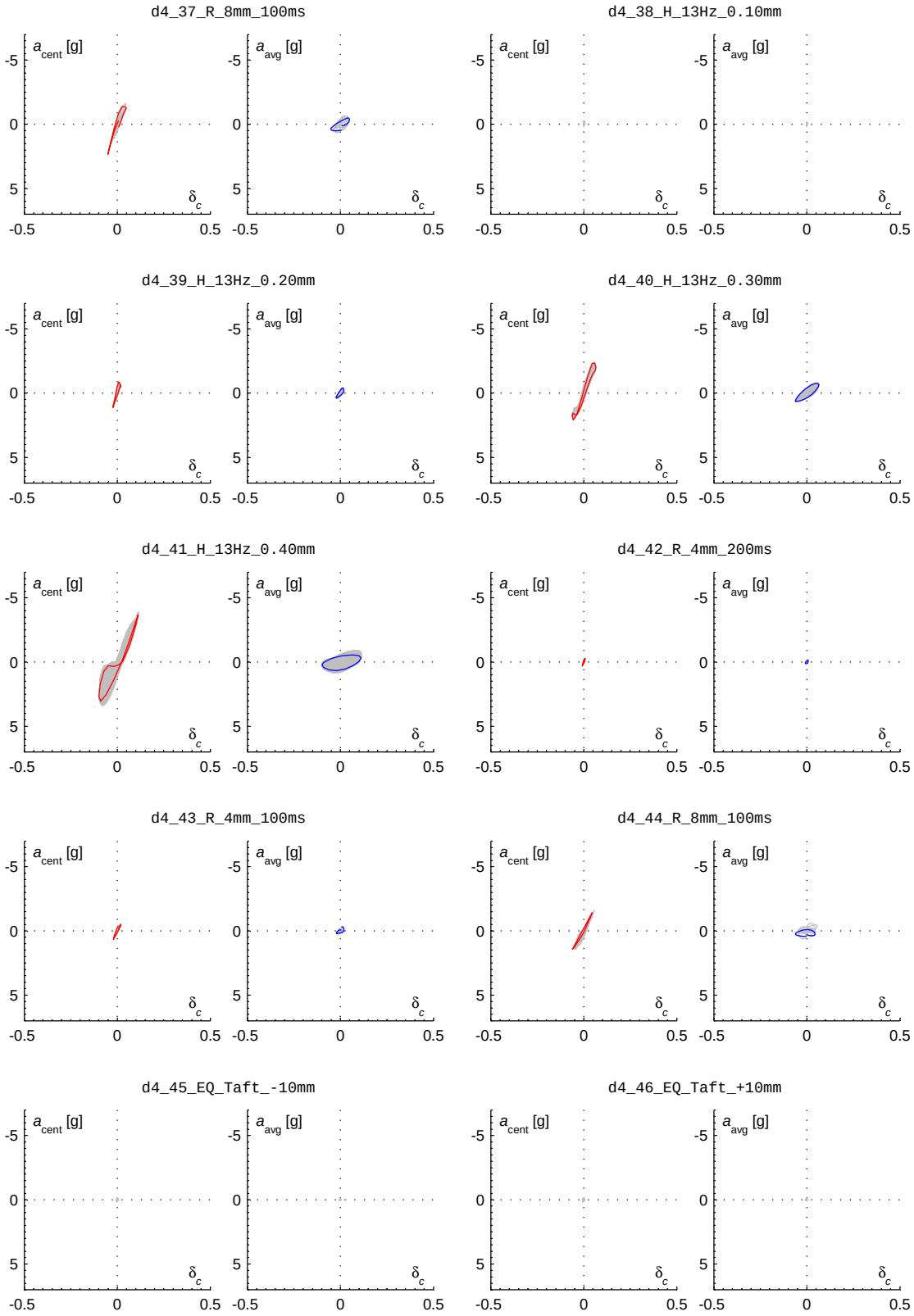
d4_37_R_8mm_100ms
d4_38_H_13Hz_0.10mm
d4_39_H_13Hz_0.20mm
d4_40_H_13Hz_0.30mm
d4_41_H_13Hz_0.40mm
d4_42_R_4mm_200ms
d4_43_R_4mm_100ms
d4_44_R_8mm_100ms
d4_45_EQ_Taft_-10mm
d4_46_EQ_Taft_+10mm
a_cent [g]
a_avg [g]
δ_c
-5
0
5
-0.5
0
0.5

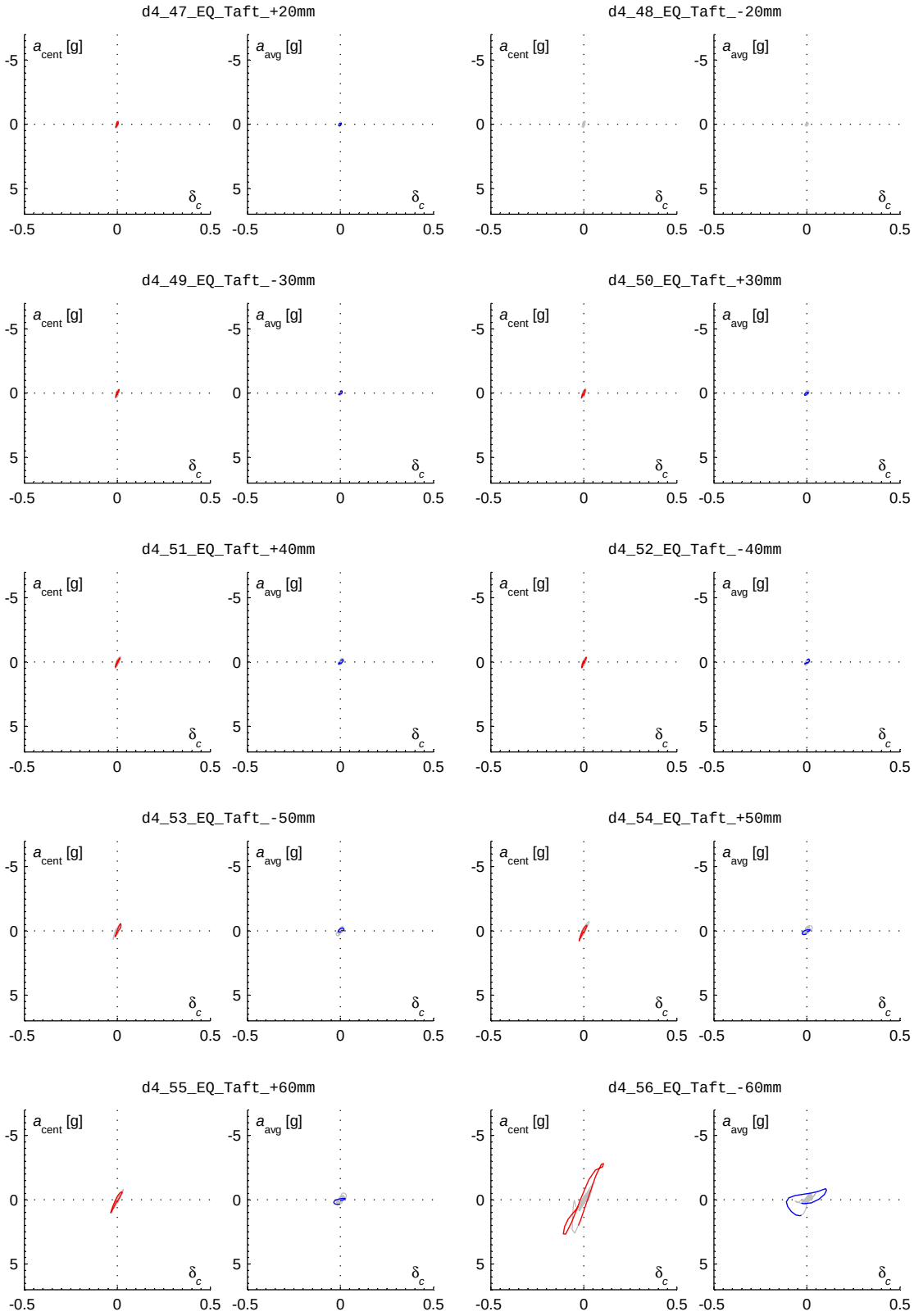
d4_47_EQ_Taft_+20mm
d4_48_EQ_Taft_-20mm
d4_49_EQ_Taft_-30mm
d4_50_EQ_Taft_+30mm
d4_51_EQ_Taft_+40mm
d4_52_EQ_Taft_-40mm
d4_53_EQ_Taft_-50mm
d4_54_EQ_Taft_+50mm
d4_55_EQ_Taft_+60mm
d4_56_EQ_Taft_-60mm
a cent [g]
a avg [g]
δc
-5
0
5
-0.5
0
0.5

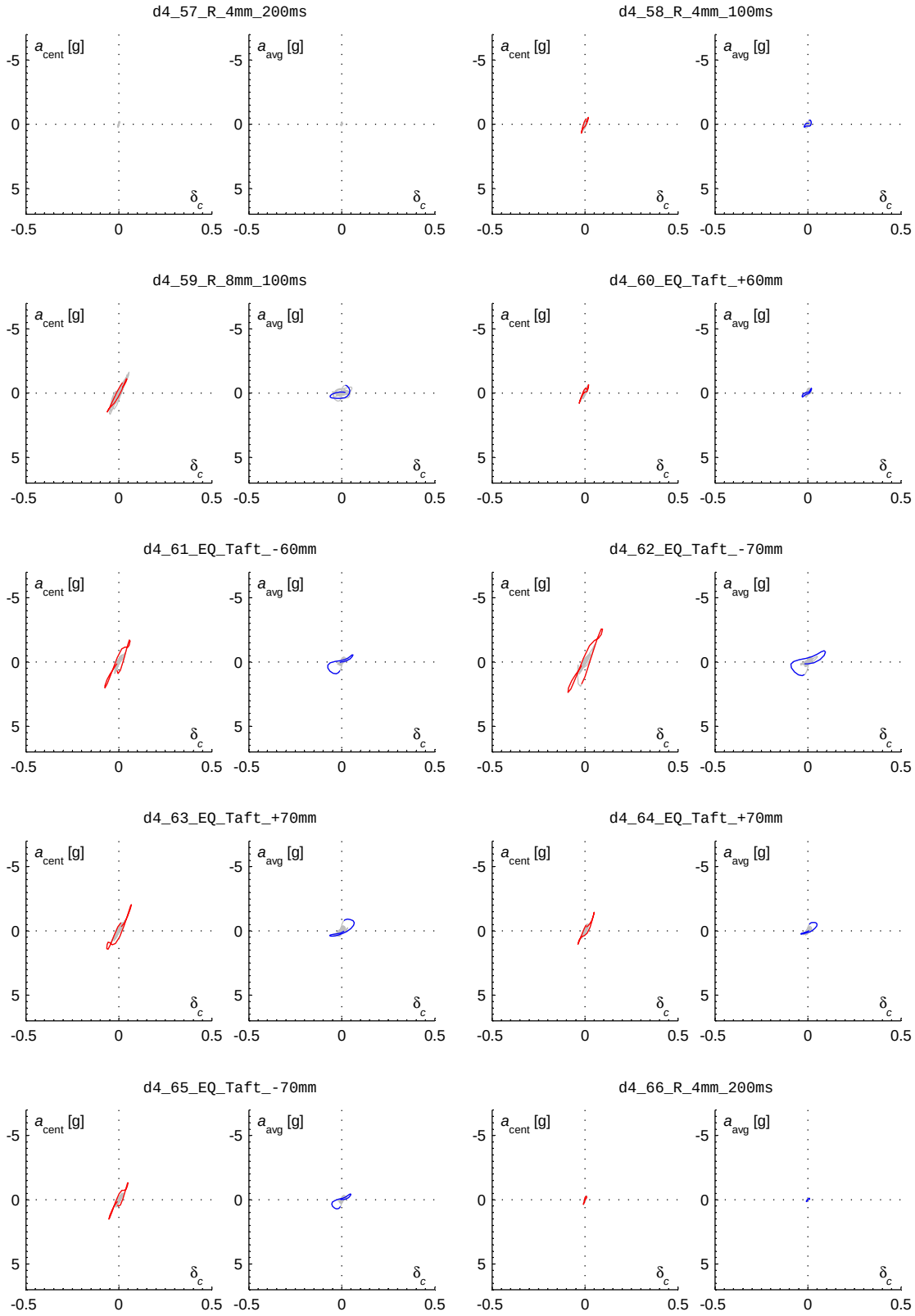
d4_57_R_4mm_200ms
d4_58_R_4mm_100ms
d4_59_R_8mm_100ms
d4_60_EQ_Taft_+60mm
d4_61_EQ_Taft_-60mm
d4_62_EQ_Taft_-70mm
d4_63_EQ_Taft_+70mm
d4_64_EQ_Taft_+70mm
d4_65_EQ_Taft_-70mm
d4_66_R_4mm_200ms
a_cent [g]
a_avg [g]
δ_c
-5
0
5
-0.5
0
0.5

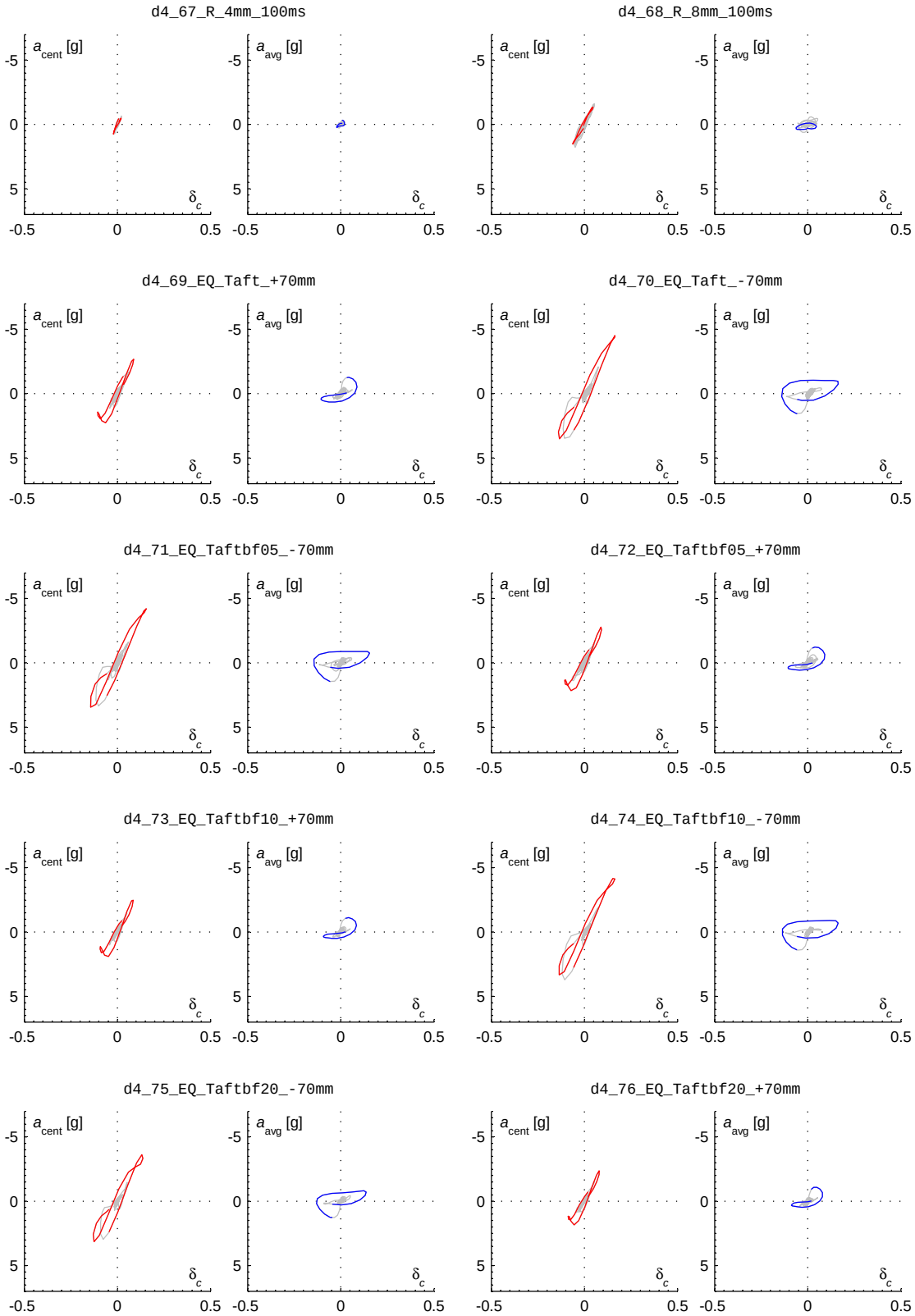
d4_67_R_4mm_100ms
d4_68_R_8mm_100ms
d4_69_EQ_Taft_+70mm
d4_70_EQ_Taft_-70mm
d4_71_EQ_Taftbf05_-70mm
d4_72_EQ_Taftbf05_+70mm
d4_73_EQ_Taftbf10_+70mm
d4_74_EQ_Taftbf10_-70mm
d4_75_EQ_Taftbf20_-70mm
d4_76_EQ_Taftbf20_+70mm
a_cent [g]
a_avg [g]
δ_c
-5
0
5
-0.5
0
0.5

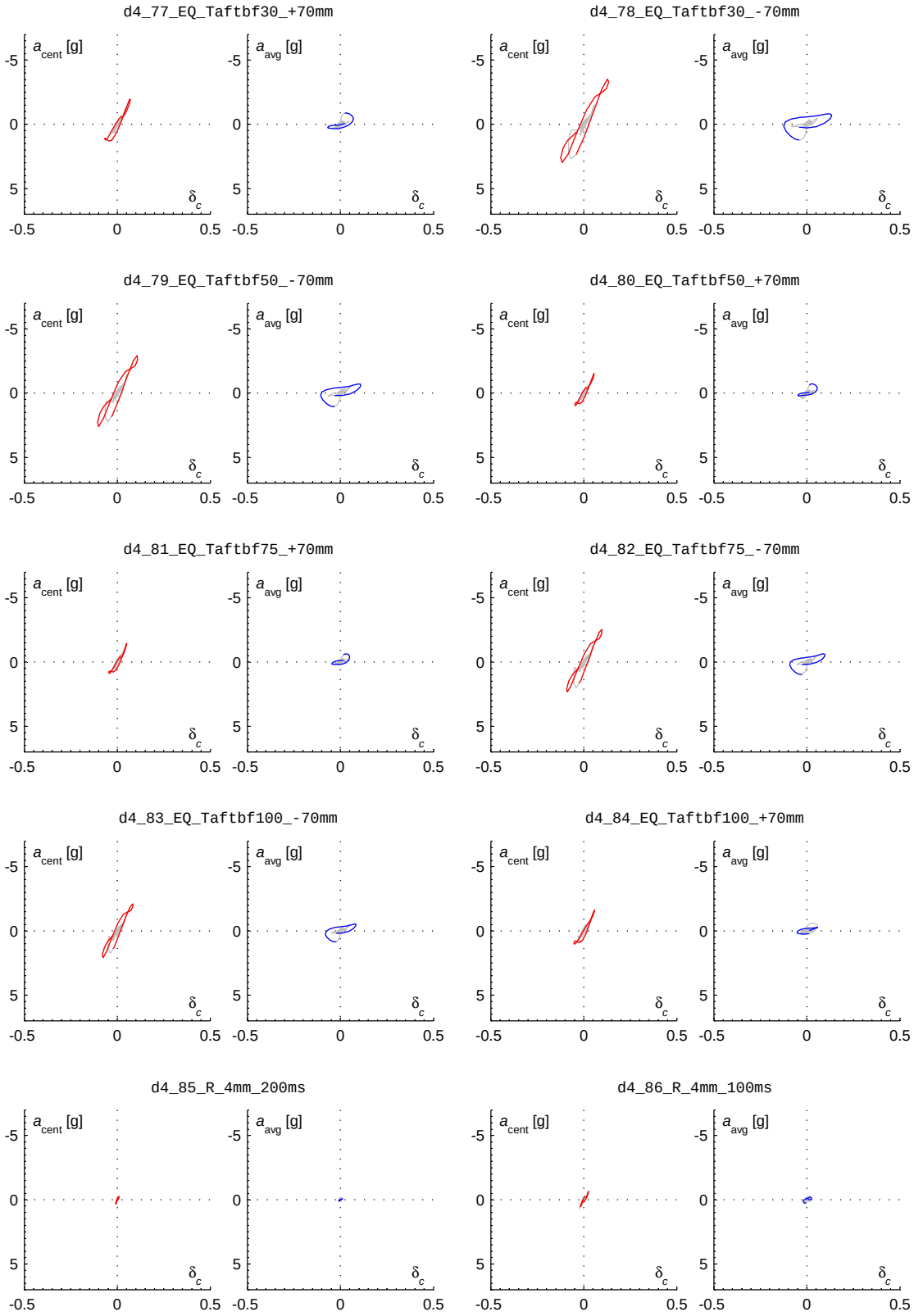
d4_77_EQ_Taftbf30_+70mm
d4_78_EQ_Taftbf30_-70mm
d4_79_EQ_Taftbf50_-70mm
d4_80_EQ_Taftbf50_+70mm
d4_81_EQ_Taftbf75_+70mm
d4_82_EQ_Taftbf75_-70mm
d4_83_EQ_Taftbf100_-70mm
d4_84_EQ_Taftbf100_+70mm
d4_85_R_4mm_200ms
d4_86_R_4mm_100ms
a_cent [g]
a_avg [g]
δ_c
-5
0
5
-0.5
0
0.5

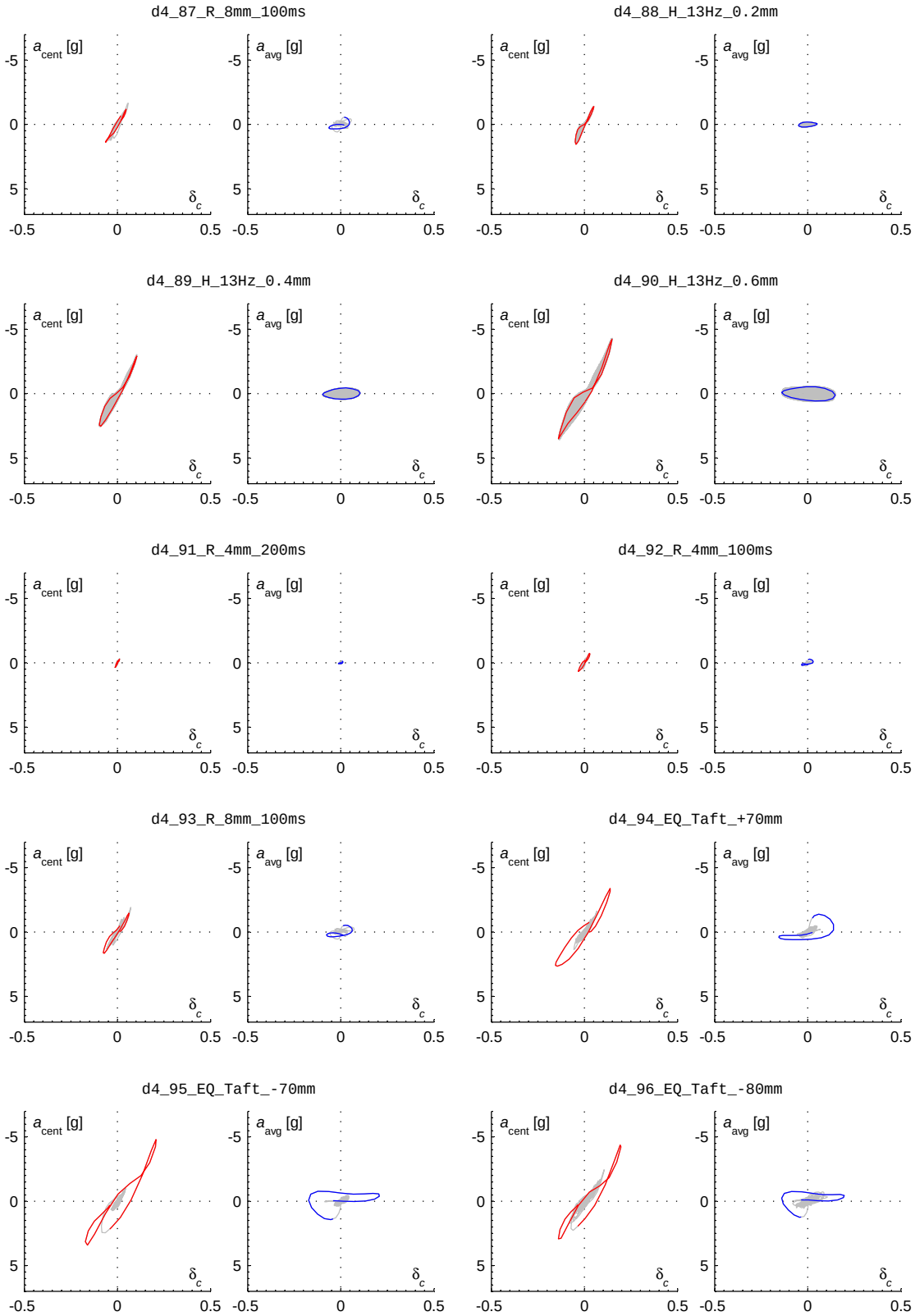
d4_87_R_8mm_100ms
d4_88_H_13Hz_0.2mm
d4_89_H_13Hz_0.4mm
d4_90_H_13Hz_0.6mm
d4_91_R_4mm_200ms
d4_92_R_4mm_100ms
d4_93_R_8mm_100ms
d4_94_EQ_Taft_+70mm
d4_95_EQ_Taft_-70mm
d4_96_EQ_Taft_-80mm
a_cent [g]
a_avg [g]
δ_c
-5
0
5
-0.5
0
0.5

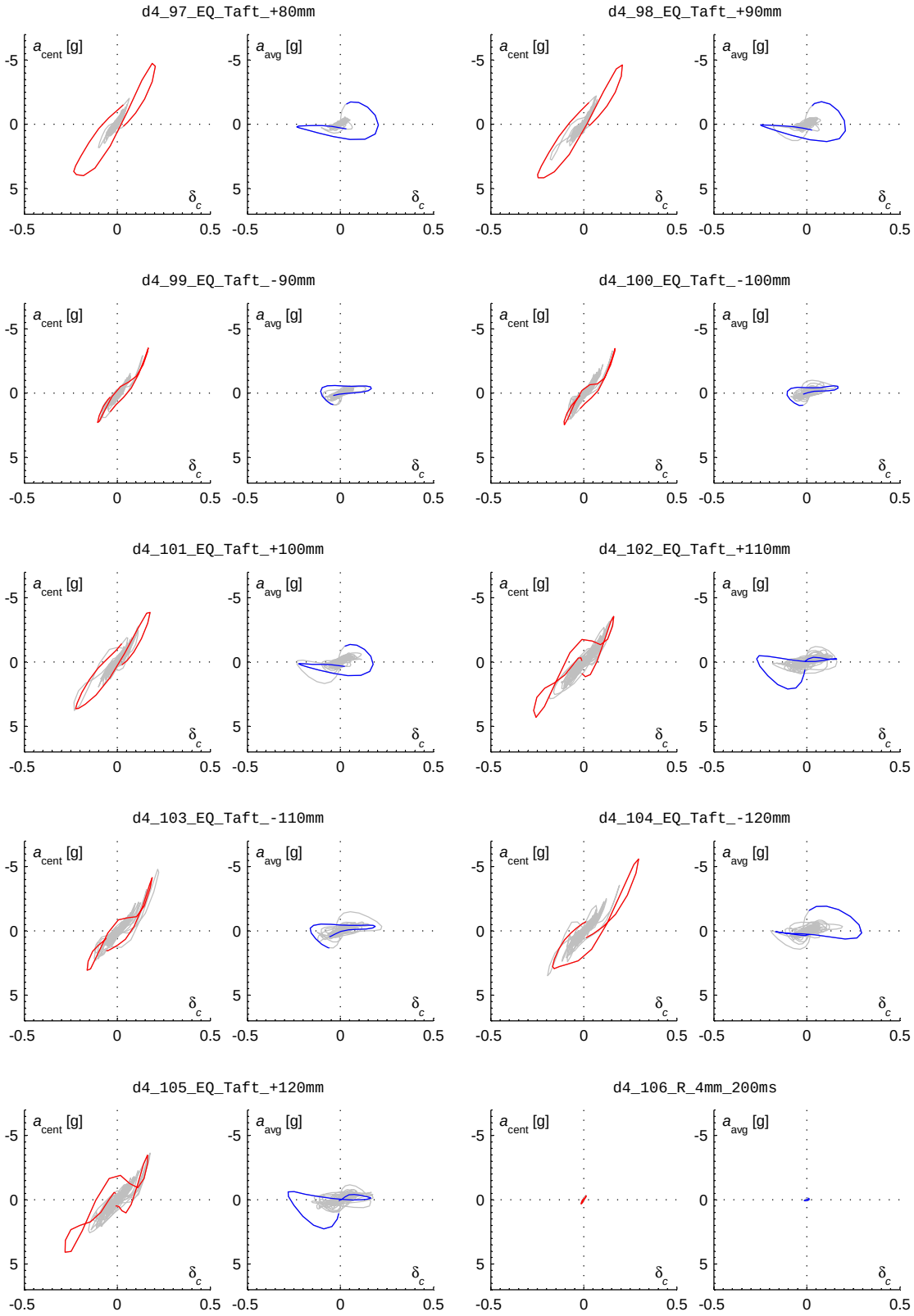
d4_97_EQ_Taft_+80mm
d4_98_EQ_Taft_+90mm
d4_99_EQ_Taft_-90mm
d4_100_EQ_Taft_-100mm
d4_101_EQ_Taft_+100mm
d4_102_EQ_Taft_+110mm
d4_103_EQ_Taft_-110mm
d4_104_EQ_Taft_-120mm
d4_105_EQ_Taft_+120mm
d4_106_R_4mm_200ms
a_cent [g]
a_avg [g]
δ_c
-5
0
5
-0.5
0
0.5

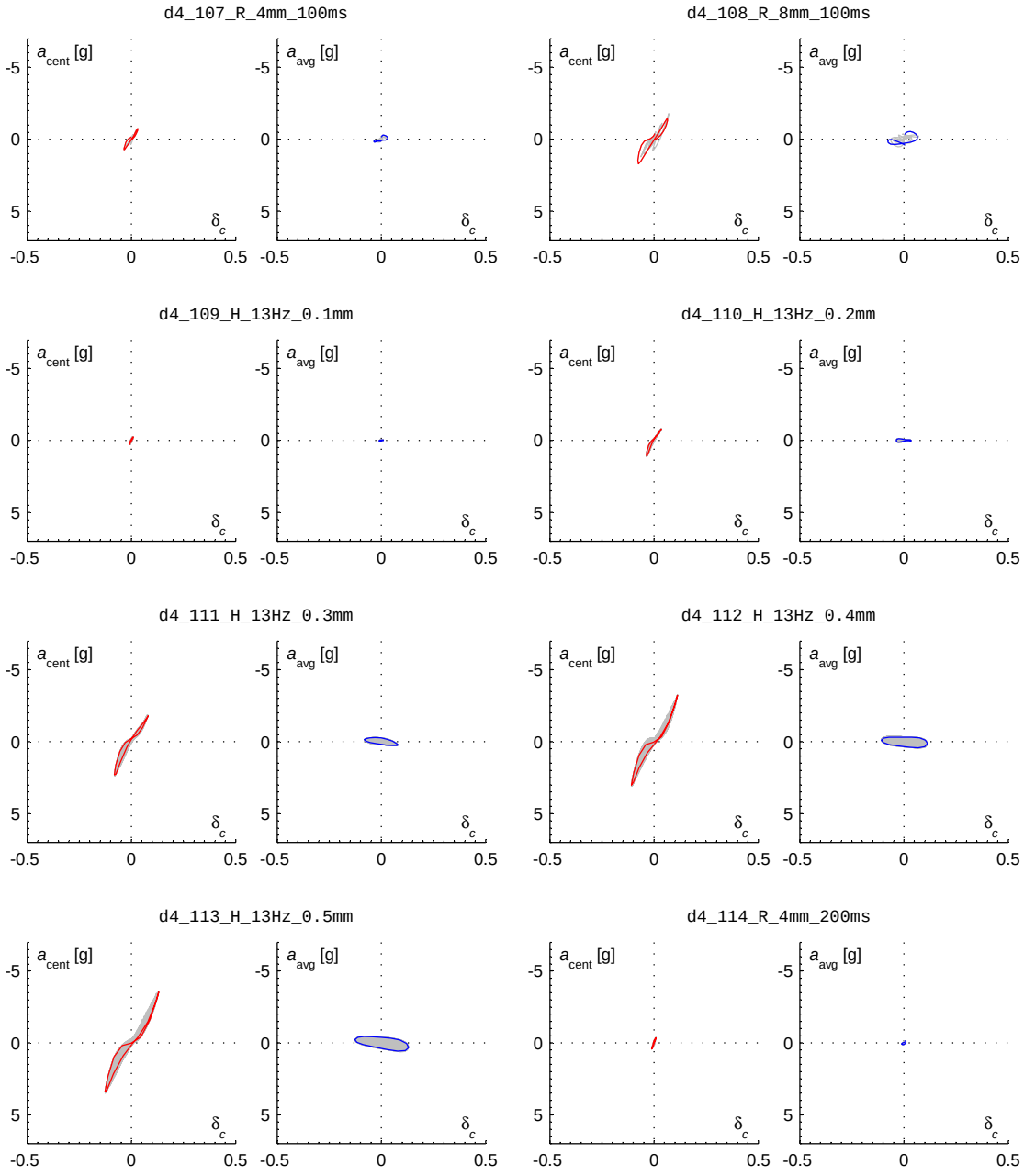
d4_107_R_4mm_100ms
d4_108_R_8mm_100ms
d4_109_H_13Hz_0.1mm
d4_110_H_13Hz_0.2mm
d4_111_H_13Hz_0.3mm
d4_112_H_13Hz_0.4mm
d4_113_H_13Hz_0.5mm
d4_114_R_4mm_200ms
a_cent [g]
a_avg [g]
δ_c
-5
0
5
-0.5
0
0.5

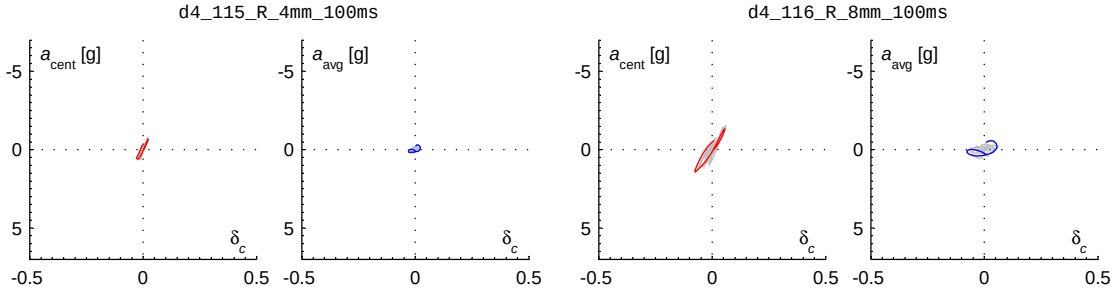
d4_115_R_4mm_100ms
d4_116_R_8mm_100ms
a cent [g]
a avg [g]
δc
-5
0
5
-0.5
0
0.5

S.7.5 Wall D5

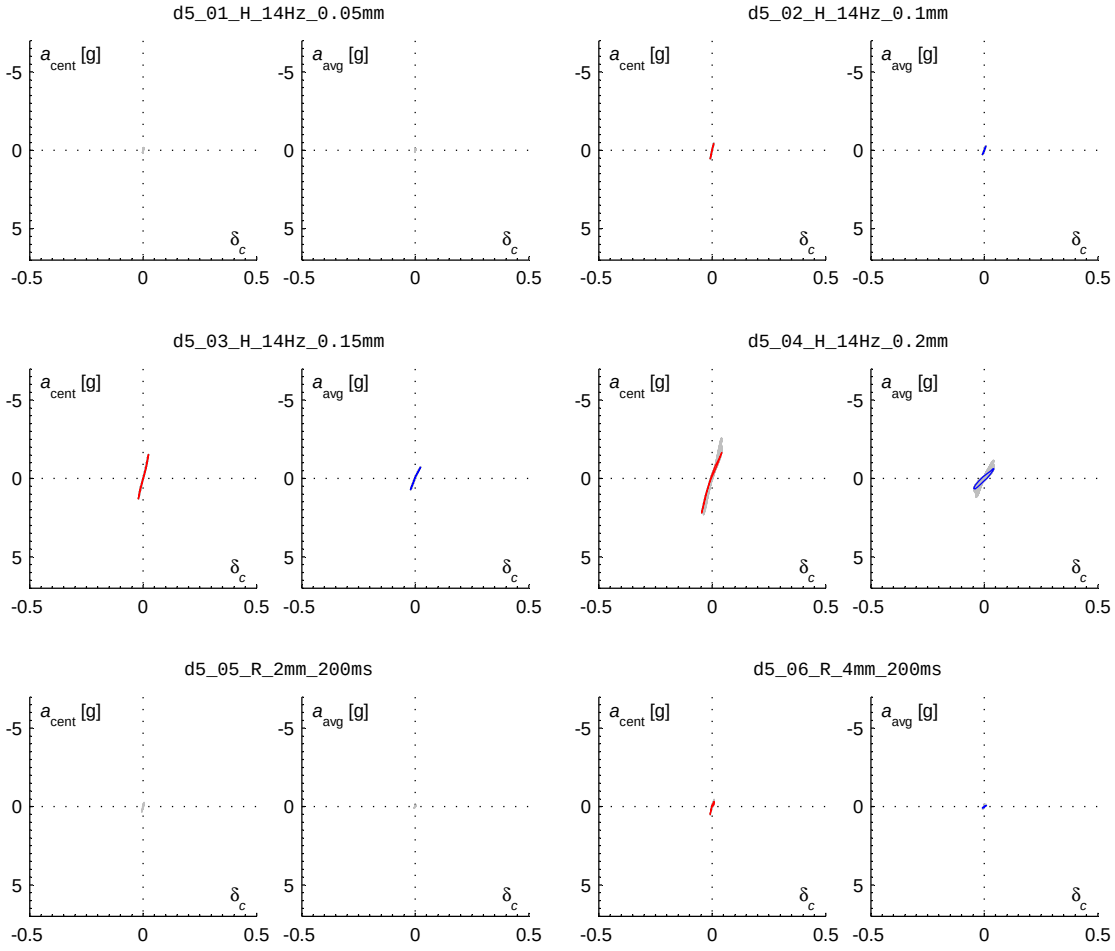
d5_01_H_14Hz_0.05mm
d5_02_H_14Hz_0.1mm
d5_03_H_14Hz_0.15mm
d5_04_H_14Hz_0.2mm
d5_05_R_2mm_200ms
d5_06_R_4mm_200ms
a cent [g]
a avg [g]
δc
-5
0
5
-0.5
0
0.5

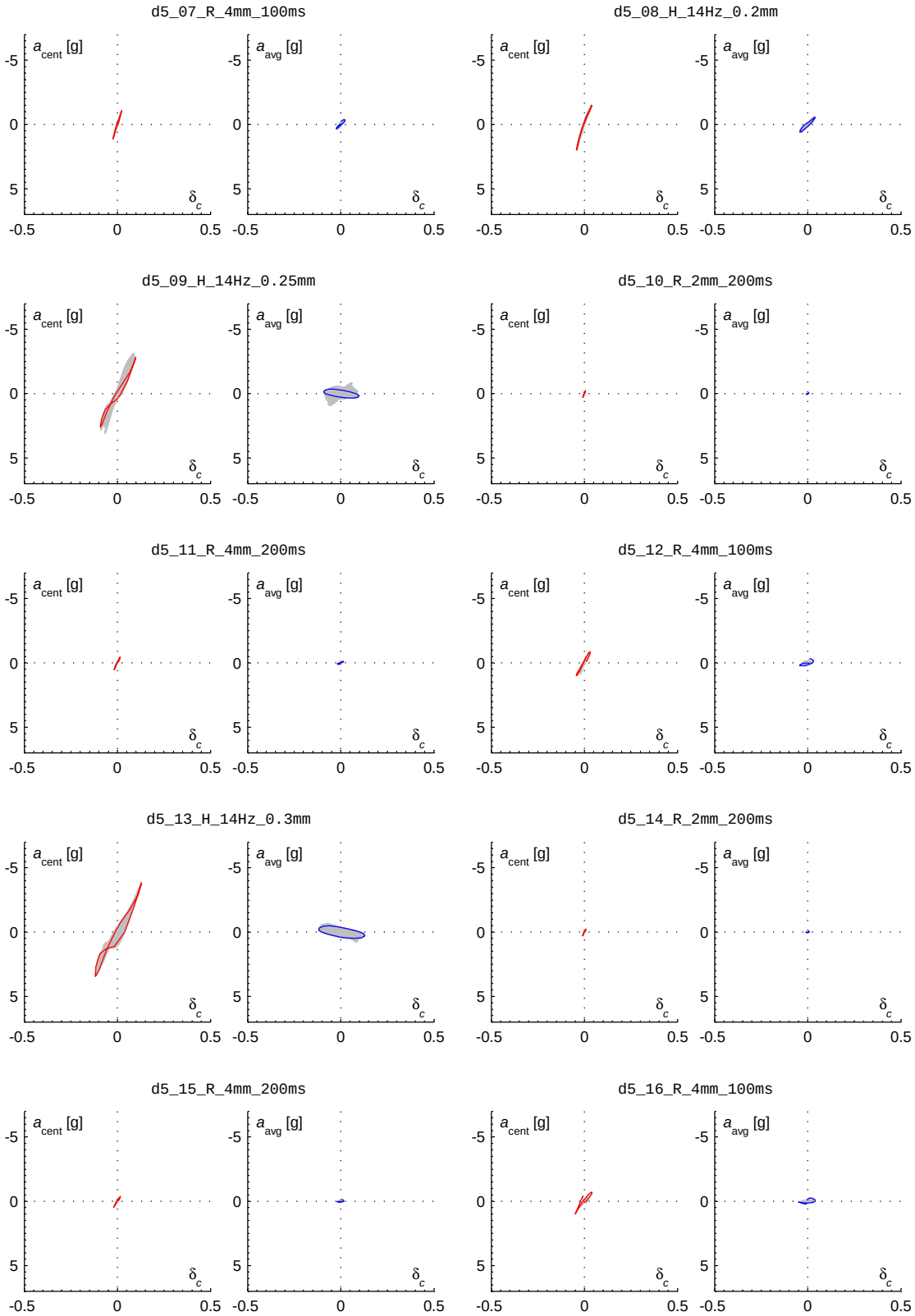
d5_07_R_4mm_100ms
d5_08_H_14Hz_0.2mm
d5_09_H_14Hz_0.25mm
d5_10_R_2mm_200ms
d5_11_R_4mm_200ms
d5_12_R_4mm_100ms
d5_13_H_14Hz_0.3mm
d5_14_R_2mm_200ms
d5_15_R_4mm_200ms
d5_16_R_4mm_100ms
a cent [g]
a avg [g]
δc
-5
0
5
-0.5
0
0.5

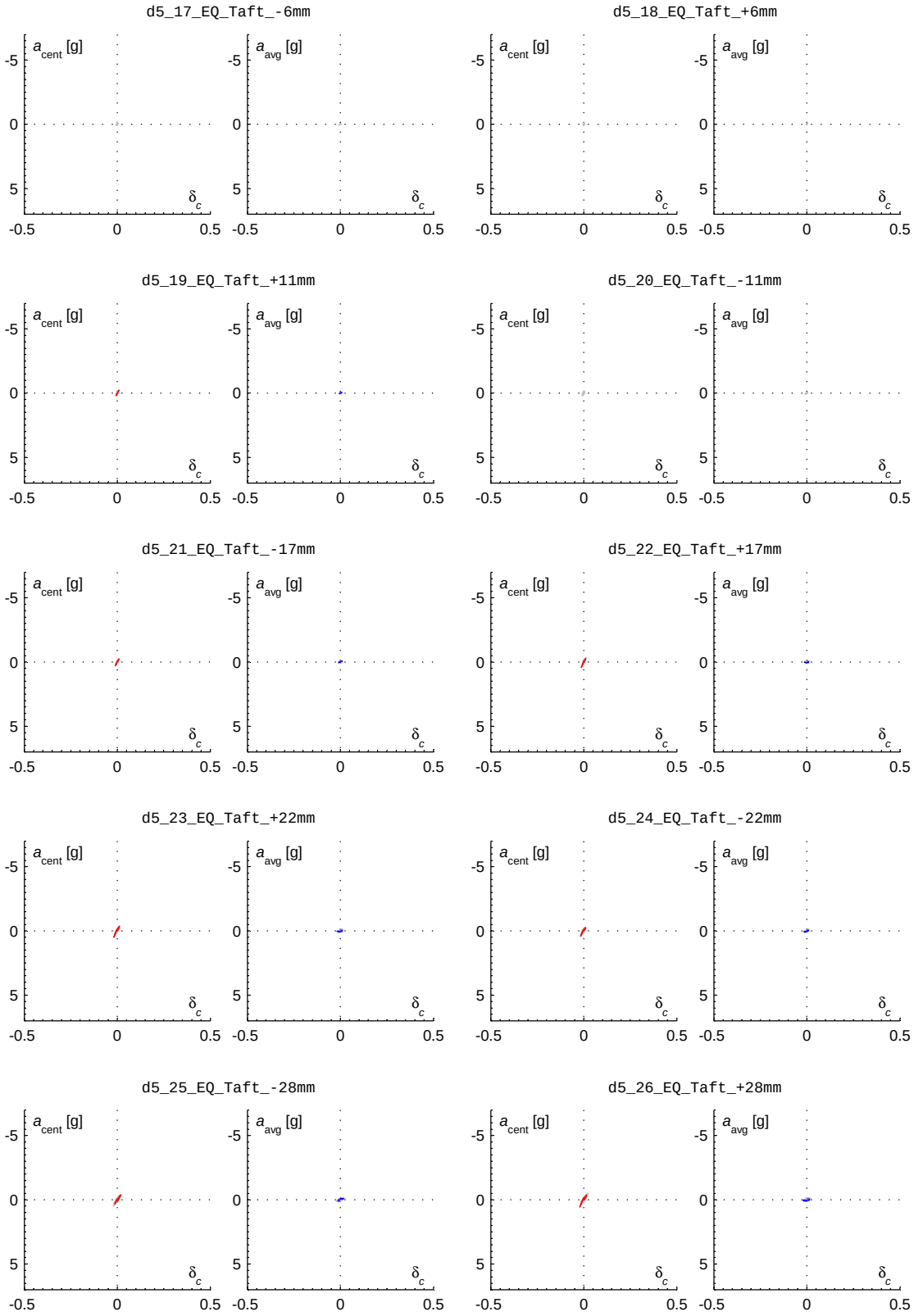
d5_17_EQ_Taft_-6mm
d5_18_EQ_Taft_+6mm
d5_19_EQ_Taft_+11mm
d5_20_EQ_Taft_-11mm
d5_21_EQ_Taft_-17mm
d5_22_EQ_Taft_+17mm
d5_23_EQ_Taft_+22mm
d5_24_EQ_Taft_-22mm
d5_25_EQ_Taft_-28mm
d5_26_EQ_Taft_+28mm
a_cent [g]
a_avg [g]
δ_c
-5
0
5
-0.5
0
0.5

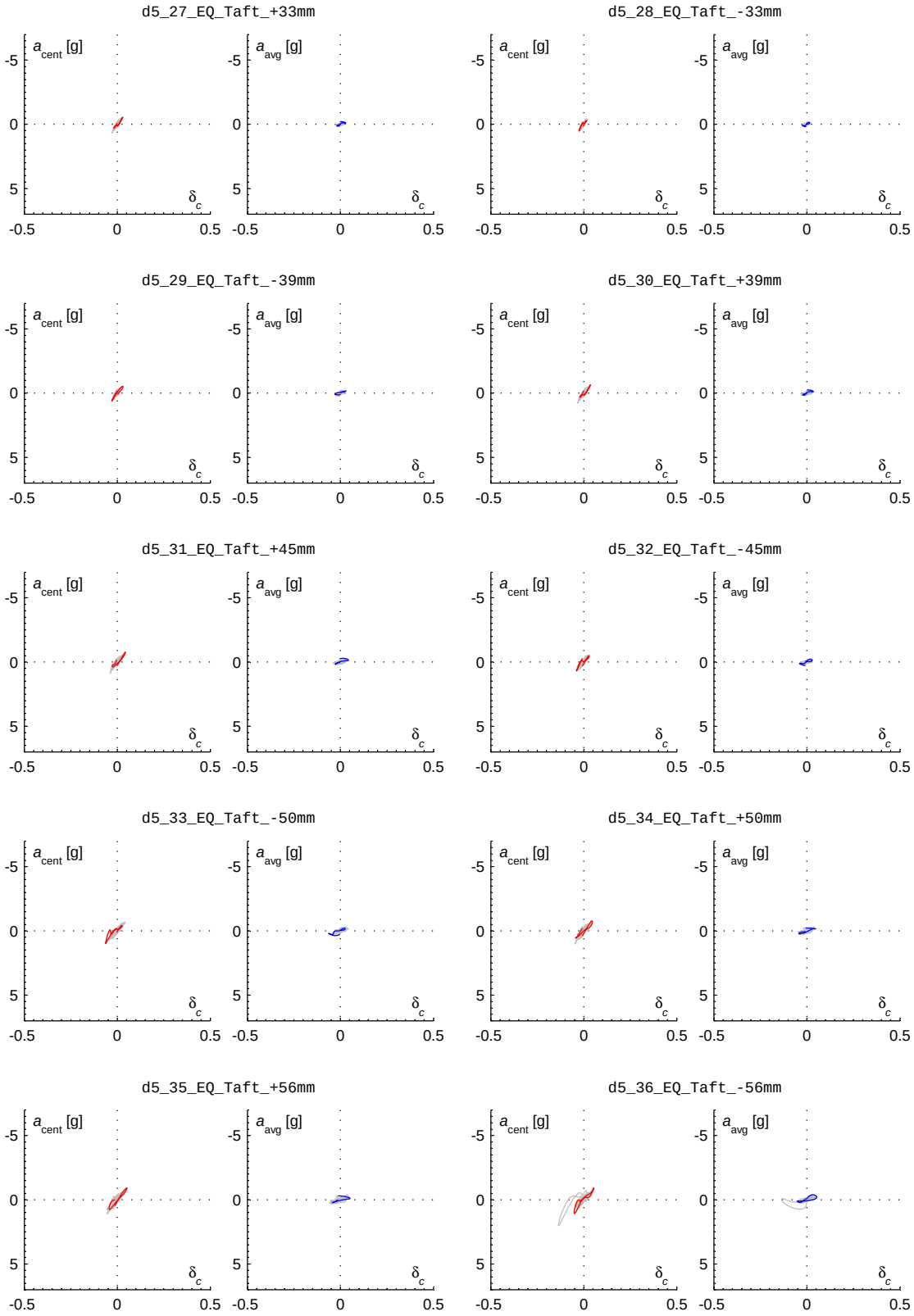
d5_27_EQ_Taft_+33mm
d5_28_EQ_Taft_-33mm
d5_29_EQ_Taft_-39mm
d5_30_EQ_Taft_+39mm
d5_31_EQ_Taft_+45mm
d5_32_EQ_Taft_-45mm
d5_33_EQ_Taft_-50mm
d5_34_EQ_Taft_+50mm
d5_35_EQ_Taft_+56mm
d5_36_EQ_Taft_-56mm
a_cent [g]
a_avg [g]
δ_c
-5
0
5
-0.5
0
0.5

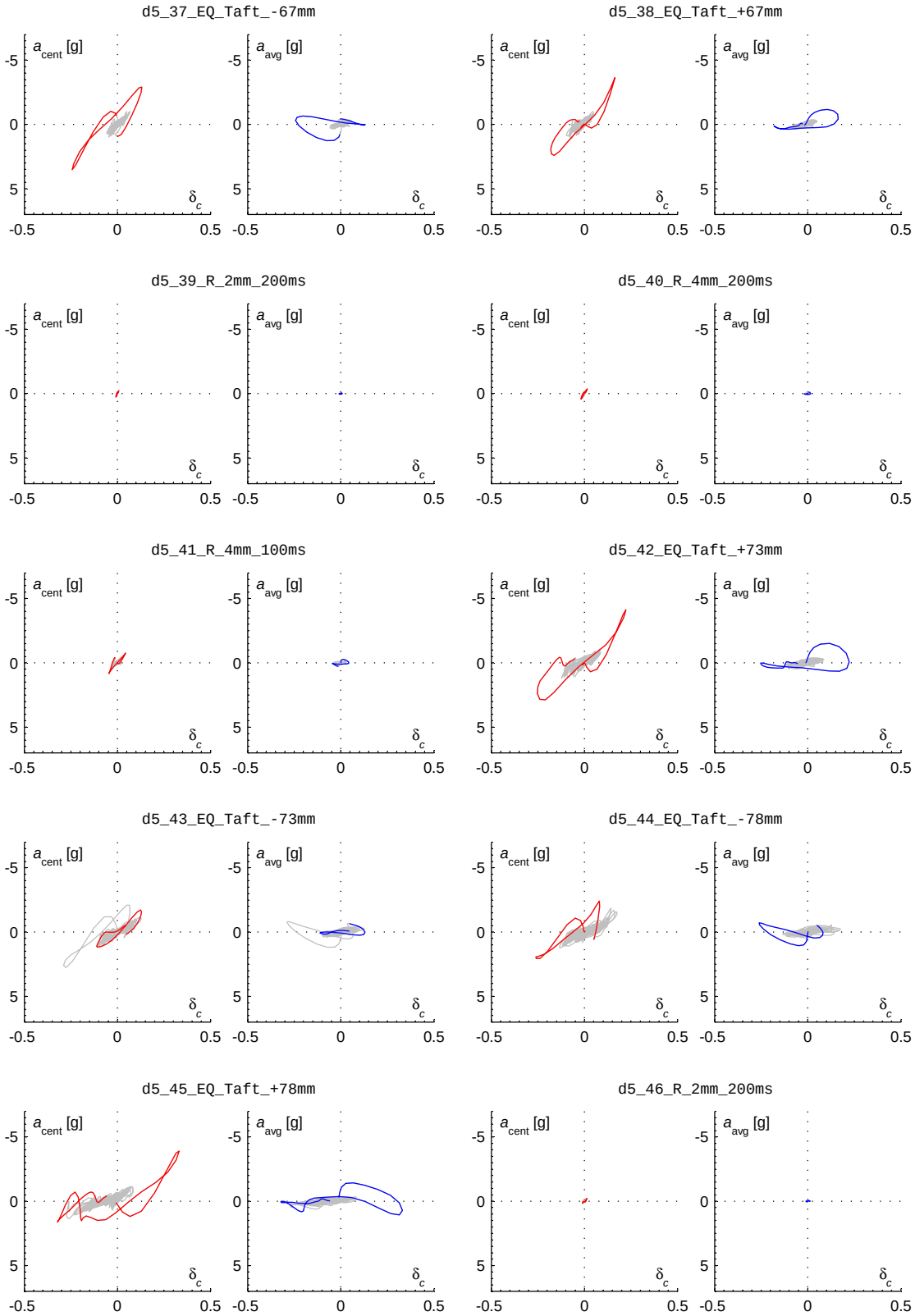
d5_37_EQ_Taft_-67mm
d5_38_EQ_Taft_+67mm
d5_39_R_2mm_200ms
d5_40_R_4mm_200ms
d5_41_R_4mm_100ms
d5_42_EQ_Taft_+73mm
d5_43_EQ_Taft_-73mm
d5_44_EQ_Taft_-78mm
d5_45_EQ_Taft_+78mm
d5_46_R_2mm_200ms
a_cent [g]
a_avg [g]
δ_c
-5
0
5
-0.5
0
0.5

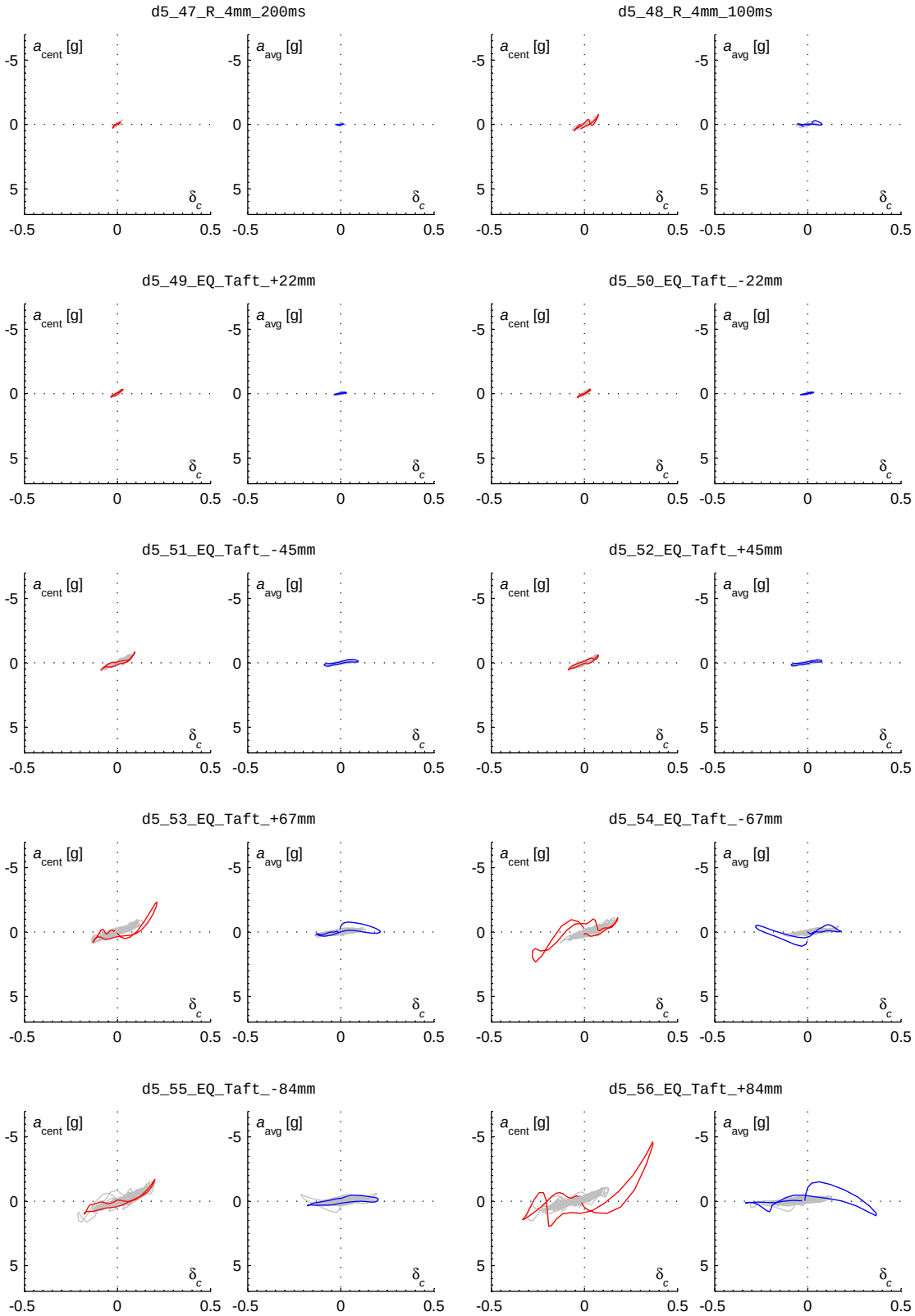
d5_47_R_4mm_200ms
d5_48_R_4mm_100ms
d5_49_EQ_Taft_+22mm
d5_50_EQ_Taft_-22mm
d5_51_EQ_Taft_-45mm
d5_52_EQ_Taft_+45mm
d5_53_EQ_Taft_+67mm
d5_54_EQ_Taft_-67mm
d5_55_EQ_Taft_-84mm
d5_56_EQ_Taft_+84mm
a_cent [g]
a_avg [g]
δ_c
-5
0
5
-0.5
0
0.5

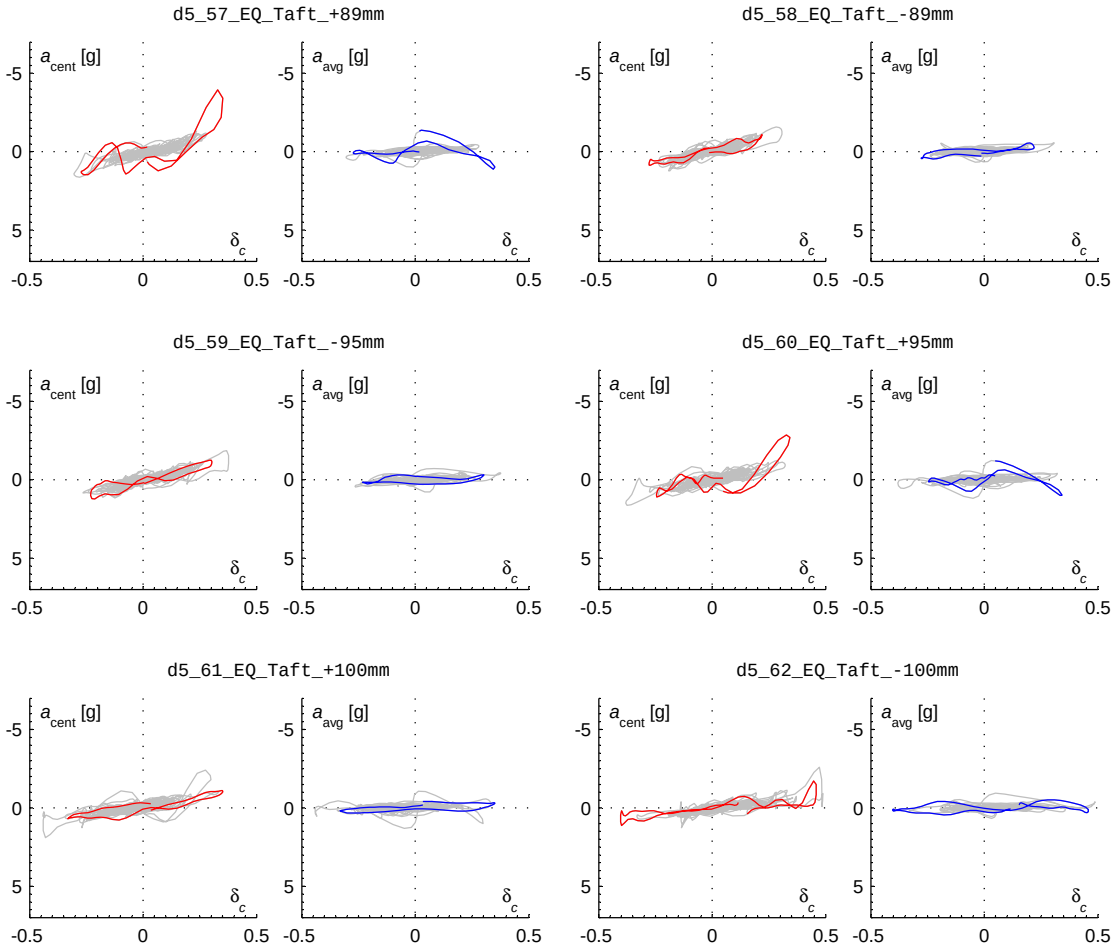
d5_57_EQ_Taft_+89mm
d5_58_EQ_Taft_-89mm
d5_59_EQ_Taft_-95mm
d5_60_EQ_Taft_+95mm
d5_61_EQ_Taft_+100mm
d5_62_EQ_Taft_-100mm
a_cent [g]
a_avg [g]
δ_c
-5
0
5
-0.5
0
0.5

S.8 Cracking Pattern Photographs

Photographs of each wall at the conclusion of testing are shown by Figures S.43–S.47.

Figure S.43: Wall D1 at the conclusion of testing.

Figure S.44: Wall D2 at the conclusion of testing.

Figure S.45: Wall D3 at the conclusion of testing.

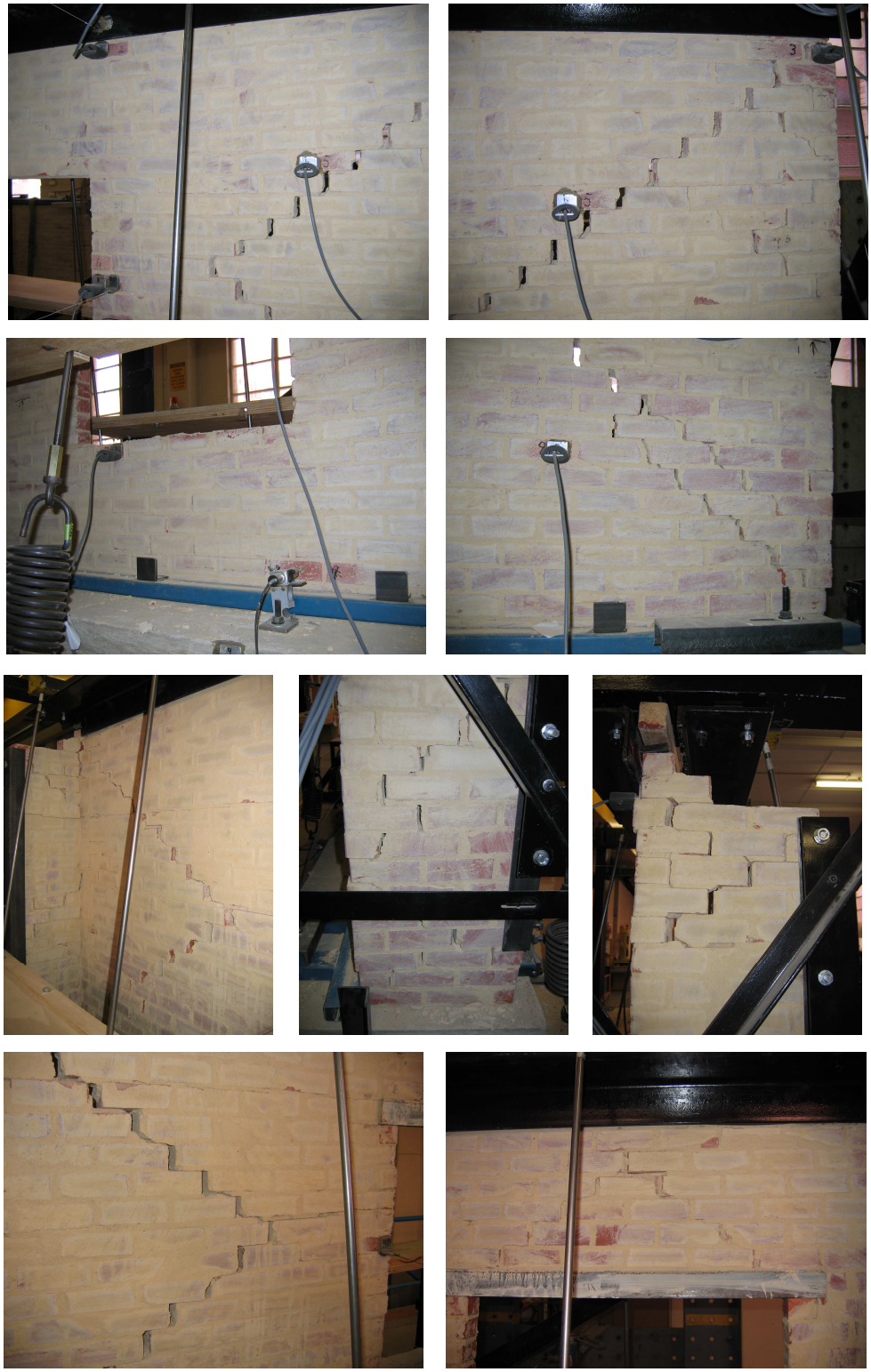

Figure S.46: Wall D4 at the conclusion of testing.

Figure S.47: Wall D5 at the conclusion of testing.

S.9 Attached Test Data

Accompanying the present Supplementary Material document is a ZIP file containing unprocessed and processed time-domain data obtained from these tests.

Both are available at the following DOI: 10.4225/55/5a0138124b6c0

All test data is sampled at a rate of 200 Hz.

Unprocessed data are contained in the subfolder `/channels`. The enclosed files provide readings from each of the ten displacement channels and six acceleration channels as defined in Figure S.15.

Processed data are provided in the subfolder `/processed`. Each file contains the following nine columns:

1. Table position, x_{tab};
2. Average support position, $x_{\text{sup.avg}}$;
3. Relative displacement between top support and table, $\Delta_{\text{sup.top-tab}}$;
4. Table acceleration, a_{tab};
5. Average support acceleration, $a_{\text{sup.avg}}$;
6. Wall central displacement, $\Delta_{\text{w.cent}}$;
7. Initially zeroed wall central displacement, $\Delta_{\text{w.cent0}}$;
8. Wall central acceleration, $a_{\text{w.cent}}$; and
9. Wall average acceleration, $a_{\text{w.avg}}$.

The process used to obtain each of the above response variables is described in Section S.4.

References

Standards Australia (2011), *Australian Standard for Masonry Structures (AS 3700—2011)*, SA, Sydney, NSW.

Vaculik, J. (2012), Unreinforced masonry walls subjected to out-of-plane seismic actions, PhD thesis, The University of Adelaide.

Vaculik, J., and Griffith, M. C. (2017), Out-of-plane shaketable testing of unreinforced masonry walls in two-way bending, *Bulletin of Earthquake Engineering*, DOI: 10.1007/s10518-017-0282-8.